Sequestering Floating Biomass in the Deep Ocean:
"Sargassum Ocean Sequestration of Carbon" (SOS Carbon)

by

Luke Alexander Gray

Submitted to the
Department of Mechanical Engineering
In Partial Fulfillment of the Requirements for the Degree of

Master of Science

at the

Massachusetts Institute of Technology

May 2020

© 2020 Luke Alexander Gray
All Rights Reserved

The author hereby grants to MIT permission to reproduce and to
distribute publicly paper and electronic copies of this thesis document in whole or in part
in any medium now known or hereafter created.

Signature of the Author……
Department of Mechanical Engineering
March 4th, 2020

Certified by……
Alexander H. Slocum
Walter and Hazel May Professor of Mechanical Engineering
Thesis Supervisor

Accepted by……
Nicolas Hadjiconstantinou
Professor of Mechanical Engineering
Chairman, Committee for Graduate Studies

Sequestering Floating Biomass in the Deep Ocean:
"Sargassum Ocean Sequestration of Carbon" (SOS Carbon)

by

Luke Alexander Gray

Submitted to the Department of Mechanical Engineering on March 4th, 2020
In Partial Fulfillment of the Requirements for the Degree of
Master of Science at the Massachusetts Institute of Technology

ABSTRACT

Sargassum seaweed has been growing ever faster due to climate change and agricultural runoff and has become a terrible problem for the Caribbean. The floating algae has been inundating Caribbean coasts in unprecedented and increasing quantities for the past decade and there are no indication of abating. When the seaweed makes landfall, it dies, rots, dyes water dark brown, creates an eyesore, and emits a terrible smell ("rotten egg" smell of hydrogen sulfide). Moreover, sargassum negatively affects tourism (decreased by as much as 25%-50% in some locations), fishing (decreased harvests & damaged equipment), industry (clogs in power plant cooling intake & fumes/particulate corrosive to machinery), human health (hydrogen sulfide & heavy metals), standard-of-living (civilian coastline with no resources to address), coastal ecology (eutrophication), and the global climate (methanogenesis in landfill & anaerobic coastal water). Responses thus far have been bootstrapped (manual cleanup predominant) and technologies recycled from other industries – containment barriers, large conveyor systems, excavators, bulldozers. These measures haven been proven to be costly, insufficient, and unsustainable.

This thesis presents the strategy of "sargassum ocean sequestration of carbon" (SOS Carbon) based on the discovery that sargassum pumped to a critical depth in the ocean ("pumping-to-depth"; identified as ~150-200m) is rendered negatively buoyant by the ambient hydrostatic pressure (air bladders that make the algae buoyant are compressed) and continues sinking to the ocean floor. Pumping-to-depth is a simple and energy-efficient (<<<10MJ/m^3) process that could generate carbon offsets (if sargassum deposited sufficiently deep; estimated to be >0.25 tCO2/tonne wet sargassum including process emissions) and enabled the design of ideal systems for low-cost, effective, long-term sargassum management. Presented herein are designs for two physical sargassum collection/disposal systems, "in-situ" and "ex-situ". This thesis documents initial investigation, early experimentation, systems analysis, concept selection, proof-of-concept tests, and the design/construction/testing of a full-scale "SOS Carbon Pilot" vessel.

ACKNOWLEDGEMENTS

Prof. Slocum: Alex, you are the greatest professional role model I have ever had. Thank you so much for the extraordinary time and attention you have given me over the past 4 years, especially the last 18 months for SOS Carbon. Machine design has become my greatest passion, and you have instilled in me an uncompromising will to use it to make the world measurably better.

Bob Gray: Dad, you have always gone above and beyond as a father – pushing us to treasure life and seize opportunities, nourishing us and making us love new things, and insisting on always doing things "the right way" – always with a healthy serving of delicious meals and ridiculously good hospitality. Now, you have really exceeded all expectations – helping me through the last two months of building in Bow. The SOS Carbon pilot tests could not have happened without you. I have been lucky to work so closely with my father on a project I am so passionate about, and I hope to get that chance again in the future.

Andres G. Bisono Leon: You have been an amazing friend and colleague over the past 18 months. You have made much personal sacrifice to see that our pilot tests became a reality. It has been one of the greatest pleasures of my life to know you, your family, and your country. Your humbleness and charm are qualities I hope to one day emulate. Your ability to connect with your own people is truly magical to watch. I hope we can collaborate more in the future on projects near and far, for the betterment of the planet and everything on it.

Folkers E. Rojas: You have been a legend in the lab since I started my freshman year. After working closely with you over the last several months, I can confirm that you have lived up to that "superstar" reputation. Thank you for your help preparing for and constructing our pilot vessel. I want to especially thank you for taking the time to have personal conversations with me, even after 15-hour days of working in the sun with sand, metal, grease, and hydraulic fluid all over us, to teach me valuable life lessons about working with others and maintaining relationships while "running at 100mph."

Rene Gruillon (Banco Popular): The support of you and the bank has been absolutely game-changing for this project. Not only that, but your personal belief in our mission has lifted me during moments of despair.

Brendan Newton (Island View Fabrication): Thank you for the skilled workmanship you gave to our project. You worked overtime to accommodate our fast-paced and erratic demand for weldments. You have amazed me with your skilled hands, but you have humbled me with your accommodation and good attitude. I am glad you got to come down to the DR to see things through! You deserved to see everything you made put together! I highly recommend Island View Fabrication: http://www.nhwelder.com/

Dieter Kunath (HydroCam Corporation): You and your son have demonstrated skilled workmanship and patience in working with me. We had some strange parts and tight schedules. You also suggested several useful fabrication improvements to the parts. I also appreciate your taking the time to share your stories as a young machine designer with me. I highly recommend HydroCam for waterjet and other machined parts: www.hydrocam.com

Bill Miskoe: Thank you for your gut checks and uplifting attitude as we planned the final details of the pilot test. I enjoyed visiting Iron Dragon and hearing about your engineering adventures.

PERG: Thanks to all my labmates that keep me sane and did me many favors while I was traveling to the Caribbean. PERG is a truly enriching place to work and I was lucky to be part of the family for 4 years.

The GC-111 Centaurus crew (Dominican Republic Navy):

T/N Marbel Rosario Ramirez Ortiz (Comandante)
T/N Yuberto Heredia Garcia (Jefe de Máquinas)
T/F Feliciano Mezquita Roso (2do Comandante)
T/C Carlos A. Rodriguez Perez (Para Servicio)
T/C Santo J. Guerrero Mojica (Para Servicio)
Sgto. Mr Wilson de la Rosa Garcia (Contra maestre)
Sgto. José Cruz Lopez (1er. Asistente)
Sgto. Anderson Ramirez Mercedes (Motorista)
Sgto. Marcelo Lopez Céspedes (Motorista)
Cabo Lenny Sanchez Liriano (Para Servicio)
Mro. Wagner Rodriguez Beltre (Para Servicio)
Mro. José Eduardo Valdez (Para Servicio)
Mro. Juan B. Perez Amador (Para Servicio)

All sponsors: We literally could not have performed our pilot tests without our sponsors. The pilot test took this project from a thesis and made it into a reality and it took my learning to the next level.

Table of Contents

0. Executive Summary

The Problem: Sargassum landfall is sapping hundreds of millions of dollars in revenue from the Caribbean tourism industry, and current bootstrapped countermeasures are capital intensive, costly to operate and maintain, visually-polluting, unsafe, and unsustainable, leaving a large demand for a low-cost, rapidly scalable, less visually-polluting, safe, sustainable, long-term solution.

The Idea: The SOS Carbon team at MIT designed, built, and tested a method for sequestering sargassum seaweed in the deep ocean by pumping it to a critical depth in the ocean (found to be 150-200m which also escapes the mixed layer of the Caribbean) where ambient hydrostatic pressure sufficiently compresses sargassum pneumatocysts (air bladders responsible for sargassum's buoyancy) such that the entire plant is rendered negatively buoyant and continues sinking to the ocean floor. This offers an ideal alternative disposal method to dubious landfilling in resort areas.

Open-Ocean In-Situ SOS Pump-to-Depth Vessels: Caribbean-wide fleet of sea-going SOS Carbon vessels that address sargassum in the open ocean (FIG 1).

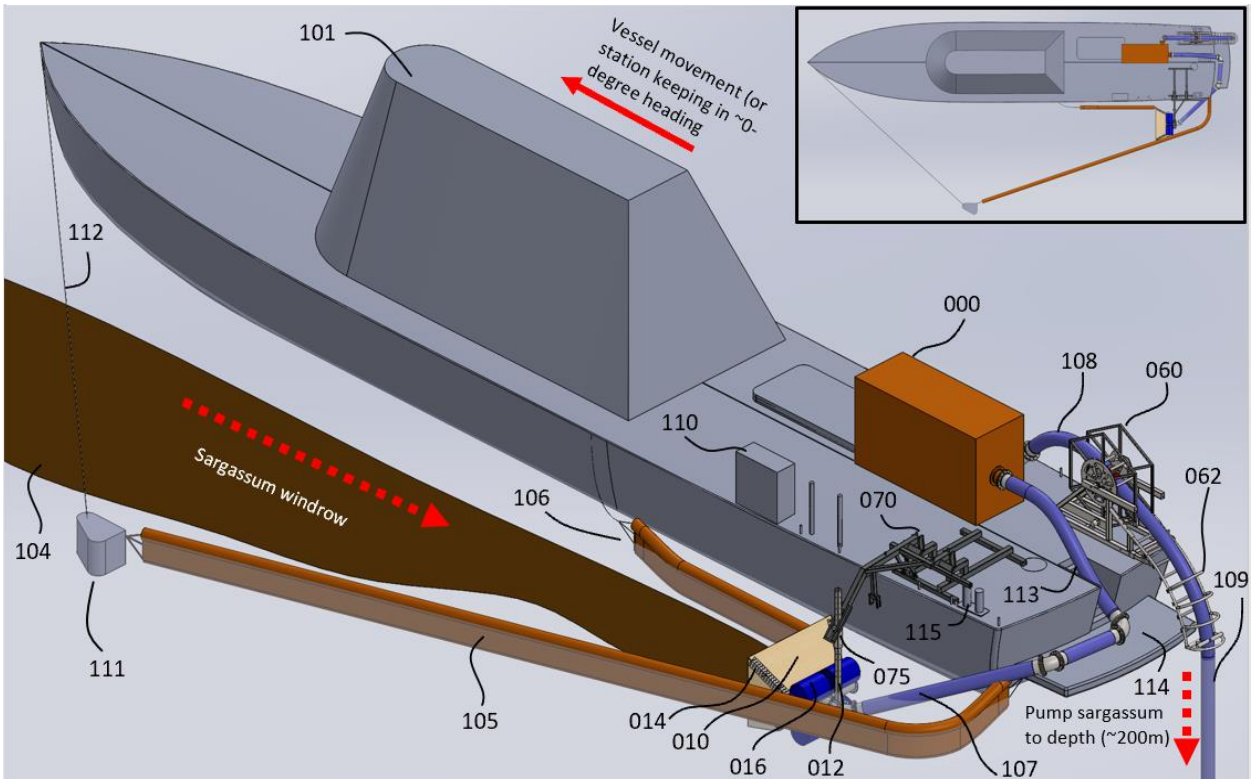

FIG 1 A 5000GPM pilot-scale version of the open-ocean, in-situ SOS pump-to-depth vessel that was designed, built, and tested. A future fleet would comprise vessels with up to 50,000GPM pumping capacity (multiple pumping systems in parallel).

FIGS 2, 3, & 4 show proof-of-concept tests, pump inlet device tests, and SOS Carbon Pilot vessel tests, respectively.

Proof-of-Concept Tests (Dom. Rep., January 2019)

FIG 2 Proof-of-concept tests (1) confirmed possible to pump-to-depth sargassum very efficiently and no outstanding risk, and (2) identified critical depth to which sargassum must be pumped.

Pump-Inlet Tests (Bow, NH, March-June, 2019)

FIG 3 Different pump inlet prototypes tested from March-June 2019. (Clockwise) Co-axial auger, transverse auger, suction tee, repurposed snowblower, suction boom. The moving auger devices (coaxial and transverse) were chosen for full-scale design.

SOS Carbon Pilot Tests (Dom. Rep., December 2019)

FIG 4 An in-situ SOS Carbon system for pumping-to-depth floating sargassum in the open ocean, which was tested in the Dom. Rep. in Fall 2019. The system illustrates how an SOS Carbon pump-based system can be deployed on a vessel of generic design (no specialty vessel required).

1. Background and Investigation

1.1 Sargassum and the Crisis in the Caribbean

Floating macroalgaes, organisms, and other pelagic debris have caused serious problems for fishing and tourism industries worldwide. In particular, Caribbean beaches are being inundated by pelagic sargassum, a type of holopelagic macroalgae that has been growing in unprecedented quantities in the Central Western Atlantic (CWA), more specifically in the Northern Equatorial Recirculation Region (NERR), and causing much economic, social, ecological and environmental damage in the region. When sargassum makes landfall, it dies, rots, dyes water dark brown, creates an eyesore, emits a terrible smell of rotten eggs (hydrogen sulfide), and inhibits swimming. This has significantly hurt tourism in Caribbean nations, where the industry directly contributes over 4% of combined GDP and supports over 700,000 jobs (WTTC, 2017). Additionally, sargassum has directly affected island life – fumes and airborne "dust" from the rotting sargassum can cause nausea, respiratory irritation, and corrosion of machinery. Direct contact from sargassum corrodes boats, breakwaters, and other man-made infrastructure. Thick mats of sargassum can stop small outboard motors, disrupting coastal villages and business activities. Fishing harvests have been severely affected, and fishing equipment damaged, in many areas (FIG 4). Eutrophication from decay of the sargassum suffocates shallow-water animals and area coverage obstructs photosynthesis of benthic plants (ie. corals). Finally, decaying sargassum in coastal waters, on beaches, and in disposal areas/landfills emits large amounts of methane into the earth's atmosphere.

Sargassum's explosion of growth is thought to be caused by warmer ocean temperatures, increased ocean alkalinity, increased nutrient upwelling of the coast of West Africa, and increased iron dust depositing from the Sahara (due to deforestation of the borders of the Sahara), and increased agricultural runoff from the Amazon and Congo rivers. Various works have used ocean models (Hybrid Coordinate Ocean Model) to backtrack from landfall locations, satellite NIR spectroscopy, synthetic particle tracking, among other methods, to corroborate the belief that the sargassum affecting the Eastern Caribbean is originating from the North Equatorial Recirculation Region (NERR) (Franks et al., 2011; J. F. R. Gower & King, 2011; J. Gower, Young, & King, 2013; Johnson et al., 2013; Putman et al., 2018). Earlier work identified Equatorial Atlantic saragassum as S. natans, which must have migrated from the Sargasso Sea many decades ago (Széchy, Guedes, Baeta-Neves, & Oliveira, 2012).

Rooted in climate change and improper land use by humans, these blooms seem certain to recur for years to come. These blooms should be seen in the broader trend of macro-/microalgal blooms, plastics accumulation, and the rise of many invasive species in our oceans, which seem to be human caused, permanent, and even accelerating phenomena in some cases.

Sargassum is one of the most common macroalgae in the world and the only holopelagic seaweed on the planet (meaning that it floats for its entire lifecycle). Sargassum was first observed in the Sargasso Sea by early explorers and was named "sargassum" after the Portugese word for "grape" because of the grape-like pneumatocysts, the bladders that give the sargassum positive buoyancy, shown in FIG 4.

In 2011, the Caribbean suffered its first season with severe sargassum invasion (Franks et al., 2011; Johnson, Ko, Franks, Moreno, & Sanchez-Rubio, 2013). From 2017-2018, then mayor-elect of Quintana Roo estimated that tourism had declined 35% due to the sargassum, and similar declines have been reported across the Caribbean (Mexico News Daily, 2018b). In Punta Cana alone, where the decline is estimated at 25%, this translates to approximately:

$$\$4.08bn \times 50\% \times (25\%) \approx (\$510{,}000{,}000)$$

(Direct Contribution of Travel & Tourism to DR GDP in 2017) × (Percent of DR Tourism in Punta Cana 2016) × (Reported Decline of Tourism in Punta Cana 2018)

of lost GDP for the Dominican Republic (Diario Libre, 2018; Dominican Annual Tourism Exchange, 2017; Euromonitor, 2016; World Travel and Tourism Council, 2018). Tourists are not only cancelling travel plans, home owners and other long-term investors are fleeing the islands. The Caribbean brand is being marred. The vice-president of the University of West Indies (UWI) stated that the sargassum problem is "the greatest single threat" to the Caribbean (CariCom, 2015). FIG 5 shows an example of a sargassum inundation not at all uncommon in the Caribbean in recent years.

FIG 5 (Top, Left) Sargassum at an unnamed private beach in the Caribbean. In the background is a $25 million villa. The dark brown color of the sargassum (and the terrible smell) is indicative of days of putrefication without being addressed. (Top, Right) Close-up view of sargassum pneumatocysts, responsible for the buoyancy of the floating macroalgae. (Bottom, Left) The fishing village located at Cabeza del Toro, between Bavaro and Punta Cana. This village is inundated with sargassum that damages fishing equipment and hurts fishing harvests.

Satellite imagery suggests that sargassum coverage in the NERR, has been increasing each year since 2011, the coverage in summer 2015 being at least 20x greater than during any time before 2011 (Wang & Hu, 2016). The severity of beaching has followed the same trend. FIG 6 shows the NERR and one NIR measurement of the sargassum coverage in this region.

While sargassum usually blooms once a year, giving rise to a "sargassum season" lasting from March through August, the 2018 & 2019 seasons extended almost until the years' ends (The Yucatan Times, 2018). The increasing severity and duration of sargassum invasions has sparked much academic research as well as physical attempts to stymie the onslaught of sargassum.

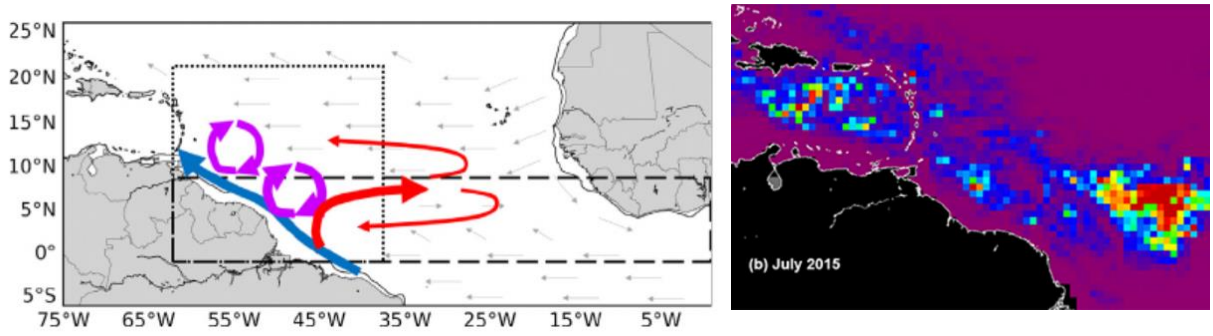

FIG 6 (a) the North Equatorial Recirculation Region (NERR), believed to be the source of Caribbean sargassum inundation (Putman et al., 2018). (b) NIR reflectometry images of sargassum spanning from the NERR to the Eastern Caribbean (Wang & Hu, 2016, MODIS Satellite Image).

A typical consolidated sargassum mat may be a few km long and a few hundred meters wide (Fig 7). In the open ocean, loosely associated "slicks" of consolidated sargassum mats, can be tens of kilometers wide by hundreds of kilometers long. A typical mat could take weeks to collect and cost hundreds of thousands of dollars to dispose of if it is allowed to make landfall. All the while tourism, coastal business, and native lives will be disrupted.

FIG 7 Consolidated sargassum mats, like the one pictured here, can be kilometers wide by tens of kilometers long. Loosely associated "slicks" of consolidated sargassum mats, can be tens of kilometers

1.2 Overview of Current Countermeasures (Specifically in Punta Cana)

Presently, the dominant management method across the Caribbean, in civilian and high-value resort areas alike, is manual cleanup. High-value resort areas have started using heavy-duty machinery and some specialized machines for removing sargassum from beaches. In even more select locations, long lengths of floating barriers have been installed immediately in front of beaches. These barriers are extremely expensive and prone to damage (from storms and biofouling). The barriers require that sargassum be constantly removed from in front of barriers using specially built barges (for example, one of two AlgeaNova barges operating in Punta Cana, in FIG 8), equipped with large conveyors, otherwise barriers can suffer damage and/or sargassum can be pushed under the floating barriers and land on the beaches, usually only 20-50m behind said barriers, as shown in FIG 9, below.

Sheer manpower and brute force methods have proven unable to effectively combat sargassum, even on the most high-priority coastlines; workers and barges are unable to respond quickly enough, or work fast enough, to keep beaches sargassum-free. All current solutions suffer from the fundamental disadvantage that they wait for sargassum to land on beaches and/or barriers before addressing it. There is no lead time afforded to the people and machines doing

FIG 8 One of 2 specialty collection barges operated by AlgeaNova (local company) in Punta Cana, DR. This aluminum barge cost ~$400,000 to construct and requires regular overhaul of the conveyors (foreign engineers from manufacturer must service) because of corrosion from saltwater and sargassum.

FIG 9 A barrier installed in front of a beach at Punta Cana. Sargassum is pushed under the beach and makes landfall unless constantly removed.

the cleanup, which means vast system scales (many workers and many machines) are needed to blanket coastlines and keep them somewhat habitable. It is a near impossible task.

In most places (civilian coastline), there is no means for sargassum management so locals are left to deal with negative effects to health and standards of living whilst compromising their own economic wellbeing to conduct cleanup efforts.

The aforementioned solutions to the problem sargassum invasions in the Caribbean are insufficient for many reasons: (1) current solutions are very expensive (requiring large amounts of manpower and special machines/infrastructure; so far requiring heavy public/private subsidy), (2) current solutions have turned resort areas into “construction zones” creating as much

disruption and visual pollution as sargassum does itself, (3) current solutions' inflexibility exposes them to a high level of risk (barriers / special machines could be rendered useless if sargassum migrates to other regions or simply stops blooming altogether, (4) current solutions exacerbate climate change by using large amounts of fuel to merely move the methane-emitting, heavy metal-leaching sargassum from one rotting place (beaches) to another (landfill or open pits), (5) special machinery/infrastructure is prone to damage (conveyors have thousands of moving parts susceptible to corrosion from contact with sargassum and barriers are prone to biofouling if not cleaned regularly) and difficult to service (requiring engineers from foreign manufacturers to make frequent service trips), and (6) current solutions are not really solutions at all because they all allow sargassum to make landfall (or come very close to making landfall in the case of floating barriers) where it causes all the same problems for tourism, human health, ecology, and the environment that have been mentioned above. Because all current systems are based onshore or just tens of meters away from shore, sargassum still accumulates on or very close civilized areas, dies, putrefies, dyes water brown, evolves a terrible smell, causes eutrophication, inhibits recreational activity, disrupts fishing, etc.

Most companies offering barrier installation and/or barrier cleaning/maintenance currently rely on heavy public private subsidy (for example, AlgeaNova, a collection company in Punta Cana, has a partnership with Grupo Punta Cana and recently received an $18 million grant to finish installing barriers in the area – barriers that will need to be replaced after 2-3 years). These companies stake their future profitability, affordability, and independency from subsidy on transforming/valorizing the sargassum they collect from barriers into saleable products.

Academic research has indeed been done on the valorization of sargassum for pharmaceuticals, nutraceutical, biomass feedstock, fertilizer, building material, biogas, bioethanol – the list goes on. The most promising valorization option for sargassum is arguably to use it as a substrate for anaerobic digestion and the production of biogas. However, the inescapable problem with sargassum valorization is its highly variable arrival rate and distribution. While ensiling and sun-drying may provide a means of preserving sargassum (Milledge & Harvey, 2016), there is a tremendous amount of research around potential products and processes that is required before any market for sargassum could incentivize and enable a large-scale, self-sustaining implementation of the current brute force solutions.

Even if there were a high-value added sargassum product readily manufacturable and with sufficient demand, operations that rely on revenues from sargassum transformation are fundamentally limited in their reach by the impracticality of extending supply chains to remote locations. Not to mention that such operations will only be incentivized to collect as much sargassum as is necessary to meet their demand, meaning that the interests of these companies may not always align with the interest to keep coastlines livable and enjoyable.

Valorization of sargassum is a noble effort, however, if sargassum really is well-suited for any kind of valorization, it is best to farm that sargassum, not collect it from the wild. There are currently large-scale sargassum farming efforts developing in the Gulf of Mexico for this purpose (ie. ARPA-E Seaweed Paddock project).

FIG 10 A barrier installed in front of a beach at Punta Cana. Sargassum is pushed under the beach and makes landfall unless constantly removed.

At present, sargassum is either buried in the beach where it lands, thrown in open pits within resort areas, or taken to landfill. FIG 10 shows some images of pre-trucked piles of sargassum in Punta Cana (Sept. 2018). The potential presence of contaminants like arsenic and cadmium, which sargassum is known to readily absorb in the ocean (Davis, Volesky, & Vieira, 2000) calls these methods into question (UNAM study found alarming levels of arsenic and cadmium in samples from Puerto Morelos and Playa del Carmen, Mexico (Mexico News Daily, June 2019); our own mass spectrometry study at MIT also found very high levels of arsenic in sargassum from Punta Cana, taken in Fall 2018).

In 2015, then Vice Chancellor of the University of the West Indies stated that approximately $120 million and 100,000 workers would have to be deployed across the Caribbean to completely solve the sargassum problem (CariCom, 2015). While vague and unsupported by any numbers, statements like these are not at all uncommon. The sargassum problem is one of the greatest threats facing the Caribbean, and there is no lack of concern nor lack of attention span for new ideas. The current solutions demonstrate that there is a strong political and financial will to keep beaches/civilian coastline clean.

2. Systems Analysis & Concept Selection

NOTE: Section 2 was written during the first months of the project, when the strategy was still being called “open ocean sinking” and the system was still being called “Deep Ocean Sargassum Sequestration (DOSS)”. This section is left unedited so that the reader may see the original evolution of thinking that lead to the concept that ultimately came to be called “Sargassum Ocean Sequestration of Carbon (SOS Carbon)”.

2.1 Overall Strategy Selection: “Open Ocean Sinking”

Fundamentally, there are only so many things you can do with sargassum – redirect it, collect it, redirect it then collect it (at a more desirable location), or none of the above. The final action taken with the sargassum can be either transport to a landfill, harvest for transformation, or disposal at sea (sink). FIG 11 shows the original matrix used to organize these strategies and identify open-ocean sinking as a promising option.

Sargassum Strategies	On Land				Offshore				Open Ocean			
Redirect Only												
Redirect → Management Point					Harvest	MSW	Kill	Sink	Harvest	MSW	Kill	Sink
Stationary Management Only	Harvest	MSW	Kill	Sink	Harvest	MSW	Kill	Sink	Harvest	MSW	Kill	Sink
Mobile Management Only	Harvest	MSW	Kill	Sink	Harvest	MSW	Kill	Sink	Harvest	MSW	Kill	Sink

Not Possible/Desirable	Being Done/Not Sufficient	Possible Future Solution	Worth Pursuing

FIG 11 The original, high-level matrix used to identify “open ocean sinking” as a promising strategy.

It was recognized that a fleet of open-ocean in-situ “sinking vessels” (latter referred to as SOS pump-to-depth vessels) could have all the following advantages over current solutions:

- **Out-of-sight** - no visual/noise pollution from barriers or onshore collection machinery (as if sargassum was never a problem).
- **Smaller system scale** - more lead time (compared to onshore measures) means large swathes of coast are protected by a small # of vessels.
- **Low-cost** - so long as critical # of resorts buy in, this is potentially the lowest variable cost achievable by any system. The cost of emergency response services could also be shared by multiple small island nations, or long stretches of civilian coastline.
- **Non-permanent** - pumps/ships have high resale value (could even be rented seasonally), unlike onshore barriers/specialized machinery.
- **Mobile** - protects large swathe of coast and can be redeployed (should sargassum migrate to different locations around world).
- **Sustainable, long-term solution** - longer lifetime (>10 years) than barriers for similar capital investment (barriers replaced every 2-3 years).

2.2 Sargassum Buoyancy Experiments: What Makes Sargassum Sink?

An artificial saltwater bath, with 35ppt sodium chloride, was created to test various concepts for rendering sargassum negatively buoyant. Sargassum used was collected from the Dominican Republic, washed, sundried, and then vacuum bagged for transport. When the sargassum is re-wetted it regains an

appearance and consistency similar to live sargassum in the wild. The pneumatocysts in the dried sargassum were 100% intact. Observations from the experiment are recorded here.

An important, perhaps obvious, observation is that everything except sargassum pneumatocysts, meaning the stems and leaves, are negatively buoyant and will readily sink when completely wetted, even if previously dried (all entrained air bubbles, held by surface energy and Van der Waals forces, should be removed by agitation underwater). Even if 90% of a sargassum plant is crushed between two flats plates and completely wetted, the remaining air bladders can keep the plant afloat. Pneumatocysts are the sole reason that sargassum is buoyant.

Wet sargassum pneumatocysts are like underinflated balloons, buckling before they burst. Therefore, the bladders require a large external pressure differential (positive or negative), applied mechanical pressure and/or displacement to break. In the laboratory setting, rupture was accomplished by using large, flat jaws to crush the saragassum, as well as by using pointed probes to apply concentrated force. The actual mode of breaking could be a combination of pressure differential, mechanical stress concentration, and surface shearing as the sargassum deforms. Unless crushed with enough force to completely flatten, even a broken bladder will remain open and refill with air. This entrained air is enough for a broken bladder to provide a buoyant force comparable to an intact bladder. The measured pressure, mechanically applied to vesicles of known dimension and measured with a force gauge, was found to be approximately 25MPa (approximately 80N applied to a 2mm diameter vesicle). This value is important to some of the concept evaluations presented later in this paper. Another experiment in a pneumatic chamber indicated that a pressure differential of greater than 30MPa would be required to explode the vesicles, suggesting that mechanical stress concentration and surface shear did contribute to imploding under mechanical compression in the former experiment.

Dry or aged sargassum pneumatocysts are more brittle and easier to break (sometimes without initial buckling), but require a large amount of entrained air to be removed before they will sink in saltwater. Applying considerable pressure between two flat plates, and doing this underwater, is the best way to ensure that bladders are broken with a high fidelity and that bladders do not maintain or refill with air, respectively. Even one bladder can support a significant amount of vegetation. It is not recommended that any strategy attempting to sink sargassum rely on bursting only a fraction of the bladders – close to 100% of bladders must be popped, and all entrained air removed, in order to render sargassum negatively buoyant. Of course, there is also the option of removing all bladders from the sargassum plant (pneumatocysts are not the reproducing part of the plant), however breaking up or cutting sargassum with this resolution and level of precision is more difficult that simply burst the bladders, and will leave a large mass of pneumatocysts floating, which will continue to reach coastline.

Knowing sargassum vesicle's buckling tendency exists, another PERG experiment endeavored to find out how sargassum vesicles respond under vacuum. It was found that sargassum vesicles of the maximum size (7mm) could remain intact under external pressure 30x less than atmospheric. Being the limit of the pneumatic cylinder used, we were unable to find the negative pressure differential at which rupture would have occurred. This finding suggests that tensile stress in the vesicles is likely not the cause of rupture in compression, rather, the stress concentration produced on the highly curved ring of a compressed sargassum vesicle is likely the principle cause of rupture under conditions of mechanical compression.

Another important observation is that the sundried, long-dead sargassum used to perform these experiments had 100% of its air bladders intact. Therefore, killing sargassum does not necessarily mean that it will sink. Because sargassum does naturally senesce and sink in the open ocean, is tempting to

FIG 12 Before and after photos of saragassum that was buoyed in a tightly packed net for 19 days. Due to disrupted nutrient cycling and/or blocked photosynthesis, the sargassum died and became negatively buoyant due to waterlogging.

imagine solutions wherein sargassum is simply killed and allowed to sink, eliminating the need for a mechanism. However, sargassum sinks in the open ocean due to down-welling currents that drag it to a depth where hydrostatic pressure implodes bladders or due to heavy encrustation by bryozoans at the surface, not because of a direct relationship between dying and negative buoyancy. However, it was observed that dried, long-dead sargassum becomes slowly waterlogged if left in saltwater over the period of several days, which does render it negatively buoyant. Upon this laboratory observation, we directed an experiment in Punta Cana where a net of tightly packed sargassum was left buoyed just off the coast and checked on regularly. Our hypothesis was that disrupted nutrient cycling and/or blocked photosynthesis from the crowded nature of the netted sargassum would cause it to die, subsequently becoming waterlogged and negatively buoyant. The experiment showed that the laboratory phenomena would also occur in the wild (although slightly slower because of more nutrient-rich water in the neritic waters of the Caribbean). FIG 12 shows before and after photos of the sargassum used in the experiment.

As sargassum is currently collected in nets by the lone barge currently operated by the startup Algae Nova, this is a method of disposal that could be used immediately (instead of dumping on the next beach or transporting to landfill, which is the company's current practice).

Dried sargassum is very flammable although it is not known whether a large fire could be sustained without other fuel. Burned pneumatocysts are extremely brittle - if not compromised by combustion itself, even slight agitation after incineration results in the disintegration of the entire bladder. However, completely burned sargassum is not negatively buoyant due to oxidation layers contributing to the buoyant force. Burned particles actually demonstrate a reversed buoyancy trend, pneumatocysts sinking and leaves floating, due to surface-area-to-volume ratios. It is also not known how much PICS, and what relative quantities of dioxins, dibenzofurans, and other harmful byproducts, are produced by burning sargassum.

To conclude the findings of the current study on the nature of sargassum's buoyancy and the loss thereof, an experiment was conducted wherein a sargassum net of known volume was submerged and weighted in the open ocean in order to obtain a conservative estimate of the buoyant force required to overcome in order to sink the sargassum, which is key to the analysis presented later in this paper. The buoyant force of the sargassum was measured to be 60 N/m^3 bulk (netted) volume of sargassum.

Prior work has studied the pressure-time dependence that governs natural sargassum sinking in the wild, but the work bore no mention of forced sinking as a method to manage invasive sargassum (Johnson, 1977). The study confirms the necessary depth that cause nearly all vesicles to "fail" immediately (either collapse or irreversibly rupture under hydrostatic pressure), causing sargassum to become negatively buoyant, and this depth is about 135m. Due to the monotonically increasing ambient pressure that sargassum experiences as it is slowly submerged under the influence of natural down-welling currents in nature, the actual depth at which sargassum loses buoyancy could vary (Johnson, 1977). The study further notes that vesicles of different sizes (can range from 2-7mm) require different hydrostatic pressures to fail and that unless a vesicle is irreversibly ruptured, it could theoretically re-inflate if carried back to a shallower depth by upwelling currents. The study therefore hypothesizes the need for sargassum to not only reach a critical depth, but also to escape the mixed layer of the ocean in order to ensure sinking in nature. Finally, the study hypothesizes the ability of sargassum to actively control its buoyancy via its bladders, in order to survive sustained prolonged submersion while being entrained in down-welling Langmuir currents (Johnson, 1977).

In light of the work done by Johnson (1977) and the considerable experimental effort of the present study, it was believed that there exist only a few ways to actively and irreversibly sink undesirable sargassum with a high fidelity:

(1) Allow sargassum to die and become waterlogged – then dump once negatively buoyant.
(2) Crush the sargassum, thereby rupturing a sufficient fraction of vesicles, and compressing the plant as a whole, such that the crushed sargassum is negatively buoyant even at surface depths.
(3) Pump the sargassum to a depth where hydrostatic pressure causes the plant to become negatively buoyant (by sufficient compression, not by irreversible rupture of vesicles).
(4) Mechanically push the sargassum to a depth where hydrostatic pressure causes negative buoyancy (again, by sufficient compression, not by irreversible rupture of vesicles).
(5) Explode the sargassum vesicles by pulling vacuum.

2.3 Sinking Method Concept Generation

A series of matrices, starting from DOSS ("Deep Ocean Sargassum Sequestration"- the name of the strategy at that time) and becoming successively more granular, were used to search for optimal solution concepts to be subject to more detailed analysis. It should be noted that many of these concepts introduced novel ways of rendering sargassum negatively buoyant, or otherwise irreversibly sinking sargassum, not listed above. These concepts were quickly dismissed. The concepts selected for detailed analysis comprise the five vetted methods of sinking, identified in the previous section. The matrices are included in their entirety so that the reader may appreciate the full breadth of the solution space explored.

FIG 13 shows the initial matrix layer of solution strategies generated to accomplish open ocean sinking and the concept matrices derived from the selected strategies, which are defined by an integral technology, principle, or process. Strategies and concepts were selected for further analysis based on (1) the technical risk, (2) the speed with which it could be implemented, (3) the impact it could have on the sargassum problem, and (4) being cheap enough for resorts to pay for.

FIG 13 The concepts for sinking sargassum were generated by expanding the "open ocean sinking" matrix from Figure 1 above. The coarse 2x2 is formed by the simple observation that sargassum can only be sunk by either changing the buoyancy and allowing it to sink naturally, or by adding weight to forcibly submerge it – this forms one reciprocal pair. Likewise, this process can either be done continuously or discretely (with starts and stops) – a second pair of descriptors. Changing buoyancy can only be changed by increasing mass, decreasing volume, or killing the sargassum (thereby lysing the pneumatocysts and decreasing the volume, rendering it negatively buoyant). Forcible sinking can only be done by pushing or pulling the sargassum down. Presented above is the layer of solution strategies inspired by these pairs of descriptors. Propagated from there are matrices with specific concepts generated by using similarly comprehensive reciprocal pairs of descriptors. Concepts chosen for more detailed analysis are highlighted in GREEN: (1) weighted nets with distributed collection, (2) weighted nets with concentrated collection, and (3) rolling crusher.

Ultimately, four concepts for sinking sargassum were chosen for further consideration:

(1) Method #1: "Kill and Release" – kill the sargassum by sequestering inside a receptacle, then tow to a sink site and simply release.
(2) Method #2: "Crusher" - sargassum bladders crushed and air removed rendering the entire plant negatively buoyant.
(3) Method #3: "Pump-to-Depth" – sargassum is pumped to a depth where hydrostatic pressure renders it negatively buoyant.
(4) Method #4: "Weighted Cage" – sargassum is collected inside a weighted cage, with an open bottom, and forcibly sunk, eventually reaching a depth where hydrostatic pressure renders the sargassum negatively buoyant.

While there are numerous reasons why each of these concepts were chosen for further analysis, it can be readily observed that each of these winning concepts directly employs one of the viable sinking

methods identified in the previous section: (1) Killing, (2) Crushing, (3) Pumping, and (4) Pushing. Exploding the sargassum by applying negative pressure differential did not pass this stage of consideration because a large, negative pressure differential is needed and we have conceived no way to do this in a time- and energy-efficient manner. One thought was to force the sargassum through a Venturi valve where bladders would explode because of the pressure differential. The size of the valve needed to sustain minimum throughput and the neck dimension needed to create the necessary pressure drop, call for an enormous amount of propulsion power, and introduce the risk of clogging, respectively.

2.4 System Concept Generation

The remaining four sinking methods were incorporated into actual system concepts for Punta Cana. These systems are primarily separated by ex-situ and in-situ systems. In the former category, sargassum is collected in a different location from the "sink zone." In the latter, sargassum is sunk in a continuous process without ever being stored, collected, or transported. FIG 14 shows all possible

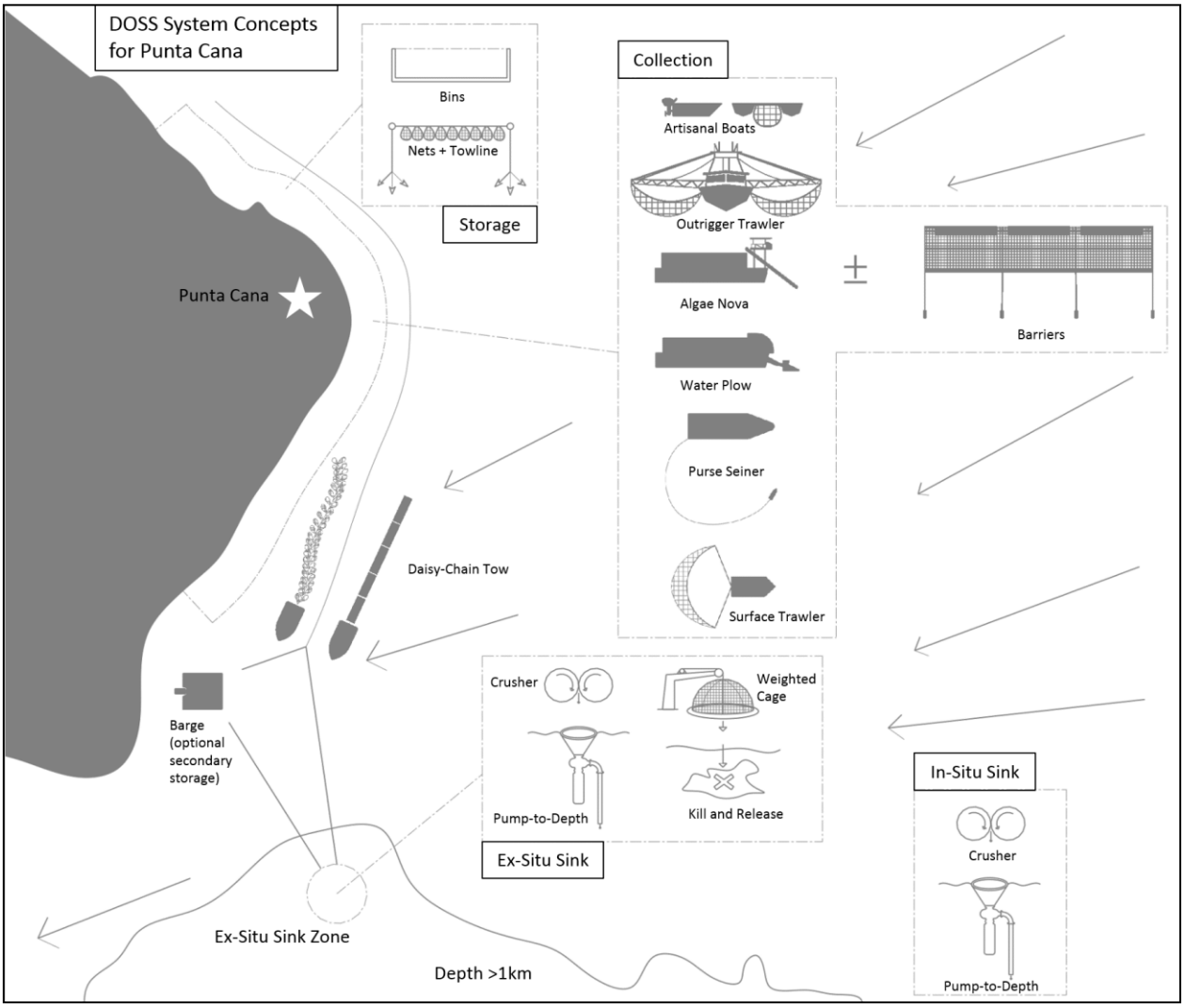

FIG 14: All possible permutations of the constituent collection vessels, storage devices, transportation vessels, and sinking methods that comprise the DOSS system concepts.

permutations of the constituent collection vessels, storage devices, transportation vessels, and sinking methods (again, the system was still being called “DOSS” at this time).

Of the system permutations generated by the elements illustrated in Figure 7, three were selected for their obvious advantages over similar solutions:

1. Ex-situ Distributed Sinking (EDS) – A combination of collection mechanisms – artisanal boats, outrigger trawlers, Algae Nova barges, purse seiners, and surface trawlers – with or without the assistance of concentrating barriers near the shore, would constantly collect and deposit sargassum in primary storage located regularly along the protected coast. Once containers are full, a primary transport daisy-chains these receptacles together and tows them down the coast to an anchored barge, depositing the sargassum there before returning the receptacles to their original location. After a longer period of time (perhaps a year) the barge is pushed out to a “sink zone” and the sargassum is sunk by any of Methods #1-4 described earlier. The system concept essentially represents a municipal waste system for sargassum where collection, transport, and disposal all occur in the ocean.
2. In-situ Concentrated Crushing (ICC) – A seaworthy vessel is outfitted with pushed, outriggered, or towed crushing devices to compress incident sargassum as it moves, rendering it negatively buoyant, without ever removing it from the water. Such a vessel may stay at sea for months at a time, its path being optimized by analyzing satellite or drone imagery.
3. In-Situ Pump-to-Depth (IPD) – A seaworthy vessel outfitted with a pushed, outriggered, or towed device that continuously pumps sargassum below the mixed layer of the ocean, and to a depth where hydrostatic pressure sufficiently compresses the sargassum such that it becomes negatively buoyant. Such a vessel may stay at sea for months at a time, its path being optimized by analyzing satellite or drone imagery.

These system concepts were evaluated based on technological readiness, potential impact at scale, potential speed of implementation, and cost to coastal entities (although the tools can easily be adapted to make calculations relevant to other areas in the Caribbean). The following sections include further elucidation of each concept selected for analysis, the analysis, and the results thereof.

2.4.1 Detail and evaluation of selected concepts

2.4.1.1 Ex-situ Distributed Sinking (EDSa)

While the exact combination of storage, collection, transportation, and final disposal method, may comprise any of the elements illustrated in FIG 14, for the purposes of technoeconomic analysis, it is necessary to define an exemplary system. For the purposes of this analysis, concept "EDSa" comprises a system wherein local fisherman (in artisanal fishing boats) are incentivized to collect sargassum using ordinary fishing vessels, attach the nets of sargassum to centrally located, anchored, buoyed towlines to be towed en-mass to a sink zone, where the sargassum is sunk by Method #1: "Kill and Release." FIG 15 illustrates such a system off the coast of Punta Cana.

FIG 15 (Left, a) A bird's-eye-view of a sargassum collection system wherein local fisherman are incentivized to collect sargassum in fishing nets using working boats, and attach that sargassum to centrally located tow lines, to be strung together and towed by a larger vessel to a "sink zone."

The envisioned system will relied on a plurality of working/fishing boats, each assigned to collect up to a few kilometers of coast/beach. Every working boat will bring individual nets of sargassum to towlines located at regular distances along the protected coastline, central to where collection is happening. If barriers are used to concentrate sargassum and increase collection efficiency, collection will be happening as close as 30 meters from shore (effective barriers are not cheap and so built as close to shore as possible; barriers can be $100-300/m). If barriers are not used, then collection should be farther away from shore, 10-20km even, to afford enough time to collect progressing sargassum. The positions of these towlines can be measured and communicated with solar powered sensors and AIS/VHF transmitters/receivers attached to the buoys, respectively. The towlines could be made of buoyant

Dyneema mooring line with integral attachment points for sargassum nets. The termini, and perhaps midpoints (depending on the length of the towline), could be attached to buoys, each anchored with three Vryhof anchors in a tri-link configuration.

In one payment scheme, working boat operators could take pictures of each properly filled and attached secured net with a serial tag they are provided by the secondary collection and disposal entity (so they these operators can receive pay for each bag and carbon accounting/verification is up to standard).

Once a tow line is filled, a tug/supply vessel operated by the secondary collection and disposal entity will make a trip down the coast and collect lines that are full, daisy-chaining individual tow lines together, and tow these lines to a "sink zone," an area deep enough such that, if sargassum is sunk there, no photosynthesizing plants are covered and currents cannot reach the sunken debris. Fortunately, the Caribbean is a relatively deep sea, hosting some of the deepest points in the entire Atlantic – the Muertos Trough, the Puerto Rico Trench, and the Venezuelan Basin all exceed 3km in depth. The sink zone should be inside the EEZ of the country performing the operation and avoid major shipping lanes. The nearest location to Punta Cana with a depth >1000m is approximately (18°18’41”N, 68°20’18” W), so it is suggested this location be considered as a preliminary “sink zone.” An approximate location of this sink zone is illustrated in Fig 14.

A redundant line will be left at each location to ensure collection is continuous. Meanwhile, when the tow line loaded with sargassum reaches the sink zone, the sargassum therein being long-dead from blocked sunlight and interrupted nutrient cycling during storage and transportation, nets will be opened and sargassum will simply be emptied into the ocean. Then the tow boat will return the towlines (with nets still attached) to their original locations so that fishermen may retrieve nets and sustain collection activity (there is no incentive to steal nets as each company/individual is allowed a limited number of serial tags).

Simple analysis of the cost of fuel for the selected vessels to move the estimated amounts of inbound sargassum across the distances, and at the prescribed speeds, shows the potential economic feasibility of a towline system with distributed collection for the 50km stretch of beach at Punta Cana (Supplementary Material 1). While this analysis shows potential to operate the EDS system profitably, it calls for an enormous number of artisanal boats and workers to completely protect Punta Cana. The number of boats constitutes a large fraction of the current fishing fleet in the Dominican Republic. It is hard to imagine how such a large fleet of workers and boats could be gathered and maintained, all without disrupting the already petering fishing industry. Therefore, for the purposes of comparison, a slightly altered version of EDS is described below.

2.4.1.2 Alternate Ex-Situ Distributed Sinking (EDSb) system

As illustrated in FIG 14, there are many combinations of storage devices, collection vessels, transport vessels, and sinking methods that could make up the EDS system. The collection mechanism in EDSb, capable of higher collection rates per vessel per day, resolves the issue of capital required by the artisanal boat scheme in EDSa.

Yet another option for ex-situ collection are specialized vessels. The most successful solution to the sargassum problem to date is the combined barrier and collection barge system operated by Algae Nova. The company currently protects about 500m of beach in Punta Cana, Dominican Republic. Barriers stop sargassum from making landfall and their specially designed barge keeps sargassum from accumulating outside the barrier and pushing underneath or damaging it. The barges can collect sargassum very efficiently, and Algae Nova claims a collection capacity of 700m^3 per day. Because these barges collect the sargassum into nets, this would be very appropriate for disposal using the towline sinking system already described in EDSa. This may eliminate the company's current problem of what to do with the collected sargassum: transportation to landfill is costly so sargassum is currently emptied back into the water in a less critical area of coastline. Not only does this dumping not solve the sargassum problem, it potentially causes more severe inundation for neighboring resorts downstream. This dumping activity will never be allowed on a large scale (nor would it be practical if Algae Nova hopes to acquire contracts to protect neighboring resorts). Not only is landfill disposal prohibitively expensive, but it also effects copious emissions of methane (Caribbean landfills lack landfill gas recovery).

Currently Algae Nova hopes to generate extra revenue from transforming sargassum into bioplastics, however, it could take a significant amount of time before this business could consume all the sargassum hitting the Punta Cana coast. The reliance on transformation is almost certainly limiting Algae Nova's growth. Sinking provides a cheaper and more convenient alternative to landfill disposal, which could allow companies like Algae Nova to grow much faster.

That is why EDSb comprises a system similar to EDSa, but wherein Algae Nova barges are used as the collection vessels. Because Algae Nova barges rely on barriers as part of their collection mechanism (the barges are not maneuverable enough, or stable enough, to collect in the open ocean), EDSb assumes the entirety of Punta Cana is protected by barriers. Therefore towlines in EDSb should be located as close to barriers as possible, leaving enough static depth to allow the secondary collection and disposal vessels to access them. Nets of sargassum can be transported from Algae Nova barges to towlines by lighter craft like working boats or jet skis. Algae Nova barges should be located at least every few kilometers.

In alternate systems to EDSa and EDSb, the various storage, collection, transportion, and disposal methods illustrated in FIG 14, and discussed briefly here, could be used in concert to protect the beaches at Punta Cana. The EDSa and EDSb systems are considered "minimum viable products" to accomplish SOS. The systems can be implemented quickly, on a small scale, to provide some immediate relief from sargassum invasions, and also prove the critical hypothesis that it is viable and advantageous to sink sargassum in the ocean. Once proven, EDS could evolve into a diverse set of companies, each employing different collection mechanisms and catered to by a central (perhaps municipal) secondary collection and disposal entity.

For example, over half the fished tuna in the world is caught by "purse seiners." Purse seiners use large nets up to 2000m long and up to 250m deep. An accessory boat tows the net around a large area of fish, detected using onboard sonar or radar. The net is attached to the main purse seiner, forming a closed loop in the water. Then purse strings are pulled tight as the net is hauled in. Once the fish inside are sufficiently crowded near the side of the purse seiner, they are scooped into a refrigerated hull. One could imagine doing this exact thing to collect sargassum into a purse seine net, but sink the sargassum instead of bringing the catch onto the ship. Alternatively, the large-scale option of a fishing trawler dragging a

buoyed net along the surface of the water could be used to collect sargassum into large nets. There are also many specialized vessels, in addition to Algae Nova barges, that could be used for primary collection.

In addition to the variety of primary collection and storage mechanisms that could be used in EDS, the is also the possibility of utilizing a secondary storage location. This secondary storage, likely accomplished by a large barge located at the southernmost point of the protected area at Punta Cana (closest to the suggested sink zone at 18°18'41"N, 68°20'18" W as illustrated in FIG 14), would reduce the frequency of sinking trips, concentrating the sinking efforts to only a few trips per year (depending on the size of the barge), when the barge, itself, is towed to the sink zone. This secondary collection must, of course, implement effective countermeasures against storms and other risks that threaten to release sargassum back into the environment. This barge would represent a significant investment and require constant monitoring (most likely by the secondary collection and disposal entity), which means it will likely only be implemented in the case EDS becomes the established sargassum collection mechanism in Punta Cana. It is uncommon to find barges greater than about 400ft X 100ft. While sargassum could be stacked to increase the volumetric carrying capacity, such a barge couldn't reasonably carry more than about 20,000 cubic meters of sargassum. This is less than the carrying capacity of a daisy-chain of towlines. It will take a super-barge, or another secondary storage device of similar size, capable of carrying approximately 100,000 cubic meters of sargassum, to make this extra step in the EDS system worthwhile.

2.4.1.3 In-situ Concentrated Crushing (ICC)

The first of two in-situ systems envisioned will use rolling crushers, deployed from a mobile vessel, to crush continuously crush sargassum and render it negatively buoyant (Method #2). There are three potential implementations of this mechanism: pushed, onboard, and outriggered. The pushed embodiment of this system calls for a modified tanker/landing craft's bow ramp to be outfitted with a pair of rolling crushers. The cylinders could be rigidly attached to the bow ramps, the dipping into the water and the plane formed between their axes being parallel to the bow ramp. This ramp may or may not be controlled by an active heave compensated winch such that it remains in the water even in rough seas. Alternatively, the rolling pair could be arranged perpendicular to the direction of the ship motion, floating in the water (not rigidly attached to the ship, and with a coefficient of friction and/or submerged depth and/or diameters such that the sargassum is lifted out of the water and into the contact patch of the cylinders.

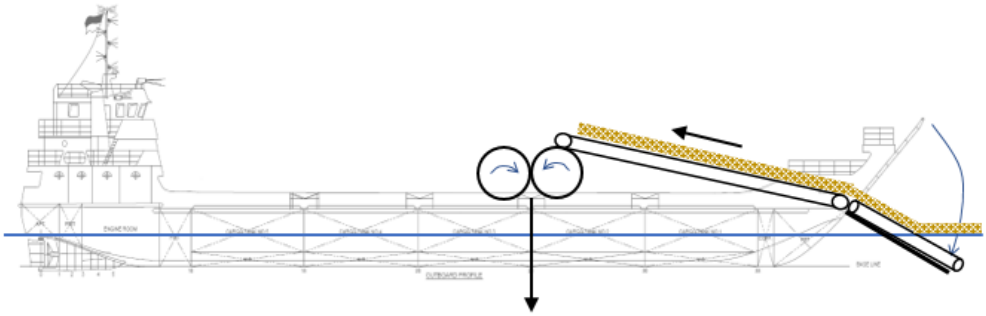

FIG 16 A crude representation of a landing craft with the following modifications: (1) a collection conveyor mounted to the bow ramp, (2) a "turtle separation" conveyor, (3) a conveyor supported on load cells for measuring throughput, (4) a rolling crusher installed on the deck, and (5) a "moon pool" cut into the hull.

The onboard implementation of rolling crushers involves placing one, or several, pair(s) of rolling crushers onboard the landing craft, which has a large deck space in front of the bridge. The bow ramp would be outfitted with a conveyor that dips into the water, lifting sargassum out of the water and depositing it into the rolling crushers. The conveyor system could also incorporate a separating section to remove turtles from the sargassum (similar to a separator used to separate chicks from their egg shells in hatcheries). Next, a conveyor supported by load cells could provide verification of the amount of sargassum collected and crushed (and this measurement can be corroborated by inline NIR optical spectroscopy). The rolling crushers used could be those already used in mineral processing facilities. After being crushed and rendered negatively buoyant by the crushers, the sargassum could be jettisoned through one or more "moon pools" cut into the hull of the ship, thereby reentering the ocean and sinking. FIG 16 roughly illustrates a landing craft with these modifications. It is recommended that the acquired vessel be "unrestricted" class, or, at least 70m in length to ensure stability at sea. Both the pushed and the onboard implementations could benefit from the use of a concentrating funnel to increase the collection width.

Another embodiment of ICC may involve outriggered rollers on the port and starboard sides of a ship, driven by outboard actuators, that are deployed in and crush sargassum in the water, without the need to remove it from the water. The implementation could be deployed on either a landing craft or supply-type ship – any vessels with enough deck space for the hydraulic arms, HPUs, repairs, and maintenance.

Regardless of the ICC implementation or the vessel used (landing craft or supply-type), it is recommended that the vessel be rented for a short time to prove out the concept for several months. Instead of moon pools, sargassum can merely exit on additional conveyors that jettison it through the gunwales of the ship. Once the ship is eventually purchased all of the modifications can be made to make it as efficient as possible.

ICC, in its various embodiments, has significant advantages over EDS:

1. The system is more flexible. It is able to operate in multiple theaters, optimizing its path to increase utilization of machines, decrease distances traveled, and ensure enough buffer to fully completely eliminate sargassum rafts before they come close to shore.
2. The system is relatively isolated, making operations immune to antagonism from external stakeholders, it requires no permanent infrastructure, and is not constrained by the availability of assets it does not wholly own or employ. It will be rare for the ship to enter any ports as if can be refueled by barges and most repairs can be done onboard.
3. The system will require less capital and it can likely be implemented faster. The marine brokerage industry is quite nimble, modifications to vessels are routine, and financing terms are flexible.
4. This system could be rapidly deployed to new areas in the Atlantic or satellite bodies of water that are suddenly hit with sargassum as a result of changing currents and boundaries of the sargassum in the Sargasso or Equatorial seas (Butler & Stoner, 1984).

A cost study, similar to that performed for EDS, was performed for ICC, wherein the assumed embodiment, for the purposes of realistic calculations, was the landing craft with conveyor, on-deck crushing, and moon pool jettison. To illustrate the potential of a carbon offset revenue model (to be discussed in a later section), hypothetical profit from the sale of carbon credits is also tabulated. FIG 17 shows the results of this analysis with example numbers.

Quantity Description	Value	Reference/Explanation
Approximate annual flux of sargassum that comes within the vicinity of Punta Cana (m^2/year)	1.3.E+08	Starting with this value calculated previously based on steady-state in CWA, rate of growth and migration.
Length of coastline at Punta Cana (km)	50	
Approximate daily flux of sargassum DURING sargassum season near Punta Cana (m^2/day)	3.5.E+05	The is the amount we need to collect to 100% eliminate… This is overestimate.
Observed daily flux of sargassum at Punta Cana DURING sargassum season (m^2/day)	350,000	Based on 60 bags a day collected by Algae Nova --> This is the value we shall use below.
Initial capital requirement of this system in Punta Cana		
Cost to acquire tankers ($/boat)	$ 2,500,000	According to various marine brokerages.
Contingency for costs related to tankers	25%	(adding moonpool, conveyors, heave compensator, turtle separator, etc.)
Number of tankers required to solve the problem for Punta Cana	1	One boat meets the collection capacity requirement to solve the problem for Punta Cana.
Total cost to acquire the tugs ($)	$ 3,125,000	This is about 1/5th the cost to cover all of Punta Cana in Algae Nova barriers.
Calculations of power requirements for all vessels during towing and transit		
Density of saltwater (kg*s^2/m^4)	104.49	at 20C according to International Towing Tank Conference
Kinematic viscosity of saltwater (m^2/s)	1.05E-06	at 20C according to International Towing Tank Conference
Length of tanker (m)	75	Ocean Marine Brokerage Services (LCT- Landing Craft 13792)
Moulded breadth of the tanker (m)	14	Ocean Marine Brokerage Services (LCT- Landing Craft 13792)
Draught of the tanker (m)	3.5	Ocean Marine Brokerage Services (LCT- Landing Craft 13792)
Deck space (m^2)	800	
Fuel capacity of tanker (gallons)	122,000	Ocean Marine Brokerage Services (LCT- Landing Craft 13792)
Average speed of the tanker (m/s)	3	
Fuel consumption at this speed (MT/day)	6	
Stern thrust capacity of the tanker (hp)	1,000	Is this per engine and are both always running?
Reynold's # for the tanker	2.13E+08	
Form factor of the tanker (used to calculate pressure resistance from skin friction)	0.7	
1. Calculated viscous resistance coefficient (friction and pressure)	0.0031	(USNA, "Resistance and Powering of Ships") and this checked against other flat-plate correlations below.
2. Calculated viscous resistance coefficient (friction and pressure)	0.0027	Check: Smooth, flat, turbulent plate… C_d=0.074/(Re_x)^0.2 (Re_L from 5e5 to 1e7)
3. Calculated viscous resistance coefficient (friction and pressure)	0.0036	Check: Rough flat, turbulent plate… C_d=(1.89-1.62*log(e/L))^-2.5 (Re_L from 5e5 to 1e7)
4. Calculated viscous resistance coefficient (friction and pressure)	0.0034	Check: Rough flat, turbulent plate… C_d=(2.635-0.618*ln(e/L))^-2.57 (e/L from 6.7e-3 to 6.7e-8)
5. Calculated viscous resistance coefficient (friction and pressure)	0.0032	Check: C_d=1.328*((R_tr)^(-0.5))*(Re_tr/Re_L)+0.523/(ln(0.06*Re_L))^2-(Re_tr/Re_L)*0.523/(ln(0.06*Re_tr))^2 (Re_tr=500,000 for smooth)
Wave-making resistance as a percentage of viscous resistance	18%	(USNA, "Resistance and Powering of Ships")
Total resistance on the tanker from viscous and wave-making resistance (kN)	26	
Net power train efficiency of large ships	24%	(USNA, "Resistance and Powering of Ships")
Contingency for added wave resistance	50%	(Tomasz Cepowski, 2016)
Power required by large towing boat during a loaded trip to sink site (hp)	653	Power produced by engine not delivered to water.
Does the selected towing vessel have enough stern thrust power?	YES	In reality I know it is enough power because this is a real ship… these numbers are VERY conservative.
Calculation of cost		
Diesel fuel cost ($/gallon)	$ 3.00	
Fuel efficiency of the boat (lbs/hp*hr)	0.6	Calculated based on the spec'd horsepower and fuel consumption of the selected tanker.
Density of diesel (lbs/gallon)	6.9	
Width of the conveyor (m)	14	Ocean Marine Brokerage Services (LCT- Landing Craft 13792)
Losses over the side of the conveyor	0%	
Fuel consumed by tanker per MT wet sargassum collected calculated from spec'd consumption (gallons/m	0.0005	Ocean Marine Brokerage Services (LCT- Landing Craft 13792)
Fuel consumed by tanker per MT wet sargassum collected calculated from spec'd power (gallons/m^2)	0.0005	Ocean Marine Brokerage Services (LCT- Landing Craft 13792)
Fuel consumed by tanker per MT wet sargassum collected calculated from power above (gallons/m^2)	0.0003	I use this higher value based on a very crued estimate of the drag coefficient.
Fuel cost per m^2 of sargassum ($/m^2) conservative	$ 0.001	
Number of operators onboard the tanker	10	Mechanics, drivers, spotters.
Hourly rate of each tug operator ($/hr)	$ 30	
Labor cost per m^2 sargassum ($/m^2)	$ 0.002	
Distance from site of operation to refueling site (km)	50	The the nearest point >1000m deep
Days to transit to and from refueling sites (days)	0.19	One-way
Total days of fuel onboard (days)	64	Workers will need to go back more often than this so perhaps that transport vessel could bring fuel?
Utilization of tankers	21%	6 months out of the year, during daylight hours, assuming time to transit for refueling…
Average size of a consolidated sargassum mat (km^2)	5	Consolidated mats can be 1km x 10km and loose slicks can be 10km x 100km
Max capacity of LCC per day (km^2/day)	1.8	Observation: We could work on one mat for several days… at nearly 100% efficiency.
Working efficiency of tankers	100%	Assuming we work on one consolidated mat all day and transit to new mats during the night…
		^^ we need to be really good about route optimization and locating sargassum…
Cost per m^2 of sargassum ($/m^2)	$ 0.005	Adding fuel and labor costs from above.
Total kilometric cost of collecting and sinking 100% of sargassum in Punta Cana ($/km/year)	$ 11,989	
Total annual cost of collecting and sinking 100% of sargassum in Punta Cana ($/year)	$ 599,433	
Number of tourists that visit Punta Cana every year	6.34E+06	(Statista, 2016)
Cost per tourist ($/person/year)	$ 0.09	Could be charged as a tax…

FIG 17: Spreadsheet wherein profitability analysis of ICC is performed. Power requirement is calculated based upon spec sheets from a selected vessel (LCT 13792). Operating profit is calculated according to the offset claims minus the cost of fuel and labor required.

Despite this promise, the primary technical challenges facing ICC are fourfold:

Bearings – Several ICC implementations call for bearings to be submerged and endure very abrasive marine conditions for long periods of time (seawater, and sargassum, itself, is extremely corrosive). While it is not at all impossible to get custom stainless steel, thin chrome layer, or otherwise coated ball bearings that will resist corrosion in seawater, there are some limitations on the performance, likely on load and speed. Ceramic bearings may offer an expensive alternative to metal bearings that could achieve higher performance while resisting corrosion. Another interesting option is the use of “seawater lubricated” bearings used to support propeller shafts on icebreaking ships in the North Atlantic. These bearings are hydrodynamic and are made from self-lubricating, elastomeric polymers (Ogle & Carter, 2015). Normally, propeller shafts are supported inside sealed, oil-lubricate sterntubes with highly engineered seals, but

these seals are particularly vulnerable to damage in abrasive waters. A last resort to bearing corrosion would be to constantly flush metal bearings with an environmentally friendly lubricant in a semi-closed system.

Misalignment – A line contact can only be made between two rigid cylinders if there is zero angular misalignment between their axes. If there is any angular misalignment in the plane formed by the axes of the cylinders, there will be edge loading, which means the loss of line contact, loss of crushing, and likely damage at the edge. If there is any angular misalignment out of the plane formed by the axes, the line contact will immediately become a point contact, again leading to loss of crushing and likely also damage to the surfaces. In ICC, it would be very hard to avoid a compromising amount angular misalignment between such large cylinders in non-isolated conditions. One obvious countermeasure may be to use soft materials at the crushing interfaces, relying on the relatively larger contact patch to be less sensitive to angular misalignment. One might also consider the use non-cylindrical rollers. The combination of a cylinder and a conical crusher, for example, yields a contact patch wider at the base of the cone and thinner at the top. Two conical crushers of inverted orientation create a contact patch that is thin in the middle and wide at the top and bottom – perhaps advantageous for countering angular misalignment out of plane. Non-cylindrical crushers, necessarily rotating on skewed axes, exhibit differential surface velocities, creating shearing action in addition to compression. While this may useful for masticating sargassum, it will almost certainly cause increased wear in the surfaces. There is a large rabbit hole of options for dealing with misalignment, which all increase the complexity of design and fabrication. These large, custom components could be extremely vulnerable to damage, and repairs would be extremely expensive.

Throughput and Power – There is little confidence in the analytical model used to predict throughput and specific energy consumption of crushing sargassum between rolling pairs of cylinders with close to zero clearance. Therefore, it is hard to design such a system without iterative testing, which may reveal throughput is a limiting factor or that specific energy consumption is higher than predicted.

Residual Buoyancy – Lastly, while it is known that rupturing close to 100% of sargassum's bladders does make the plant negatively buoyant, there may still be entrained air that can keep the plant afloat for an unknown period of time. We cannot presume that ocean mixing will remove air over time as the associative forces responsible for entrained air are quite strong (in laboratory experiments, air entrained in already ruptured bladders had to be removed by hand, bladder by bladder, leaf by leaf, before sinking was accomplished). Even if crushing causes complete annihilation of vesicles and leaves such that they cannot entrain air, discharging the remnants of sargassum onto the surface of the ocean leaves the possibility that the saragssum will be carried, by ocean currents, to undesired locations, before finally coming to rest (shallow areas with photosynthesizing plants, critical habitats, or even coastal areas).

Despite the major comparative advantages of ICC over EDS, significant design complexity is foreseen. The next solution concept provides another method for sinking saragssum in-situ, which lacks the mechanistic complexity of ICC.

2.4.1.4 In-situ Pump-to-Depth (IPD)

The third and final concept to be proposed herein is an in-situ sinking system wherein sargassum is continuously pumped to a depth below the mixed layer of the ocean and to a depth where the ambient hydrostatic pressure is sufficient to compress the sargassum and render it negatively buoyant. This system would employ powerful centrifugal slurry pumps to accomplish this. FIG 18 shows the general layout of IPD.

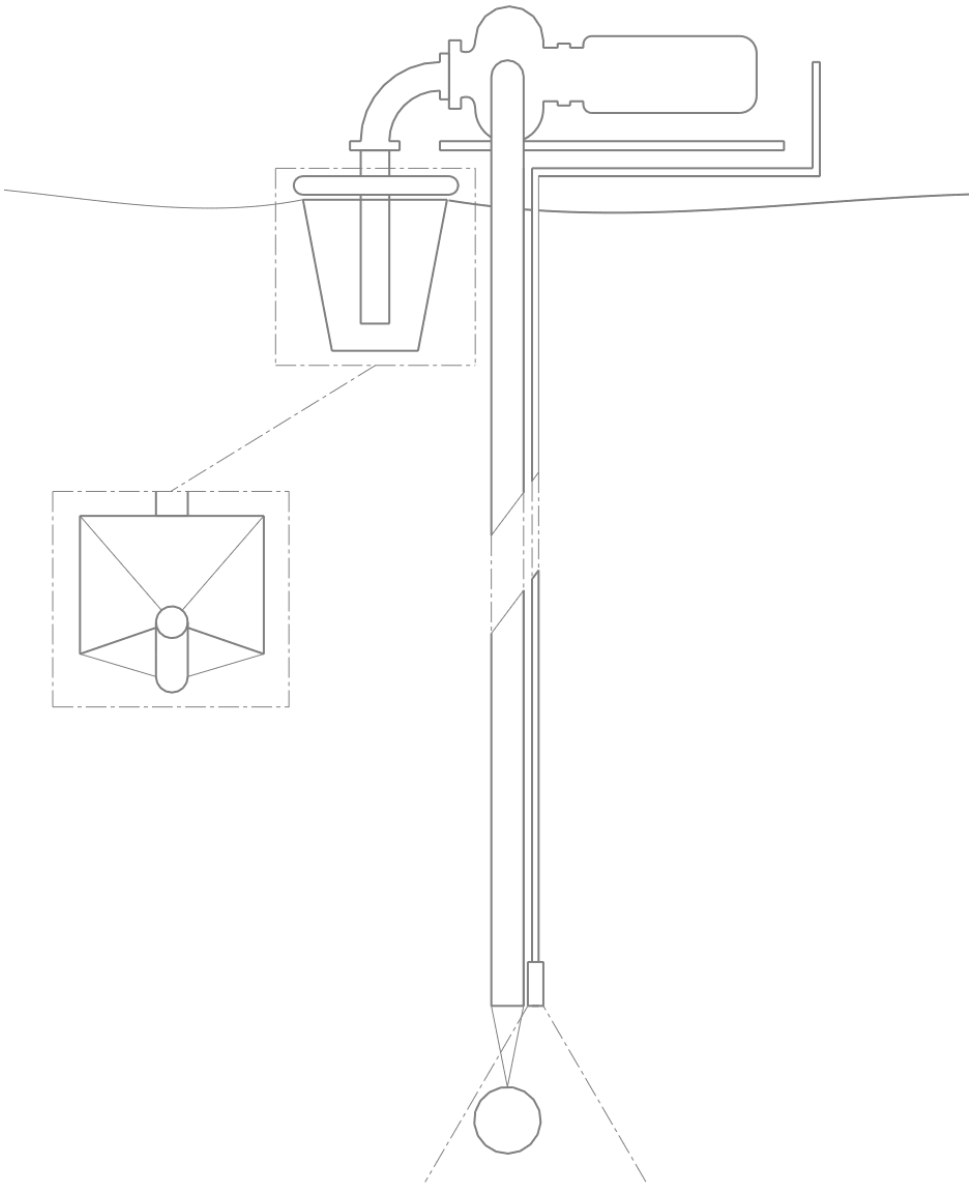

FIG 18 A depiction of an In-situ Pump-to-Depth (IPD) version of SOS, where sargassum is pumped from the surface to a depth where it escapes the mixed layer of the Caribbean and where hydrostatic pressure sufficiently compresses the sargassum such that it becomes negatively buoyant.

Johnson (1977) found that a depth of about 135m seawater is required to induce negative buoyancy in wild sargassum pulled down by Langmuir currents. The mixed layer of the Caribbean is relatively shallow, ending between 90-100m. Therefore, to goal depth in IPD is 135m.The analysis tool depicted in FIG 19 calculates the energy consumption and cost of pumping sargassum to the required depth. Low specific energy consumption and low mechanistic complexity are the main features that made IPD so attractive as a SOS system.

In-Situ Continuous Pump-to-Depth (ICPD)

Quantity	Value	Reference / Explanation
Data from prior art and PERG experiments...		
#1 Pumping depth for irreversible rupture of vesicles (m)	2500	Depth to irreversibly rupture all vesicles (based on PERG force gauge experiment --> 80N was required on 2mm diameter vesicle. Pressure required in hydrostatic suspension may differ because shearing and stress concentration effects may differ).
#2 Pumping depth for total failure of vesicles (m)	135	Depth to immediately lose buoyancy by rupturing ~100% of vesicles, large (4-7mm) and small (2-4mm) (some fraction of large may only buckle/crease and not irreversibly rupture, meaning they could recover if somehow transported to shallower depths again)... (Johnson, 1977)
#3 Pumping depth for partial failure of vesicles (m)	35	Depth at which large vesicles begin to buckle/crease, with some small amount of rupturing (perhaps small vesicles, while still intact, will also be compressed enough s.t. negative buoyancy of the entire plant is achieved).
#4 Pumping depth for round-trip loss of buoyancy (m)	500	Depth s.t. round-trip to ~10m causes negative buoyancy... assuming 5cm/s static rate of rise and time-pressure relation in (Johnson, 1977): z=102-23log(t)
Pumping depth used in calculations below (m)	135	MUST CHANGE THIS CELL DEPENDING ON STRATEGY ... 130 meters is chosen for now because there is too much uncertainty around the phenomena present at other depths...
Pressure required to rupture sargassum vesicles (Pa)	2.50E+07	Determined by PERG experiment wherein individual bladders of known dimensions were crushed between two plates and the force required to do so was measured. Surface shear and stress concentration in the deformed state may have influenced.
Maximum mixed layer depth (MLD) in the Caribbean (m)	90	Relatively shallow compared to other parts of the ocean... changes between 10m and 90m throughout the year - deeper Dec to March and shallower Sept to Nov... from data atmoshperic analysis on data 1993 to 2015 (R.A. Montoya-Sanchez, 2018)
Max expected upwell speed (m/s)	0.2	Should keep in mind that 12m/s winds can create 10cm/sec upwell/downwell speeds and this could bring sargassum back to a depth where unruptured vesicles recover buoyancy... (Johnson, 1977)
Rate-of-rise of positively buoyant sargassum (m/s)	0.05	This is average - exact speed depends on depth... (Johnson, 1977)
Sinking rate of negatively buoyant sargassum (m/s)	0.03	Once the sargassum has escaped the mixed layer, it may take one or two days for the sargassum to reach the ocean floor (Johnson, 1977).
Drag coefficient on sargassum	0.97	From a simple force balance between buoyant force, gravitational force, and drag force where the terminal velocity is observed to be 0.03 m/s (Johnson, 1977)
Net buoyant force of the saragassum per unit bulk volume (N/m^3)	24	Calculation given known average rate-of-rise in the wild and estimated drag force on a single plant of average size.
Net buoyant force of the saragassum per unit bulk volume (N/m^3)	60	Determined via PERG experiment in the DR wherein a bag of known volume was weighted until net negative buoyancy was achieved yielded 60N/m^3.
Design Parameters...		
Width of the funnels (m)	0.74	
Length of hose (m)	135	Length chosen based on the depth-strategy chosen from above...
Distance from free surface to pump inlet (m)	1	Do not want to suck in air and/or lose suction on water (NPSH is checked below).
Pump inlet diameter (m)	0.375	There may also be piping and complex entrance geometry that will call for more sophisticated loss analysis later.
Pump outlet diameter (m)	0.3	For whichever pump is currently being evaluated.
Impeller outer diameter (m)	0.584	Representative and used to calculate the pump Reynold's # below.
Volute inner diameter (m)	0.635	Representative and used to calculate the pump Reynold's # below.
Impeller speed (rpm)	1000	Representative and used to calculate the pump Reynold's # below.
Pump entrance loss coefficient, k_ent, pump	0.25	This should be set at 0.25 for a typical pump entrance.
Pump exit loss coefficient, k_ent, pump	0.25	Should be set at 0.25 for hose that is just slightly bigger than the pump outlet diameter.
Hose entrance loss coefficient, k_ent_pipe	0.55	ould be set at 0.25 for a normal pipe entrance, but 0.3 is added because of the 90 degree elbow required to direct flow down. This value could be increased of a valve or orifice is placed at the entrance (in the Strategy #4 where we attempt to crush sargassum using the pressure head in the
Hose exit loss coefficient, k_exit	1	This should be set at 1 for a normal pipe exit, but could be increased of a diffuser or orifice is placed at the end (in the Strategy #4 where we attempt to crush sargassum using the pressure head in the pump)
Volumetric flow rate, Q (m^3/s)	0.221	Prescribed by slurry velocity and hose inner diameter specified above...
Speed of sargassum slurry (m/s)	3.12	
Inner diameter of hose, D (m)	0.3	Outlet diameter of the biggest cable deployed submersible dredge pump from EDDY PUMP. "Hose" chosen because must be flexible for deployability... can be constrained with a sufficient weight hanging at its end.
Accumulation of sargassum in system due to differential velocity?	NO	sargassum, could cause a velocity differential in the vertical direction (up to 0.2 m/s), causing sargassum to accumulate where diameter increases. To prevent this, pipe/hose diameters must monotonically decrease. We are ignoring this contraint in most cases because sargassum is cor
Desired percent volume of solids of the slurry at inlet	30%	Actual volume percentage not percent bulk volume...Depends on funneling width and other equipment geometry --> this is an important design parameter and critical to test ability to control this feed characteristic to predict friction / power losses, prevent clogging.
Method # 1: Non-Settling Homogeneous Newtonian Equivalent Fluid Model		
*Usually for very fine particles (<400 micron) and very small "hindered settling velocities," fluids will exhibit homogenous or pseudohomogeneous behavior, like a single-phase fluid, with the solids and fluid moving at the same velocities, and the delivered/in-situ concentrations of solids being identical. For such fluids it is appropriate to use an equivalent fluid model using mean in-situ density and viscosity according to the concentration of the solids. However, non-settling homogeneous fluids tend to exhibit non-Newtonian behavior. The relationship between shear stress and strain rate should be elucidated. This cannot be implicitly calculated from first principles - it requires Rabinowitsch-Mooney technique wherein a tube viscometer is used to attain the rheogram ln(τ_o) vs. ln(8*V_m/D) where τ_o=(D/4)*(dP/dx). The slope of this log-log rheogram could then be transformed into a real rheogram where τ_o =τ and 8*V_m/D (the shear rate for Newtonian fluids) is "scaled up" by (3n + 1)/(4n) where n is the slope of the log-log rheogram (Wilson et al., 2006). This scale up technique require laboratory data with a tube viscometer. These instruments may not be applicable to large particles like sargassum (the homogeneous model may also not be appropriate). Without the ability to implicitly or empirically obtain the viscosity of the sargassum-seawater slurry. My intuition is that dilute sargassum slurries will exhibit Netwonian behavior with a viscosity close to that of water. More concentrated slurries may exhibit a yield stress followed by a constant viscosity. Given this Newtonian expectation (which is quite reasonable for large particles only affected by gravity and contact forces), I elect to apply the equivalent fluid model, using an averaged in-situ density and a concentration-dependent, equivalent, constant viscosity calculated using equations from Krieger and Eiler, respectively, presented in (Shook & Roco, 1991, Pages 62-63). We reasonably assume that the slurry is in the turbulent regime without taking into account that the solids may damp turbulent oscillations allow for greater velocities under laminar conditions.*		
Area consumption rate of sargassum (m^2/s)	2	
Speed of the towing/deployment vessel required (m/s)	3	This value cannot change - if more sargassum needs to be put through then the width of the funnel must be increased.
Volumetric flow rate (GPM)	3500	Pump should be operating within 10% of its BEP according to Table 5.2 (Davidson & Bertele, 2000)
Roughness of pipe, e/D	0.00002	Conservative for smooth plastic pipes of 7 microns roughness coefficient (Engineering Toolbox).
Friction factor of the pipe	0.014	While the equivalent fluid model usually excludes any solids effects on the friction factor, I use the equivalent viscosity of the fluid. It should be known that for solids concentrations lower than the "loose packed" concentration (~30%) the visocity should be assumed equal to water.
Net Positive Suction Head (NPSH), absolute (Pa)	110,239	Check: This needs to be positive (preferably with healthy margin) to prevent cavtiation and attrition of impeller and casing...
Now the head contributions are calculated in turn...		
Static head contribution from buoyancy of slurry (Pa)	8,144	Slurry is slightly less dense than seawater... otherwise it wouldn't take any energy (besides hydraulic losses) to pump... this is a significant portion of the total pressure head required (calculated below)... change in avg. density of slurry actually doesn't matter...
Velocity head contribution from pump inlet losses (Pa)	518	There may also be piping and complex entrance geometry that will call for more sophisticated loss analysis later... relatively small contribution to total head required.
Velocity head contribution from pipe inlet losses (Pa)	2,781	May be able to get the exact loss coefficient from manufacturer...
Velocity head contribution from kinetic pressure energy across pump (Pa)	(2,985)	The downstream component of this term exactly cancels the velocity head contribution of the exit losses below (unless the exit loss coefficient is a value other than 1).
Velocity head contribution from pipe friction losses (Pa)	31,582	Major portion of losses from pipe friction losses... as is to be expected...
Velocity head contribution from pipe exit losses (Pa)	5,056	Again, this exactly cancels the pressure head contribution of the kinetic pressure energy of the fluid above (unless the exit loss coefficient is a value other than 1).
Pressure head required (Pa)	45,112	$P_H = (\rho_{seawater} \times g - \rho_{slurry} \times g) \times$ (Length of Hose + Distance from Free Surface to Pump Centerline) − (Change in Kinetic Energy Across the Pump) + (Pump Entrance Losses) + (Hose Entrance Losses) + (Hose Friction Losses) + (Hose Exit Losses)
Slurry viscosity effect on head?	Negligible	Condition: (Kinematic Viscosity in cSt) < (Flow in l/s)^(0.5) * (Head in m)^(0.25) ...head should not be affected by viscosity of the solid-liquid mixture of sargassum and seawater... however, frictional effects need to be taken into account when calculating power below...
Power required to compress the slurry (kW)	8	pressures downstream from pump are > 135 m seawater, sargassum is actually fully compressed, and the pressure head contribution from buoyancy is actually negative. This cell calculates the power that is required to compress the sargassum as it goes through the pressure differential of
Pressure head required assuming compressed slurry (Pa)	65,515	This is a check: Cool to see that using the compressed density of the slurry (from above), which makes the head contribution due to buoyancy negative, and adding in the work required to impose that adiabatic compression, we get a similar pressure head requirement...
*** Pressure head is like several hundred kilograms pushing down on the control volume of sargassum inside the hose... you can get a similar number (weight required) by using the measured buoyancy per unit volume from above... good to see agreement!*		
Pump "hydraulic efficiency"	17%	Assuming the lowest reasonable starting efficiency for a centrifugal pump with Q*H^0.5=450 of 25%, and applying the recommended centrifugal slurry pump correction factors in (Davidson & Bertele, 2000, pages 116-117) Hydraulic efficiency only accounts for impeller, volute and casing
Viscosity correction factor	0.9	Viscosity not significantly different from water...
Solids pump correction factor	0.8	Re_p > 2000000 so additional pump losses (beyond secondary flow losses and local losses) are to be expected.
Slurry correction factor	1	Can ignore large discrete particels so long as the hose diameter is greater than three time the largest expected particle size (to prevent jamming) (Davidson & Bertele, 2000)... this equation only appropriate for low viscosity Newtonian fluids.
Absorbed Power (kW)	81	I am assuming a submersible electric pump with a variable speed drive for now (allows a soft start so used a lot for deepwater and difficut applications)... hydraulic submersibles have the advantage of better throttling and being somewhat safer, but you pay a lot for this ($300,000 /HPU)
Driver power rating (kW)	633	Minimum power rating of the driver according to P=(1.12+0.1/H^(0.25)+1/(Pump Efficiency))*(Energy Absorbed) I have also added a 10% margin because I plan to use a pump with integrated electric motor where the impeller may be changed at some point (Davidson & Bertele, 2000, page 15
Diesel-electric efficiency	25%	The motor is integral with no belts, gear boxes or other transmission so there is no correction for that... the last correction is just for the efficiency of the diesel generator onboard the deployment vessel (or the deck generator we may choose to install).
Fuel-energy consumed per bulk unit volume sargassum (MJ/m^3)	13	Assuming there is 3m^3 bulk volume for every 1m^3 actual volume of sargassum (yearly throughput measured in bulk volume).
Energy density of diesel (MJ/L)	40	
Cost per gallon diesel ($/gal)	$ 3.00	
Cost to sink bulk cubic meter sargassum ($/m^3)	$ 0.25	TREMELY CONSERVATIVE... normally the fluid-equivalent model doesn't use an equivalent viscosity (there is no solids-effect on the friction factor)... sometimes pseudohomogeneous fluids don't exhibit any relative density solids-effect at all... losses are that of water (Carstens & Addie, 1
Cost added by fuel consumption of deployment vessel		
Now include the costs towing and of the deployment vessel...I assume that the towed modules are solids rectangular prisms, assume the deployment vessels are much larger than required, include numerous contingencies, and assume a low fuel efficiency for the ships, the maximum amount of sargassum expected every year and the price per tourist per year is still very reasonable...		
Width of the modules (m)	0.7	
Draught of the modules (m)	2	
Length of the modules (m)	2	
Reynold's # of the towed module	2.56E+06	
Form factor of modules (to calculate pressure resistance from skin friction)	2.573056	
1. Calculated viscous resistance coefficient (friction and pressure)	1.38E-02	(USNA, "Resistance and Powering of Ships") and this checked against other flat-plate correlations below.
2. Calculated viscous resistance coefficient (friction and pressure)	1.38E-02	Check: Smooth, flat, turbulent plate... C_d=0.074/(Re_x)^0.2 (Re_L from 5e5 to 1e7)
3. Calculated viscous resistance coefficient (friction and pressure)	7.78E-03	Check: Rough flat, turbulent plate... C_d=(1.89-1.62*log(e/L))^-2.5 (Re_L from 5e5 to 1e7)
4. Calculated viscous resistance coefficient (friction and pressure)	7.23E-03	Check: Rough flat, turbulent plate... C_d=(2.635-0.618*ln(e/L))^-2.57 (e/L from 6.7e-3 to 6.7e-8)
5. Calculated viscous resistance coefficient (friction and pressure)	1.10E-02	Check: C_d=1.328*((R_tr)^(-0.5))*(Re_tr/Re_L)+0.523/(ln(0.06*Re_L))^2-(Re_tr/Re_L)*0.523/(ln(0.06*Re_tr))^2 (Re_tr=500,000 for smooth)
Wave-making resistance as a percentage of viscous resistance	18%	(USNA, "Resistance and Powering of Ships")
Total resistance on a single module from viscous and wave-making resistance	694	
Contingency for added wave resistance	50%	(Tomasz Cepowski, 2016)
Power required to tow a single module during sinking operation (hp)	4	Power produced by engine not delivered to water.
Moulded breadth of the deployment vessels (m)	14	Crowley Ocean Class Tug
Draught of the deploment vessels (m)	6.5	Crowley Ocean Class Tug
Length of the deployment vessels (m)	45	Crowley Ocean Class Tug
Reynold's # of the deployment vessels	5.75E+07	
Form factor of deployment vessels	1.8	(to calculate pressure resistance from skin friction)
1. Calculated viscous resistance coefficient (friction and pressure)	6.42E-03	(USNA, "Resistance and Powering of Ships") and this checked against other flat-plate correlations below.
2. Calculated viscous resistance coefficient (friction and pressure)	5.89E-03	Check: Smooth, flat, turbulent plate... C_d=0.074/(Re_x)^0.2 (Re_L from 5e5 to 1e7)
3. Calculated viscous resistance coefficient (friction and pressure)	6.18E-03	Check: Rough flat, turbulent plate... C_d=(1.89-1.62*log(e/L))^-2.5 (Re_L from 5e5 to 1e7)
4. Calculated viscous resistance coefficient (friction and pressure)	5.75E-03	Check: Rough flat, turbulent plate... C_d=(2.635-0.618*ln(e/L))^-2.57 (e/L from 6.7e-3 to 6.7e-8)
5. Calculated viscous resistance coefficient (friction and pressure)	6.48E-03	Check: C_d=1.328*((R_tr)^(-0.5))*(Re_tr/Re_L)+0.523/(ln(0.06*Re_L))^2-(Re_tr/Re_L)*0.523/(ln(0.06*Re_tr))^2 (Re_tr=500,000 for smooth)
Wave-making resistance as a percentage of viscous resistance	18%	(USNA, "Resistance and Powering of Ships")
Total resistance on a deployment vessel from viscous and wave-making resista	41,407	
Net power train efficiency of large ships	24%	(USNA, "Resistance and Powering of Ships")
Contingency for added wave resistance	50%	(Tomasz Cepowski, 2016)
Power required by deployment vessel during sinking operation (hp)	1,042	Power produced by engine not delivered to water.
Distance from site of operation to refueling location (km)	20	
Fuel efficiency of the deployment vessel (lbs/hp*hr)	0.4	Reasonable for an ocean-class supply boat.
Density of diesel (lbs/gallon)	6.9	
Fuel capacity of the deployment vessel (gallons)	250,000	Crowley Ocean Class Tug
Total days of fuel onboard (days)	172	
Utilization of the modules	25%	Only during tourist season and only during daylight hours...
Working efficiency of the modules	80%	Losses through the funnel/between modules...
Number of modules required to protect Punta Cana	10	Again, not necessarily the same as the number of boats...
Number of modules towed by a single boat	5	Whether, towing, deployment and remote operation, outrigging, pushing is the best concept still to be decided...
Number of boats required in Punta Cana	2	
Added cost per cubic meter sargassum from vessel fuel consumption ($/m^3)	$ 0.05	
Annnual amount of sargassum to be sunk (m^3/year)	6.41E+06	in Punta Cana (700m^3/km/day) along 50 kilometers of beach... considered a conservative estimate. This is perhaps the number with the most uncertainty - will we have to collect more than the amount that lands on shores - how well can we predict what sargassum will end up on beaches
Number of international tourists in Punta Cana every year	6.34E+06	(Euromonitor, 2016)
Cost per tourist per year ($/tourist/year)	$ 0.30	Levied as a "tourist tax" on all international flights into Punta Cana International Airport (PUJ)? Highly dependent on the amount of sargassum that is received.

FIG 19 One embodiment of an in-situ concentrated system wherein sargassum is pumped, using powerful slurry pumps, to a depth where hydrostatic pressure will render it negatively buoyant. Analysis shows this is an extremely efficient and carbon negative option for protecting Caribbean beaches from sargassum inundation.

It is not currently known what kind of flow characteristics the sargassum will exhibit when pumped. Therefore, the tool presented in FIG 19 uses several models to calculated head loss: (1) Non-Settling Homogeneous Newtonian Equivalent Fluid Model, (2) Dilute Settling Heterogeneous Model, (3) Sliding Bed Model, and (4) Plug Flow Model, each appropriate under different assumptions and operating

conditions. Until experiments reveal the regimes, and the transitions between them, the most conservative model will be used for system costing.

The IPD system could be either outriggered or towed, stationary or moving. A stationary system could comprise a system similar to a purse seine fishing method, except that a boom with a submerged curtain, instead of a siene net, is used to encircle a mat of sargassum and draw is near the main collection vessel. As sargassum is crowded near the vessel, “sump-inlets” similar to that shown in FIG 20 could be used to control solids concentration, remove entrained air, and feed slurry to pumps onboard or , which then transport the slurry to the required depth through long hoses. A supply-type vessel, or any vessel with sufficient deck space to host the required number of pumps could be used as the deployment vessel. Again, the stationary IPD system is best applied to large, consolidated mats of sargassum that tend to form in near-shore areas (10-30km).

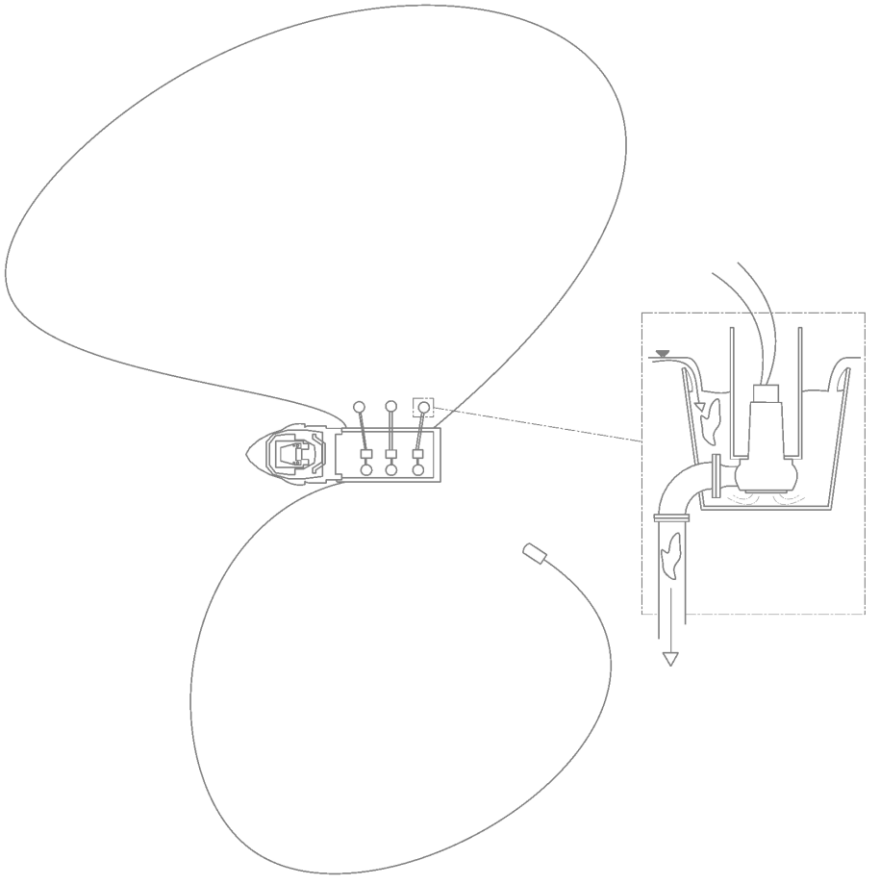

FIG 20 A stationary implementation of IPD wherein long booms are used to encircle mats of sargassum and crowd it close to a ship, similar to a purse seine fishing method. Stationary “sump-inlet” are used to control solids concentrations and remove entrained air while feeding the sargassum-seawater slurry to pumps that transport it, through a long hose, to a depth where the sargassum encounters sufficient hydrostatic pressure to render it negatively buoyant.

Long “windrows” of sargassum, formed by Langmuir cells in the open ocean, could be better managed by a moving implementation of IPD. Outriggers bearing “planing-inlets” could be used to drive through a windrow (or a consolidated mat), pushing sargassum underneath the free surface of the water, feeding the slurry to suction piping. FIG 21 shows such a system.

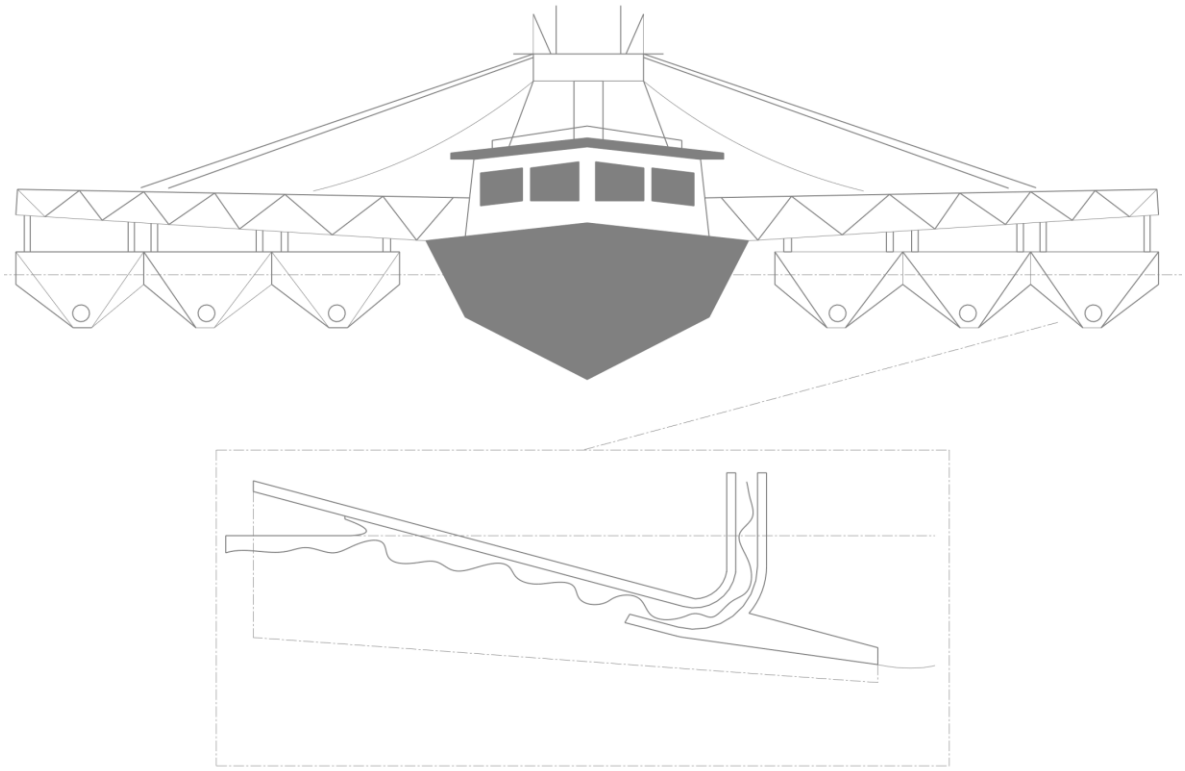

FIG 21 An example of how IPD could be implemented on a moving platform. The envisioned system calls for "planing-inlets" to be outriggered from a vessel (similar to a shrimping trawler), to concentrate and force sargassum underwater towards suction piping as the vessel moves.

Various embodiments of the "planning-inlet," so named because the hydrodynamics mimic those of a 0-degree deadrise planing hull, are depicted in FIG 22.

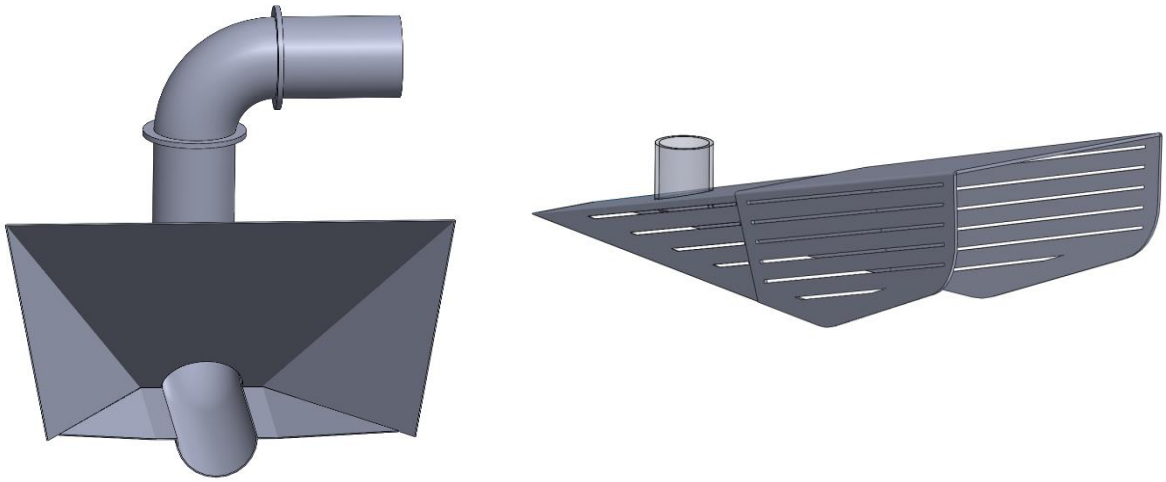

FIG 22 Embodiments of a moving "planing-inlet" use to drive sargassum underneath the free surface of the ocean, before feeding it to suction lines. (Left, a) An embodiment with the contingency of an added auger eliminated clogs in the suction piping. (Right, b) Another embodiment of the planing-inlet with various drag-reduction features.

The major design considerations for the inlet devices are: (1) controlling solids concentration, (2) meeting net positive suction head required (NPSHR), (3) avoiding clogs, and (4) low drag (in the case of the planing-inlet only).

In the stationary design, solids concentration is controlled by the location of the inlet at the surface, air entrainment is avoided by placing the suction bell at a sufficient depth, and clogging is prevented by a coarse grate. There are two methods to control the depth of the sump in the water: static and dynamic. Static depth can be maintained by simply making the sump negatively buoyant and

Flow of water over the edge of the sump is analogous to flow over a rectangular weir, which is known to follow the relationship (by application of Bernoulli):

$$Q_{weir} = \frac{2}{3} C_d b \sqrt{2g} h^{3/2}$$

Where b is the width of the weir, h is the head of water above the weir, and C_d is the "discharge coefficient" evaluated for rectangular weirs as:

$$C_d = 0.602 + 0.083 \frac{h}{P}$$

Where P is the height of the weir. Making the analogy to the cylindrical sump, $C_d = 0.602$, P→ ∞, and the flow rate over the edge of the sump is:

$$Q_{weir} = \frac{2}{3} \times (0.602) \times \pi d_1 \times \sqrt{2g} \times (0.1)^{3/2}$$

Where d_1 is the diameter of the sump and 0.1 is the desired depth of the sump relative to the free surface (to enforce a high solids concentration). Given $Q_{weir} = Q_{pump}$ by steady-state, the diameter of the sump is defined by (rearranging):

$$d_1 = 5.662 \times Q_{pump}$$

The geometry of the sump is also constrained by the necessary relations:

$$V_{sump} > Q \times (60\ seconds)$$

$\frac{Q}{A_{C,sump}} > 0.2 \equiv$ max expected rate-of-rise of buoyant sargassum

to allow sufficient reaction time in the case that flow to the sump is blocked and ensure that sargassum enters the suction piping at the bottom of the sump, respectively. Once a pump and optimal flow rate, Q, are chosen, the buoyancy of the sump can be engineered such that it will operate around a stable equilibrium with h=0.1m.

Net positive suction head is not a major concern with this design because it is assumed, in the stationary system, sump-inlets will operate close to the ship, or that pumps will be submerged inside the sump, so suction piping will not be excessively long.

In the planing-inlet, solids concentration is defined by the width of the collector, entrained air is avoided by forcing sargassum underwater (by the relative motion between the water and the planing

section of the inlet) before it encounters suction, clogging is met by the contingency of adding an auger into the suction inlet, and low drag will be achieved by optimized geometry of the planing manifold.

For the purposes of analyzing the planing-inlet, an analogy to a 0-degree deadrise hull is made. A planing plate, as pictured in FIG 23, will experience a positive dynamic distribution along its wetted area, with the maximum pressure occurring at the leading edge. Because the pressure along the wetted area of the plate is higher than for a streamline at the free surface, there is also a reduction in velocity for flow along the planing plate. As a result of the positive dynamic pressure distribution, there is a lift force generated. Due to both the dynamic pressure distribution, and viscous drag, a net drag force is also exerted on the planing plate.

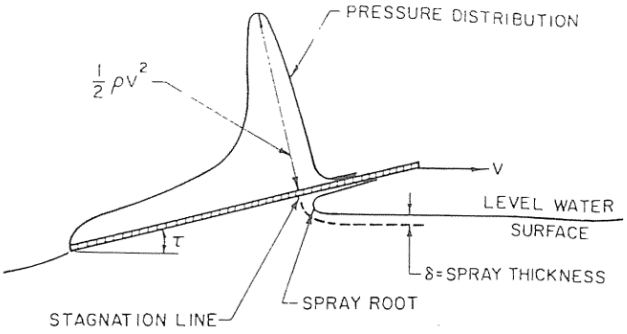

Figure 16: An illustration of planing physics relevant to the design of the "planing-inlet" design, central to the moving implantation of IPD (Savitsky, 1964).

Given the camber (degrees), τ, the beam (m), b, the depth of the trailing edge (m), d, and the forward velocity (m/s), V, of the planing body, it is possible to calculate the mean bottom velocity, the mean dynamic pressure, the lift, and the drag forces on the planing object. First of all, the wetted length of the plate, defined by the static waterline, can be calculated as:

$$\lambda_1 = \frac{d}{\sin(\tau)}$$

The actual wetted area, caused by the "spray" that can develop at the leading edge at high speeds, can be calculated as:

$$\lambda = \lambda_1 + 0.3 \quad for \quad 0 \leq \lambda_1 \leq 1$$

$$\lambda = 1.6\lambda_1 - 0.3\lambda_1^2 \quad for \quad 1 \leq \lambda_1 \leq 4$$

Evaluating the speed coefficient as $C_v = V/\sqrt{gb}$, the total dynamic lift (excluding buoyancy) can be calculated as:

$$\Delta = \frac{1}{2} C_l \rho b^2 V^2 \quad \text{where} \quad C_L = \tau^{1.11}\left(0.012\lambda^{\frac{1}{2}} + \frac{0.0055\lambda^{\frac{5}{2}}}{C_v^2}\right)$$

$$\text{for} \quad 2° \leq \tau \leq 15° \quad \text{and} \quad 0.6 \leq C_v \leq 13$$

The average dynamic pressure on the bottom wetted surface is the normal projection of the net dynamic lift onto the plane, divided by the wetted area:

$$p_d = \frac{\Delta}{\lambda b^2 \cos(\tau)}$$

The max dynamic pressure (at the leading edge of the plane) is expressed as (by Bernoulli):

$$p_{d,max} = \frac{1}{2}\rho V^2$$

The "mean bottom velocity," the mean velocity on along the wetted surface of the plane is (by Bernoulli):

$$V_m = V\sqrt{1 - \frac{2p_d}{\rho V^2}}$$

Finally, the total drag on the plate can be calculated as the sum of the pressure and viscous terms as:

$$D = \Delta \tan(\tau) + \frac{\frac{1}{2}C_f \rho V_m^2 \lambda b^2}{\cos(\tau)}$$

These relations are solely drawn from (Savitsky et al., 1964). They can be used to determine dimensions of the planing-inlet according to the primary constraint:

$$V_m \sin(\tau) > 0.2 \;\equiv \text{max expected rate-of-rise of sargassum}$$

As well as the desire to minimize drag and weight. FIG 24 shows a tool that uses these equations to optimize a small-scale planing hull shown in FIG 22.

Quantity	Value	Reference/Explanation
camber angle, t (degrees)	15	Angle between plane and free surface.
beam, b (m)	0.3	Collection width.
depth of the trailing edge, d (m)	0.3	Safe distance underwater.
lambda_1 (m)	1.16	Wetted length ignoring spray.
lambda (m)	1.46	Actual wetted length with spray.
forward velocity, v (m/s)	1.5	Boat through water.
Speed coefficient, c_v	0.87	
Lift coefficient	0.65	for 2< t < 15 and 0.6 < c_v < 13
Dynamic lift, L_d (N)	68	Not including buoyancy.
Average dynamic pressure, p_d (Pa)	533	Lift force over projected wetted area.
Average absolute pressure, p (Pa)	101533	Adding atmospheric pressure...
Average bottom velocity, v_1 (m/s)	1.10	Less that free stream velocity... Bernoulli
Max absolute pressure, p_max (Pa)	102159	At leading edge: full velocity head in plus P_atm.
Min bottom velocity, v_min (m/s)	0	At leading edge where spray forms.
Check: v_down at leading edge > 0.2	YES	Must exceed the rate-of-rise of sargassum.
Turbulent friction factor	-	(Schoenherr, 1932)
Turbulent friction factor	0.004	(Prandtl, 1927)
Drag, D (N)	18	Reasonable to hold by hand.
Pump centerline to free surface, l (m)	0.5	Suction lifting losses associated with this...
NPSHA	8.39	Must be greater than 3m head.
Using a planing hull analogy with 0-degree deadrise - all physics from (Savitsky, 1964)		

FIG 24 A tool that uses planing hull equations, assuming 0-degree deadrise angle, to analyze the dynamics of the "planing-inlet.

It should be noted that planing hull analogy does not take account for the negative dynamic pressure created as a result of suction through the pump inlet on the trailing edge of the plane. This gradient is relatively small compared to the positive gradient created by planing. Overall, the planing hull exhibits even greater NPSHA due to the initial velocity head of the fluid and the net positive dynamic pressure at the suction inlet created by planing. Therefore, as long as entrained air is avoided, NPSH is not a concern. The planing inlet design in FIG 22 features cutouts that reduce drag and allow the escape of trap air bubbles.

Prototypes of the sump-inlet and planing-inlet designs are to be tested in a small-scale experiment. These devices should provide good control of volumetric solids concentration while reducing the risk of air entrainment and cavitation. The slurry pumps, along with these inlet devices, constitute modules may be parallelized or divided up, and implemented on a variety of platforms.

The IPD system has many of the same advantages of the ICC system presented in section 2.2: the system is more flexible, it is able to operate in multiple theaters, it can optimize its path to increase utilization of machines, decrease distances traveled, and ensure enough buffer to completely eliminate sargassum rafts before they exit the sink zone. The IPD system is decoupled from stakeholders, requires no permanent infrastructure, and is not constrained by the availability of assets it does not wholly own or employ. Not only this, but IPD provides a simpler and cheaper way of sinking sargassum, avoiding the complexity inherent to ICC. The flexibility IPD affords should preclude many obstacles faced during implementation. For the purposes of concept evaluation in section 2.4.2, the moving implementation of IPD is adopted.

2.4.2 Concept Evaluation

Extensive calculations were performed to predict the performance of each system. For full detail, the reader is referred to the excel tool (Supplementary Material 1). This section will present calculations of some criteria deemed especially important to concept selection:

System scale – the size of the system, measured in number of vessels, modules, or people, that is deemed possible or necessary to stop 100% of sargassum from reaching Punta Cana, whichever is smaller.

Levelized cost (per tourist) – the annual cost of each operation amortized over all the international tourists in Punta Cana each year.

Annual carbon offset – the potential carbon offset that could be accomplished by each system, at full system scale, by sinking 100% of sargassum inbound to Punta Cana every year.

These metrics, and other heuristic observations/implications about each system will also be discussed – speed of implementation, reduction in sargassum landfall, lifecycle cost, and flexibility.

As discussed in section 2.4.1, the EDS system could be implemented with a variety of collection mechanisms. For the purposes of comparison, two different EDS systems were analyzed: (1) with artisanal fishing vessels as the sole collection vessels, and (2) with Algae Nova barges as the sole collection vessels, respectively. Both systems will benefit from the use of barriers to concentrate sargassum, which increases collection efficiency, and both systems will use towlines as the primary storage devices. These systems will be denoted EDSa (artisanal) and EDSb (barge), respectively. EDSa, EDSb, ICC, and IPD, will now be evaluated in parallel.

It should first be made clear that the amounts of sargassum making landfall in Punta Cana is not well quantified. Resort operations directors either do not keep, or are unwilling to share, receipts of sargassum pickups or other records of collection amounts. Based on the known steady-state amount of sargassum in the Central Western Atlantic (CWA, the source area) of 2000-3000 km^2 (Wang & Hu, 2015; Wang & Hu, 2016), using the known doubling rate of sargassum in phosphorous-poor water of 33 days (Lapointe, 1986), and assuming close to 50% of sargassum exiting the CWA is carried towards the Caribbean by the North Equatorial Recirculation Region (which is reasonable based on satellite imagery; Wang & Hu, 2016), the time-averaged rate of sargassum exiting the Caribbean can be readily calculated as:

$$\left(\frac{2000\ km^2}{33\ days}\right) \times \left(\frac{1000\ m}{1\ km}\right)^2 \times (0.1\ m) \times 50\% = 3.03 \times 10^6 \left[\frac{m^3}{day}\right]$$

This number may be useful for calculating net costs and carbon offsets for a hypothetical concentrated effort to stop sargassum from entering the Caribbean completely, however, it would be inappropriate to use this number to extrapolate sargassum landfall in Punta Cana, specifically. A better estimate might be rigorously obtained from NIR reflectometry analysis in the Mona Passage. Lacking the resources and continuous enough datasets to perform this analysis, we resort to making an estimate based on first-hand observation. We find that our estimate based on first-hand experience agrees well with collection publicized max collection capacity of the Algae Nova barge, which is about 700 cubic

meters per kilometer per day, or about 7000 square meters per kilometer per day. This the number that will be used for the purposes of Calculation in Punta Cana.

System scale can be calculated as the number of vessels required to collect 100% of the sargassum inbound to the Caribbean. The collection rate of artisanal vessels is estimated to be about 10 cubic meters per boat-hour. This is a reasonable amount based on a max net size of D = 2m and L = 5m that the boats can handle, and an average towing distance of 1km from collection sites to tow lines (located at least every kilometer of coast), and a normal 8-hour working day. Adopting a collection efficiency of 80% assuming only basic communication between resort and collection workers (no satellite guidance or communication to help direct resources), and recognizing that the crude process of effectively trawling with small fishing boats may prevent workers from collecting 100% of sargassum, the EDSa system scale can be calculated as:

$$\left(\frac{700\ m^3}{km-day}\right)\times\left(\frac{1\ boat-hour}{10\ m^3}\right)\times\left(\frac{1\ day}{8\ hours}\right)\times\left(\frac{1}{80\%}\right)=11\ \left[\frac{boats}{km}\right]$$

While some coastline in Punta Cana may be naturally clear of sargassum due to local geography and human infrastructure, the length of critical coastline is taken to be about 50km. Therefore, the total number of boats required by EDSa to protect all of Punta Cana is about 550 vessels, which is a significant portion of the country's total fishing fleet. Considering the challenge of furbishing and maintaining such a large fleet of vessels, for what is suggested as a short-term solution, we propose a revised system scale of 5 boats per kilometer and a total fleet of **250 boats** in Punta Cana. Because of this reduced scale, the system will likely have less efficacy, in terms of sargassum landfall reduction, compared to other SOS systems.

The advertised collection rate of Algae Nova barges is 175 cubic meters per boat-hour (based on 700 cubic meters per day and two 2-hour collection runs per kilometer per day). This agrees with first-hand observation. The collection efficiency is taken to be 100% as the barge has a wide collection width, high maneuverability, and the ability to collect very close to barriers. Rounding up, the EDSb system scale can therefore be calculated as:

$$\left(\frac{700\ m^3}{km-day}\right)\times\left(\frac{1\ boat-hour}{175\ m^3}\right)\times\left(\frac{1\ day}{8\ hours}\right)=0.5\ \left[\frac{boat}{km}\right]$$

The high collection rate and collection efficiency afforded by Algae Nova barges and barriers, respectively, suggests that one barge could handle more than one kilometer of beach. While the company currently works on a contractual, resort-by-resort basis, it could be possible to centrally locate a single barge between two areas of responsibility, but it is unrealistic to expect a single barge to protect a piece of coastline greater than 4-5km in length. The barges require significant maintenance (with 7+ hydraulically driven mechanisms, and the requirement to constantly clean corrosive sargassum out of critical mechanisms), so it is not recommended that these barges be pushed past the current 4-hour daily duty. For the purpose of comparison, the system scale of EDSb is taken to be **30 barges** to protect all of Punta Cana.

The scale of in-situ systems is relatively easier to justify. ICC, with an average speed of 3 m/s and a collection width of 14m, the projected collection rate is calculated to be 15,000 cubic meters per boat-hour. Assuming operation 8 hours per day (with ~4 hours of daylight for maintenance and repairs) and a

collection efficiency of 90% (the vessel transits at night and works on a single, concentrated mat for up to several days at a time), the system scale can be calculated as:

$$\left(\frac{700\ m^3}{km-day}\right)\times\left(\frac{1\ boat-hour}{15{,}000\ m^3}\right)\times\left(\frac{1\ day}{8\ hours}\right)\times\left(\frac{1}{90\%}\right)\times(50\ km)=0.32\ [boats]$$

While the occasional "perfect storm" of severe weather, nutrient upwelling, and conspiring ocean currents, among other phenomena, may cause an abnormal amount of sargassum to be inbound to Punta Cana, ICC's large collection rate and unrestricted seafaring ability should enable it to intercept most mats of sargassum at distances, which afford complete elimination. Therefore, **1 boat** is taken to be the expected scale of the ICC system.

IPD has several implementation concepts that deploy a different number of pumps per boat. Using an EDDY Pump 8" pump operating at the best efficiency point of 3500 GPM (or approximately 800 cubic meters per pump per hour), assuming a 30% solids concentration, a loose packed concentration of 30% (similar to natural floating solids concentration), and a 90% collection efficiency (like ICC, IPD maximizes collection efficiency by transiting at night and working on single mats of sargassum for up to days at a time), the system scale required by IPD to collect 100% of sargassum inbound to the Caribbean can be calculated as:

$$\left(\frac{700\ m^3}{km-day}\right)\times\left(\frac{1\ pump-hour}{800\ m^3}\right)\times\left(\frac{1\ day}{8\ hours}\right)\times\left(\frac{30\%\ loose}{30\%\ slurry}\right)\times\left(\frac{1}{90\%}\right)\times(50\ km)\approx 6\ [pumps]$$

If the pumping modules are to be towed in a continuous process, then all pumps could be towed by a single boat. Likewise, if pumps are to be deployed in a stationary setting (with sargassum concentrated around inlet-sumps via a method similar to purse seine fishing), all pumps could be deployed off the deck of a large supply-type ship. Lastly, if pumping modules are to be deployed as outriggered, moving collectors, then all pumps could still be deployed on the deck of a single supply-type ship, or as integrated submersible modules suspended from the outriggers. It is too soon to specify an exact deployment scheme for IPD. However, in order to maximize the utility of each pump, maximize the flexibility afforded by the modularity of the independent pumps, and minimize the overall complexity of each vessel, we might expect these pumps to be deployed on up to **3 boats**, which may or may not still work in unison under most circumstances. This number will be taken as the IPD system scale for now.

Algae Nova has been producing about 1 barge a year at a cost of approximately $400,000 (private communication). Therefore it is estimated that while EDSa may be implemented, on a meaningful scale, within a few months, EDSb may take years to fully implement. ICC and IPD, on the other hand, require relatively few pieces of infrastructure. While ICC could generate more technical challenges (no predicate technology) than IPD, delivery of and modifications to ships can happen relatively quickly - on the order of a few months. IPD, with the possibility for a simple, modular design, could also be implemented on the order of months.

Before shifting focus to cost and carbon offset calculations, it should be noted that EDSa and EDSb, in addition to collection vessels, will required tens of kilometers of barriers and regularly placed holding pens/towlines (to temporarily hold sargassum before transport to secondary storage, or to a sink zone), if implemented at the specified scales. If secondary storage is called for, then a large barge will also be required.

In terms of lifecycle costs, EDSa and EDSb exhibit the highest up front investment, requiring tens of kilometers of barriers ($100-$300/m), tens and/or hundreds of collection vessels, hundreds of people, several large towing vessels, and, perhaps, a large secondary storage barge. While artisanal vessels may have some re-sale value at the end of the system lifetime, Algae Nova barges will not. While the ICC system, depending on the implementation (towed, outriggered, pushed, onboard), may require significant modifications, the system only requires a single ship in Punta Cana. Therefore, the lifecycle cost of ICC is expected to be an order of magnitude less than that of EDSa and EDSb. IPD, with its potential modular design, will not require major modifications, and lifecycle cost is also expected to be low.

The focus of this analysis will now turn to cost calculations. Specific energy consumption (SEC; J/m^3 sargassum) and levelized cost of sinking (LCOS; $ per tourist per year) are useful for system optimization and concept selection, respectively. Being intimately related metrics, they will be calculated in parallel.

As mentioned in section 2.1, a spreadsheet tool was developed to calculate the fuel consumption for the selected vessels to move the estimated amounts of inbound sargassum across the distances, and at the speeds, prescribed by EDS. The model uses basic geometric dimensions of the selected vessels and adds contingency for head-on wave resistance and powertrain efficiency. The drag coefficients due to viscous friction and normal pressure distribution on the vessels are calculated as:

$$C_d = (1+K) \times \frac{0.075}{(\log_{10}(Re)-2)^2} \quad \text{where} \quad K \equiv \text{Form Factor} = 19 \times \left(\frac{2\times B}{L}\right)^2$$

Where Re is the Reynolds number describing the viscous and inertial characteristics of the flow around the vessel, B is the moulded breadth of the vessel, and L is the length of the vessel. Power required for each of these vessels in different modes of operation (unloaded vs. towing) is defined as:

$$P_{req} = V \times \left(\left(\frac{1}{2}\right) \times \rho \times S \times C_d \times V^2\right) \times (1+W)$$

Where V is the prescribed velocity of the vessel in that mode of operation, ρ is the destiny of the seawater, S is the wetted surface area of the vessel, and W is a contingency to account for added wave-making resistance. In both the calculation of drag coefficients and wetted surface area, the vessels are conservatively assumed to be rectangular prisms with the same moulded breadth, length, and draught as the actual vessel. The power required by the vessels and the towlines, calculated using the methods described above, are then added together in the appropriate combinations to represent different scenarios: loaded and unloaded transit for both the working boats and the larger towing vessels. Lastly, contingencies for added wave resistance (from head-waves) and efficiency of the vessels' engines are added to achieve a conservative estimate of the actual power consumed as diesel fuel by each vessel, in each mode of operation.

$$P_{actual,m} = \sum \left(V \times \left(\left(\frac{1}{2}\right) \times \rho \times S \times C_d \times V^2\right) \times (1+W) \right)_m \times \left(\frac{1+w}{\eta_{eng}}\right)$$

Where m is the mode of operation (working boat/towing vessel, loaded, unloaded), w is the added wave resistance (calculation assumes the vessels are always moving against waves), and η_{eng} is the assumed efficiency of the diesel engines.

Assuming the artisanal vessels in EDSa are 3m X 1.5m (L X W), with a 0.5m draught, the sargassum nets having D=2m and L=5m, and boats are moving at an average speed of 3 m/s during transit and 1 m/s during towing, the powers required were calculated as 35hp and 74hp for transiting and towing, respectively (not out of the realm of possibility, but clearly very conservative). Likewise, assuming the large towing vessel, with dimensions 45m X 14m (L X W), with a 6.5m draught (Crowely Ocean Class tug), moving an average speed of 3 m/s during transit and towing, and assuming 5 towlines are towed at once, each carrying 1000 nets of sargassum, the powers required are 924hp and 970hp for unloaded and loaded transit, respectively (again, taken to be quite conservative based on the known capabilities of these ships). Given that each towline has a specified number of nets with known volume, the net volumetric carrying capacity of an entire daisychain in EDSa is readily calculated as 80,000 m^3. The specific energy consumption of EDSa during one complete operational micro-cycle can be calculated as:

$$SEC_{EDSa} = \left(\frac{0.7\ lbs}{hp \times hr} \times \frac{500m}{1bag} \times \frac{5000\ bags}{1\ daisychain} \times \left(\frac{35\ hp}{3\ m/s} + \frac{74\ hp}{1\ m/s}\right) + \frac{0.6\ lbs}{hp \times hr} \times \frac{90{,}000\ m}{1\ daisychain} \times \left(\frac{924\ hp}{3\ m/s} + \frac{970\ hp}{3\ m/s}\right)\right) \times \frac{1\ hr}{3600\ s} \times \frac{1\ gallon}{6.9\ lbs} \times \frac{1\ liter}{0.264\ gallons} \times \frac{40\ MJ}{1\ liter\ diesel} \times \frac{1\ daisychain}{80{,}000\ m^3} = 14.0\ \left[\frac{MJ}{m^3}\right]$$

Where 0.7 lbs/hp-hr and 0.6 lbs/hp-hr are the fuel consumption of the artisanal boats and the large tug boats, respectively. The distances traveled by the artisanal boat and tug boats, during each round trip, are 1km and 180km respectively (sink zone is taken to be 40km southeast of Punta Cana). Assuming an hourly rate of $30 for both artisanal boat operators and tugboat operators alike, total cost per cubic meter can be calculated as:

$$LCOS_{EDSa} = \left(\left(\frac{0.7\ lbs}{hp \times hr} \times \frac{500m}{1bag} \times \frac{5000\ bags}{1\ daisychain} \times \left(\frac{35\ hp}{3\ m/s} + \frac{74\ hp}{1\ m/s}\right) + \frac{0.6\ lbs}{hp \times hr} \times \frac{90{,}000\ m}{1\ daisychain} \times \left(\frac{924\ hp}{3\ m/s} + \frac{970\ hp}{3\ m/s}\right)\right) \times \frac{1\ hr}{3600\ s} \times \frac{1\ gallon}{6.9\ lbs} \times \frac{\$3.00}{1\ gallon}\right.$$
$$\left. + \left(\frac{500m}{1bag} \times \frac{5000\ bags}{1\ daisychain} \times \left(\frac{1}{3\ m/s} + \frac{1}{1\ m/s}\right) \times \frac{1\ boat \times hr}{3600\ s} \times \frac{2\ people \times hr}{1\ boat \times hr} + \frac{90{,}000\ m}{1\ daisychain} \times \left(\frac{1}{3\ m/s} + \frac{1}{3\ m/s}\right) \times \frac{1\ boat \times hr}{3600\ s} \times \frac{5\ people \times hr}{1\ boat \times hr}\right) \times \frac{\$30.00}{1\ person \times hour}\right) \times \frac{1\ daisychain}{80{,}000\ m^3}$$
$$\times \frac{700\ m^3}{km \times day} \times 50\ km \times \frac{365\ days}{1\ year} \times \frac{1}{6.34 \times 10^6\ tourists} \approx 2.02\ \left[\frac{\$}{tourist \times year}\right]$$

Now apply the same analysis that was performed for the vessels in EDSa to the vessels in EDSb. Assuming the Algae Nova barges are 8m X 5m (L X W), with a 0.5m draught, the sargassum nets have D=1m and L=2.5m, and barges are moving at an average speed of 2 m/s regardless of the payload (no towing; sargassum is collected onboard and draught increases slightly, but negligible compared to the static power requirement of the barges), the power required by the barges is calculated to be 200hp. Assuming five towlines are pulled in every daisychain (2000 bags on each and approximately 2 cubic meters in every bag), the power requirements for the towing vessels are 924hp and 947hp during transiting and towing, respectively (towing power requirement lower than that of EDSa because Algae Nova currently uses smaller nets, decreasing the form factor of the daisychain). The net volumetric carrying capacity of an entire daisychain in EDSb is readily calculated as approximately 20,000 m^3. The specific energy consumption of EDSb during one complete operational micro-cycle can be calculated as:

$$SEC_{EDSb} = \left(\frac{0.65\ lbs}{hp \times hr} \times \frac{15\ m}{1bag} \times \frac{10{,}000\ bags}{1\ daisychain} \times \left(\frac{200\ hp}{2\ m/s}\right) + \frac{0.6\ lbs}{hp \times hr} \times \frac{90{,}000\ m}{1\ daisychain} \times \left(\frac{924\ hp}{3\ m/s} + \frac{947\ hp}{3\ m/s}\right)\right) \times \frac{1\ hr}{3600\ s} \times \frac{1\ gallon}{6.9\ lbs} \times \frac{1\ liter}{0.264\ gallons} \times \frac{40\ MJ}{1\ liter\ diesel} \times \frac{1\ daisychain}{20{,}000\ m^3} = 13.2\ \left[\frac{MJ}{m^3}\right]$$

Where 0.65 lbs/hp-hr and 0.6 lbs/hp-hr are the fuel consumption of the Algae Nova barges and the large tug boats, respectively. The distances traveled by the artisanal boat and tug boats, per round trip, are 1km and 80km respectively (sink zone is taken to be 40km southeast of Punta Cana). Assuming an hourly rate of $30 for both Algae Nova barge operators and tug boat operators alike, total cost per cubic meter can be calculated as:

$$LCOS_{EDSb} = \left(\left(\frac{0.65\ lbs}{hp \times hr} \times \frac{15\ m}{1\ bag} \times \frac{10{,}000\ bags}{1\ daisychain} \times \left(\frac{200\ hp}{2\ m/s}\right) + \frac{0.6\ lbs}{hp \times hr} \times \frac{90{,}000\ m}{1\ daisychain} \times \left(\frac{924\ hp}{3\ m/s} + \frac{947\ hp}{3\ m/s}\right)\right) \times \frac{1\ hr}{3600\ s} \times \frac{1\ gallon}{6.9\ lbs} \times \frac{\$3.00}{gallon}\right.$$
$$+ \left(\frac{15\ m}{1\ bag} \times \frac{10{,}000\ bags}{1\ daisychain} \times \left(\frac{1}{2\ m/s}\right) \times \frac{1\ barge \times hr}{3600\ s} \times \frac{5\ person \times hr}{1\ barge \times hr} + \frac{90{,}000\ m}{1\ daisychain} \times \left(\frac{1}{3\ m/s} + \frac{1}{3\ m/s}\right) \times \frac{1\ boat \times hr}{3600\ s} \times \frac{5\ person \times hr}{1\ boat \times hour}\right) \times \frac{\$30.00}{1\ person \times hr}\Bigg) \times \frac{1\ daisychain}{20{,}000\ m^3}$$
$$\times \frac{700 m^3}{km \times day} \times 50\ km \times \frac{365\ days}{1\ year} \times \frac{1}{6.34 \times 10^6\ tourists} = 1.10\ \left[\frac{\$}{tourist \times year}\right]$$

Note that if a secondary storage site is to be used to facilitate only a few mass transports to the sink zone(s) and reduce the number of trips made by individual tugs, specific energy consumption and levelized cost of EDSa and EDSb could enjoy significant reductions.

In-situ systems' specific energy consumptions and levelized costs are, again, somewhat easier to calculate because these systems are more concentrated and better defined as economic subjects. ICC calls for a large ship (collection width is intimately tied to the width of the vessel unrestricted seafaring ability implies a certain aspect ratio), whose dimensions are taken to be 75m X 14m (L X W), with a 3.5m draught (taken from and exemplary ship on a marine brokerage). The power required to move the ship at an average speed of 3 m/s is calculated to be 653hp. The specific energy consumption contribution from propulsion then:

$$SEC_{propulsion} = 653hp \times \frac{0.6\ lbs}{hp \times hr} \times \frac{1\ hr}{15{,}000 m^3} \times \frac{1\ gallon}{6.9\ lbs} \times \frac{1\ liter}{0.264\ gallons} \times \frac{40\ MJ}{1\ liter\ diesel} \approx 0.573\ \left[\frac{MJ}{m^3}\right]$$

With the experimental value of *p*=25MPa required to irreversibly rupture sargassum bladders, assuming *n* stainless steel cylindrical crusher pairs with E=200GPa, height *H*=2m, diameter *D*=1m, and active length *l*=0.5m, the power it takes to crush sargassum can be approximated as:

$$SEC_{crush} = (25 \times 10^6 Pa) \times \frac{10Hb}{l \times \eta_{bearing}\eta_{motor}\eta_{HPU}} \approx 0.849\ \left[\frac{MJ}{m^3}\right]$$

Where the contact patch width, b, can be expressed by Hertzian Line Contact theory as $p_{avg}D/\pi E$. Here, the actual value calculated is the power required to continuously elastically deform the rollers together assuming 0% efficiency. This is taken as a conservative estimate for the power required to crush sargassum in the absence of prior data on the pressure vs. %-compression relationship of sargassum (such a curve could make this analysis much more representative). Adding the SEC of crushing and propulsion, the total specific energy consumption of ICC can be calculated as:

$$SEC_{ICC} = SEC_{crush} + SEC_{propulsion} \approx 1.42\ \left[\frac{MJ}{m^3}\right]$$

Adding labor cost for 10 workers onboard the vessel, each with an hourly rate of $30, the levelized cost for ICC can be readily calculated as:

$$LOCS_{ICC} = \left(SEC_{ICC} \times \frac{1\ liter}{40\ MJ} \times \frac{0.264\ gallons}{1\ liter} \times \frac{\$3.00}{1\ gallon} + \frac{1\ boat \times hr}{15{,}000 m^3} \times \frac{10\ person \times hr}{1\ boat \times hr} \times \frac{\$30}{1\ person \times hr}\right)$$
$$\times \frac{700 m^3}{km \times day} \times 50\ km \times \frac{365\ days}{1\ year} \times \frac{1}{6.34 \times 10^6\ tourists} \approx 0.10\ \left[\frac{\$}{tourist \times year}\right]$$

In order to calculate SEC for IPD, the specific pumping power must first be evaluated. As previously mentioned, there have been four models developed to predict the pressure head in IPD: (1) Non-Settling Homogeneous Newtonian Equivalent Fluid Model, (2) Dilute Settling Heterogeneous Model, (3) Sliding Bed Model, and (4) Plug Flow Model, each appropriate under different assumptions and operating

conditions. The most conservative model is considered to be the Equivalent Fluid model, which is used to calculate the required pressure head as:

$$P_H = \left(\rho_{seawater} \times g - \rho_{slurry} \times g\right) \times (L + l) - (\Delta KE_{pump}) + (Pump\ Entrance\ Losses) + (Hose\ Entrance\ Losses) + (Hose\ Friction\ Losses) + (\text{Hose Exit Losses})$$

Assuming an EDDY Pump 8" pump at best efficiency point of 3500 GPM (800 cubic meters per pump per hour), starting with a hydraulic pump efficiency of 17%, then applying viscosity, slurry, and solids correction factors of 0.9, 1, and 0.8, respectively (according to dimensionless correlations in Davidson & Bertele, 2000), the specific energy consumption contribution from pumping is calculated as:

$$SEC_{pump} = 1.47\ \left[\frac{MJ}{m^3}\right]$$

The additional power requirement of a driver is ignored because, for now, it is assumed the system will only operate at a single, known best efficiency point, with no variable speed requirement.

Assuming the moving implementation of IPD, with 6 pump modules towed, in parallel, by a vessel with dimensions 45m X 14m (L X W), and draught 3.5m, the propulsion power of the entire system is calculated as 835hp (by the same methods described above). Therefore, the specific energy consumption contribution of propulsion power is readily calculated as:

$$SEC_{propulsion} = 835hp \times \frac{0.6\ lbs}{hp \times hr} \times \frac{1\ hr}{4{,}800\ m^3} \times \frac{1\ gallon}{6.9\ lbs} \times \frac{1\ liter}{0.264\ gallons} \times \frac{40\ MJ}{1\ liter\ diesel} \approx 2.29\ \left[\frac{MJ}{m^3}\right]$$

And the total specific energy consumption of IPD is:

$$SEC_{IPD} = SEC_{pump} + SEC_{propulsion} = 3.76\ \left[\frac{MJ}{m^3}\right]$$

Adding in labor cost for 5 workers onboard the towing vessel, with an hourly wage of $30, the levelized cost of IPD is calculated as:

$$LOCS_{IPD} = \left(SEC_{IPD} \times \frac{1\ liter}{40\ MJ} \times \frac{0.264\ gallons}{1\ liter} \times \frac{\$3.00}{1\ gallon} + \frac{1\ boat \times hr}{4{,}800 m^3} \times \frac{5\ person \times hr}{1\ boat \times hr} \times \frac{\$30}{1\ person \times hr}\right) \times \frac{700 m^3}{km \times day} \times 50\ km \times \frac{365\ days}{1\ year} \times \frac{1}{6.34 \times 10^6\ tourists} \approx 0.21\ \left[\frac{\$}{tourist \times year}\right]$$

It should be noted that all the numbers used herein are exemplary believed to be reasonable and somewhat optimized for the imagined systems. Cost calculations do not include maintenance, downtime, or overhead costs. The analysis presented here is just a small fraction of that performed in the spreadsheet tools (Supplementary Material 1).

The focus of this analysis will now turn to calculation of carbon offset for EDSa, EDSb, ICC, and IPD, respectively, as carbon sequestration and emissions reductions are an exciting and critical consequence of the SOS strategy.

Section 4.1 contains a detailed discussion on carbon offsets, the potential magnitudes in the Caribbean and Punta Cana, respectively, as well as a discussion of how this activity might subsidize, or even profit, SOS operations as a primary revenue model. Sinking sargassum generates carbon offsets in

three ways: (1) permanently sequestering the net carbon content in sargassum's biomass in the deep ocean, (2) reducing landfill input, and (3) increasing the overall biological pumping capacity of the Caribbean by allowing increased area coverage of highly productive phytoplankton in sargassum's stead. Before the offset potential of each SOS system can be calculated, the "specific carbon offset value" (SCOV) of sargassum must be calculated in terms of MTCO2 per MTWS (MT wet sargassum). Taking the mass of dry sargassum as a percentage of wet weight to be 8% (Gower, 2006), the mass of carbon as a percent of dry weight of sargassum to be 50% (Gower, 2006), and taking the mass of molecular CO2 as a multiple of the mass of constituent carbon as 3.67 (based on molar masses), the specific offset value of sargassum, due to intrinsic carbon content, can be calculated as:

$$\left(\frac{0.08\ MTDS}{1\ MTWS}\right) \times \left(\frac{0.5\ MTC}{1\ MTDS}\right) \times \left(\frac{3.67\ MTCO2}{1\ MTC}\right) = 0.147\ \left[\frac{MTCO2}{MTWS}\right]$$

Using the EPA WARM excel-based tool, using dry weight of landfill source reduced, approximating sargassum as "food waste," assuming no landfill gas recovery (LFGR; not common in Caribbean nations; World Bank Group, 2006), and an average distance to landfill of 20 miles, it can be readily calculated that sargassum represents an additional 0.404 MTCO2 per MTWS. We will ignore the specific carbon offset value contributed due to an increased biological pumping capacity of the Caribbean because it would require an unprecedented kind of U.N. clean development mechanism (CDM) methodology to be issued (exactly what impact sargassum coverage has on phytoplankton productivity is unknown). For now, the specific carbon offset value of sargassum can be calculated as:

$$0.147\ \left[\frac{MTCO2}{MTWS}\right] + 0.404\ \left[\frac{MTCO2}{MTWS}\right] = \ 0.551\ \left[\frac{MTCO2}{MTWS}\right]$$ "total specific carbon offset value" (TSCOV)

Before calculating a total offset for SOS operations in Punta Cana, the emissions of each SOS concept must be subtracted from this value. The exercise of calculating fuel consumption for each system has already been done in the course of evaulating SEC and LCOS. Taking 23lbs CO2 as the emissions content of a gallon of diesel (EIA, 2017), the "specific carbon offset penalty" (SCOP) of the consumed fuels in each SOS system can be calculated as:

$$SCOP = SEC_X \times \frac{1\ liter}{40MJ} \times \frac{0.264\ gallons}{1\ liter} \times (0.1m\ mat\ thickness) \times \left(\frac{1\ m^2\ wet}{4\ kg}\right) \times \left(\frac{1000\ kg}{1\ MTWS}\right) \times \left(\frac{23\ lbs\ CO2}{1\ gallon\ diesel}\right) \times \left(\frac{1\ kg\ CO2}{2.2\ lbs\ CO2}\right) \times \left(\frac{1\ MTCO2}{1000\ kg\ CO2}\right)$$

Where the result is in MTCO2/MTWS. The specific carbon offset values of sargassum for each SOS system are:

$$SCOV_{EDSa} = TSCOV - SCOP_{EDSa} = 0.527\left[\frac{MTCO2}{MTWS}\right]$$

$$SCOV_{EDSb} = TSCOV - SCOP_{EDSb} = 0.528\left[\frac{MTCO2}{MTWS}\right]$$

$$SCOV_{ICC} = TSCOV - SCOP_{ICC} = 0.548\left[\frac{MTCO2}{MTWS}\right]$$

$$SCOV_{IPD} = TSCOV - SCOP_{IPD} = 0.544\left[\frac{MTCO2}{MTWS}\right]$$

The assumed flux of sargassum at Punta Cana (700m^3/km/day) is equivalent to 511,000 MTWS/year (using 4000g/m^2 as wet density; Parr, 1939). Assuming this annual tonnage is completely sunk, SOS systems in Punta Cana could net an annual offset of approximately:

$$Annual\ Offset_{EDSa} \approx\ 269{,}000 \left[\frac{MTCO2}{year}\right]$$

$$Annual\ Offset_{EDSb} \approx\ 270{,}000 \left[\frac{MTCO2}{year}\right]$$

$$Annual\ Offset_{ICC} \approx 280{,}000\ \left[\frac{MTCO2}{year}\right]$$

$$Annual\ Offset_{IPD} \approx\ 278{,}000 \left[\frac{MTCO2}{year}\right]$$

The flexibility of the SOS systems can be viewed in three separate ways: (1) sensitivity to, and the resulting operating range of, system parameters, (2) ability to change implementation of the system without compromising performance, and (3) the scalability of the system.

Sensitivity analysis suggests that EDS demonstrates a high sensitivity to the speeds of the working boats and the large tugs, the cost of the nets, and the volume of each net. These systems are so large, in terms of quantities of people and machines, that any unforeseen inefficiency will have a large impact. There may be significant disturbance on the real-life EDS systems in the form of: weather, sargassum distribution and arrival rates, boat traffic, worker availability, corruption, dissatisfied external stakeholders, dissenting internal stakeholders, damage to assets, coastal environmental concerns, consumables prices, and human error.

Although the EDS system, as it is currently envisioned, suffers from high sensitivities, the system can grow organically, each resort negotiating terms with highly diverse companies each utilizing what they believe to be the most efficient collection mechanism. If this distributed collection system does take hold in Punta Cana, or in other places around the Caribbean, it will invite the ingenuity of thousands. With a reliable entity (private or municipal) to gather and dispose of the collected sargassum (using tug and towlines or another combination), the EDS system could be a sustainable, scalable model, because every stretch of coastal community has the strong incentive to keep their coastlines clear. In this way, EDS is very congruous with the current strategy of distributed collection by locals, except that it provides a way to collect and dispose of sargassum in the water, thereby avoiding the tragedy and more difficult cleanup that occurs when sargassum makes landfall.

While ICC and IPD exhibit high sensitivity to throughput and vessel speed, the small system scales, and the nature of each technology, allows superior control of these parameters. As already discussed, both systems could be implemented in a number of ways, being pushed, towed, outriggered, or onboard. This affords great flexibility in the processes of design, optimization, and perhaps even during implementation. While certain ICC designs may be tied to a specific vessel, the possibility for modularity of IPD could allow it to be deployed on a wide variety of platforms. Both ICC and IPD, because of the relatively low system capital and high portability, represent systems that could scale up to protect the entire Caribbean.

2.5 Summary and Comparison of SOS Concepts in Punta Cana

The table below will suffice to summarize the performance of each system in Punta Cana relative to important criteria.

Criteria	EDS (+ artisanal boats)	EDS (+ Algae Nova barges)	ICC	IPD
System Scale	250 boats	30 barges	1 boat	1-3 boats
Speed of Implementation	1-3 months	1-3 years	3-6 months	3-6 months
Reduction of Sargassum Landfall	~50%	~100%	~100%	~100%
TRL	Very High	High	Medium	High
Lifecycle Cost	High	Very High	High	Medium
Flexibility	Low	Low	High	Very High
Collection Rate	Low	Low	Very High	Very High
Visual Pollution	Very High	Very High	None	None
Specific Offset (MTCO2/MTWS)	0.527	0.528	0.548	0.544
Annual Offset (MTCO2)	269,000	270,000	280,000	278,000
SEC (MJ/m^3 sarg.)	14.0	13.2	1.42	3.76
LCOS from ops. ($/tourist/year)	$2.02	$1.10	$0.10	$0.21

IPD was selected as the concept deserving of developmental focus, owing to its low capital requirement, high throughput, high technological readiness, modularity, low visual pollution, negative carbon footprint, low energy consumption, low operation cost, and potential to scale into a Caribbean-wide fleet of massive capability. Not only this, but given the fact that analysis of IPD was so conservative, there is the possibility to achieve better performance than that forecast. Our active pursuit became to complete and test designs of IPD briefly shown in section 2.3.

3. In-situ Pump-to-Depth Proof-of-Concept Tests (01/18-31/2019)

Given the promise of the IPD implementation of SOS, a preliminary test was performed to validate the critical hypotheses of IPD:

(1) Sargassum will become negatively buoyant if it is transported below a critical depth of seawater. Sargassum will thus sink without being carried back up by any upwelling currents in the Caribbean.
(2) The head and power required by the In-situ Pump-to-Depth (IPD) system is consistent with the analysis already done.

For the purposes of informing subsequent full-scale design, it was also considered useful to:

(3) Identify risks such as clogging, corrosion/wear, deposition/stratification.
(4) Test inlet devices ("sump-inlet," "planing-inlet," and "chute-inlet"). Confirm designs do not pose risks to pump's Net Positive Suction Head (NPSH) due to swirling, entrained air, etc.

The successful verification of **(1)** will confirm the findings of (Johnson, 1977) and justify the fundamental principle of IPD – that sargassum at a sufficient depth will continue to sink. **(2)** will confirm the accuracy of the current sargassum-seawater flow models and the economic viability of IPD. **(3)** could identify considerations that are currently overlooked, that should receive serious attention as the detailed design stage commences. **(4)** will provide important insight as to how the sargassum needs to be "funneled" from the surface to the pump inlet.

3.1 Drop Camera Experiment (Critical Depth Identification)

To test hypothesis (1), that there exists a critical depth beyond, which sargassum becomes negatively buoyant, small sargassum specimens were lowered beneath the free surface inside an open-bottom, optically clear cylinder while a drop camera on the end of a 150m video cable tether captured video. At the critical depth, sargassum exits through the bottom of the cylinder. FIG 25 shows the open-bottomed cylinder with the affixed drop camera, video cable, and added weight.

FIG 25 Left, the open-bottomed cylinder, affixed drop camera, video cable, and added weight. Sargassum was inserted into the open-bottomed cylinder and lowered below the free surface while video was captured to identify a critical depth where buoyancy is lost and the sargassum exits the cylinder.

Several videos captured the negative buoyancy transition of sargassum at depths between 75 and 150m. FIG 26 shows sargassum at 150m seawater depth. While the sargassum experienced packing as the results of its buoyancy at the surface and because of pressure drag during descent, which prevented it from completely exiting the cylinder, the sargassum slips downward slowly over the course of about a minute after reaching the final depth.

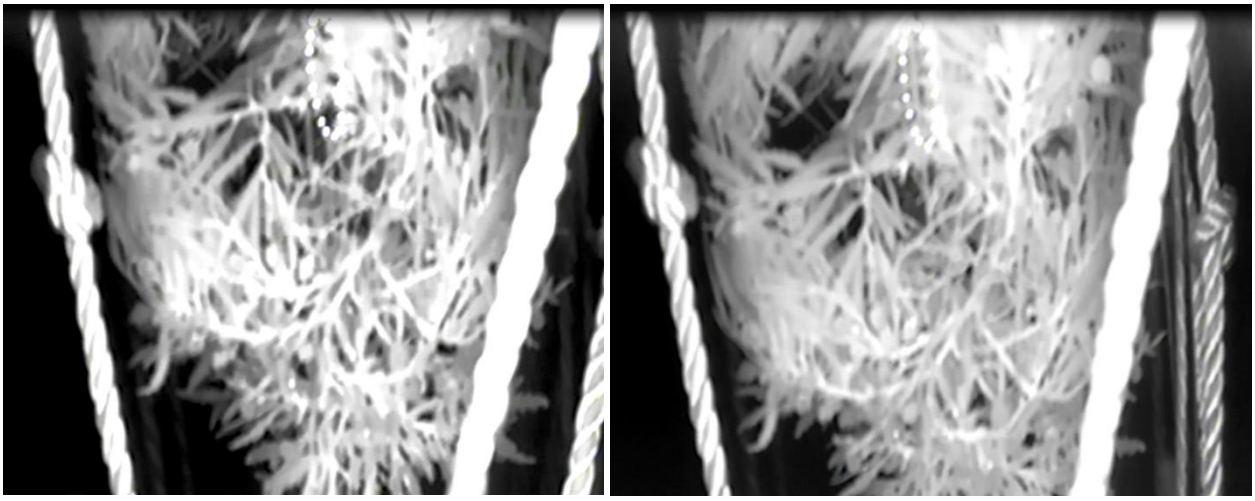

FIG 26 Left, the open-bottomed cylinder, affixed drop camera, video cable, and added weight. Sargassum was inserted into the open-bottomed cylinder and lowered below the free surface while video was captured to identify a critical depth where buoyancy is lost and the sargassum exits the cylinder.

This first drop in FIG 26 showed that there is a critical depth beyond which sargassum becomes negatively buoyant. However, because there was significant packing, the experiment was unable to identify the exact depth at which buoyancy was lost. Several other drops were performed implementing a cone and/or a smaller sample of sargassum in order to prevent upward packing and give an accurate depth reading where sargassum loses buoyancy. FIG 27 shows two of these drops at the moments when sargassum exited the cylinder.

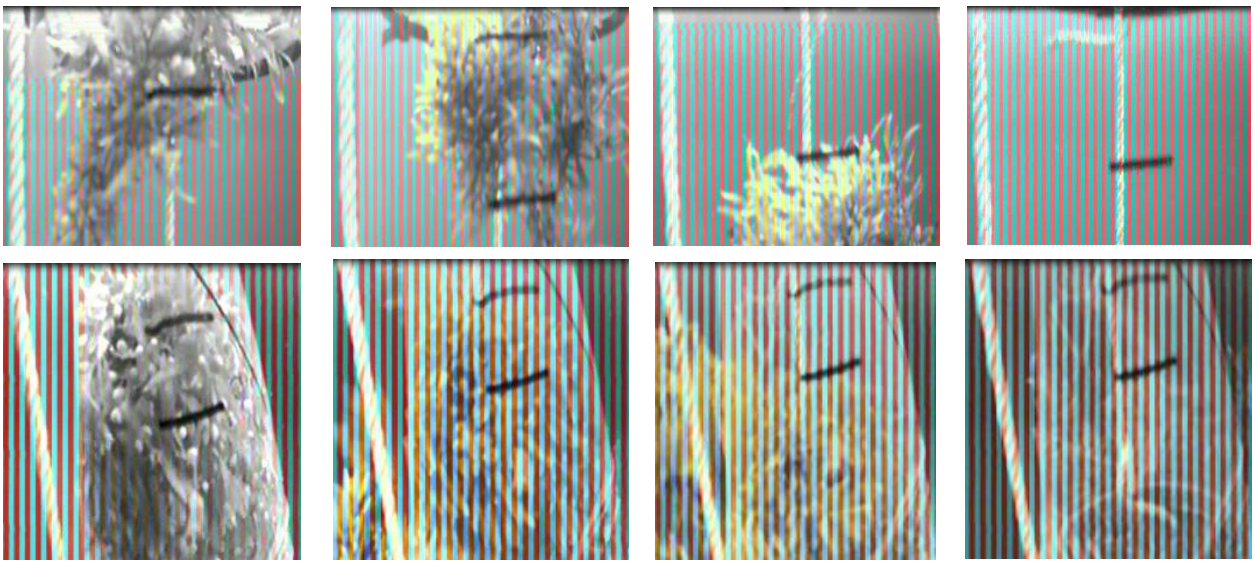

FIG 27 Two drop camera attempts wherein specific depths were identified where sargassum became negatively buoyant and exited the cylinder. (Row 1) Four consecutive frames in which sargassum lost buoyancy at 75m depth. (Row 2) Four consecutive frames in which sargassum lost buoyancy at 150m of depth. The depths at which sargassum became negatively buoyant in these experiments all fell between 75m and 150m.

These countermeasures successfully prevented packing and lead to several consective drops where all sargassum simultaneously exited the cylinder at identifiable depths. These critical depths fell in the range between 75m and 150m (the maximum length of the video cable). This range may have manifested as a result of the time pressure relationship of sargassum's loss of buoyancy, predicted by (Johnson, 1977).

$$z_{critical} = 102 - 23\log(t) \qquad [m]$$

Because of this expected time-pressure relationship governing sargassum's loss of buoyancy at depth, in seawater, we will assume a conservative goal-depth of 200m for the purposes of evolving economic models for IPD, and may even make provisions to pump to 250m during full-scale prototype demonstrations. This decision is corroborated by our knowledge, from PERG laboratory experiments, that the maximum pressure the vesicles can withstand before permanently rupturing is about 25MPa. The full-scale IPD test will use either a drop camera or an ROV to verify that this depth is sufficient to ensure sinking.

3.2 Pump-to-Depth and Inlet Device Tests

The first of two pumping experiments endeavored to pump sargassum from the surface to depth, through a 180m hose. By showing that this could be done using a small pump and narrow hose, we showed that the pressure head and power requirement of pumping high concentrations of sargassum is economically viable. This experiment also showed that there is no exceptional risk of clogging presented by sargassum. We are especially indebted to the Dominican Republic Navy for allowing us to use the patrol ship GC-108 Capella docked the Cap Cana Marina as the platform for this experiment. FIG 28 shows the Dominican Navy vessel used to perform this test, along with the pump, inlet device, hose, and portable generator. The following discussion will address the design and results of this experiment.

FIG 28 The Dominican Navy patrol-ship GC-108 Capella, docked at Cap Cana Marina, being loaded with pump, inlet device, hose, and portable generator prior to departure. We are especially grateful to Lieutenant T/N Ronaldo Osovia Fernandez ARD and his crew for their outpouring of support.

For ease of implementation and availability in the Dominican Republic, a small electric submersible pump was rented, knowing that the performance of this pump is far lower than that which could be achieved by a much larger pump (ie. performance will only get better with increasing pump size). The rented pump was a Sulzer ABS Scavenger EJ 100D4MS. The pump was sized based on the system loss curve generated by the conservative equivalent-fluid model. The approximate operating point of **380 GPM and 45 ft head** is identified in FIG 29, below.

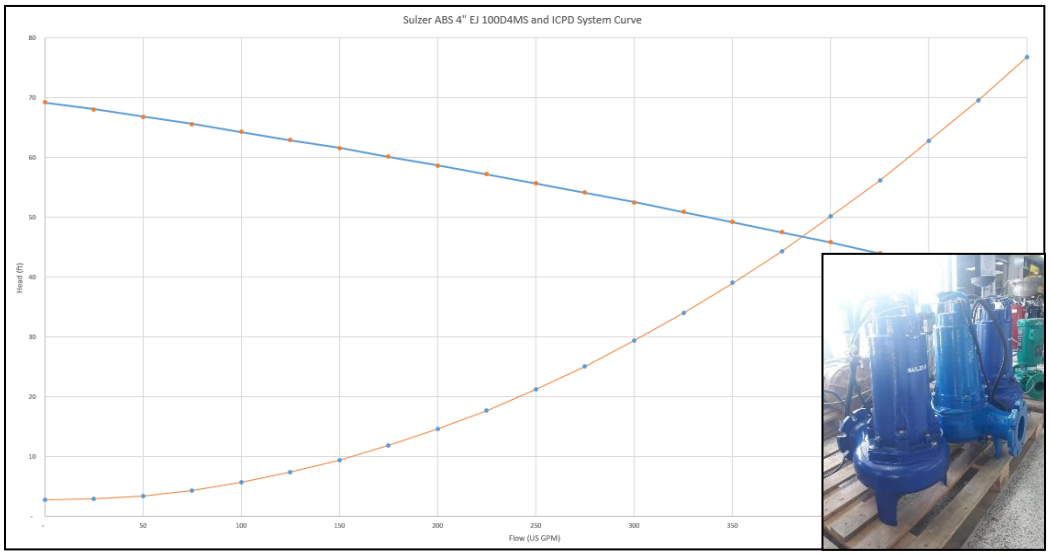

FIG 29 The system head loss curve and rental pump Q-H curve. The shown operating point (380 GPM) was also been confirmed by Dalsan rentals in SDQ.

The open ocean pumping experiment utilized the stationary sump-inlet as a means of feeding sargassum into the submersible pump. In this particular case, the pump was place directly inside of the sump mimicking the typical wet-pit installation of dewatering pumps. The sump-inlet controls solids concentration by enforcing that only fluid near the free surface (where sargassum is floating) is able to enter the pump. The sump-inlet therefore ensures a high, but controllable, solids concentration, such that water is not unnecessarily pumped, ensuring specific energy consumption is low (J/m^3 sargassum). The flow of fluid over the edge of the sump is similar to flow over a rectangular weir. The geometry of the prototype sump was defined by the constraint:

$$\frac{Q}{A_{sump}} = \frac{Q}{\pi\frac{d^2}{4} - \frac{\pi d_{motor}^2}{4}} > 0.2\ \left[\frac{m}{s}\right] \equiv \text{Max rate-of-rise of sargassum}$$

Where $d_{motor} = 0.3m$. This constraint ensures sargassum flows to the bottom of the sump and doesn't accumulate in the sump at the surface. The diameter of the sump is therefore chosen to be:

$$D_{sump,max} \approx 0.5m \approx 19.5"$$

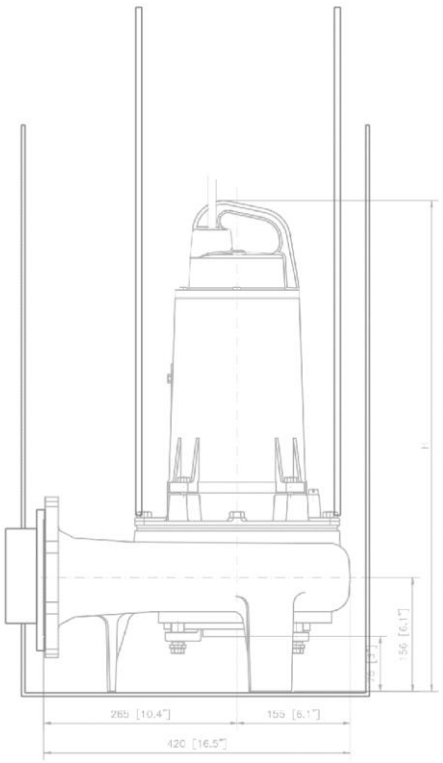

FIG 30 Sump-inlet device, wherein the Sulzer submersible pump sits. Seawater and sargassum flows into the device from the top.

To give sufficient reaction time in the case that the sump-inlet is blocked and the water level inside the sump decreases rapidly (the Sulzer pump cannot tolerate running dry), the height of the sump was therefore evaluated as:

$$H \times \frac{\pi d^2}{4} \geq Q \times 3 \ \ seconds$$

$$H = 0.762m \approx 30"$$

Given these desired dimensions, McMaster-Carr 3678K14 was used to provide the structure of the sump (shown in FIG 30). Discharge from the pump immediately exited the sump through a hole cut near its base (and packed on the periphery of the exit piping) and entered the vertical hose. Whereas the final design of the sump-inlet calls for passive control of the sump at a specified distance below the free surface, the height of the prototype sump was controlled by hand through short tethers as shown in FIG 31. Also shown in FIG 31 is the vinyl, lay-flat hose deployed from the starboard side of the boat, weighted at its end to keep the hose stable in the vertical configuration, and held open by a rolled piece of sheet metal.

FIG 31 (Left) The sump-inlet prototype, wherein the slurry pump sits. Seawater and sargassum flows into the device from the top and exits through the hose in the base (already deployed over the starboard side of the boat). (Right) During open ocean pumping experiments, the sump-inlet prototype was suspended between a Dominican Republic Navy ship and a small artisanal boat, its depth in the water being controlled by hand, through short tethers.

Aboard the GC-108 Capella, we motored approximately 4km from the coast, to reach a depth of approximately 250m. A trailing artisanal boat operated by Carlos Manuel Perdarma Costillo and his crew, was filled with sargassum before entering the surf. After deploying the hose and the pump/sump-inlet prototype in the water between the Capella's starboard side and the artisanal boat, we pumped the entire boatload of sargassum down to the benthos over the course of approximately 5 minutes. FIG 32 shows sargassum entering the sump-inlet during these experiments.

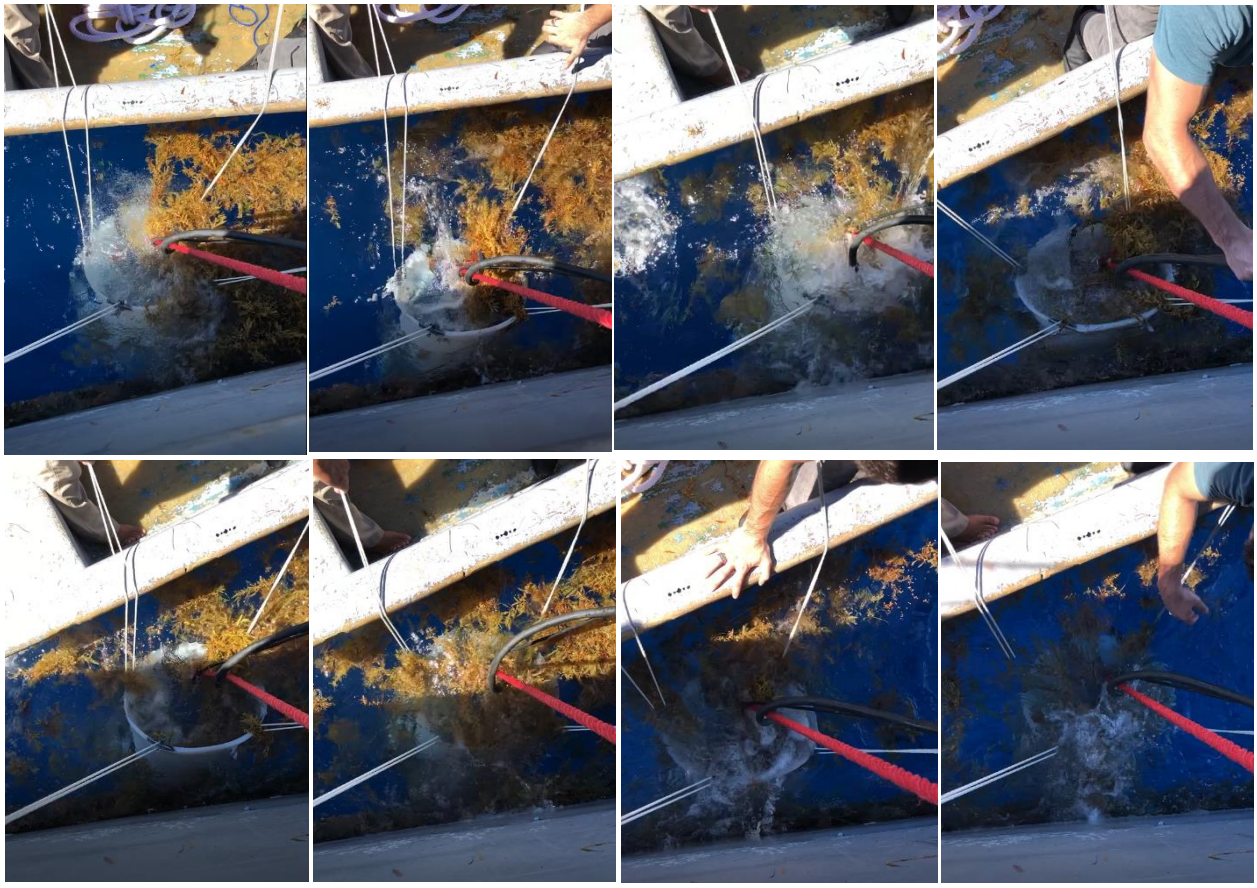

FIG 32 Consecutive photos taken during the open ocean pumping experiments during the span of 30 seconds. Approximately 2 cubic meters of sargassum was pumped in total.

Near the end of the pumping experiment, a clog developed at the exit of the hose (at 180m). This became evident upon hauling the hose back aboard the GC-108 Capella. The clog developed due to the fixturing at the end of the hose and because the weight was secured too close to the hose's exit. However, this clog, shown in FIG 33, conveniently serves as evidence that sargassum was transported the entire distance. While dewatering the hose after the completion of the open ocean pumping experiment, there were no additional clogs found.

FIG 33 The severed end of the hose used during the open ocean pumping experiments. A clog developed at the terminus of the hose, at the end of the pumping experiment, due to the concentrated fixturing, as well as the proximity of the affixed weight, at the end of the hose. There were no other clogs along the entire length of the hose.

Having shown that pumping sargassum, at high concentration, to the prescribed depth was technically and economically feasible, the final experiment aimed to test the performance of the two main inlet designs discussed in section 2.3: (1) the stationary “sump-inlet” and (2) the moving “chute-inlet.” In order to observe the dynamics of these two devices in a relatively controlled environment, we chose to perform this experiment in the back of the Cap Cana Marina.

FIG 34 The combined sump-inlet/chute-inlet prototype being deployed in the back of the Marina at Cap Cana. This device allowed the observation of both the stationary sump-inlet and the moving chute-inlet dynamics with the same wet-pit pump installation inside the sump.

A combined prototype was constructed that could demonstrate both the concept of the stationary sump-inlet and the moving chute-inlet. This prototype is shown in FIG 34 as it is being deployed. With the pump located inside of the sump and discharge exiting through the bottom thereof, similar to the open ocean pumping experiment, sargassum can flow into the top of the sump, demonstrating the principal of the stationary sump-inlet. A second pipe entering the sump near the surface is fed by a chute constructed out of plywood. When pumping commences and the water level in the sump is below this second inlet to the sump, sargassum and seawater from the chute will enter the sump at a constant rate of approximately 150 GPM, as prescribed by the geometry of the inlet piping (there was no way to exert direct suction in the chute-inlet as the submersible pump had no provisions for securing suction piping). The moving chute-inlet was pulled, by hand, long the marina wall as sargassum was thrown into its path. A hose of only about 10m in length was used on the discharge side of the pump. Constrictions and a diffuser were

imposed on the hose to ensure an operating point similar to that in the open ocean pumping experiment (and within the healthy operating range of the Sulzer pump).

The stationary sump-inlet demonstrated excellent dynamics. Despite the wooden obstructions around the top of the sump, sargassum readily flowed into the sump from a distance of approximately 1.5D away from the central axis of the sump. FIG 35 shows the sump-inlet operating in the Cap Cana Marina. In the optimized design, passive control of the sump near the surface of the water, increased sump size, and a smoother weir shape, will all contribute to higher flowrates and more consistent solids concentrations.

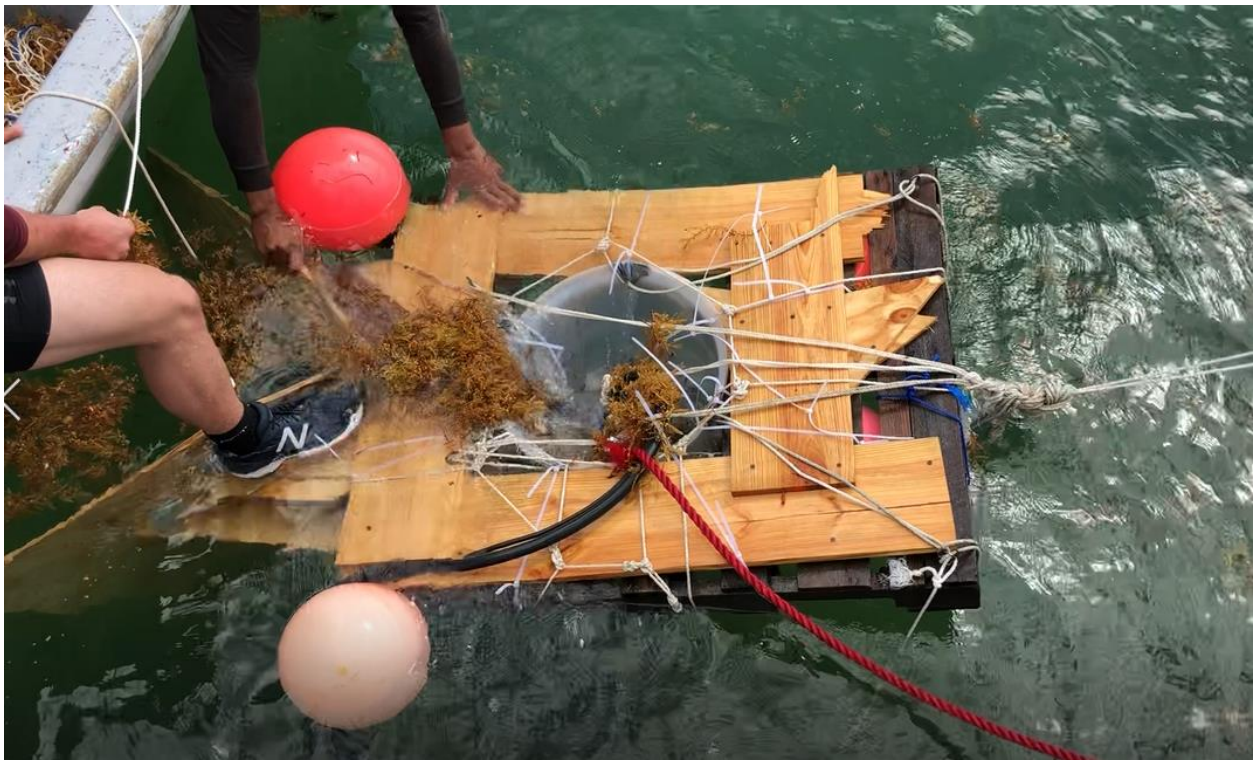

FIG 35 Video captured of the stationary "sump-inlet" in the calm waters at the back of the Cap Cana Marina. Similar to the open ocean pumping experiment, the depth of the weir below the free surface of the water was controlled manually. This inlet device performed as expected, ensuring a high volumetric flow with high solids concentration of sargassum.

The moving chute-inlet, while not as well-implemented, showed promising performance as well. Because of the difference between the constant inlet and outlet volumetric flow rates, the sump was at risk of running dry, so the moving chute-inlet experiments could only last about 2-3 seconds before the sump needed to be re-submerged. As a result of the small pressure gradient (merely due to the small ~0.1m static head present) acting across the 2ft inlet tube, the chute-inlet exerted relatively little pull on sargassum, it was difficult to "mow" large amount of sargassum as intended, and eventually a clog formed when the chute-inlet was fed too much sargassum, as shown in FIG 36. In the future, an auger will be added for automatic clog relief in the chute-inlet.

FIG 36 (Left) Video captured of the moving "chute-inlet" in the calm waters at the back of the Cap Cana Marina. The chute-inlet was pulled along the marina wall as sargassum was thrown into its path. (Right) A clog that developed at the inlet piping due to the low suction exerted. This risk will be remedied with an auger in the future.

While the stationary sump-inlet proved to be a more effective way of feeding sargassum into the pump at the current scale, both the stationary sump-inlet and the moving chute-inlet will be designed for implementation in a full-scale test.

The drop camera experiments proved critical hypothesis (1), and the open ocean pumping experiments proved (2). Open ocean pumping experiments also shed light on objective (3) and inlet device tests accomplished objective (4) shedding light on the risks to be addressed in ongoing design. Overall these field tests confirmed the economic and technical viability of IPD, justifying further design and full-scale tests, as well as working more closely with Caribbean governments to grant permits and develop preliminary implementation models.

Once full-scale designs are prototyped, and full-scale testing commences, it may also be useful to:

(5) Measure the friction factors and/or identify the flow regime of the live sargassum from the surface of the sea as it is pumped down at different rates and solids concentrations.
(6) Identify the dynamics of loss of buoyancy by underwater video of sargassum vesicles (bladders) as they reach the different release depths.

(5) will allow us to improve the accuracy of current sargassum-seawater flow models and predict design points in the full-scale system. The conditions leading to certain advantageous flow regimes could even become design goals. **(6)** will not only confirm the findings of (Johnson, 1977), further clarifying the exact mechanisms by which sargassum loses buoyancy in the wild, but it will also inform us whether or not loss of buoyancy in IPD is permanent. If loss of buoyancy is not permanent, attention must be paid to the depth of the mixed layer of the ocean where IPD is implemented to ensure that ocean currents cannot carry sargassum back up to a depth where it regains buoyancy.

The outpouring of support that we received from locals during these field tests in the Dominican Republic (01/2019) was absolutely humbly. We would like to specially acknowledge:

Silvano Suazo, Director of Marina at Cap Cana

Jose Luis, Manager of Marina at Cap Cana

Carlos Manuel Perdomo Castillo

Daniel Duarte Sanchez

Jose Luis Jimenez Almonte

T/N Reinaldo Osoria Fernandez ARD

SGT Juan Hose Lopez Vargas

T/C Rafael Augusto Herra Cordero ARD

MRO Porfirio Elias Nova Bello

MRO Jeyer Jose Ramirez Hernandez

MRO Oliver Melendes Pineda

4. System Concepts

Having shown a proof-of-concept of the pump-to-depth process and identified the critical depth to which sargassum must be pumped, concepts for the actual at-scale SOS systems were detailed. The SOS system concepts were still bifurcated fundamentally by the “in-situ” and “ex-situ” descriptors.

4.1 Nearshore Collection + SOS Carbon Pump-to-Depth Barge (“Ex-Situ”)

Phase 1 (near shore artisanal collection + SOS pump-to-depth barge disposal): Near shore collection of sargassum along beaches and barriers using artisanal vessels & nets and disposal via pumping-to-depth in the ocean from a sea-going hopper barge (FIG 37).

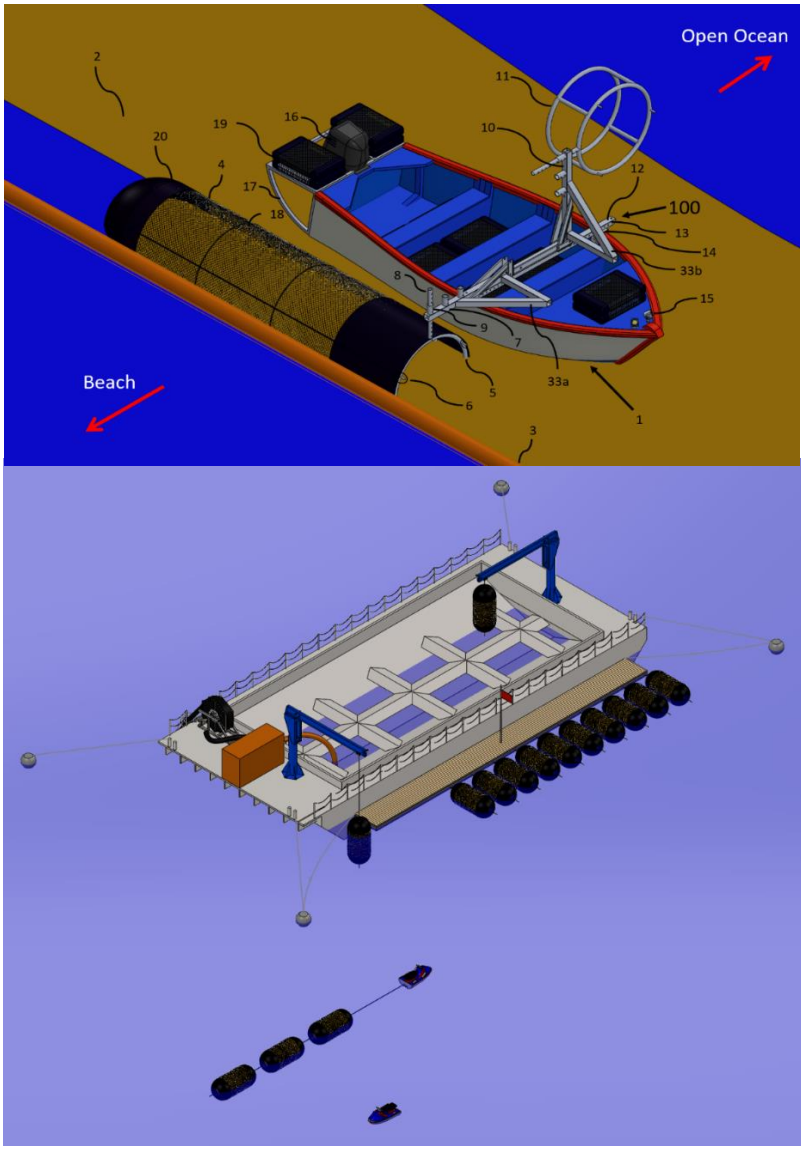

FIG 37 (Top) Artisanal sargassum collection vessel outfitted with hardware for deploying nets. (Bottom) SOS pump-to-depth barge moored offshore from beaches where sargassum collection is happening. Jet skis shuttle nets of sargassum. The SOS barge is towed out periodically for pumping-to-depth.

4.2 Offshore SOS Carbon Pump-to-Depth Vessel ("In-Situ")

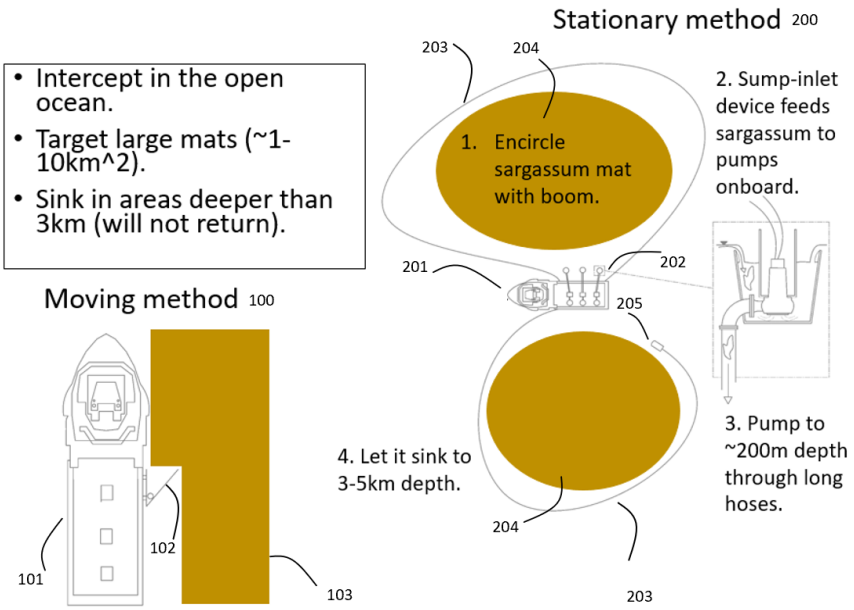

FIG 38 Two methods for using booms to gather sargassum mats towards SOS Carbon pump suction inlet devices.

4.2.1 Moving Method

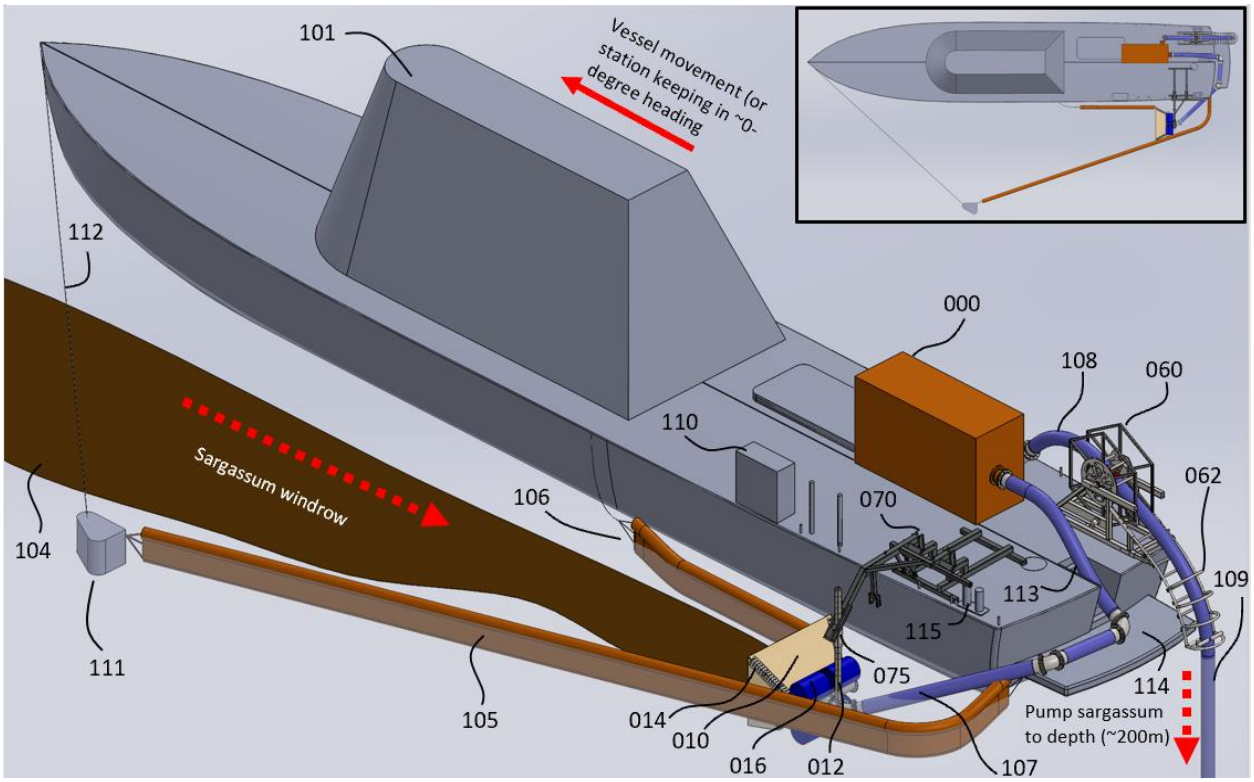

FIG 39 A 5000GPM pilot-scale version of the open-ocean, in-situ SOS pump-to-depth vessel that was designed, built, and tested. A future fleet would comprise vessels with up to 50,000GPM pumping capacity (multiple pumping systems in parallel).

4.2.2 Stationary Method

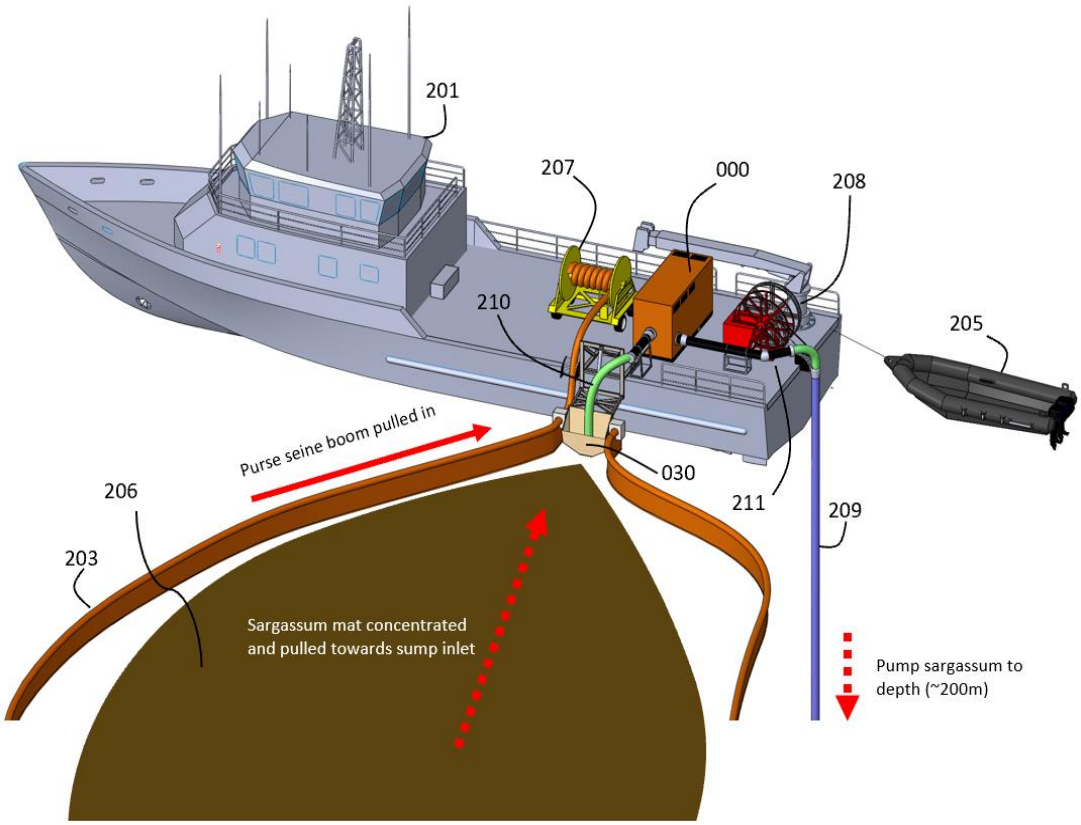

FIG 40 A pilot-scale SOS Carbon vessel, stationary while using a long boom in a "purse seine" fashion.

4.3 System Concept Summary

- Artisanal boat collection:
    - **Lower-cost** - fixed & variable; compared to specialized conveyor machinery with high capex and cost-of-ownership/operation.
    - **Rapid/cheap scale up/down** - compared to specialized conveyor machinery with fixed capacities, relative immobility, costs everyday (even when no sargassum), and months of build-time.
    - **Less visual/noise pollution** - these vessels (fishing boats & water taxis) are already part of the local scenery; compared to large, noisy, specialized conveyor machinery that draws much attention.
    - **Higher-capacity** - operation all day compared to specialized conveyor machinery only taken out periodically throughout the day (because cumbersome, maintenance-intensive, and noisy/visually unpleasant).
    - **Higher degree of cleanliness** - it is prohibitively expensive for specialized conveyor machinery to operate when only small amounts of sargassum present and it is impossible to clean immediately next to barriers/beaches with such large, hard-to-

maneuver machines. Therefore, barriers always have accumulated sargassum, which rots, smells, dyes water brown, bio-fouls barriers, and dissolves into particulate that passes through barrier mesh and lands on beaches. Artisanal vessels can operate continuously and the marginal cost of collection stays relatively low even for small sargassum influx. Therefore, with high-quality, aptly installed barriers and high rate of artisanal vessel collection, it is possible for beaches to be ~100% clean - even "cleaner than before" sargassum blooms started (something no one has believed possible until now).

- SOS pump-to-depth barge (alternative to landfill/open-pit dumping)
    - **Less visual/noise pollution** - sargassum taken away and disposed via water rather than carried through resort areas, trucked through tourist streets, and dumped in landfill within resort areas (current practice).
    - **Lower-cost** - up to 4X cheaper than landfill (assuming $50/wet tonne dumping fee, HOWEVER, Punta Cana hotels dump in ***open pits*** within resort areas for FREE).
    - **No methanogenesis** - potential additional revenue stream with sale of carbon offsets and a low-cost alternative for fighting "flight shame" (by offering SOS carbon offsets to tourists, through airlines and trip planners).
    - **No health/public relations threat** - no hydrogen sulfide ("rotten egg smell") and no toxic leaching into groundwater (sargassum arsenic levels found to be ~125mg/kg, >500x more concentrated than in seawater).[1]

- Phase 2 (open-ocean in-situ SOS pump-to-depth vessels):
    - **Out-of-sight** - no visual/noise pollution from barriers or onshore collection machinery (as if sargassum was never a problem).
    - **Smaller system scale** - more lead time (compared to onshore measures) means large swathes of coast are protected by a small # of SOS vessels.
    - **Low-cost** - so long as critical # of resorts buy in, this is potentially the lowest variable cost achievable by any system. The cost of emergency response services could also be shared by multiple small island nations, or long stretches of civilian coastline.
    - **Non-permanent** - pumps/ships have high resale value (could even be rented seasonally), unlike onshore barriers/specialized machinery.
    - **Mobile** - protects large swathe of coast and can be redeployed (should sargassum migrate to different locations around world).
    - **Sustainable, long-term solution** - longer lifetime (>10 years) than barriers for similar capital investment (barriers replaced every 2-3 years).

Both of these systems had tremendous promise for reducing costs, visual pollution, and providing a sustainable, long-term solution. However, it was recognized that offshore in-situ SOS Carbon pump-to-depth vessels possessed higher risk because it requires (1) real-time satellite identification, drift calculation, & navigation of/to sargassum mats in the wild, and (2) pump-collection in the high seas (whereas the pump inlet and sargassum in the SOS Carbon pump-to-depth barge share a common inertial reference frame – likely making the process more

[1] Refer to Appendix B "Toxicity Analysis of Sargassum in Punta Cana"

controllable). Without a clear determination as to which system was destined for future use (it was actually believed that the lowest path-of-resistance option would be to implement the ex-situ system first, and then replace its slowly by the in-situ system over time), the SOS Carbon team elected to test an SOS Pilot vessel precisely because it was the riskier of the two system concepts and de-risking could be had for both system concepts, from a single test: to show that the in-situ system worked would provide validation for both systems at once and, if the in-situ system proved unviable due to the harsh realities of operating in waves (pump inlet feed efficiency and safety, among other challenges), it could still be shown that sargassum could be fed into the pump manually in controlled conditions.

5. Inlet Device Designs and Testing

Several inlet devices were designed/built/tested/evaluated as a means of (1) metering flow of sargassum, (2) maximizing feed efficiency, and (3) preventing suction-side clogs/aspiration. Each inlet differed in its fundamental operating principle:

- **Co-axial auger**
- **Transverse auger**
- **Sump**
- **Repurposed snowblower**
- **Suction boom/"tee"**

Design/testing and evaluation of each of these devices is described hereafter.

FIG 41 Different pump inlet prototypes tested from March-June 2019. (Clockwise) Co-axial auger, transverse auger, suction boom, suction tee, repurposed snowblower.

5.1 Auger Devices

Auger devices use augers to meter the flow of sargassum into suction piping. FIG 42 shows prototypes of the co-axial and transverse auger devices, respectively. Augers are surrounded by funneling structures that direct sargassum towards the augers as the device moves through the water.

FIG 42 Prototypes of the co-axial and transverse auger devices tested using pine shavings as a surrogate for sargassum.

Both auger designs were ultimately chosen for further development and use in the SOS Pilot vessel. FIGS 43 & 44 show final designs of the co-axial and transverse auger devices.

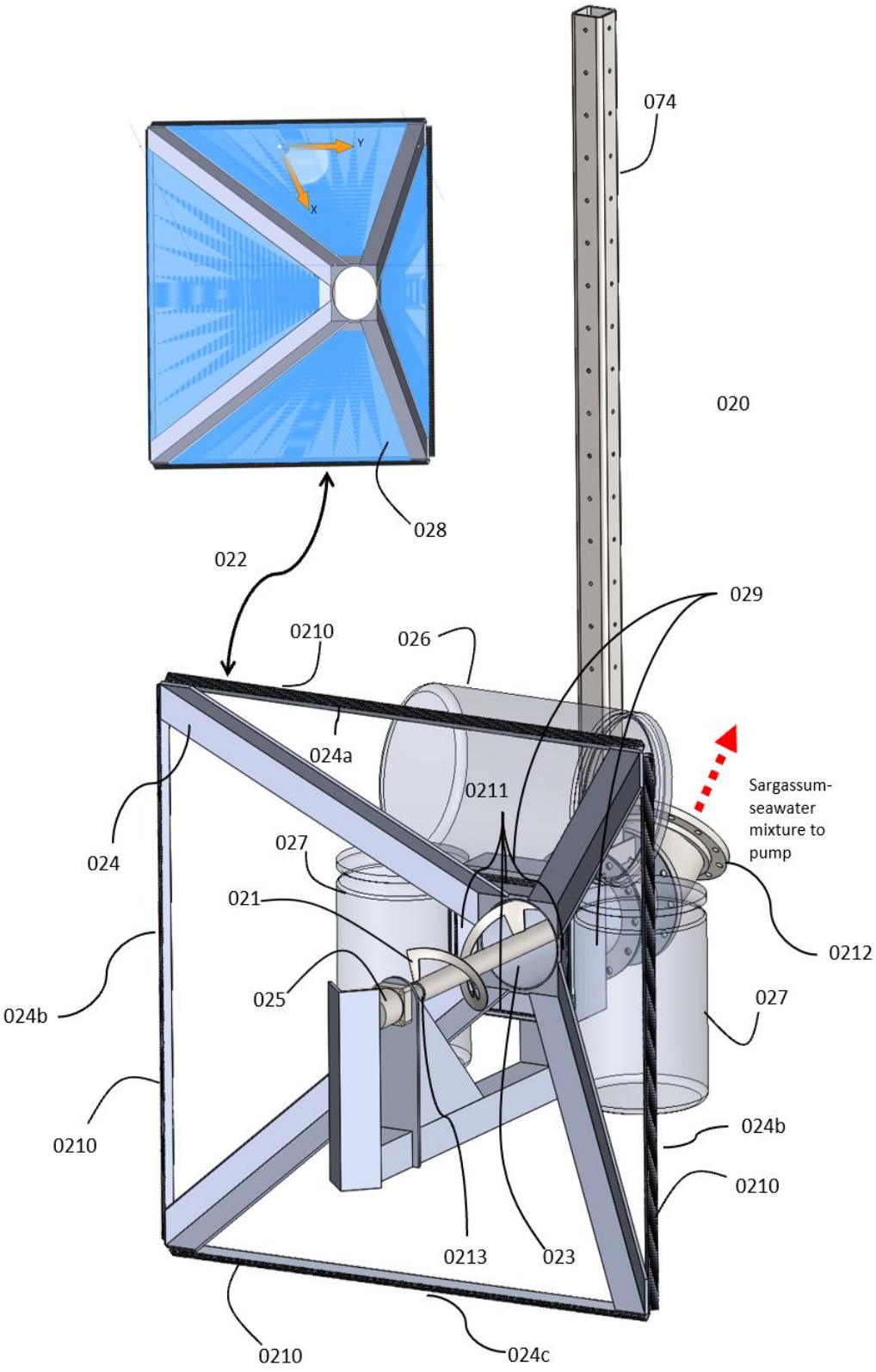

FIG 43 The transverse inlet device uses a left-handed/right-handed auger to prevent stable archway formation and feed sargassum into the suction inlet at a constant rate.

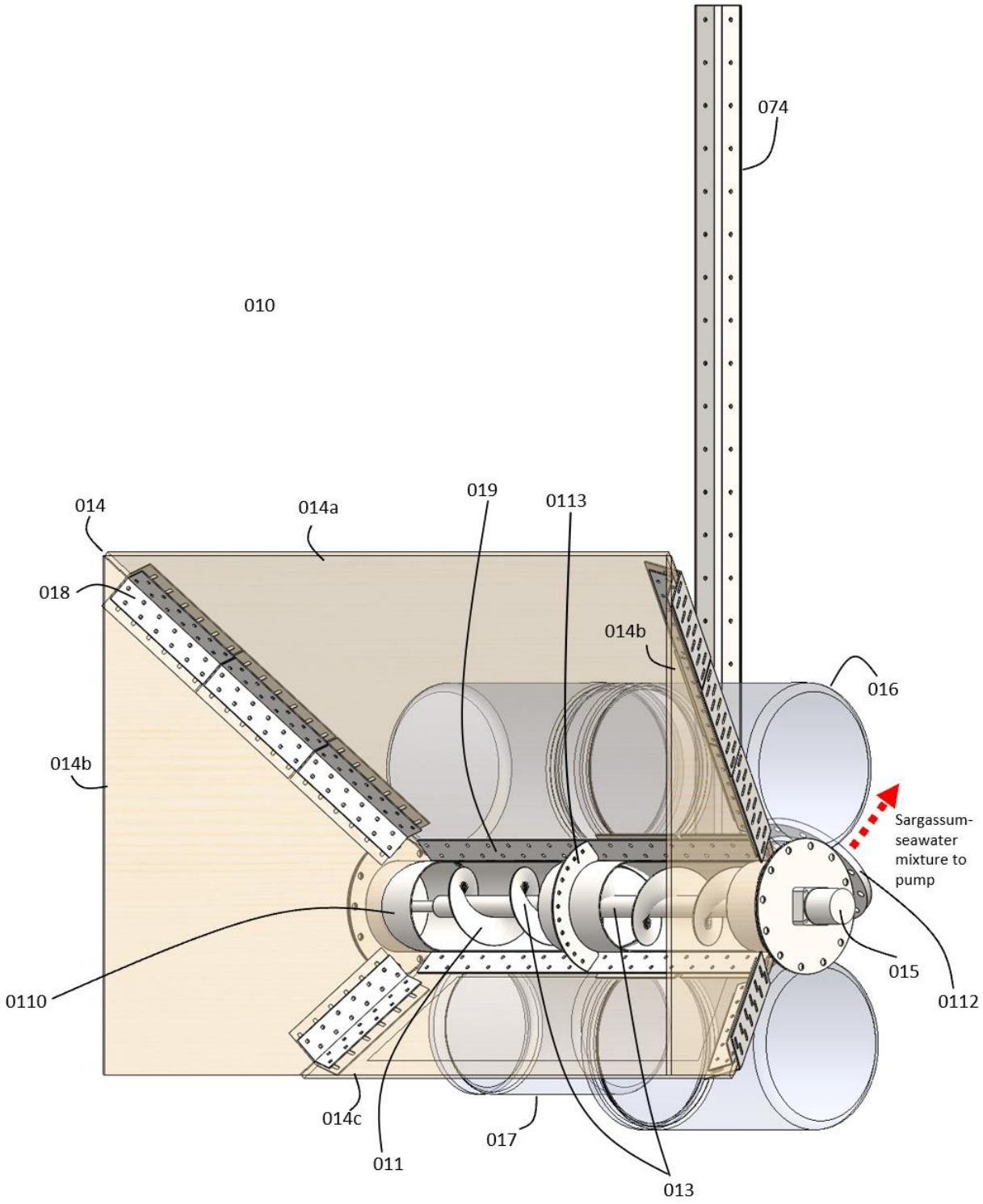

FIG 44 The transverse inlet device uses a left-handed/right-handed auger to prevent stable archway formation and feed sargassum into the suction inlet at a constant rate.

For more detail on the design of the auger devices, and thorough annotation of FIGS 43 & 44, refer to Section 7 “Patent Specifications (Detailed Technology Description)”. More details on the construction and testing of the final designs are provided in Section 6 “SOS Carbon Pilot Vessel”.

5.2 Sump Inlet

The prototype of the sump inlet was shown in the previous section as it was used as the pump inlet during proof-of-concept pump-to-depth experiments. FIG 45 shows the scaled-up design of a rectangular sump, sized for a 5000GPM pump.

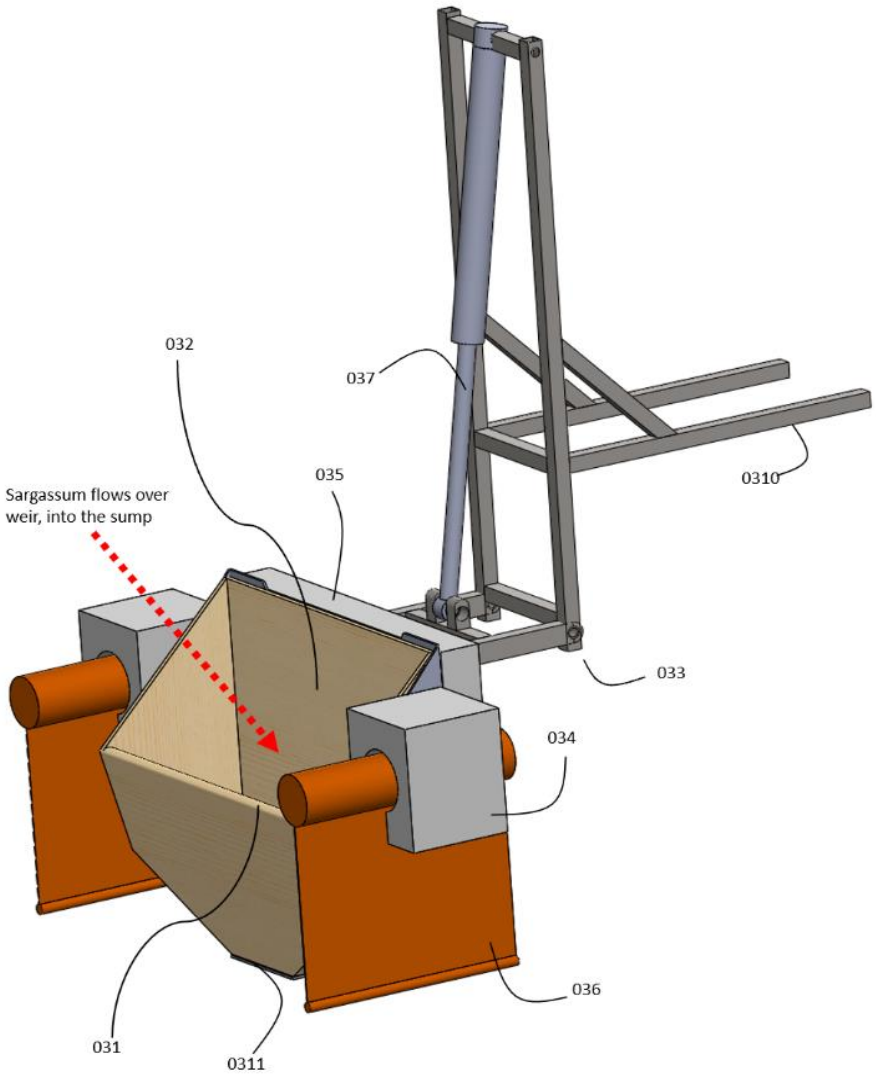

FIG 45 The design of a wave-following, retractable, rectangular sump, sized for use with a 5000GPM pump.

The fundamental working-principle of the sump-inlet is that a wave-following weir limits the depth at which solids and liquids can enter, imposing a consistent volumetric solids concentration, and induces a sufficient downward velocity inside the sump to transport sargassum downwards, towards suction piping, against its natural rate-of-rise (~0.05-0.2m/s).

The necessity to induce sufficient downward velocity to overcome the natural rate-of-rise of sargassum suggests a sump shape with a high (perimeter):(cross-sectional area) ratio such that the sump can sustain larger volumetric flowrates (by increasing its perimeter – the length of the weir) without sacrificing downward velocity (which decreases as cross-sectional area increases like ~$(\text{perimeter})^2$), which would result in sargassum simply accumulating at the top of the sump. FIG 46 shows the downward velocity of seawater in various sump geometries vs. the volumetric flowrates. There is a maximum flowrate for each sump geometry/size, beyond which the sump does not provide sufficient downward velocity. The sump shapes analyzed in the model comprise: (a) a circle, (b) a square, (c) a triangle, (d) a rectangle with b/a=10, (e) a circle with drafted walls, (f) a square with drafted walls, (g) a triangle with drafted walls, and (h) a rectangle with drafted walls. The latter four sumps have short, steep, positive drafts between the inlet edge and the core of the sump such that the effective perimeter/cross-sectional area is increased and the volumetric flowrate range is extended.

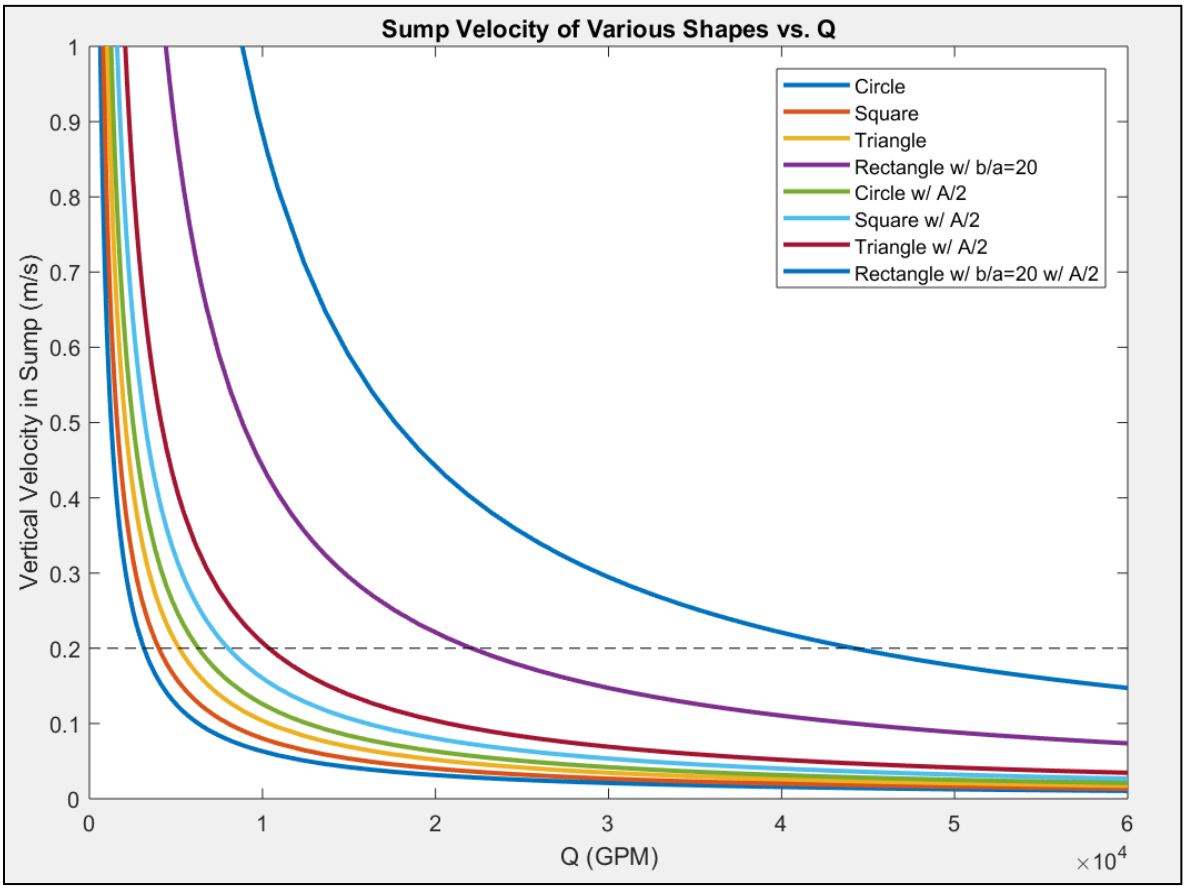

FIG 46 A MATLAB model output showing the limiting volumetric of sump-inlets of varying size/geometry. A sump shape/size is not viable if it does not induce a downward velocity of at least 0.2 m/s. This constraint suggest the use of a shape with a high perimeter/cross-sectional area ratio, such as a high aspect-ratio rectangle.

Circle	Square	Eq, Triangle	Rectangle b/a=γ
$\frac{P}{A}=\frac{4}{D}$	$\frac{P}{A}=\frac{4}{a}$	$\frac{P}{A}=\frac{4\sqrt{3}}{a}$	$\frac{P}{A}=\frac{2(1+\gamma)}{b}$

A rectangle has been chosen as the sump shape of the full-scale prototype. This shape maximizes the perimeter-to-area ratio, thereby also maximizing the permissible volumetric flowrate without compromising downward velocity inside the sump (which is necessary to transport sargassum towards inlet piping). The aspect ratio of the rectangular sump should be as high as possible (limited only by the length of the vessel and the diameter of the suction piping). A slender rectangular has a much smaller footprint than a circular sump rated for the same volumetric flowrate, meaning that it takes less space (it could perhaps even be stored in an outboard position) and can be deployed immediately next to the ship (decreasing the size and complexity of the deployment mechanism). A rectangular sump is easier to make, transport, install, and maintain. A rectangular sump is lighter and more compact than a circular sump of equivalent rated volumetric flow, meaning it will have less effect on ship dynamics. Lastly, a rectangular sump lends itself to sealing against the collection boom(s).

With this deterministic choice of sump shape, we could quickly converge on the detailed geometry of the sump. The approximate sump geometry is illustrated in FIG 47 The drafted bottom decreases material use and hydrodynamic forces on the sump. A filleted leading edge maximizes flowrate to decrease the chance of dry-running and allowing the leading-edge to remain close to the free surface, maximizing volumetric solids concentration. The remaining planes are all flat, zero draft tessellations.

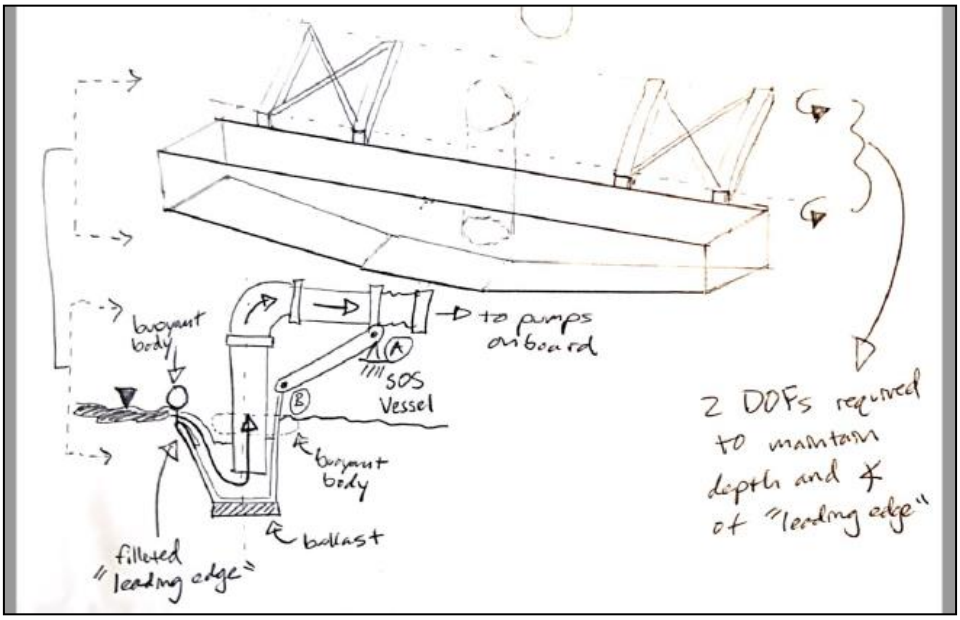

FIG 47 An illustration of the sump inlet geometry, comprising a rectangular prism with drafted floor. Sargassum and seawater flow over the leading edge into the sump. The cross-sectional area of the sump is small enough such that the volumetric flowrate out (via the pump) causes sufficient downward velocity inside the sump to pull sargassum down (against its natural rate-of-rise) towards suction inlet piping. 2 degrees of freedom (DOFs) are required to maintain the depth and orientation of the leading edge.

There will be one sump for every pump, so that each of the sump-pump-pipe-hose modules can act as independent units (as opposed to one sump per multiple pumps or one pump with multi-suction inlet). This allows variable sinking rate and allows continued operation in the case that one module is out of service. Only the distal edge of the sump acts as the "leading edge," lying below the free surface and sustaining a flow of sargassum and seawater over it (the proximal edge of the sump is above the waterline).

SEE APPENDIX D - "SUMP INLET HYDRODYNAMICS MODEL" FOR A DETAILED MODEL THAT WAS USED TO CHOSE THE SIZE, EXACT GEOMETRY, BALLAST, BUOYANCY, MATERIALS, AND CONSTRAINT.

The hydraulics of the sump-inlet are, by definition, unstable. Given a constant volumetric flowrate out, to the onboard pump, that flowrate must be matched or exceeded by the volumetric flowrate over the leading edge of the sump, or else the sump risks running dry and causing damage to the pump. If the volumetric flowrate to the pump Q_{pump} exceeds the flow over the leading edge Q_{LE}, even for a moment, the water level in the sump will decrease, making it more buoyant and causing the leading edge to rise. This results in a lowering of the head at the leading edge, the resultant decrease in Q_{LE} causing a runway emptying of the sump as the sump rises to the surface. This was observed during proof-of-concept tests.

There are several countermeasures, which may be immediately obvious:

1. Make sure that the leading edge is always submerged by lowering it relative to the CoB of the sump (setting it at a larger depth). Submerged sufficiently deep, the sump-inlet no longer exhibits a "spillway/waterfall" flow phenomena. While this solves the issue of running dry, it lowers the volumetric solids concentration of the pump feed. This lowering in solids concentration could be offset by pulling the collection boom faster (causing sargassum to pile vertically, above and below the SWL). However, this requires a boom with greater tensile strength, lower bending stiffness, a longer skirt, and taller wind guards. This adds cost, limits the length of the boom, a therefore limits mat size that can be addressed in a single operation.
2. Increase the size of the sump to increase response time before the sump runs dry. While this measure also has merit, because the cross-sectional area of the sump is limited by the constraint $Q_{pump}/A_c > 0.2 \equiv$ natural rate-of-rise of sargassum, increasing the volume of the sump can only be accomplished by increasing the draft. This exposes the sump to higher wave forcing, making the control problem more difficult and requiring reinforcing of the structure. Not to mention, increasing the volumetric capacity of the sump increases cost and the efficiency/convenience of handling.
3. Vary Q_{pump} using a variable frequency drive. While this is another viable way of avoiding dry-running, it is also not ideal because there exists a single flowrate and volumetric solids concentration that achieves the greatest hydraulic efficiency of the entire system. Therefore, varying pump flowrate as a countermeasure to dry-running not only adds complication, it also eliminates the ability to simultaneously pursue hydraulic efficiency.

4. Preload the sump underwater with a spring or with ballast located near the surface of the water. The represents a viable countermeasure, but also adds mechanical complexity and increasing the cost/weight of the sump. Moreover, this countermeasure only slows the rate of dry-running, which may be enough to avoid transient conditions that initiate the instability, but that is yet to be shown.

A combination of these solutions may prove necessary to eliminate the risk of dry-running while also maintaining a high, consistent volumetric solids concentration. However, these countermeasures address the symptoms of the sump-inlet's hydraulic instability, not the instability itself. We suggest an additional countermeasure to directly address this instability:

5. Increase the volumetric flow capacity of the leading edge of the sump-inlet by increasing its length and optimizing its surface geometry. This will increase the flow rate of fluid it can pass under a given head of water, increasing the inherent hydraulic stability of the sump-inlet and allowing the leading edge to operate closer to the free surface.

This countermeasure requires further explanation.

The spillway/waterfall flow phenomena of the leading edge of the sump-inlet is analogous to the flow of water over a "weir" in civil engineering applications, where weirs are used to control the water level in reservoirs, most notably for flood prevention in dams. For this reason, the hydraulics of weirs are well understood and a great detail of design effort has been spent maximizing their capacity. The design objective of a "free crest" or "ungated" weir is to maximize the flowrate for a given head of water (in most cases the literal height of reservoir fluid above the crest). The general equation for the flow of a weir is:

$$Q_{weir} = \frac{3}{2} \times C_d \times \sqrt{2g} \times P \times H^{3/2}$$

Where L is the width of the weir [m] and H is the head of fluid above the weir [m]. The simplest form of a weir comprises a rectangle crest, which usually exhibit a discharge coefficient of approximately 0.602. The most elementary improvement to such a weir is to evolve the rectangular crest into one that follows the natural freefall trajectory, or "nappe," of the stream. This is known as an "ogee" profile, shown in Figure Y, an usually boats an improved discharge coefficient of between 0.602-0.650 (Bureau of Reclamation, Hydraulic Model Study of Ritschard Dam Spilllways, 1991) depending on the design head of the ogee profile. In addition to the increased discharge, for a head sufficiently close to the design head of an ogee profile, the nappe is also kept attached to the wall, preventing it from separating and aerating the stream.

A further increase in flowrate can be achieved by making an undulating crest to increase the length of the weir in a given width. In civil applications, this has been accomplished with U

shapes, trapezoidal shapes, triangular shapes (called a labyrinth weir), and square shapes (called a “piano key” weir). Labyrinth and Piano key weirs are shown in F

5.3 Repurposed Snowblower

The repurposed snowblower was actually not a pump inlet at all – it does not rely on suction, rather, it is fed by left-/right-handed auger(s) and gravitational induced flow of water and floating debris into the void created when water is “thrown” out of the casing by the blower impeller. The casing of the impeller is exposed to atmosphere and therefore always at atmospheric pressure. This is an interesting property because one problem with other pump inlets tested is that the pump loses prime when any part of the inlet emerges above the waterline. In waves, if this is happening constantly, the constant de-priming and re-priming of the pump would significantly hurt process efficiency. Therefore, other pump inlet devices with inlets close to the waterline (all but the sump inlet) would need to be heavily hydrostatically preloaded to perform in waves. A repurposed snowblower would avoid this issue because it continues throwing water regardless of whether or not it comes out of the water. In the end, the repurposed snowblower concept was eliminated because the impeller of the 90hp commercial snowblower caused must disturbance of the incoming water and floating debris, significantly hurting feed efficiency. More importantly, however, the purpose of the pilot tests was to show pumping-to-depth in the open ocean; a system with a snowblower on the receiving-end would still be required to discharge into a sump onboard, from which it would then be pumped. This space requirement and complication of this additional step was simply not feasible. It should be noted that a repurposed snowblower might still be well-suited for near shore collection and deposition into a receptacle for further transport/processing.

FIG 48 Initial repurposed snowblower tests with low-power snowblower.

FIG 49 A test using a commercial snowblower to impel sargassum from the surface.

5.4 Suction Boom/“Tee”

Prototypes of the suction boom/”tee” are shown in FIG 50. The suction boom/”tee” comprises an extended suction pipe/hose, respectively, with its distal end capped/sealed, with distributed inlets spread along the entire length. The design goal of the suction boom/”tee” is to maximize the length of continuous suction region where the inlet velocity is divided but still locally high enough to entrain sargassum. Because pressure losses between inlets is much less than the pressure losses through the inlets themselves, there is approximately equal flowrate through each inlet along the entire length of the boom.

FIG 50 Different pump inlet prototypes tested from March-June 2019. (Clockwise) Co-axial auger, transverse auger, suction boom, suction tee, repurposed snowblower.

Floatation and ballast (in the case of the suction boom, chain ballast, shown in FIG 51, attached frequently along the length) creates hydrostatic preload, counteracting wave forces and internal forces from flow through the suction boom/"tee".

A large-scale SOS Carbon system for implementing pumping-to-depth may wish to use very large pumps (>100,000 GPM) to increase capacity and efficiency. A challenge exists here because very large pumps with single inlets must be fed with sargassum very quickly – otherwise the operator would pump only seawater and very little sargassum. Instead of driving the collection vessel very quickly, or pulling a boom extremely fast, the suction boom's extended length will allow collection from a wide swathe, at relatively low velocity locally. Therefore, the suction boom might be very useful, especially if large pumps are considered. It is important to note that the extended suction device not only enables the use of a large pump, but it requires it, otherwise local inlet velocity will not be sufficient to entrain nearby sargassum amidst other ocean forces.

An alternative to a flexible boom is a suction "tee" that might incorporate anti-roll floatation in the form of a "tee" to prevent roll and emergence of inlet openings on the underside of the device in large waves. Because a rigid suction boom cannot be compacted, its length is limited by the size of ship and deployment system used.

FIG 51 Prototype version of the suction boom (flexible), showing the chain ballast used to counteract forces from waves and flow of water through the boom.

FIG 52 shows scaled up desgins of both the flexible suction boom and the rigid suction “tee”.

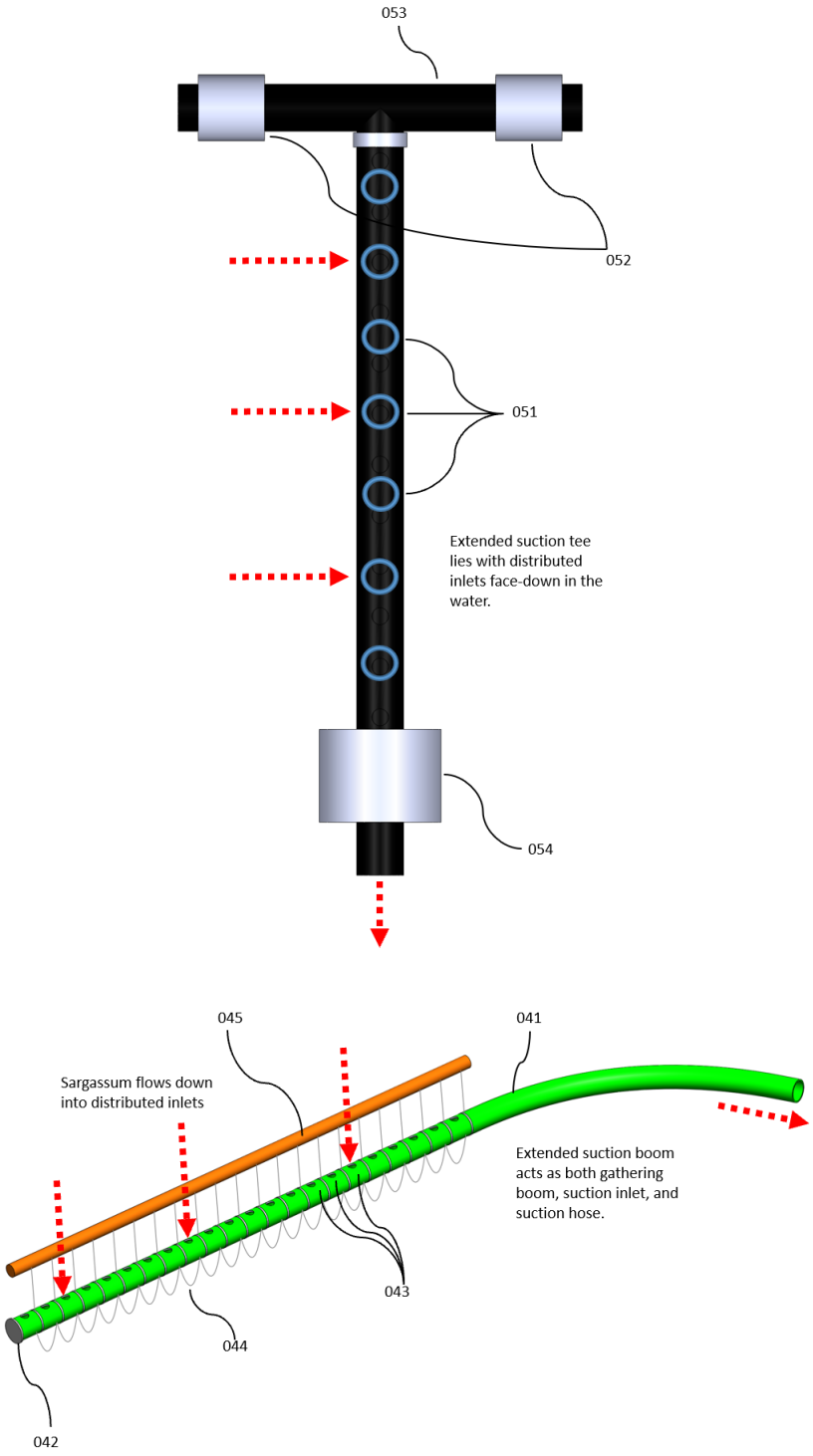

FIG 52 Scaled up designs of the suction boom/”tee”.

5.5 Inlet Device Summary

It was learned that devices which divided the flowrate up into multiple suctions (ie. the suction boom and suction “tee”) or distributed it continuously across a large area (ie. the sump) decreased the local fluid inlet velocity such that pine shavings (and other surrogates for sargassum used on Prof. Slocum’s pond in Bow, NH) were not sufficiently entrained in the flow to enter the suction plumbing. Water instead preferentially flowed up into the suction devices from deeper depths (in proximity to the free surface, gravity and surface tension likely played an important role in this non-uniform flow phenomena near the suction inlets). An interesting phenomena that occurred with these devices was the formation of “depletion zones” near the suction inlets bounded by “stable arches” of floating debris that literally reinforced themselves much the same way as structural archways are self-supporting. These feed efficiency problems could only be remedied by directing suction narrowly, squarely, and immediately at the floating debris, which adds the risk of suction line aspiration and loss-of-suction (should the suction come so close to the free surface that surface tension in broken and whirlpooling/air-entrainment occur).

The sump inlet received much design attention, but ultimately was also shelved at the time because it could not work in the moving method (the primary goal of the pilot tests). There were not enough funds or engineering bandwidth to implement the purse seine boom and containment boom reel. The sump inlet is still considered a promising device as an inlet device in the stationary method.

While the suction boom/”tee” and sump devices were shelved, the lessons learned are not to be forgotten and it is noted that these devices could prove useful with larger flowrates in the future (<100,000GPM). For example, at high flowrates, a depletion zone could be caused by a flowrate too large compared to the (forward velocity) x (collection width) (rather than by insufficient inlet flow velocity as is discussed immediately above caused by moderate flowrates spread over too much inlet area). Rather than have vessels drive faster (or pull booms faster in the case of the purse seining method) to match the pump flowrate, it is better to increase the suction area (thereby decreasing the inlet velocity locally) such that the pump flowrate is better matched and a high volumetric solids concentration is sustained (otherwise the depletion zones would persist and a large amount of seawater would be pumped per volume of sargassum, which is very inefficient).

In the end, it was recognized that the simplest, most reliable way to keep the suction inlet region fed with sargassum at moderate flowrates (3,000-10,000GPM represents a reasonably transportable pedestal or submersible pump that can be easily deployed on a moderately sized boat) was with a moving mass-flow funnel (or “vee” or “hopper”) because depletion zones are eliminated from the necking inlet area and self-help of sargassum pushing itself into the inlet. The possibility of stable arch formation is eliminated and sargassum concentration is controlled by a the use of the co-axial and transverse augers, respectively. The former device interrupts the “keystone” region of arches as they developed. The latter provides a moving surface interrupting the “feet” of forming arches. Both auger designs enforce a relatively constant solids flowrate via having at least one full flight pitch inside the suction inlet.

6. Full-Scale Pilot Vessel

The purpose of the SOS Pilot was to show that the hardware and pump-to-depth method could work at a commercial scale – keeping in mind the small size of the SOS Carbon team. So long as one pump, crane, inlet, and hose reel could be installed and operated effectively, it would provide the validation needed to pursue much larger ships with multiple pump-crane-inlet-hose sets in parallel. The scale for the system was based on a Godwin (Xylem brand) DPC300 5000GPM pump – the workhorse of the Godwin fleet – designed to be rugged and transportable for high capacity dewatering applications all around the world.

Building/shipping/installing/testing the SOS Carbon hardware took >5 months (July-December, 2019). A special thanks to Prof. Slocum for hosting the building/staging at his farm in Bow, NH; my father, Bob Gray, for helping during the critical latter stages of building; Dr. Folkers Rojas, for his mentorship and help, both in Bow and in the DR, to get the hardware working; and Andres Bisono, for securing the funds that enabled the entire project.

6.1 Funding

It was originally estimated that ~$250,000 would be required to successfully execute a full-scale SOS pilot vessel. February through June, 2019, designs, strategy, and plans for testing continued to evolve whilst the team struggled to raise the total funds from a single donor. Pitches were made to resorts, restaurants, power companies, angel funds, multinational, and domestic banks. All potential donors either saw the venture as outside their intended theme/expertise, did not understand the problem/solution well enough and determined it too risky, or, in many cases, recognized the promise of SOS Carbon and ask to instead participate in an equity investment (which we were not able or willing to do). Surely, some of these incidents were due to insufficient communication of the SOS Carbon value proposition. L. Gray can admit to being to in love with the idea and, as the design engineer, being distracted by trying to share every minute detail of the system and thereby failing to emphasize the overall value proposition. Struggling to raise funds from a single donor, team members considered, for a moment, the possibility of publishing Proof-of-Concept Test (Jan. 2019) results and leaving the project there.

Ultimately, the team sustained hope that a no-equity donation could be secured. A bank we had already pitched to – Banco Popular, largely considered the largest domestic bank in the Dominican Republic – while unable to give the entire ~$250,000 admitted that the “ASK” was small for a project with such large potential to solve what was known to be a multi-billion-dollar problem for the Caribbean. Banco Popular committed a fraction of the needed funds ($20,000) and, in only two weeks, raised equal contributions ($20,000 each) from 10 additional organizations in the DR, many of which we had previously contacted (recognized below). The only concession in return is was that, should SOS Carbon commercialize, any equity investments that donors in the Banco Popular cohort propose will be given first consideration, and a letter of agreement was signed to this effect (along with the statement that no IP was transferred, and no other promises are being made relating to test results or payback). Additional contributions of $8,000 from Grupo Ramos (the only pilot funds raised successfully before Banco Popular’s involvement) and later contribution of $20,000 from VoLo Foundation (original supporter in the early stages of the project who were interested in equity investment in exchange for the full ~$250,000 – VoLo made this fractional donation to earn the same initial consideration promised to donors in the Banco Popular cohort in the future) brought the total contribution from all donors to $248,000. The piecewise donations that

made up this total lowered the barrier to entry for each donor, and each commitment added momentum to the cause. A similar approach is suggested for others pursuing academic projects of this scale. The project also benefitted from the goodwill of Godwin (Xylem Inc.) who donated the 5000GPM pump free of rent, the Maritime Affairs Ministry in the DR who helped with the import taxation waive for equipment entering the country, and The Dominican Republic Navy who hosted us at the Las Calderas Naval Base in Bani, DR, and allowed us to install and test the SOS pilot system on a navy ship, the GC-111 Centaurus (and where the equipment still resides at the time this thesis was submitted, February 2020).

All of the supporters (both monetary and goodwill) are recognized here:

During the funding struggle from February to June, 2019, L. Gray and Prof. Slocum continued designing and testing inlet devices at personal expense (an attitude of confidence in our technology that we hoped would further encourage potential donors to commit).

6.2 Pilot Vessel

The design of the pilot depended greatly on the vessel to be used. At the start, the team was considering several specific vessels for either purchase or rental, and layouts were made for each (FIG 53).

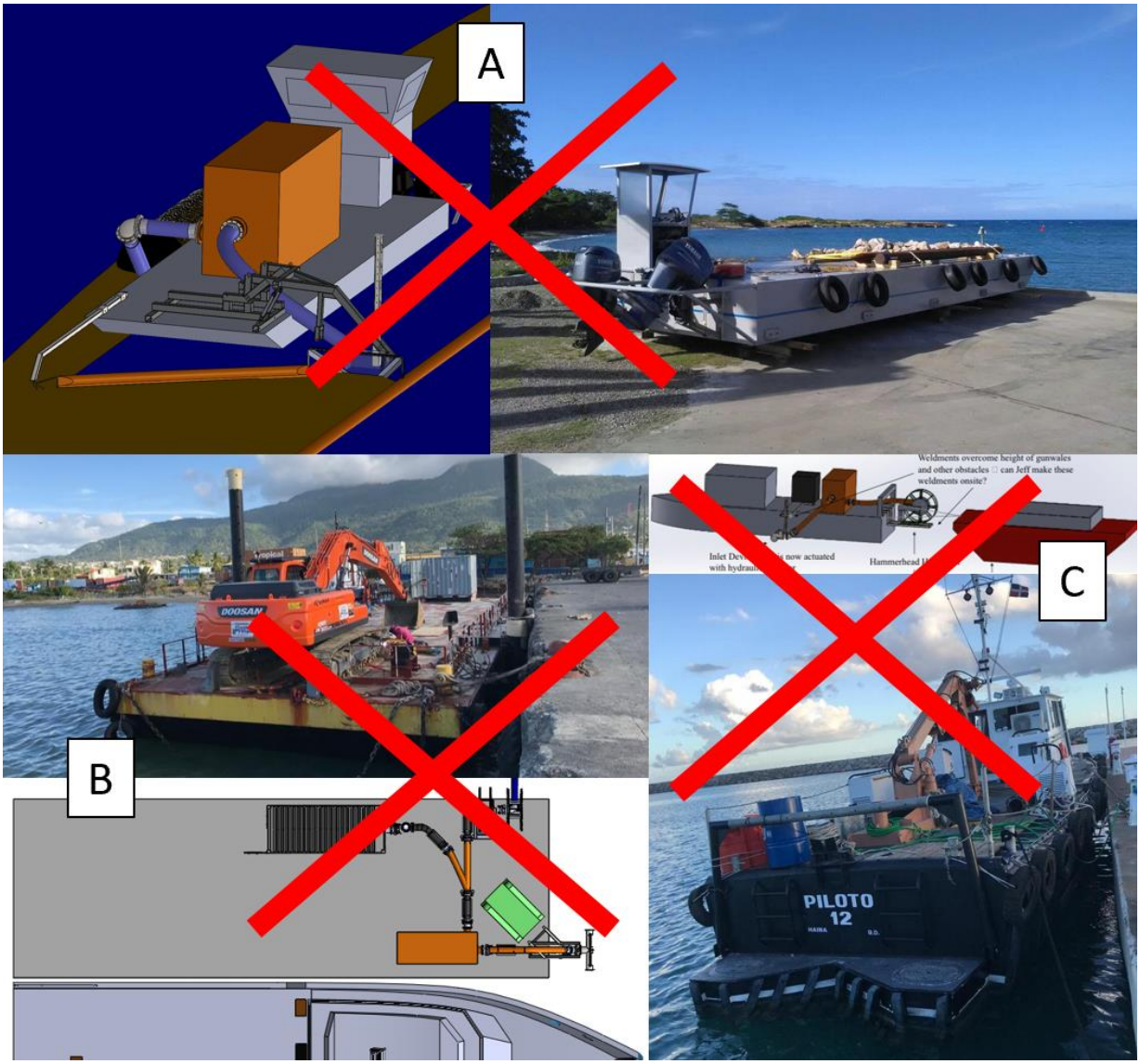

FIG 53: (A) a low-draft deck utility boat, (B) a construction barge, (C) a small tug.

Tests of an early inlet device deployment mechanism that used a skid steer to deploy the inlet from the front of a barge/deck utility boat were completed with Godwin in Bridgeport, NJ (FIGS 54 & 55).

FIG 54 An early deployment mechanism for the inlet devices when the team was considering mounting the equipment on the bow of a barge. The inlets were held inside an adjustable z-axis on a frame that was forked by a skid-steer, which could also be used as an HPU for the augers.

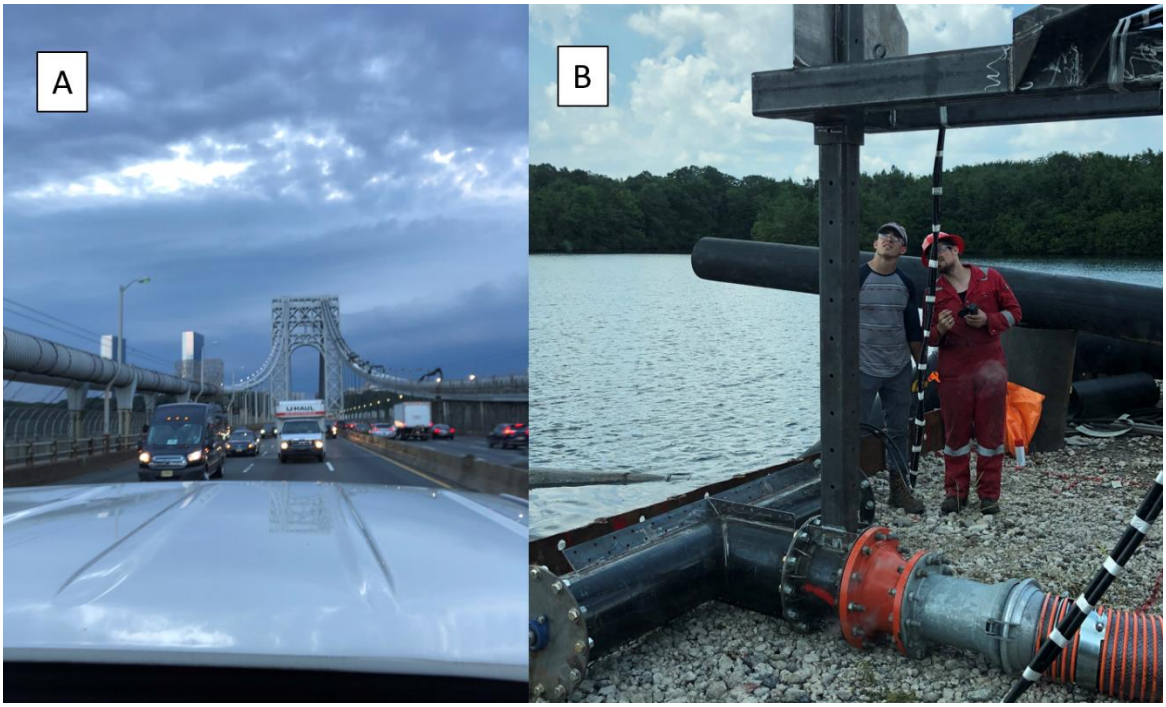

FIG 55 Early tests of the transverse inlet device with DPC300 pump in the Godwin test ponds in Bridgeport, NJ. The tests were considered a dress rehearsal and verified the feed efficiency of the transverse inlet at the real flowrate (again, using pine shavings as a surrogate for sargassum).

Ultimately, a partnership was formed with the DR Navy to use one of their ships (at no cost; as the team had done in January, 2019, during proof-of-concept tests). The original intention was for all the construction and testing to be done in Punta Cana, out of the Cap Cana Marina. However, it became evident that the Las Calderas Naval Base in Bani, DR, which also manages a shipyard next-door, was better equipped – with a crane, accessible power, a machine shop, etc (FIG 56). This area (west of SDQ) still receives enormous amounts of sargassum. Therefore, in the end, the SOS Carbon team chose to use the GC-111 Centaurus navy vessel (FIG 57), and stage the pilot out of the Las Calderas base. This saved significant cost (no cost to rent/buy boat AND accommodations in the barracks were free), the Centaurus captain/crew proved very helpful hands, and the resources nearby bailed us out of several unexpected issues.

FIG 56 The ultimate location of the SOS Carbon Pilot – Las Calderas Naval Base, outside Bani, DR.

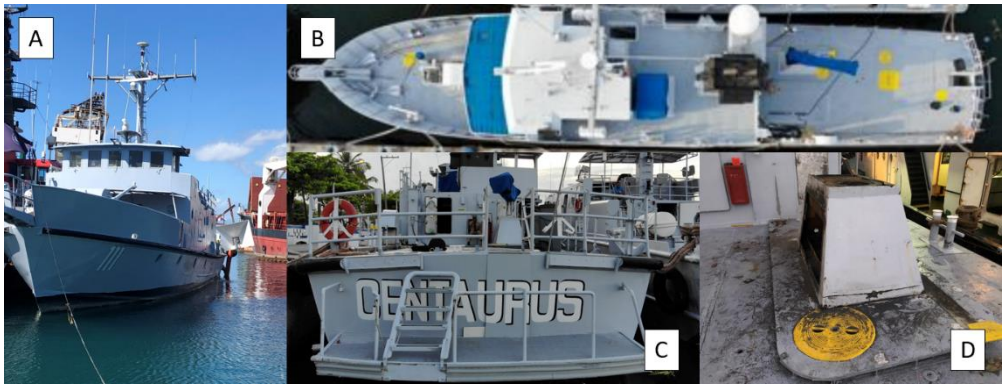

FIG 57 The GC-111 Centaurus, the DR navy vessel used as the platform for the SOS Carbon Pilot. The vessel was determined to have sufficient space, stability, and deck strength to accommodate the SOS Carbon hardware. Several railings and an out-of-repair crane (D) were removed.

With the goal to have equipment on the water testing in the DR in September, 2019, the SOS Carbon team looked for a means of deploying the pump inlet devices without designing/building a custom crane-arm. A CAT 303.E mini excavator was rented and a compatible bucket purchased. The z-axis sleeve was welded to this bucket and the transverse device assembled thereupon. The kinematics of using an excavator to deploy the inlet devices over the port-side of the Centaurus was tested next to a containment wall at Prof. Slocum's farm (FIG 58). This was the early plan for how to deploy the inlet devices from the Centaurus (excavator would be chained to the deck of the Centaurus).

FIG 58 The GC-111 Centaurus, the DR navy vessel used as the platform for the SOS Carbon Pilot. The vessel was determined to have sufficient space, stability, and deck strength to accommodate the SOS Carbon hardware. Several railings and an out-of-repair crane (D) were removed.

In the end, delays on other pieces of hardware afforded the time necessary to design and build a custom crane for deploying the inlet devices. This was not only safer, but it simplified the control of the deployment (1 DOF only). This lead to the final SOS Carbon Pilot vessel layout in

FIG. 59. Thanks to Folkers Rojas for creating the detailed CAD model of the deck from his reconnaissance trip in September, 2019.

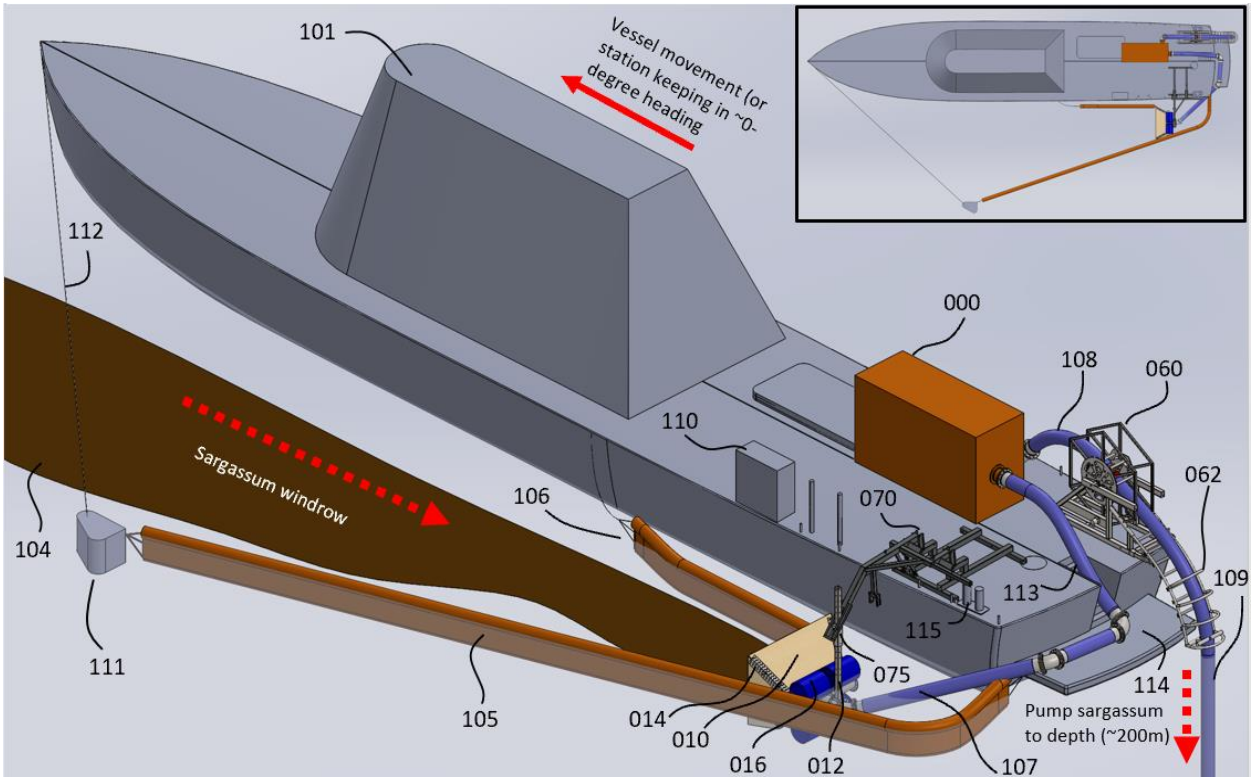

FIG 59 The final layout of the SOS Carbon Pilot vessel, using a custom-built crane arm for deploying the pump inlet. NOTE: the J-boom did not ultimately get used.

Without the auxiliary hydraulics of the excavator, the SOS Carbon team decided to use the HPU onboard the GC-111 Centaurus (FIG 60). Folkers Rojas did a preemptive trip to trace lines in the engine room and make sure the pump worked as it had not been used in a long time. Cain Shultz from TST hydraulics helped to identify the flowrates of the 3-stage pump and spec a control valve for all three of our functions (hose reel, crane, auger).

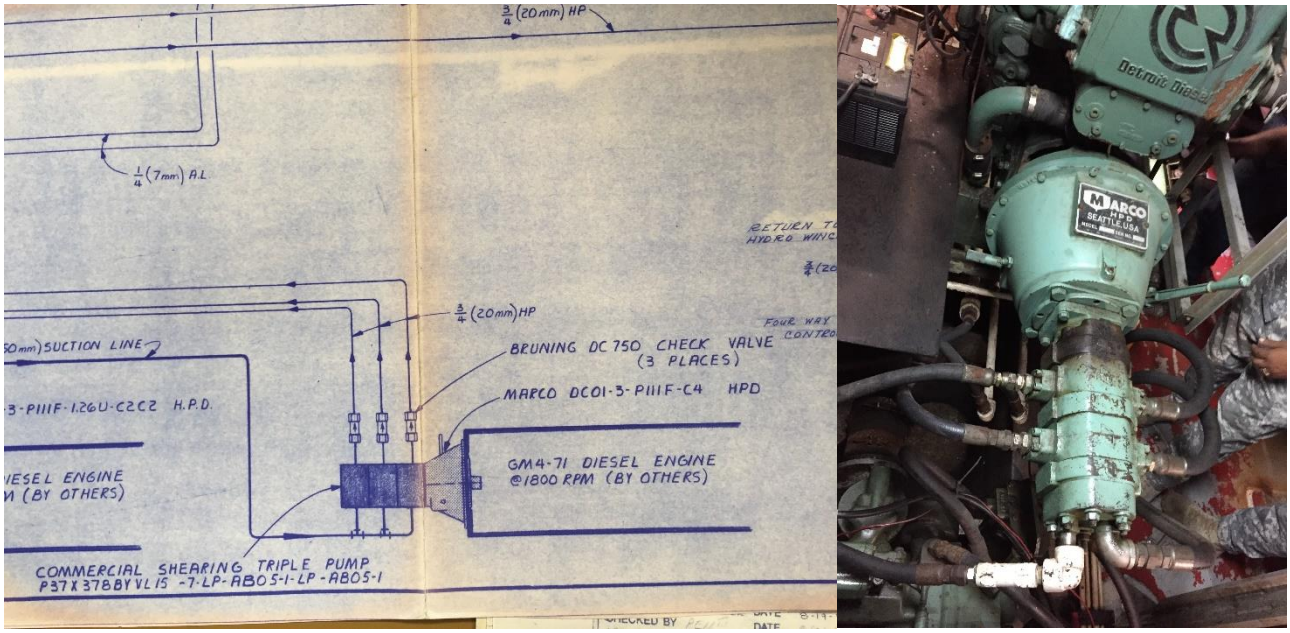

FIG 60 A schematic of the Detroit Diesel engine and 3-stage pump onboard the GC-111.

With this layout finished, all that was left to do was build, ship, install, and test.

6.3 Building (Bow, NH)

Fabrication and staging of the pilot hardware was done in Bow, NH, at Prof. Slocum's farm. Luke Gray spent 5 months, over 1800hrs, designing and building the hardware for the pilot tests. This is not including the many hours contributed by Prof. Slocum, Folkers Rojas, Bob Gray, and Andres Bisono. Thanks to Prof. Slocum for hosting me many nights, for contributing greatly to design and testing, and particularly for the complete design of the crane arm to replace the excavator boom, which was a major safety risk left outstanding. Thanks to my father Bob Gray for hosting me many nights, and for stepping in to help during the latter 2 months of building to problem solve and be an extra hand. Without any one of these people, the pilot tests simply would not have happened. There were also many NH businesses contracted:

- Raw materials were sourced from Cohen Steel Supply (Concord, NH).
- Weldments were produced by Brendan Newton at Island View Fabrication (Andover, NH).
- Machined parts were provided by Dieter Kunath at HydroCam Corp. (Concord, NH).
- Hydraulics were provided by Cain Shultz at TST Hydraulics (Merrimack, NH).
- Lay-flat fracking hose was sourced from Hammerhead Industrial Hose (Houston, TX).

Brendan Newton deserves special recognition for the skill and speed of work he exhibited. He operated under a very constrained timetable, working into the night several times leading up to the ship date. A number of his weldments are shown in FIG 61.

FIG 61 (A) finished weldments of the hose reel (base and wagon-wheel) arriving at Prof. Slocum's farm, (B) 2ea 48" coaxial augers (spoked and solid) and 2ea 80" transverse augers (spoked and solid), (C) the z-axis that rides inside the rotating sleeve on the end of the crane and connects the inlet devices to the suction hose, (D) the stinger for guiding the hose over the dive deck on the back of the GC-111 Centaurus, (E) the transverse inlet device.

The SOS Carbon hose reel was assembled and tested, in Bow, on October 6th 2019 (FIG 62). The hose reel is designed to hold 200m of lay-flat fracking hose (0.25"-thick polyurethane and >100,000lbs tensile strength).

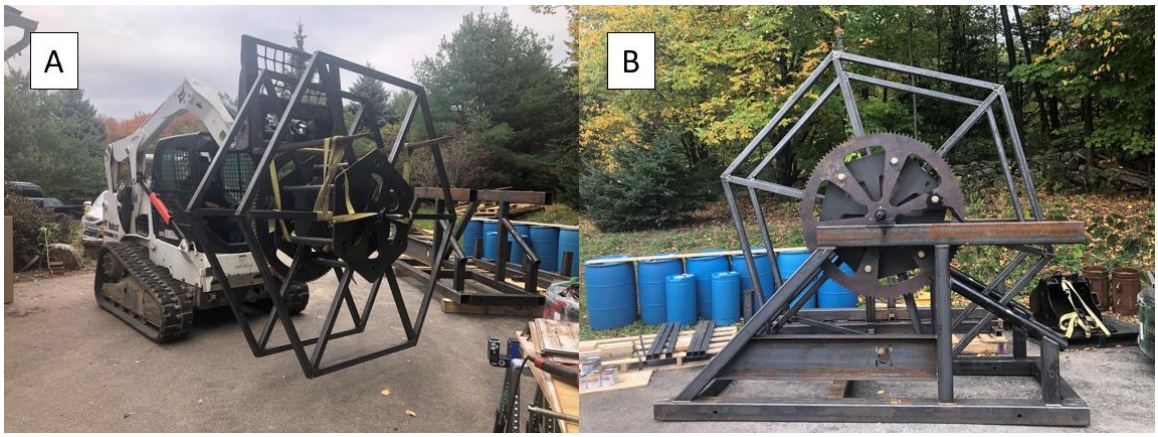

FIG 62 (A) hose reel wagon wheel speared by Prof. Slocum's skid steer, (B) The hose reel assembled.

The crane arm was assembled and tested, in Bow, on October 13th 2019 (FIG 63).

FIG 63 (A) the boom arm of the crane, speared by Prof. Slocum's tractor, being assembled onto the crane arm base, (B) the crane assembled.

For more detail on the design of the hose reel, crane arm, and inlet devices, please refer to section 7 "Patent Specifications (Detailed Technology Description)".

Once the hose reel/crane had been assembled/tested and all spare parts/tools needed for installment acquired finishing touches were applied: all steel was wire-brushed/primed/painted with safety colors (FIG 64), SOS Carbon branding/safety warnings added (FIG 64), and everything packed inside/on custom, heat-treated crates/pallets (recycled from local depots/hardware stores or bought hand-me-down from local companies). Expensive tools and spare parts prone to corrosion in salty sea-air were wrapped in polycarbonate bags. The packaging was built (thanks to Bob Gray and his nail-gun) according to the 40ft container layout in FIG 65. Everything was made to fit precisely (tight-packing reduces movement in transit) and spare steel was used as dunnage to take up any remaining space. The entrance to the container has slightly smaller dimensions than the inner dimensions of the container. From the beginning, the hose reel/crane (etc.) had been designed to fit into an intermodal container like this. For example, the hose reel wagon wheel was made hexagonal (as opposed to rolled, round tubing) with tip-to-tip distance 102" so that it could hold all 200m of hose, but still fit into the 40ft container entrance with flat-to-flat distance 89". Lastly, all contingencies for how equipment might shift during transit, and what impact it could have, were considered. Sharp edges were blocked or padded and additional wood dunnage was added to take up small spaces.

Shipping was handled by CTC Logistics. The original shipping date of October 8th was pushed back until October 15th so that the crane arm and stinger could be completed. A telescopic telehandler, with a reach of 42ft to load all the way into the back of the container, was rented for the day. Loading the container took <5 hours (FIG 66). Then, the container was on its way to Camden Yards (where it would be loaded onto a boat for the voyage to Rio Haina port in

the DR). Prior to being loaded into the 40ft container, each piece was weighed using a large floor scale and labeled (FIG 67). When the container reached the export port, it would be weighed and confirmed by logistics company. Then a bill of lading and actual cost would be reported.

FIG 64 (A) Bob Gray applying SOS Carbon decals on the funnels of the inlet devices, (B) Luke Gray priming the transverse auger inlet device.

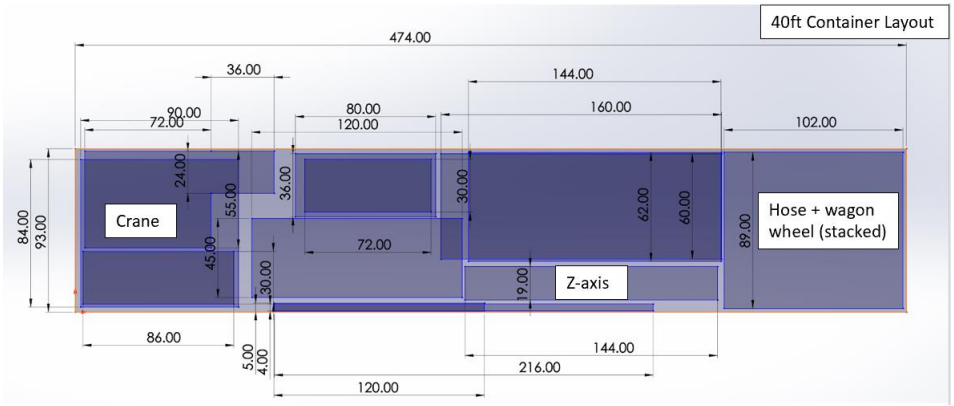

FIG 65 Layout of equipment inside the 40ft container sent to the DR.

The import into the DR and Rio Haina port was expedited by the Ministry of Maritime Affairs (ANAMAR). Import was registered as “temporary admission” so all port duties and import taxes were waived (this would have been close to 20% of the stated value of the goods). Having each piece of equipment explicitly labeled may have helped expedite release from customs in DR.

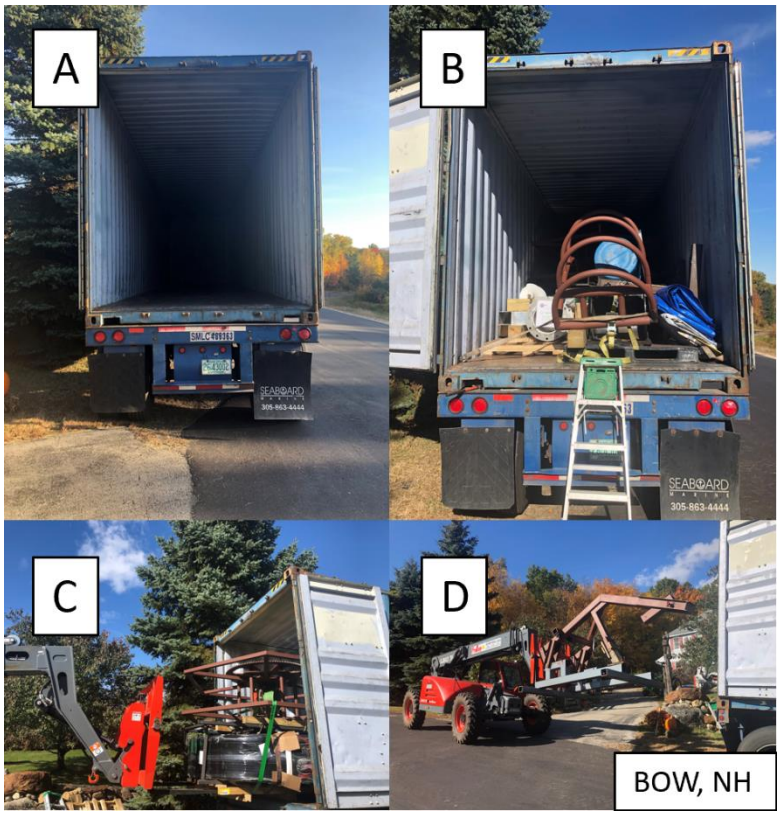

FIG 66 (A) 40ft container before being loaded in Bow, NH, (B) 40ft container after being loaded in Bow, NH, (C) hose reel base being loaded in Bow, NH, (D) crane (assembled backwards) being loaded in Bow, NH.

FIG 67 Labels with name and weight of each piece loaded into the container were secured to each respective piece.

6.4 Installation (Las Calderas Naval Base, Dominican Republic)

The 40ft container from Bow, arrived at the navy base on November 2nd, 2019 (FIG 68).

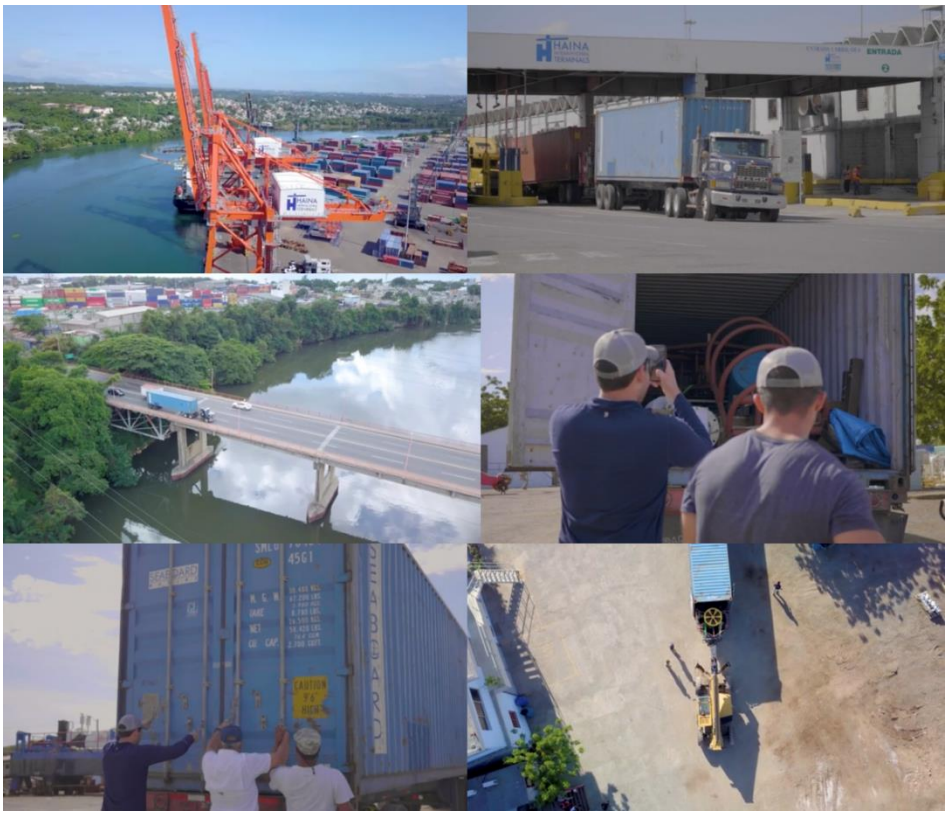

FIG 68 40ft container from Bow being delivered to navy base and unloaded.

Luke Gray, Folkers Rojas, and Andres Bisono, spent the first week of November, 2019, assembling the hose reel/crane and mounting these machines onto the GC-111 Centaurus. Prof. Slocum came for several days to see the equipment mounted and to do a preliminary test of the hose reel (November 8th, FIG 69).

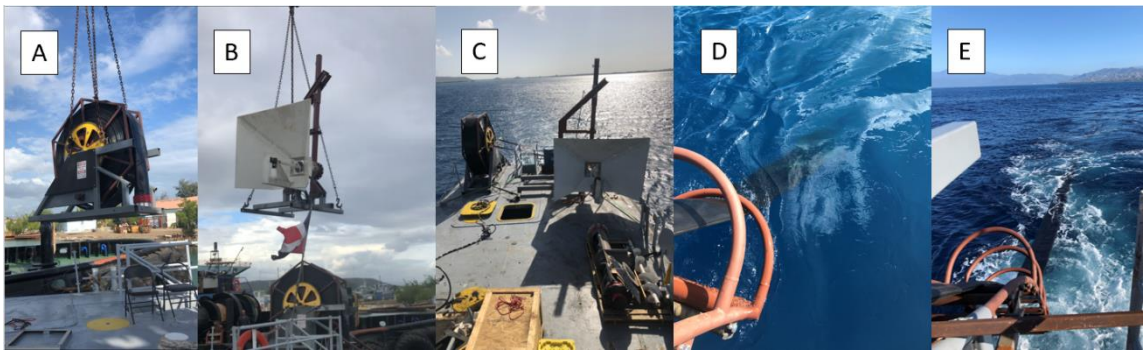

FIG 69 (A) pilot hose reel being loaded onto navy vessel, (B) crane and coaxial inlet being loaded onto the navy vessel, (C) first voyage to test hose reel, (D) the layflat hose being deployed for the first time, (E) hose towed at 3 knots (discovered that vessel must move <1 knot for hose to stay vertical).

This week of building was the most grueling and technically challenging. The hose reel, crane, and coaxial inlet device (decided that this would be tested first because more promising and lighter-weight of the two auger devices) were assembled in the staging area, a dirt area on dry land just next to the GC-111 docking area, adjacent to the Daniela Sofia (crane ship used to later lift the equipment onto the navy vessel). IMCA, the biggest equipment rental company on the island and an SOS Carbon Pilot Donor, donated a mini excavator and telehandler to help with assembling the equipment in the staging area (FIG 70).

It was decided that layflat hose would remain on the storage reel until it arrived in the DR. If we attempted to transfer hose to the pilot reel in Bow, NH, and failed, it would be very hard to get the hose back onto the storage reel. See FIG 70 for an illustration of how the how was ultimately transferred, and FIG 71 for modifications made to the storage reel prior to shipment, to facilitate transfer this pre-planned transfer.

FIG 70 (A) crane and coaxial inlet being assembled in staging area. (B) the staging area in which the layflat hose can be seen getting transferred from the storage reel onto the pilot hose reel. (C) The GC-111 crew finishing tightening all 400+ bolts in the coaxial inlet funnel. (D) Close-up of the layflat hose being transferred onto the pilot hose reel. The storage reel spins freely on two steel sawhorses. The telehandler supports/tensions the hose while also providing hydraulic power to the pilot hose reel.

FIG 71 The lay-flat hose storage reel had plates and a central tube added to it such that it could be easily transferred to the pilot hose reel once in the DR. Credit to Bob Gray for this idea. (A) Brendan Newton welding channel onto the side of the lay-flat hose storage reel. (B) Close-up of welded channel and central 3.5" tube turning freely inside. The layflat hose was protected from spatter by a welding blanket.

The November 8th test showed the hose reel would operate exactly as it was designed. It was discovered that with only one of the two 200lbs pipe sections hanging from the end of the layflat hose (FIG 72), and no flow being pushed through the hose, the pilot vessel could not move faster than 1 knot without the layflat hose rising to the surface (this speed could be increased later on when layflat hose pressurized by pump and second 200lbs pipe section added).

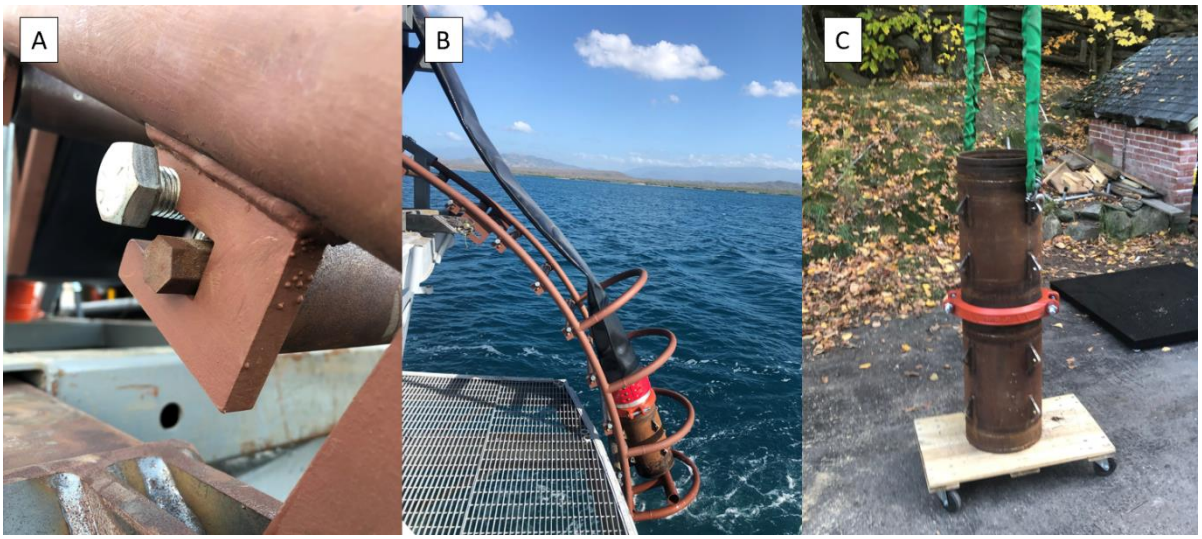

FIG 72 (A) stinger roller hex-end held inside slots and retained by ¾-10 bolt, (B) the stinger conveying the layflat hose over the stern of the GC-111 (during transit, the hose weight rests on a removable cover on the end of the stinger, and tension is let off the hose), (C) showing how more hose weights may be added together with Victaulic clamps (padeyes on hose weights also allow heavy chain to be hung from shackles).

Because, after the November 8th test, the pump was still in transit from Lakeland, FL (Godwin Branch 19 was the closest location with an available DPC300) the team returned home that weekend. ~1 week later, Luke Gray and Andres Bisono returned to finish installment aboard the GC-111.

The DPC300 pump arrived on November 15th and immediately loaded onto the GC-111 (FIG 73). The pump came with 5ea 10ft kanaflex hoses and 2 crates of 45°/90° camlock fittings and 12-bolt-to-camlock adapters (FIG 74).

FIG 73 (A) pump arriving at the Las Calderas navy base (November 15th), (B) pump being lifted onto the GC-111.

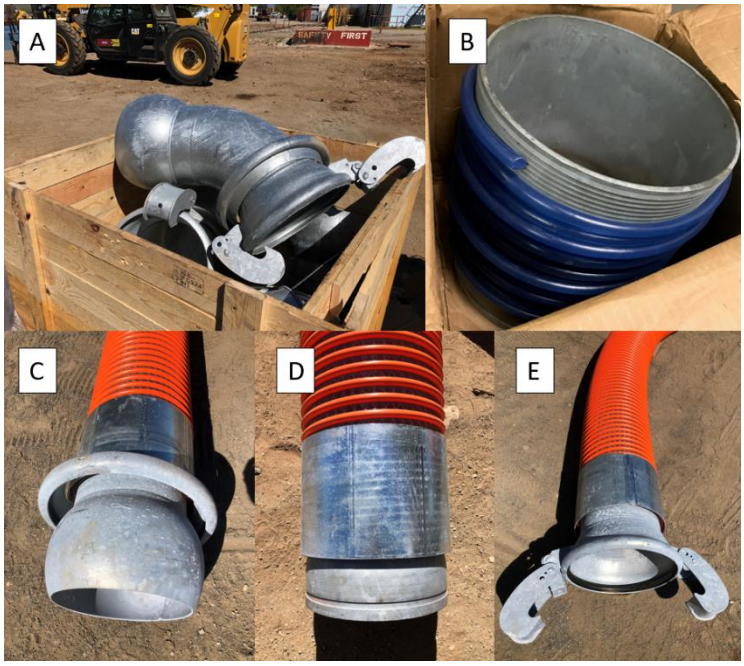

FIG 74 (A) crate with galvanized camlock fittings, (B) banding coil used to crimp fittings onto the ends of kanaflex hose, (C) male camlock fitting on the end of a kanaflex hose, (D) Victaulic groove fitting on the end of one kanaflex hose (bought by SOS Carbon team and sent to Godwin Branch 19 for instalment in a single hose for connecting to the layflat hose, through the hose reel), (E) female camlock fitting on the end of a kanaflex hose.

Kanaflex hoses were the most “lightweight” (200lbs/10ft section + 75lbs fittings on both ends; compared to other hoses of this size/pressure rating) and flexible option available, giving us the best chance of making the needed connections. Still, installing the three consecutive lengths of suction hose needed was physically strenuous and required the entire crew (FIG 75).

FIG 75 (A & B) pilot vessel repositioned for hose instalment, (C) the GC-111 crew wrestling with a section of kanaflex hose, (D) first attempted hose layout with only 20ft of suction hose (this required tight bend such that hose needed to be disconnected from pump for crane to lift inlet out of the water).

The ultimate layout of the 30ft of kanaflex suction hose is shown in FIG 76. The stern dive deck and stairway of the GC-111 proved especially useful for making the necessary bends.

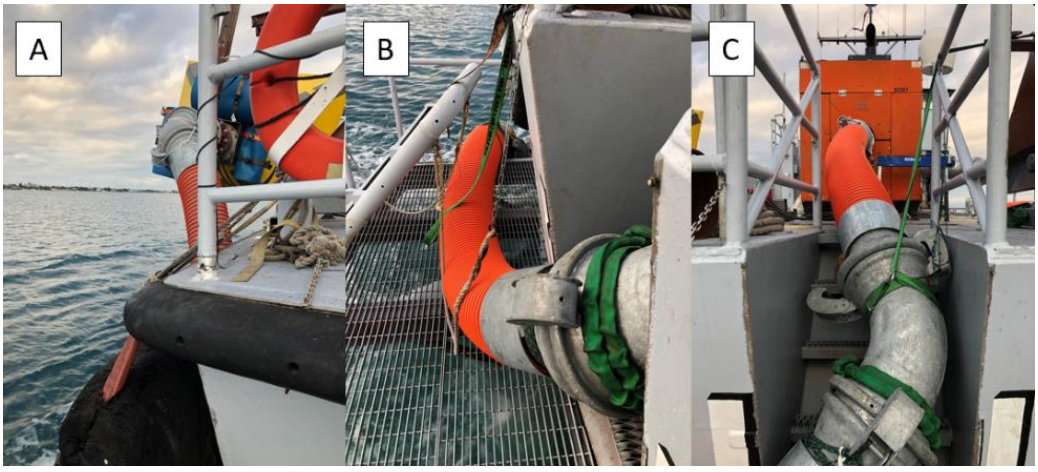

FIG 76 (A) connection from inlet device to the first section of kanaflex hose, (B) second section of kanaflex hose resting on the stern dive deck (secured by ratchet straps), (C) third section of kanaflex hose traveling up the stern stairway and connecting to the pump (secured by ratchet straps).

Note it is not recommended that more than 30ft of suction hose be used (to prevent clogging and cavitation) when installing these systems on other vessels in the future. Using the full 30ft of hose on the GC-111 made it possible to leave the suction hose completely connected (no need to make any connections in the field). The crane arm could move through its full range of motion without comprising any of the suction hose connections.

With the pump hoses installed, the next thing to do was to test the pump and inlet at the mooring (FIG 77). The pump battery was delivered with <12 volts and had to be charged to >13 volts in order with the engine to start – this was a chronic issue throughout testing.

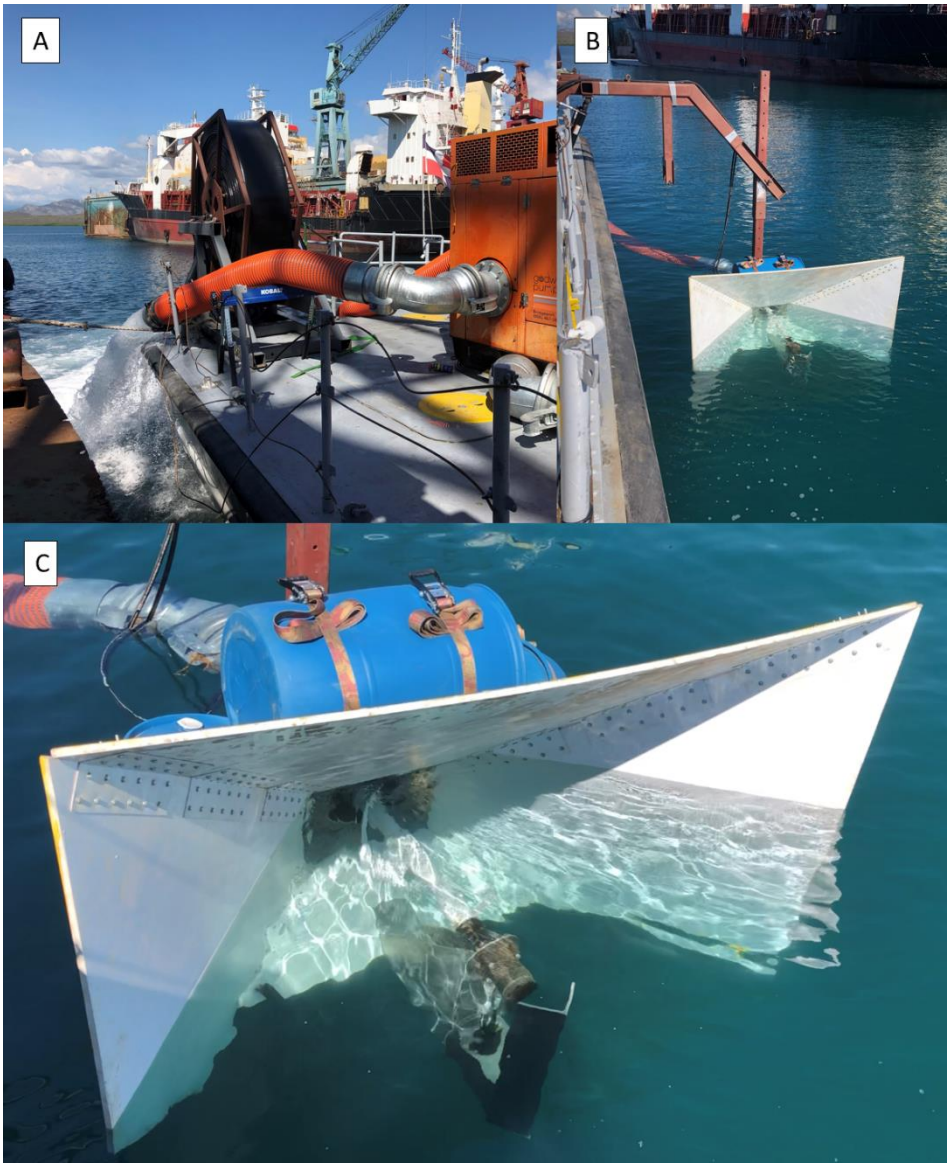

FIG 77 (A) ~5000GPM discharge of the DPC300 during testing at mooring, (B) inlet device deployed during test of pump at mooring, (C) close-up of inlet device, during test of DPC300 pump, showing flowlines inside the funnel.

These tests confirmed that the pump was operating optimally, 1800rpm was determined to be the best engine speed (based on the perceived engine load and reported fuel consumption), and one leak in the suction line was discovered and corrected.

Before the pilot vessel could begin testing, all equipment needed to be secured for excursions outside the protected bay, and into the open ocean. Up until this point, the hose reel and crane had been simply gravity preloaded and secured with ratchet straps. However, for going to the open ocean, equipment needed to be pinned. To this end, the hose reel and crane were designed with 1" OD holes on the square tubing that made up their bases. Pairs of padeyes were to straddle this square tubing, at each hole, and a 7/8" high-strength pin inserted through and secured with a linchpin. There were two types of padeyes designed for this purpose (FIG 78): one was non-adjustable and the other had sets of staggered holes to be used in uneven areas of the deck where non-adjustable padeyes could not line up with the holes in equipment bases. These adjustable padeyes could be moved laterally to ensure that there would always be one combination of holes that aligned and accepted a pin. This worked beautifully and will be extremely useful for installing SOS equipment on ships, in the future. The adjustable padeyes were also removable so they posed no tripping hazard when SOS equipment not onboard - 5058 bolt pads with helicoil inserts were welded to the deck and 3/8" steel angle with staggered holes could be bolted/unbolted thereupon – see FIG 78. Non-adjustable (irremovable) padeyes were only used where pinholes aligned and near the perimeter of the deck where they will not pose a tripping hazard should the pilot equipment ever be removed temporarily.

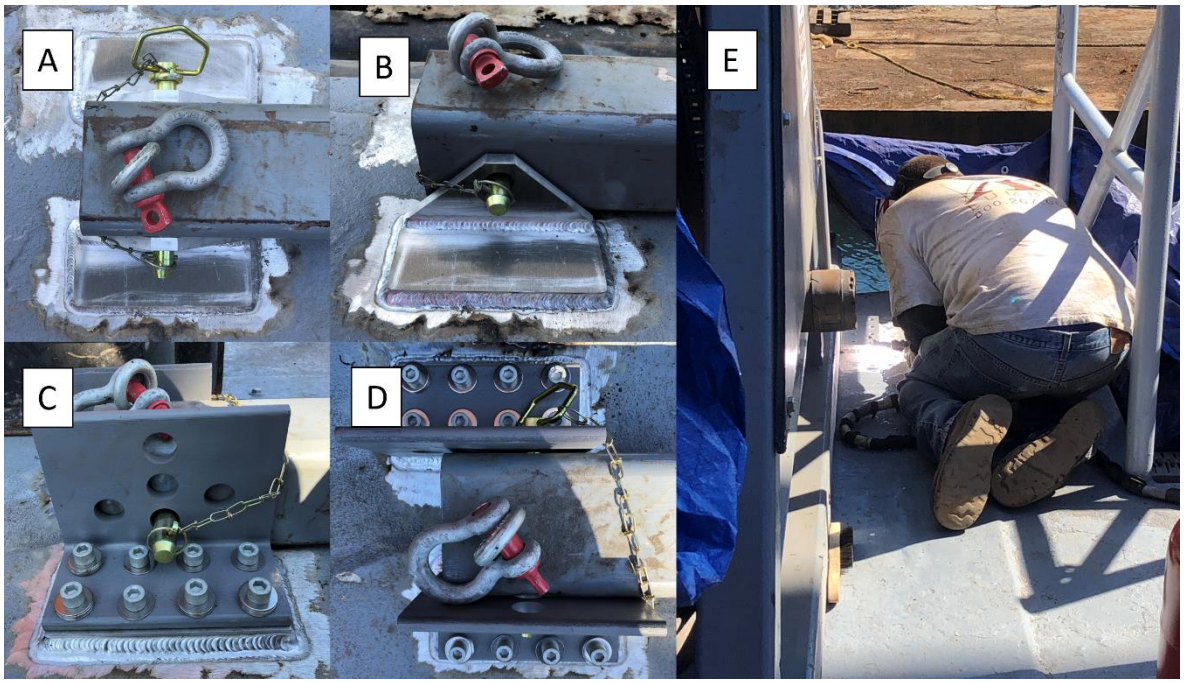

FIG 78 (A) top-down view of a pair of non-adjustable padeyes securing the crane base, (B) side-view of a non-adjustable padeye, (C) side view of an adjustable padeye, (D) top-down view of a staggered pair of adjustable padeyes, (E) Brendan Newton welding a padeye to the GC-111 deck, next to the hose reel base).

The team brought Brendan Newton, from Island View Fabrication, to the DR for 3 days to make the critical welds between these padeyes and the shipdeck (the ship was 5058 Al, so all padeyes and filler were also). Previous welds by a welder from the shipyard were unsatisfactory – the machine used did not have the amperage necessary for full penetration welds and the welder failed to preheat. For Brendan Newton, we secured a larger welding machine, meant for aluminum, and a propane tank with a weed-burner attachment for convenient preheating. Both the hose reel and the crane were pinned at four points. The DPC300 was secured with chains and turnbuckles (FIG 79).

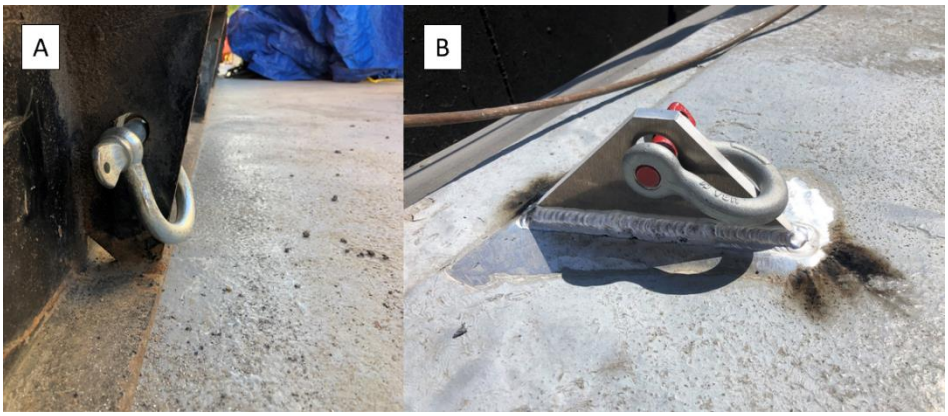

FIG 79 Single non-adjustable padeyes were welded to the GC-111 deck (B) and connected to the skid of the DPC300 (A) with shackles and chains w/ turnbuckles. 4 chains were used in total – one on each corner of the pump.

FIG 80 The team worked past midnight on November 18th to finish welding work and fix a constraint issue with the co-axial auger (notice co-axial device removed; discussed more later on). The team was accustomed to working dawn to dusk, but power usually shut off around 5:00pm. This night, the team rented a generator to run the aluminum welding machine. Also pictured is a local welder sealing a hatch that had been cut to remove the engine for repairs at one time.

The team contributed to the general well-being of the ship by installing new railings, replacing the bow anchor control valve, and sealing a hatch in the stern deck that had been cut to remove the engine for repairs at one time in the past (FIG 80).

One of the last tasks, before the pilot vessel was ready for testing, was to install the hydraulics for controlling the three functions: hose reel, crane, and auger. A 3-spool valve was used for all controls. The valve tapped from the 12GPM stage of the pump, through ¾" JIC that we fit with quick disconnects (the other two stages of the pump were shorted). ½" hose lead to all functions. All functions operate separately so plenty of power/flow was always available to each (except for when we forgot to turn the inlet auger off, which sapped fluid power from the crane cylinders – this was easy to notice and fix). All motors and cylinders had quick disconnect fittings and rubber caps for quick removal and safe storage. The control valve was mounted on the bow-starboard corner of the crane base (FIG 81) as it was a vantage point for all functions.

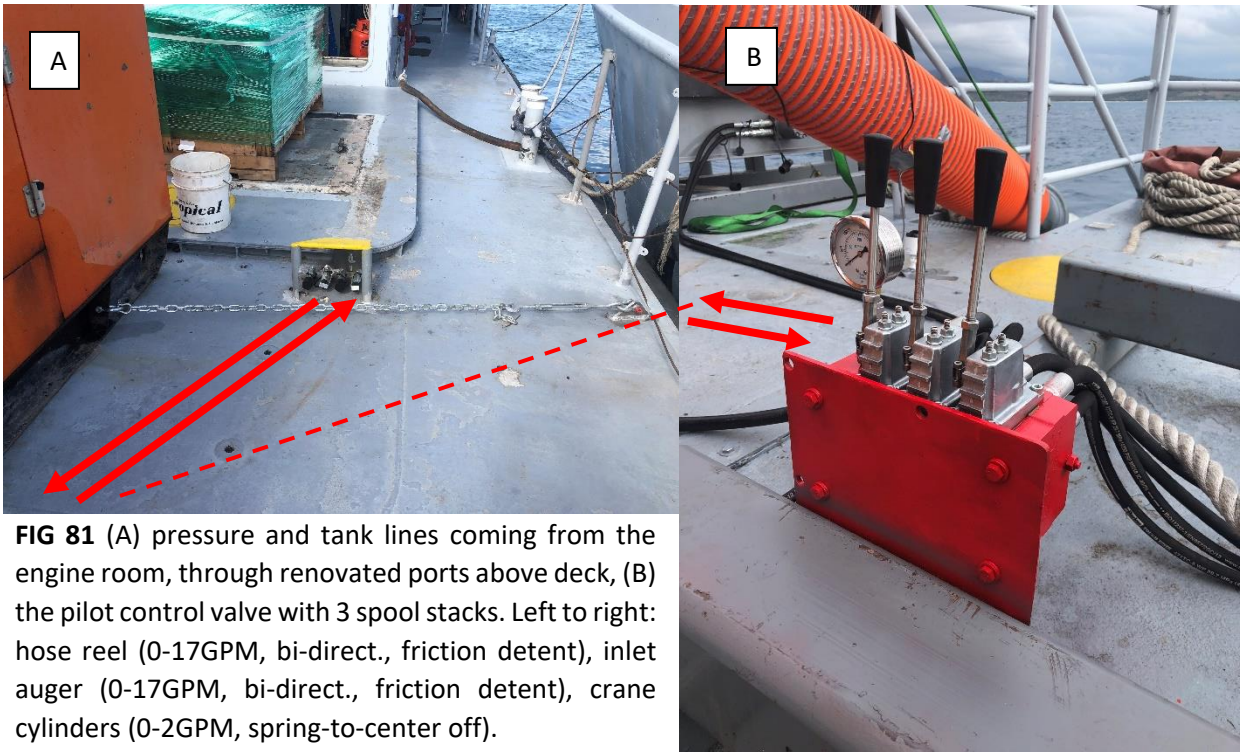

FIG 81 (A) pressure and tank lines coming from the engine room, through renovated ports above deck, (B) the pilot control valve with 3 spool stacks. Left to right: hose reel (0-17GPM, bi-direct., friction detent), inlet auger (0-17GPM, bi-direct., friction detent), crane cylinders (0-2GPM, spring-to-center off).

The last task to complete, before testing could commence, was to install and adjust the buoyancy of the inlet device. In order to wave-follow reliably heavy hydrostatic preload was required. The coaxial inlet device and z-axis together weighed about 800lbs and required ~100 gallons of water displaced to float with the central axis of the coaxial inlet 18" below the still water line. This was accomplished with empty, cylindrical 55- and 30-gallon tanks (we brought

plenty – bought second hand vinegar tanks in Bow, NH) rachet strapped and tightened into vees formed by the inlet funnel panels and aluminum plates welded onto the funnel sandwiching brackets (these plates had slots at the bottom of the vees that the straps ran through). See FIG 82. This kinematic constraint, and heavy preload from the straps, kept the barrels from moving and loosening the straps. We used two 55-gallon tanks, one horizontal on the top funnel panel, and one on the outboard side, and one 30-gallon tank, on the inboard side. The tanks were sealed with silicone sealant as they were easily crushed by the ambient hydrostatic pressure without it. The center of the 55-gallon tank coincided with the still water line (this worked out nicely, but if it didn't we could have added solid ballast or let water into the tanks). This provided a waterline area of 800in^2 from the tank – which was evidently plenty of hydrostatic stiffness given the inlet could wave follow very reliably even in short-wavelength waves. The z-axis post was kept greased with water-proof, tacky chain grease to reduce resistance to the linear sliding motion when wave-following.

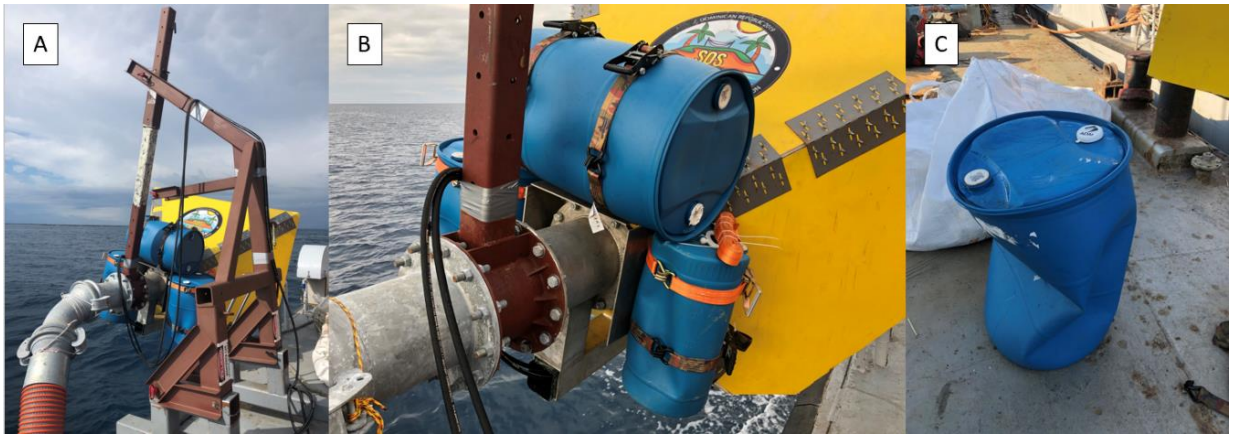

FIG 82 (A) crane and coaxial inlet in the "up" position on the portside of the GC-111 during transit (note the yellow chain grease on the z-axis for reducing resistance to linear sliding during wave-following), (B) close-up of the suction hose/z-axis/inlet device 12-bolt connection (note the 55-/30-gallon tanks strapped into vees formed by the funnel panels and aluminum plates), (C) a tank that wasn't properly sealed with silicone and was crushed in operation by hydrostatic pressure.

Just as everything was ready to begin open-ocean testing with sargassum, the construction had run into early December. Because sargassum landfall usually dwindles during December/January/February each year (while, increasingly, it is becoming a year-round problem), there were no large mats of sargassum to test on. Not only that, but it was difficult to find enough sargassum to make our own mat (our plan B was to fill a DR navy landing craft ship with a truck-full of sargassum and "create" a mat in the bay at the navy base). A researcher at a French satellite company CLS, told the team that they expected to see sargassum landfall near Pedernales, near the border between the DR and Haiti. Luke and Pedro drove from Las Calderas to Pedernales looking for/asking about sargassum in every town/village (FIG 83). Despite many promising leads and many helpful fishermen/motorcyclists, they did not bring any sargassum back.

FIG 83 (A) Pedro talking to locals outside Barahona, (B) a trash-laden beach near Pedernales, (C) a beautiful beach near the bay of Ocoa, (D) a typical path taken from the main road to the beach in the undeveloped area between Las Calderas and Haiti.

Fortunately, Punta Cana does receive sargassum year-round and we were able to drive several truckloads of sargassum from Punta Cana to the navy base, on several occasions, to finish testing (FIG 84). This sargassum (because there was precious little) was thrown from the ship, directly into the inlet. The results section will discuss future plans for more tests with real, wild mats of sargassum.

FIG 84 (A) a truckload of sargassum delivered to the navy base, from Punta Cana, for pilot tests (this was done several times), (B) close-up of sargassum delivered from Punta Cana to the navy base, showing freshness (sargassum was always collected and brought the evening before tests), (C) the GC-111 crew helping to jettison sargassum overboard during testing.

Before getting into test results, it is important to, at some point, document life at the base during these months of construction. FIG 85 shows the barrack accommodation and a typical meal (plantains and meat). The SOS Carbon bought groceries for the ship so that everyone was eating well through the duration of the project (work involved long grueling days of manual labor).

FIG 85 (A) SOS Carbon team room in the barracks at Las Calderas, (B) common corridor in the Las Calderas barracks, (C) a typical dinner on the GC-111: plantains and meat.

6.5 Lessons Learned

Not everything went as expected/planned when building the SOS Carbon Pilot. Enumerated here are mistakes/misfortunes, and how they were resolved.

1. **Co-axial auger constraint:** The coaxial auger was designed to be cantilevered from the White Hyde motor shaft to avoid putting a support bearing in the suction pipe, in the path of water and sargassum. While the bearing set in these motors was strong enough to support these loads, it and the coupling connection was not stiff enough to prevent the auger from impacting the inside of the pipe – a misjudgement likely due to an optimistically low eccentric load assumption in design calculations. The impacting steel auger cut the inside of the schedule 40 aluminum pipe, creating a terrible noise and prompting fear that it would continue to cut until the pipe had lost all structural integrity. Therefore, in the end, the team decided to install a support bearing, inside the pipe, on the previously cantilevered end of the co-axial auger (see FIG 86 for more detail). This was a quick fix, and didn't seem to cause any outstanding clog risk during testing. This sort of design is thus recommended for a production device.

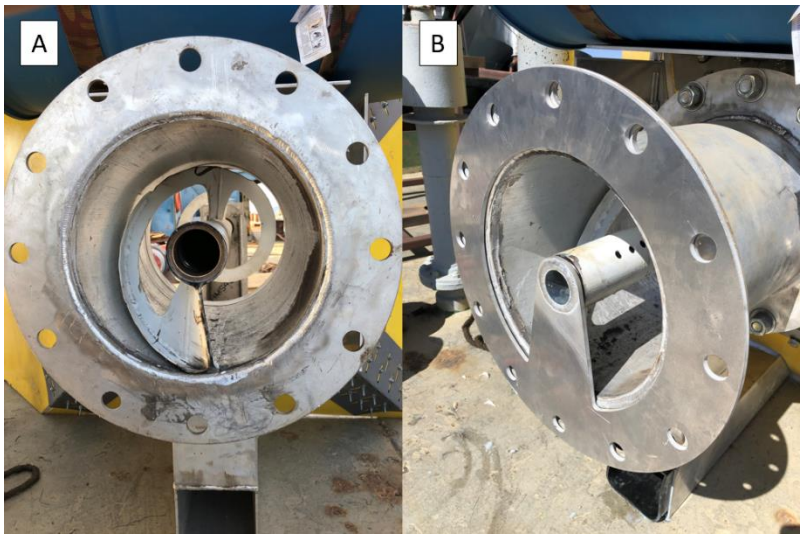

FIG 86 (A) The cantilevered end of the co-axial auger before the support bearing was added (note the damaged interior of the aluminum pipe from the impact of the unsupported steel auger). (B) The support bearing comprised a simple waterjet piece of aluminum that was caulked and bolted between the inlet device and the z-axis. The plate supported an oil-impregnated bushing that inserted into the center tube of the previously unsupported end of the co-axial auger.

The learning lesson here is to never cantilever a rotating object with tight clearances unless you are quite confident in your model of stiffness and input loading (eccentric and other).

2. **Custom fitting installment:** A custom fitting in the end of the layflat hose enabled us to bolt it to the center of the pilot hose reel and also connect the kanaflex discharge hose (from the pump) to it, using a victaulic groove/clamp connection. This custom fitting was made by Hammerhead Industrial Hose as it was just a slight modification to one of their off-the-shelf layflat hose fittings. See FIG 87 for more detail

on hose this connection was made in operation. The function of this modification worked perfectly. It was installing these fittings where the team ran into some trouble.

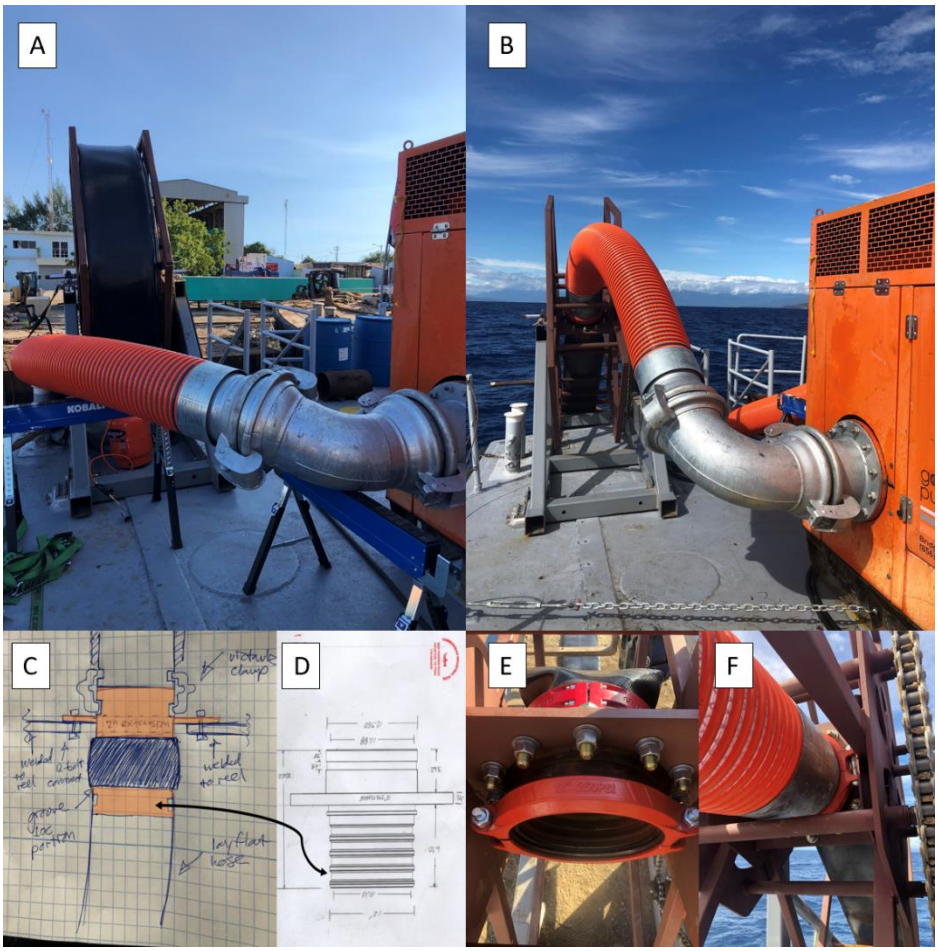

FIG 87 (A) the pilot at mooring with the layflat hose completely reeled up and the discharge kanaflex hose from the pump left disconnected, (B) the pilot vessel at sea with the layflat hose completely unreeled and the discharge kanaflex hose connected to the layflat hose via a custom fitting in the center of the hose reel, (C) L. Gray's original drawing indicating the changes needing to be made to the layflat hose vendor's off-the-shelf hose fitting, (D) the layflat hose vendor's dimensioned drawing for the custom fitting, showing how an off-the-shelf hose fitting would be cut and a ¾" 12-bolt IPS flange would be welded in the middle, (E) a close-up of the custom layflat hose fitting, bolted to a plate in the center of the hose reel, with a Victaulic groove/clamp extending from the opposite side such that the kanaflex discharge hose (from the pump) could be connected, (F) a close-up of the connection between the kanaflex discharge hose and the 200m layflat hose, via the custom layflat hose fitting bolted to the center of the hose reel.

Hammerhead Industrial Hose insisted all that was needed to insert the barbed end of the fitting into the layflat hose was a small amount of P-80 emulsion (a lubricant that turns tacky when dried so it does not compromise the tension load capacity of the connection). The SOS Carbon team acquired this

lubricant, but quickly ran out when it was discovered that it was taking too much time to even get a starting length of hose onto the barbed end (the emulsion turned tacky after just a few minutes). Hammerhead believed we had received a slightly undersized hose and that usually is shouldn't be so difficult to install the fitting. Nevertheless, the team began pursuing other options (FIG 88). It took 2 full days of different tactics – brute force, differential heating, many different tools, many different maneuvers, increasing amount of other lubricants – until the fitting was installed (the farther the barbed fitting was inserted, the more friction the team fought, and the harder it was to keep inserting).

FIG 88 (A) Folkers Rojas pouring boiling water around the custom fitting in an attempt to stretch the end of the layflat hose, using the thermal expansion of the metal fitting, such that there might be more clearance when the system came back to equilibrium, (B) the GC-111 crew applying brute force to try to coax the layflat hose onto the custom fitting, (C) the custom fitting completely installed in the end of the layflat hose, (D) the groove-loc collar securing the custom fitting inside the layflat hose.

In the end, Hammerhead revealed that they have a special tool called a "hose expander" that opens up the ends of the hoses such that barbed ends are inserted more easily. They failed to mention this up until that point and insisted we would be able to do this assembly, ourselves, in the field.

The learning lesson here is to never trust vendors when they tell you that you can perform assembly on their parts that they themselves normally perform in house, using special tools.

3. **Crane cylinder retrofit:** Originally, the cylinders driving the rotation of the crane were 2" bore 3000PSI Prince tie-rod cylinders with 18" stroke (B200180ABAAA07B). These cylinders were donated by a local engineer in New Hampshire. The previous owner had elected to remove the stock clevis ends from the rods and install spherical/self-aligning ends (see FIG 89). The kinematic design of the crane arm was based on the retraced and extended length of these specific cylinders.

Because the crane lost its mechanical advantage near the top of its range of motion, the original 2" cylinders were replaced with 2.5" bore 3000PSI Prince tie-rod cylinders, also with 18" stroke

(B250180ABAAA07B), to ensure that the inlet device could always be lifted from the water, even if water had entered the floatation tanks (adding weight to the lift).

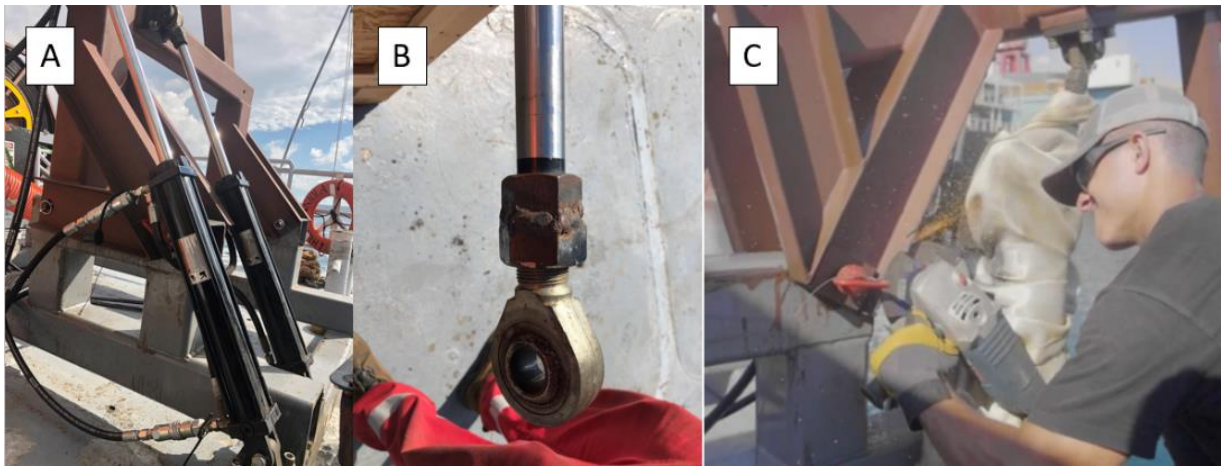

FIG 89 (A) the pair of tie rod cylinders driving the rotation of the crane arm, (B) the spherical/self-aligning rod-ends installed in the tie-rod cylinders, by the previous owner, (C) L. Gray creating extra clearance for the larger 2.5" bore tie-rod cylinders that were installed.

The challenge with installing the larger cylinders was that, although the 2" and 2.5" cylinders were from the same product line, from the same manufacturer, and had the same stroke (18") and retracted length (28 ¼"), L. Gray did not account for the ~¼" increased retracted length that was afforded by the spherical rod-ends the previous owner had installed on the 2" cylinders, which the crane arm had been designed around. Because of this mistake, the range of motion of the crane arm, with the newly installed 2.5" cylinders, was slightly less than it has been previously. Because the system had been designed to require the full stroke of the cylinders, the safety pinholes, meant to secure the crane in the upright position, no longer lined up sufficiently to insert a pin.

The solution to this problem was to remove the custom spherical rod ends from the 2" cylinders and put them onto the new 2.5" cylinders, to recoup the lost ~¼". This required considerable effort as these spherical ends had not been made to be removed and, unfortunately, required that flats be ground into the rod of the 2" cylinders (making them non-functional).

The learning lesson here is that half a day of construction was wasted panicking about a problem that could have been prevented with just a few minutes of careful planning months earlier. Be careful when recycling old parts and designing your whole system around them – especially if those recycled parts have been modified by the previous user. It also would have been advisable to use a cylinder with a longer stroke, anyway, so that the ~¼" deficit did not create such a big problem (it is also safer to keep cylinders from being loaded when fully extended).

6.6 Pilot Test Results

The final product of the SOS Carbon Pilot tests is nicely captured in FIG 90, below.

FIG 90 An in-situ SOS Carbon system for pumping-to-depth floating sargassum in the open ocean, which was tested in the Dom. Rep. in Fall 2019. The system shows how an SOS Carbon pump-based system can be deployed on a vessel of generic design (no specialty vessel required).

The SOS Carbon Pilot vessel accomplished all its critical goals:

- Pilot vessel construction finished
- System tested 4 consecutive days
- ~15m^3 sargassum pumped-to-depth
- DR Navy crew trained to operate independently
- Several system improvements made (to be discussed)
- Energy consumption (<10MJ/m^3) confirmed (less than $0.20 diesel/m^3 sargassum)

The SOS Carbon Pilot vessel was completed on December 2nd, 2019 and a week of tests ensued with truckloads of sargassum delivered from Punta Cana several times. These tests, and all previous tests until that point, were recorded by a security camera system installed, for this purpose, on the GC-111, by the SOS Carbon team (FIG 91).

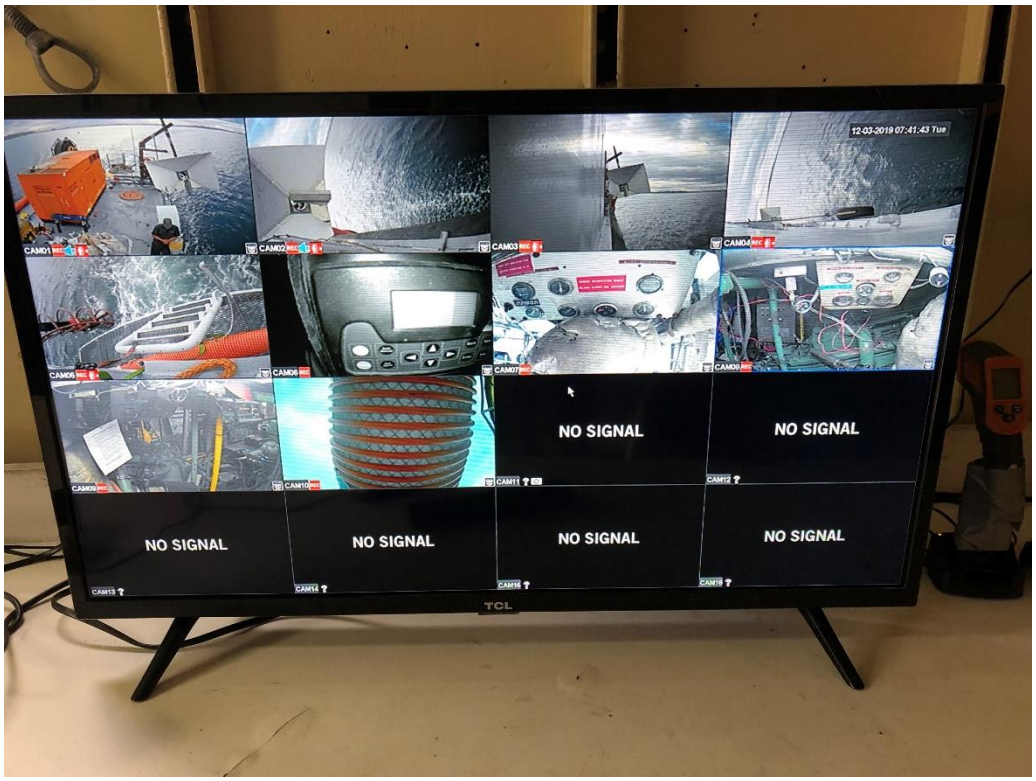

FIG 91 A security camera system ("NightOwl") of 10 cameras installed around the GC-111 for the purpose of recording all construction and testing of the SOS Carbon Pilot.

Throughout these days of testing, the pilot system consistently showed that it could pump sargassum to depth at a very high solids concentration (FIG 92 & 93) without ever experiencing a single clog in the pump volute or inlet auger.

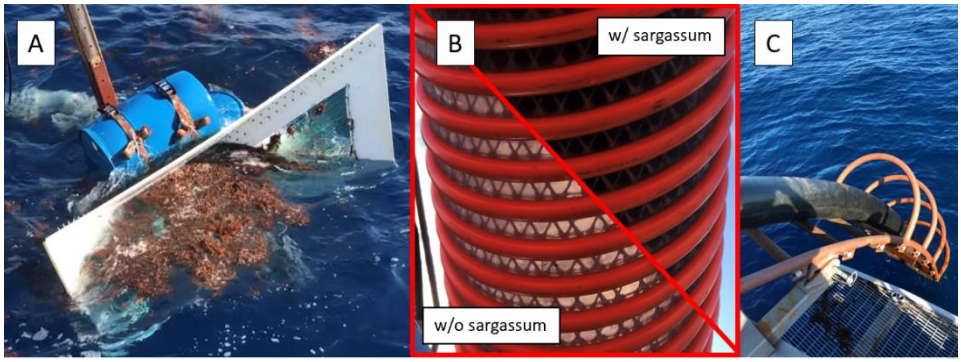

FIG 92 (A) sargassum entering the co-axial auger inlet device, (B) sargassum (dark region) flowing through the kanaflex suction hose at ~4m/s velocity, (C) the 200m layflat hose completely deployed, with 5000GPM of seawater and sargassum flowing through it.

FIG 93 Snapshots of the kanaflex suction hose over a range of times during a single test, showing the consistently high solids concentration achieved without any clogs.

The team learned that solids concentration is maximized when the co-axial auger operates at ~60rpm such that sargassum is fed rapidly, but that the auger does not spin so fast that the repulsive centrifugal flow, from the auger acting as a paddle, does not hurt feed efficiency (this was determined with the 12” OD, 30” pitch, spoked auger).

The GC-111 crew was able to consistently deploy all equipment and safely make the connection between the pump discharge hose and the 200m layflat hose (at the center of the hose reel), even in the open ocean (FIG 94).

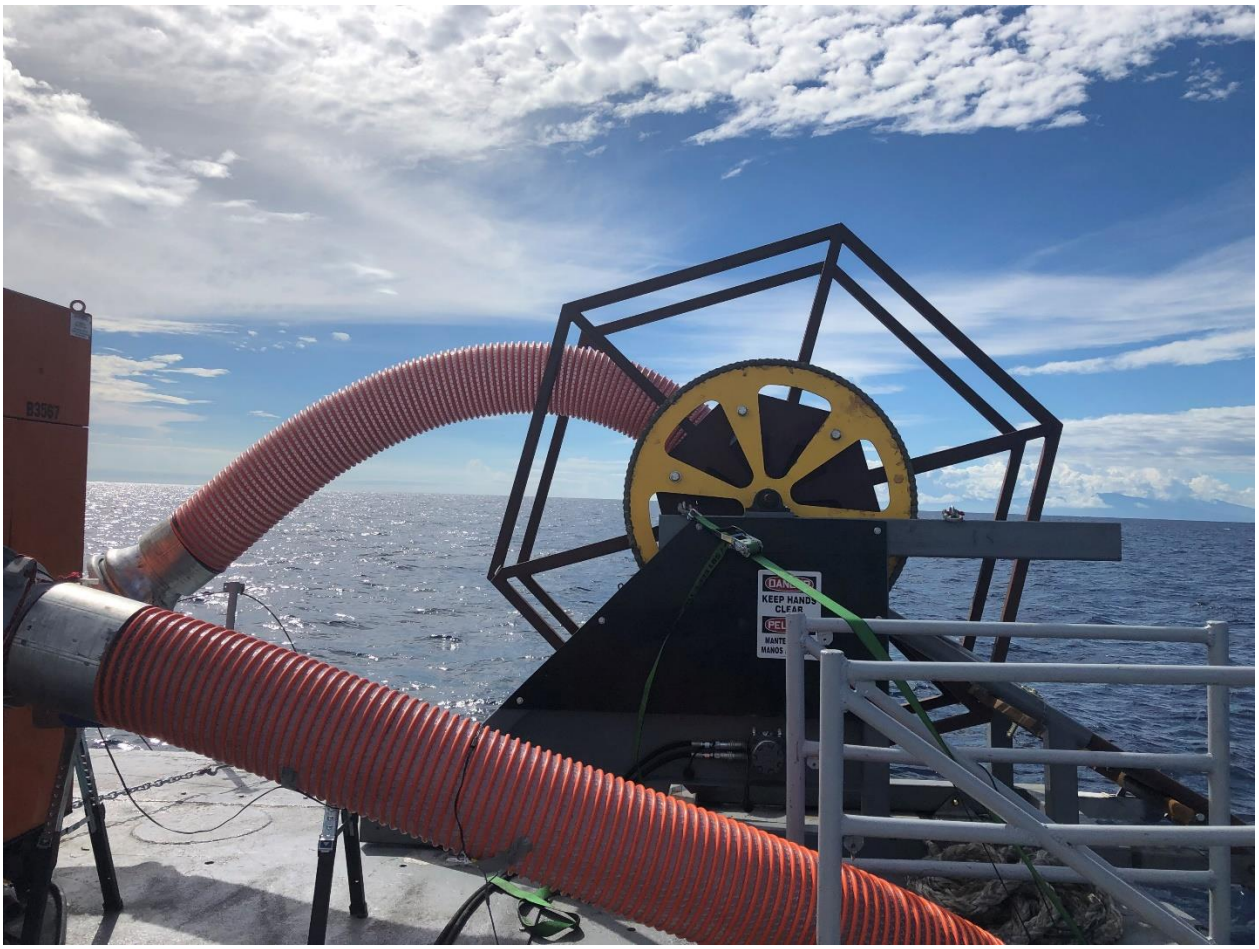

FIG 94 Hose connections made successfully during first open ocean tests.

In addition to accomplishing its goals, the team also made a critical improvement to the inlet funnel. Because the funnel was originally made from solid, ¾" marine plywood, it displaced a large amount of seawater as it wave-followed, plunging in and out of the water. In high waves, water exiting the inlet region as the wedge-like top panel plunged into the water, flowed around the edges of the funnel to fill the void left on the opposite side of the top panel. This manifested itself as vortices formed near the edges of the funnel, at the free surface of the ocean, that tended to pull sargassum out of the inlet region with it – obviously not an ideal characteristic of the funnel, even if it only afflicts the system in high waves.

The remedy to this loss of efficiency was to make the funnel pervious to water, to the greatest extent possible, without compromising structural integrity. This was done by cutting windows in the solid funnel and then covering the windows with a tight-knit, radially symmetric weave of high-strength fishing line. The weave was made radially symmetric about the coaxial inlet's central axis, as opposed to making a fishing-net-like mesh, so that sargassum would not get caught – it would be conveyed directly towards the suction inlet. This modification already existed as a contingency and the tools/parts to make these modifications had already been

acquired. The team started with making the modification to one side and, when it proved to work, the modification was made to the other side as well (FIG 95). This modification took ~2hrs per side.

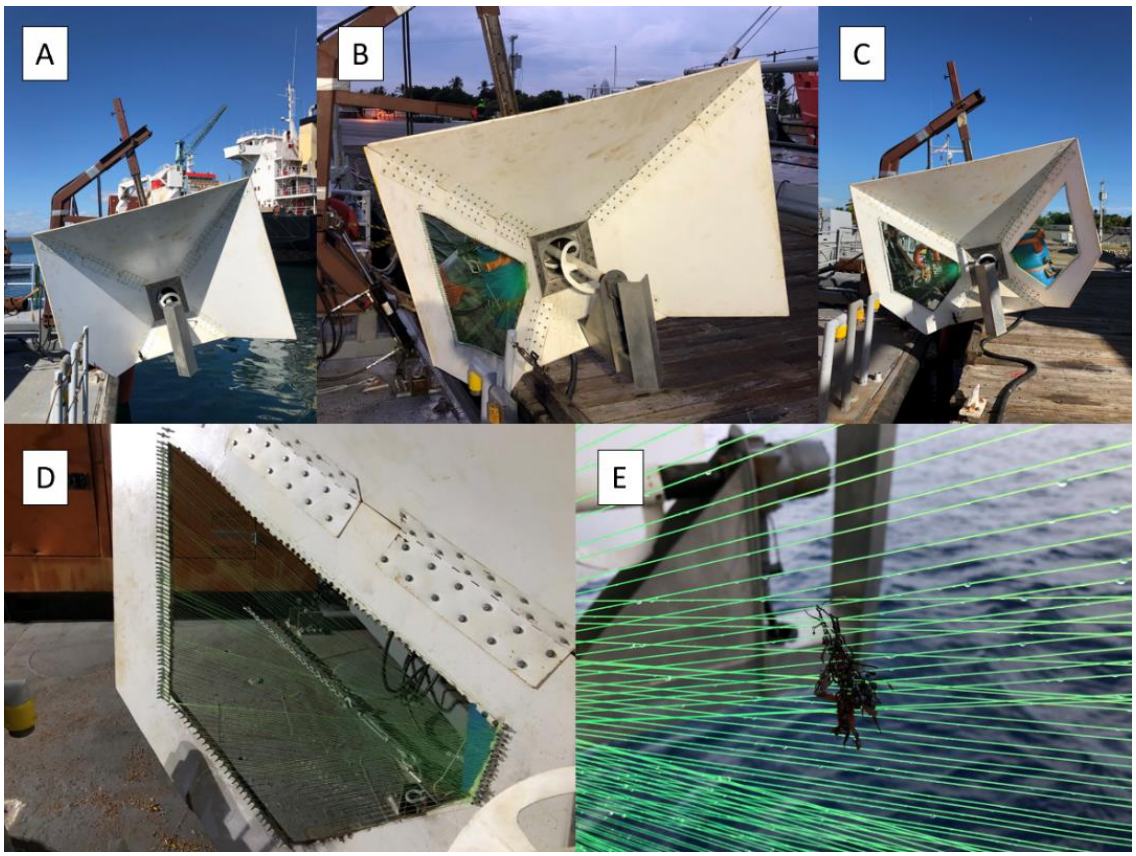

FIG 95 (A) solid funnel prior to pervious modification being made, (B) the funnel with one side made pervious, (C) the funnel with both sides made pervious, (D) a close-up of the radially symmetric weave of high-strength fishing line, (E) a close-up showing the tightness of the weave of fishing line, compared to a small fragment of sargassum left after testing one day.

The pervious modification was very effective at eliminating the vortices and the associated detriment to feed efficiency in high waves (FIG 96). The change reduced the hydrodynamic forces on the funnel, which is good for longevity as well. It is recommended funnels always be designed to be pervious in the future.

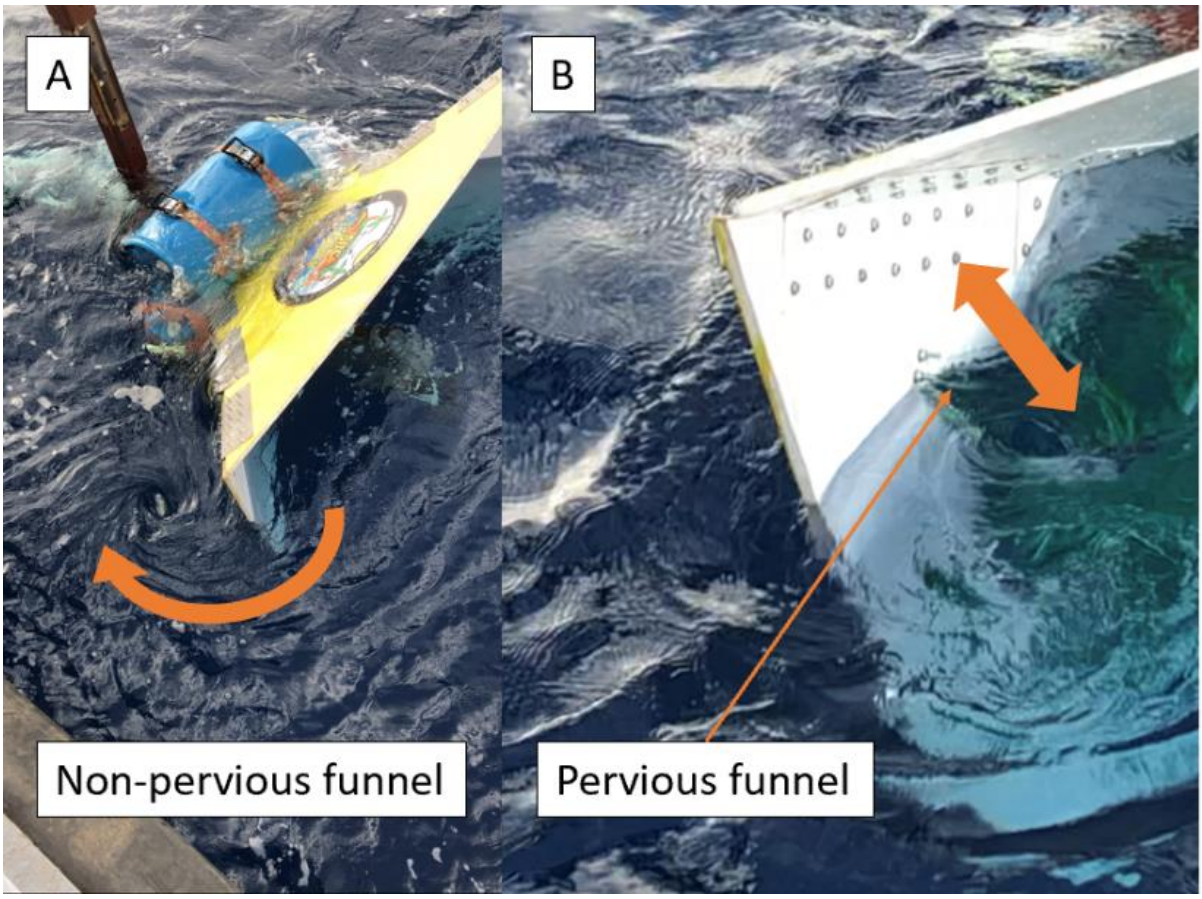

FIG 96 (A) The coaxial inlet device funnel before the pervious modification was made. A vortex can be seen forming just outside the funnel, which tended to pull sargassum out of the inlet region. (B) The coaxial inlet device funnel with the pervious modification made. After this modification, the funnel no longer suffered from the negative impact of vortices.

The final update to SOS Carbon Pilot donors happened on January 17th, 2020, in the Banco Popular headquarters, in Santo Domingo, DR (FIG 97). Donors were quite pleased with the results and the discussion centered around how this technology is to be scaled.

Banco Popular hired a videographer to visit the navy base to take drone and other professional footage, during project milestones, and produced a very professional promotional video for the project (FIG 98).

FIG 97 Banco Popular headquarters in Santo Domingo, Dominican Republic.

FIG 98 A promotional video of the SOS Carbon Pilot vessel project, created by Banco Popular, the lead pilot donor. The video is currently posted at: **https://app.frame.io/presentations/28933801-9175-49cf-a2b1-5e82c27eb9ef**

A special thanks is owed to the Dominican Republic Navy and the GC-111 crew. They lived and breathed the construction of the pilot vessel with the MIT team. They endured long, hard days of grueling manual labor. They also contributed to solving many of the issues we had during construction. FIG 99 shows a picture of the GC-111 returning from its final day of testing and the GC-111 crew celebrating after a good day of testing.

FIG 99 (Top) the GC-111 returning from the final day of SOS Carbon Pilot testing. (Bottom) The GC-111 crew celebrating after a successful test.

7. Patent Specifications (Detailed Technology Description)

The SOS Carbon team filed 3 provisional patents over the course of a year, each covering exclusive developments. MIT (Trademark and Licensing Office and the Department of Mechanical Engineering) waived all rights to the intellectual property after some deliberation over whether or not MIT could see itself effectively prosecuting/licensing/litigating such a patent. After the SOS Carbon Pilot tests, the inventors (L. Gray & A. Slocum) filed a Patent Cooperation Treaty (PCT) application with the USPTO. Included hereafter are the figures, specifications, and claims that

The entire family of inventions produced by the inventors is vast, and captured in the tree in FIG 100 (not meant to be readable, but rather illustrate the extent of ideation; for which prior art has now been generated, but not claimed as only a select few are preferred embodiments).

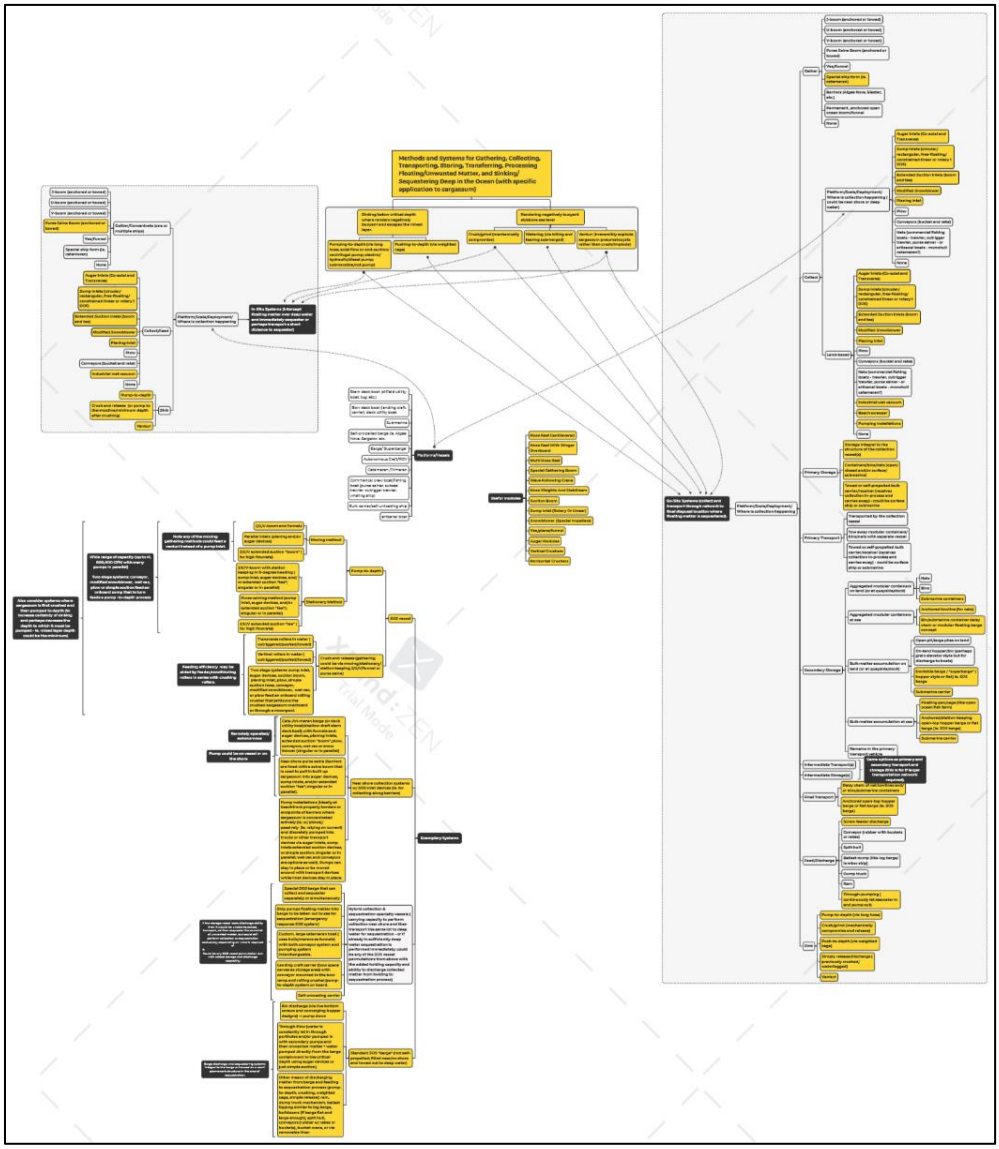

FIG 100 The complete taxonomy of all ideas related to SOS Carbon's technology.

7.1 Utility Patent Specifications

METHOD AND MECHANISM FOR COLLECTING FLOATING BIOMASS AND SEQUESTERING IT IN THE DEEP OCEAN

FIELD OF THE INVENTION

The present invention relates to methods and mechanisms for collecting floating biomass (or other unwanted matter) and sequestering it at great ocean depths to prevent its harmful effects and also essentially permanently sequester its carbon. This submission describes several methods and mechanisms developed to address the inundation of Caribbean beaches by pelagic sargassum, a type of holopelagic macroalgae that has been growing in unprecedented quantities and causing much economic, social, ecological, and environmental damage in the region.

STATEMENT REGARDING FEDERALLY FUNDED RESEARCH

This invention was made without US government support.

BACKGROUND

BACKGROUND IS REDACTED BECAUSE ALREADY INCLUDED IN SECTION 2

OBJECTS OF THE INVENTION

The primary method described herein for sequestering sargassum is to gather and pump sargassum to a critical depth in the ocean at which its pneumatocysts (air bladders responsible for its buoyancy) are sufficiently compressed such that the sargassum becomes negatively buoyant and continues sinking on its own. This method is hereafter referred to as “pump-to-depth” (IPD). This critical depth of about 150-200m also happens to exceed the mixed layer of the Caribbean (90-110m depending on the time of year) so that sargassum will not be carried back up to a depth where it may become positively buoyant again (the compression imposed by hydrostatic pressure at the critical depth of 150-200m does not necessarily irreversibly rupture the sargassum pneumatocysts – this would require a much greater depth and much more pumping energy expenditure).

Accordingly, the following objects of the invention include:

A principal object of this invention, therefore, is to provide a simple, low-cost system to intercept sargassum in the open deep ocean and collect and pump-to-depth where it will remain in stasis for eons thereby effectively sequestering the carbon it has absorbed from the atmosphere and the excess nutrients and heavy metals from oceans polluted by human activities.

A further object of the invention is to direct the sargassum in-situ, by one of various funneling or booming techniques, into the intake of a centrifugal or axial flow pump, the output

of which is connected to a hose or pipe that projects either into a container for collection, transport, and later pump-to-depth, or pump it directly down to a critical depth at which the sargassum will keep sinking, on its own, to the bottom of the ocean.

A further object of the invention is to use augers/screw conveyors of various designs and orientations (transverse and/or co-axial with the pump/suction inlet) to controllably feed pump inlets to prevent clogging and optimize feed efficiency.

A further object of the invention is to use spring-loaded containment, serration/interrupted flighting, and compliant materials to prevent the wedging of jetsam/flotsam in auger flighting.

A further object of the invention is for the auger systems to deliver the material collected to sharp blades to reduce the size of individual solids entering the collection pumps.

A further object of the invention is to use a sump, wherein seawater and sargassum flows over a weir at a prescribed depth, to better direct suction at the surface where sargassum is, collect the sargassum, and meter its flow into a pump inlet.

A further object of the invention is to make said sump wave-following by free-floatation or a linear and/or rotary 1-2 degree of freedom system with appropriate hydrostatic preload, stiffness, and damping to keep the sump weir at an appropriate depth below the free surface of the water, such that the sump does not run dry and provides consistent, high solids concentration to the pump inlet, in a wide range of sea states and headings.

A further object of the invention is to use a long suction hose/pipe with inlets distributed along its width/length, such that it acts as both a suction device and a collection boom and enables the utilization of pumps with very high flowrates.

A further object of the invention is to use a conveyor mechanism to collect and transfer sargassum out of the water into a container, pump inlet, or rolling crusher inlet.

A further object of the invention is to use a solid funnel or wire/cable/string woven into a funnel frame immediately around the suction inlet to reduce leakage and improve suction feed efficiency. The funnel may comprise various configurations including concentrating, planing, scooping, vertical, or hybrid.

A further object of the invention is to use a vacuum with the various inlet devices, in place of a pump, for the purpose of collection of sargassum and discharge from the vacuum into a container for later pumping the sargassum to be sequestered in the deep ocean.

A further object of the invention is to use satellite imagery in combination with Lagrangian particle tracking models to optimize the path of ships performing the collection of sargassum.

A further object of the invention is to use benthic current modeling to predict the final resting place of sunken sargassum.

A further object of the invention is verification of the collection and sinking of sargassum by a fleet of ships at appropriate locations and to sufficient depth. This might be done by a combination of satellite imagery (visible and/or NIR), video surveillance, or sonar survey.

A further object of the invention is to separate the collection and sinking activities such that, for example, sargassum is collected near shore and then transported to the open ocean to be sequestered.

A further object of the invention is a special barge capable of storing collected sargassum, transporting it to sufficiently deep water, and discharging or otherwise feeding it to a system that executes one of the aforementioned sequestration methods. Such a barge may be fully integrated with equipment such that it can be towed by any ordinary tug/mover (or perhaps have its own propulsion ability).

A further object of the invention is to use hopper walls (perhaps designed for mass flow of sargassum) and fully live or partially live screw feed bottoms in the aforementioned special barge to discharge sargassum and feed it to a pump, that in turn executes pump-to-depth of the previously collected, stored, and transported sargassum.

A further object of the invention is to continuously, passively allow the entry of water, or actively pump water, into the aforementioned special barge while simultaneously pumping the sargassum and seawater mixture out of the barge, to the critical depth.

A further object of the invention is the use of stern-deck boats (oilfield utility boats, crew boats, tugs, etc.) and bow-deck boats (landing craft ships, self-unloading ships, etc.) to deploy the aforementioned gathering, feeding, and pumping systems.

A further object of the invention is the use of catamaran or trimaran barges, deck utility boats, and/or other low-draft stern-/bow-deck boats with aforementioned pump inlet devices to perform near-shore collection (and storage/transport) of sargassum.

A further object of the invention is the use of specialty hybrid boats that can collect, store, transport, discharge/feed, and sequester sargassum (perhaps using independent, interchangeable systems) so that sequestration can happen in-situ or ex-situ with the initial collection.

A further object of the invention is hybrid vessel is a catamaran that uses is hulls as funneling structures for sargassum and comprises a reconfigurable member between the hulls that can act as a conveyor for collection (when pitched down so that the front edge is in the water; negative angle of attack) and later sequestration, or as a planing pump inlet (when tipped up so the back edge is in the water; positive angle of attack) for immediate sequestration.

A further object of the invention is to use rolling crushers or venturi vacuums to irreversibly compromise sargassum pneumatocysts such that sargassum will sink by itself, from the surface, without being actively transported to the critical depth.

A further object of the invention is to move the sargassum down where the depth of the water is at least 1 km deep where it has escaped the photosynthetic layers of the ocean.

A still further object, therefore, is to intercept the sargassum over waters that are deep enough such that intrinsic carbon or any greenhouse gases (GHGs) resulting from any decomposition will not rise to the surface, but will rather for example become frozen hydrates or remain dissolved in the deep ocean waters without being transported by ocean currents or oceanic food chains.

Other and further objects will be explained hereinafter and more particularly delineated in the appended claims.

SUMMARY

In summary, in the preferred embodiment of the present invention, concentrations of floating sargassum are identified and the path of travel driven by currents predicted such that vessels can be deployed to intercept and pump sargassum directly down to critical depth at which it becomes negatively buoyant (due to hydrostatic pressure at the critical depth sufficiently compressing its bladders/pneumatocysts) so that it continues sinking to the bottom of the ocean. A ship deploys booms or funnel structures to gather and guide the sargassum towards pump inlet devices, which may comprise vees, planes, scoops, long lengths of hose/pipe with distributed suction, weirs, and/or various designs of augers to prevent clogging and provide a controlled infeed rate to one or more pumps, such that the sargassum can be directly pumped, through a downward deployed pipe or hose, to a critical depth at which it will continue to sink to the bottom of the ocean. If the sargassum is not over deep water, or in an area otherwise preventing sequestration, such as in a harbor or along an offshore barrier or beachfront, sargassum is first collected by using one of the aforementioned pump inlet devices, mounted to a variety of deployment vessels, or by other means, and deposited into a container, such as a barge, and then transported to a sufficiently deep area of the ocean, where it is then removed from the barge and sunk to depth by pumps, by simply releasing it if natural processes or active crushing have rendered it negatively buoyant. These systems are also applicable to other types of floating biomass or debris in different parts of the world, such as algae, seaweed, jellyfish, and plastic in the great garbage patch.

Best mode and preferred designs and techniques will now be described.

DRAWINGS

The present invention can be best understood in conjunction with the accompanying drawing, in which:

FIG. 1 shows two methods for collecting sargassum mats and windrows in the ocean – a moving method 001 and a stationary method 002 – and in-situ sinking said sargassum to achieve Sargassum Ocean Sequestration of Carbon (SOScarbon). The moving method 001 comprises one of the various inlet devices is being pushed through a mat of sargassum, and the stationary method 002 comprises one of various inlet devices being fed by pulled booms encircling mats of sargassum. The moving method may be assisted by the use of a J-boom, wherein the J-apex is attached to the SOS vessel and/or inlet device and the distal end is towed ahead of the SOS vessel (or held passively by a boomvane), through a mat of sargassum, such that a large swathe of sargassum is funneled towards the inlet device(s).

FIG. 2 shows the preferred embodiment of a system 100 for implementing the moving method for collecting sargassum mats and windrows in the ocean from FIG. 1

FIG. 3 shows the preferred embodiment of a system 200 for implementing the stationary method for collecting sargassum mats and windrows in the ocean from FIG. 1

FIG. 4 shows a system 300 that uses many inlets in parallel, instead of booms, to extend its collection width

FIG. 5 shows a pump inlet device 010 with a left-handed/right-handed (center-feed), transverse auger 011 for preventing arch formation and metering solids (ie. sargassum) into said pump (for clog prevention).

FIG. 6 shows a pump inlet device 020 with a co-axial auger 021 for preventing arch formation and metering solids (ie. sargassum) into said pump (for clog prevention).

FIG. 7 shows a pump inlet device 030 with a weir 031 over which sargassum and seawater flows into a sump 032 of confined cross-sectional such that sargassum is pulled down towards a pump suction hose inlet inside said sump 032.

FIG. 8 shows a flexible, extended suction boom 040 with inlets 041 distributed along its length that acts as a gathering boom, pump inlet, and suction hose.

FIG. 9 shows an rigid, extended suction “tee” 050 with inlets 051 distributed along its length that acts as a gathering boom, pump inlet, and suction hose.

FIG. 10 shows a hose reel 060 that deploys a long, lay flat discharge hose over the side of a vessel using a “stinger” 061 comprising a number of conveyor rollers 062 mounted to curved structural members 063 that extend over the edge of said vessel.

FIG. 11 shows a crane device 070 for deploying various pump suction inlet devices from the side of a vessel with 1 hydraulically powered rotary degree of freedom 071 for deployment and additional, closely coupled, rotary and linear degrees of freedom 072 and 073 to allow said inlet devices, attach to a perforated tube 074, to wave follow when deployed.

FIG. 12 shows a two-stage, or “ex-situ”, system 400 wherein sargassum is first collected and then transported to an appropriate location where it is then sequestered in the deep ocean.

FIG. 13 shows an isometric view of a sequestration barge 410 for transporting sargassum 411 and, once brought to an appropriate location in the ocean, sequestering said sargassum in the deep ocean, by first ejecting/discharging it from said sequestration barge 410 using a number of discharge augers 412 towards a pump suction inlet 413. The pump 000 then pumps the sargassum to depth.

FIG. 14 shows an end-view of the sequestration barge 410 for transporting sargassum 411 and, once brought to an appropriate location in the ocean, sequestering said sargassum in the deep ocean.

FIG. 15 shows a cross-sectional, side-view of a sequestration barge 420, an alternative to the sequestration barge 410 of FIGS. 13 and 14, which directly pumps sargassum out of a hopper compartment 424 instead of using discharge augers as in sequestration barge 410. Sequestration barge 420 uses portholes 422 and/or secondary pumps 423 to continuously fill hopper compartment 424 with seawater. The resulting sargassum-seawater mixture is then pumped out of hopper compartment 424 and directly pumped to depth.

FIG. 16 shows a system 500 for collecting sargassum 501 from the ocean surface using a number of conveyors 502 that deposit the collected sargassum into a set of rolling crushers 503 that irreversibly compromise the sargassum 501 pneumatocysts such that the sargassum 501 is rendered negatively buoyant. The sargassum is then jettisoned back into the ocean through a moon pool 504.

FIG. 17 shows outputs from a system 600 for directing sargassum collection vessels in various locations.

In the drawings, preferred embodiments of the invention are illustrated by way of example, it being expressly understood that the description and drawings are only for the purpose of illustration and preferred designs, and are not intended as a definition of the limits of the invention.

PREFERRED EMBODIMENT(S) OF THE INVENTION

The present invention comprises several methods and mechanisms for sequestering sargassum in the deep ocean. Hereafter, preferred embodiments among the many possible system permutations are described.

The primary method of the present invention is called “pump(ing)-to-depth”, wherein sargassum is permanently sequestered in the deep ocean by pumping it to a minimum critical depth in the ocean (150-200m; the depth at which sargassum becomes negatively buoyant has been found to be at least 50-100m through various experiments in which sargassum was lowered, while being videoed, inside of an open-bottom cylinder) where the hydrostatic pressure is enough to sufficiently compress sargassum pneumatocysts (the grape-like bladders responsible for sargassum’s buoyancy) such that the entire macroalgae is rendered negatively buoyant and continues sinking on its own (without any further intervention). It is important to note that pumping sargassum to said critical depth (150-200m) does not irreversibly compromise sargassum pneumatocysts or permanently compromise its buoyancy. Rather, it sufficiently compresses the pneumatocysts so that the sargassum becomes negatively buoyant below the said critical depth. However, if sargassum previously pumped-to-depth was somehow returned above the critical depth, it may become positively buoyant again. Sargassum pneumatocysts are like underinflated balloons, buckling before they burst. Because of this, irreversibly rupturing sargassum vesicles requires a much greater depth than said critical depth (150-200m), making it mechanically and energetically unfeasible. Therefore, a critical feature of the pump-to-depth method is that said critical depth (150-200m) for pumping to depth also exceeds the mixed layer of the Caribbean (usually 90-110m) so that sargassum cannot be carried back up to a depth where it becomes positively buoyant again. Ideally, pumping-to-depth will, furthermore, be performed in locations where the depth of the oceans exceeds 1km, but preferably 3km, such that when sargassum pumped to the critical depth (150-200m) sinks, on its own, and reaches the bottom of the ocean, its carbon will be essentially permanently sequestered. Hereafter “SOScarbon” (“sargassum ocean sequestration of carbon”) will be used to refer collectively to the pump-to-depth method and/or all systems used to execute said method, described hereafter.

SOScarbon system embodiments generally fall into two categories: in-situ systems and ex-situ systems. In “in-situ” systems, sargassum is intercepted offshore, anywhere deep enough for pumping-to-depth (at least 250m depth is recommended) and immediately sequestered via pumping-to-depth. By contrast, in “ex-situ” systems, sargassum is first collected along barriers or in other areas where it is not feasible to pump-to-depth, and then transported to an appropriate location for sequestration via pumping-to-depth. In-situ systems have the advantage they require no handling/transportation of sargassum, however bathymetry and other conditions may not always permit in-situ pumping-to-depth. In the current paradigm of sargassum management, wherein sargassum is collected on or near beaches, ex-situ systems could be immediately useful. Both types of systems share many of the same mechanisms, ex-situ systems comprising additional methods and mechanisms for transporting sargassum and feeding the subsequent pump-to-depth process.

The in-situ pump-to-depth version of SOScarbon has two preferred embodiments, distinguished base on how the systems “feed” on a mat or windrow of sargassum in the open

ocean – one using a moving method and the other using a stationary method. These methods are both shown in FIG.1. In FIG. 1, a moving vessel 101, equip with a generic suction inlet device 102, feeds on the edge of a sargassum mat/windrow 103, and pumps-to-depth immediately. Also in FIG. 1, a stationary vessel 201, equip with generic suction inlet devices 202 and multiple booms 203 being pulled around sargassum mats/windrows 204 by a secondary vessel 205, is fed by pulling (reeling in) booms 203, gathering sargassum mats/windrows 204 near its suction inlet devices 202, and pumps-to-depth immediately.

Note that the moving method 100 of FIG. 1 only requires that there is relative motion between the SOScarbon vessel 101 and the sargassum mat/windrow 103. The vessel 101 could be motoring in any direction or merely station-keeping in ~0-degree heading as sargassum mat/windrow 103 moves towards the vessel 101. The moving method may also deploy multiple suction inlet devices 102 in parallel and/or from both sides of the vessel 101, perhaps also using J/U/V-booms to further extend the collection width on either side (as shown in the later more detailed embodiment of method 100 in FIG. 2). To eliminate the entire sargassum mat/windrow 103, the vessel 101 may use multiple passes in the same direction relative to the direction of ocean current, use a rastering pattern in multiple directions, or feed along the outer contour of the mat/windrow 103 in a cyclical fashion. No matter the path taken to completely eliminate the sargassum mat/windrow 103, the vessel 101 may choose to use the ocean current to its advantage by motoring when moving with the ocean current and station-keeping (or motoring slower) when moving against the ocean current. This is order to both save fuel and also with the goal of maintaining a constant, relative, normal (orthogonal) velocity between the suction inlet device 102 and the seawater/sargassum at the ideal value for system operation (currently found to be ~1 knot in practice) and to reduce acute and/or cyclical loads on equipment deployed. Many more complicated feeding patterns may be developed to save fuel (minimize distance and propulsion power) and optimize suction inlet devices 102 performance. It is recommended that the vessel 101, utilizing the moving method 100 of feeding, not exceed a relative velocity with respect to the ambient seawater of more than 3m/s (~6 knots). In practice, it has proven better to stay as close as possible to 0-degree or 180-degree heading with respect to ocean waves/current in order to reduce the rolling of the vessel 101 and improve the performance of the suction inlet devices 102. In practice, is has proven better to keep the suction inlet devices slightly in the “wave shadow” of the vessel 101, whenever possible, to reduce the heaving forces on the suction inlet devices 102 (it is obviously not possible to keep all suction inlet devices 102 in the wave shadow of the vessel 101 when suction inlet devices 102 are deployed from both sides of the vessel 101).

Note that the stationary method 200 of FIG. 1 could encircle sargassum mats/windrows 204 by either the secondary vessel 205 towing the booms 203 around the sargassum mats/windrows 204 (similar to a purse seine fishing vessel except the seine net is replaced by the booms 203) or the vessel 201 could pull the booms 203 around the sargassum mats/windrows 204 itself, perhaps using floating anchors (devices that act like underwater parachutes), conventional anchors (depending on the depth of the water), or a secondary vessel 205 to anchor the opposite end of the booms 203 (note the vessel 201 would not be able to pull out multiple booms 203 without the help of the secondary vessel 205). If a secondary vessel 205 is used to any extent, it

could comprise one of a number of vessels (ie. rib boats with outboard motors or towing catamarans for towing oil booms at present), so long as it has the capacity to tow the booms 203 (at least 500hp). The booms 203 could be 100m to 3km in length using current boom/lay-flat hose reels (for deployment/recollection), allowing the encirclement of a sargassum mats/windrows 204 close to 1km^2 in area (given that it is roughly circular or, if in an elongated windrow, first concentrated using the booms 203 as J/U/V-booms that move relative to the sargassum). The booms 203 could be even longer if they are stored on and deployed from a coiling pad (similar to those used for storing and dispensing underwater cable from cable laying vessels). The booms 203 could be of various design (fence, solid floatation, self-inflating, etc.), the simplest being a normal solid floatation, round oil containment boom with a solid skirt (perhaps with the modification that the skirt is made pervious to allow water, but not sargassum, to pass) with the basic requirements that it be capable of operation in the intended sea state so as to avoid bridging, arching, overtopping, and/or submergence failure (although boom selection can become much more complicated – taking into consideration the shape of the buoyant member, coatings on the skirt, the attachment method of the ballast, etc.). It is recommended that the booms 203 be pulled in (using the storage reel/coiling pad) at 0.5 to 2m/s (this is linear speed along the length of the booms 203). Because the rate of change of area encircled by the booms 203, as they are pulled in, decreases linearly with the decrease in length of the booms 203 still in the water the pulling speed of booms 203 may be increased during the pulling process in order to maintain a constant feed rate of sargassum into the suction inlet devices 202. Because the sargassum encircled by the booms 203 can be concentrated 5-10 times during the pulling process, it is recommended that the booms 203 have skirts 1-2m in length and freeboard of 0.15-0.3m (sargassum is only weakly buoyant so as it is concentrated most of the increased thickness will remain underwater – generally there will be 10:1 submerged to unsubmerged thickness). Note also that the booms 203 could also be actual purse seine nets and the vessel 201 could be a purse seiner vessel.

The vessels 101 and 201 could be of various design so long as there is deck space, capacity, and adequate faculties for maneuverability (DP2 station-keeping ability recommended) and deployment of system components; the vessels 101 and 201 could be of stern-deck or bow-deck design. This is particularly advantageous for an entity operating an SOScarbon system because the ability to quickly install and uninstall SOScarbon systems on many different vessels means that vessels 101 and 201 could be rented only during “sargassum season”, being allocated to other work during periods when sargassum is not threatening beaches.

Note that the suction inlet devices 102 & 202 of FIG. 1 are generic and not meant to be detailed representations of devices to be used in preferred embodiment of systems for executing methods 100 and 200. Immediately following is a description of preferred embodiments of systems for executing methods 100 and 200, followed by detailed descriptions of several pump inlet devices.

The overall, preferred SOScarbon system embodiment for accomplishing pumping-to-depth via moving method 100 is shown in FIG. 2. wherein sargassum windrow 104 is intercepted offshore, in a location appropriate for pumping-to-depth (at least 250m deep) where funneling

booms 105 & 106 direct it towards a transverse auger suction inlet 010 (which is shown instead of the generic suction inlet device 102 from FIG. 1), which meters the flow of solids into a 12” pump suction hose 107. 12” pump suction hose 107 leads to 12”, 5000GPM pump 000, which discharges into 12” pump discharge hose 108. 12” pump discharge hose 108 is connected to a 12”, 200m lay-flat discharge hose 109 through an integral fitting in a hose reel 060, which deploys and recollects said 12”, 200m lay-flat discharge hose 109. The 12”, 200m lay-flat discharge hose 109 is deployed over a curved roller conveyor 062, and extends vertically downward to/past the critical depth of 150-200m. When sargassum is discharged from the end of 12”, 200m lay-flat discharge hose 109 at/below said critical depth of 150-200m, sargassum pneumatocysts are sufficiently compressed such that the entire macroalgae is rendered negatively buoyant and continues sinking to the bottom of the ocean. The said critical depth also exceeds the mixed layer of the Caribbean (90-110m) so it cannot be carried back of to a depth where it may become positively buoyant again.

The rear end of funneling boom 105 is secured to the stern of the vessel 101, and the forward end is attached to a boomvane 111, which is in turn attached to the bow of vessel 101 via bowline 112. The boomvane 111 has submerged foils that generate an outboard, opening force when seawater passes through them, which pulls the forward end of funneling boom 105 away from the vessel 101, providing a large collection width for feeding on the sargassum windrow 104 (this permits the vessel 101 to travel slower, saving fuel and reducing stress on equipment, while still feeding large quantities of sargassum to transverse auger suction inlet 010). The side of funneling boom 105 seals against the solid funnel 014 of transverse auger suction inlet 010. The rear end of funneling boom 106 is attached to, and creates a seal with, the inboard side of the solid funnel 014 of transverse auger suction inlet 010. The forward end of funneling boom 106 is attached to, and creates a seal with, the port side of vessel 101. In order to achieve a solids concentration of ~50% (by bulk volume) in the pumped sargassum-seawater mixture, with a total pumped flowrate of 5000GPM and a relative forward speed of 0.1m/s, and assuming the bulk thickness of incoming sargassum is 0.1m thick, the funneling boom 105 can be 30m long and inclined at 30 degrees from the sagittal/median plane of the vessel 101, to provide a collection width of 15m.

The transverse auger suction inlet 010 is deployed from the port side of vessel 101 using crane 070. The transverse auger suction inlet 010 is held by a post 012, which is inserted into combined rotary-linear, 2 degree of freedom, passive joint 075 of crane 070. The post 012 is retained inside passive joint 075 of crane 070 with a set of high-strength pins inserted through the patterned holes in said post 012. The passive joint 075 rotates freely and allows the post 012 to slide inside its linear degree of freedom. Because the transverse auger suction inlet 010 is preloaded on the water surface by its own weight and a number of floatation tanks 016, the transverse auger pump inlet 010 can reliably wave follow to keep the inlet opening of the 12” pump suction hose 107 at a constant depth below the free surface, despite incident waves. This is a critical functionality of all the inlet devices described herein, because it the 12” pump suction hose 107 repeatedly comes out of the water and aspirates, the 12”, 5000GPM pump 000 will lose suction and constantly have to re-prime, essentially bringing the pumping-to-depth process to a hault.

While the system embodiment contained in FIG. 2 for executing pumping-to-depth method 100 is shown with transverse auger suction inlet 010 outriggered from the vessel 101, the transverse auger suction inlet 010 could be alternatively pushed in front of and/or towed behind vessel 101, at the apex of a U-boom instead of the funneling boom 105.

The overall, preferred SOScarbon system embodiment for accomplishing pumping-to-depth via stationary method 200 is shown in FIG. 3. wherein sargassum mat 206 is intercepted offshore, in a location appropriate for pumping-to-depth (at least 250m deep), encircled by boom 203 and pulled in (by boom storage reel 207), toward sump suction inlet 030 (which is shown instead of the generic pump inlet device 202 from FIG. 1), which meters sargassum into 12" pump suction hose 210. 12" pump suction hose 210 leads to 12", 5000GPM pump 000, which discharges into 12" pump discharge hose 211. 12" pump discharge hose 211 is connected to a 12", 200m lay-flat discharge hose 209. The 12", 200m lay-flat discharge hose 209 extends vertically downward to/past the critical depth of 150-200m. When sargassum is discharged from the end of 12", 200m lay-flat discharge hose 209 at/below said critical depth of 150-200m, sargassum pneumatocysts are sufficiently compressed such that the entire macroalgae is rendered negatively buoyant and continues sinking to the bottom of the ocean. The said critical depth also exceeds the mixed layer of the Caribbean (90-110m) so it cannot be carried back up to a depth where it may become positively buoyant again. Note that generic hose reel 208 shown in FIG. 3 could be replaced by hose reel 060 shown in FIG. 2 and the 12", 200m lay-flat discharge hose 209 could be deployed/recollected from said hose reel 060, over the curved roller conveyor 062.

In the system embodiments contained in FIGS. 2 & 3 for executing pumping-to-depth methods 100 & 200, respectively, all connections between 12" pump suction hose 107 & 210 segments, 12" pump discharge hose 108 & 211 segments, 12" 5000GPM pump 000, hose reel 060 and 12" 200m lay-flat discharge hose 109 are made with 12" camlock or Victaulic groove clamps and secured to the vessels 101 & 201 with chain and/or ratchet straps. It is recommended that the 12" pump suction hose 107 & 210 segments and the 12" pump discharge hose 108 & 211 segments be lightweight, flexible hose (Kanaflex hose, for example, makes hoses reinforced radially by a metal helices that maintain bending compliance) and have swiveling camlock connections between them (using o-rings on spherical ends). The bendability afforded by these features helps with the deployment of the suction inlet devices 010 & 030 (which requires manipulation of the attached 12" pump suction hose 107 & 210 segments) and helps with making the other necessary onboard connections during deployment (connecting the 12" pump discharge hose 108 to the hose reel 060, for example). All equipment – crane 070, hose reel 060, and 12", 5000GPM pump 000 – are secured to the deck of vessel 101 using 4ea 7/8" high-strength pins on each. The pins penetrate 1" pinholes in the base of the equipment and 1" pinholes in pairs of padeyes that straddle each pin location. The said pairs of padeyes are welded directly to the deck of vessels 101 and 201. The 12", 200m lay-flat discharge hoses 109 & 209 are ballasted by weighted segment(s) of pipe (for example 3ea 0.5m-long, 12", schedule 120 steel pipe totaling 300kg) that are attached to the end of the 12", 200 lay-flat discharge hoses 109 & 209 and to each other, end-to-end, with 12" Victaulic groove clamps. Said weighted segment(s) of pipe allow sargassum to discharge through them (after traveling down the 12", 200m lay-flat discharge hoses 109 &209) and sufficiently weight the 12", 200m lay-flat discharge hoses 109 & 209 so as

to prevent the 12”, 200m lay-flat discharge hoses 109 & 209 from swaying such that the bottom of the hose raises above the critical depth (150-m-200m. The hose weights also prevent the 12”, 200m lay-flat discharge hoses 109 & 209 from vibrating (due to Von Karman), whipping, and/or twisting.

Note that in the system embodiments contained in FIGS. 2 & 3 for executing pumping-to-depth methods 100 & 200, respectively, the system layouts are particular for vessels 101 and 201. In FIG. 2, for example, the layout of 12” pump suction hose 107 makes use of the dive deck 114 and the stairway 113 (on the stern of vessel 101) to avoid a bollard 115 (which the 12” pump suction hose 107 might otherwise catch on during deployment of transverse auger pump inlet 010). This layout of 12” pump suction hose 107 also allowed it to remain attached to the 12” 5000GPM pump 000 suction at all times (rather than detaching/reattaching it from the 12” 5000GPM pump 000 every time the transverse auger suction inlet 010 is retracted/deployed using the crane 070). Additionally, assuming vessels 101 & 201 are repurposed for use as SOScarbon vessels, small modifications may be possible while retrofitting (like cutting railings and padeyes), critical infrastructure cannot be moved. For example, the crane 070 in FIG. 2 needed to be placed such that it avoided the obstacle 110 on the portside of the ship, which was a critical engine room exhaust.

The 12” 5000GPM pump 000 illustrated in both FIGS. 2 & 3 is generally representative of an end-suction/centrifugal pump made by Godwin, a Xylem Inc. brand, that makes critically-silenced, skid-mounted, automatic self-priming, integrated diesel, 5000GPM, dewatering/wastewater pumps, called DPC300. These pumps are ideal for the scale of systems depicted in FIGS. 2 & 3 because they are a manageable size (6500lbs with a 1.5m x 4.5m footprint), skid mounted (easy to transport, lift, and secure to deck), easy to use (boasting a fairly generous operating range), have an open vane impeller design appropriate for solids-handling. These pumps are offered primarily through rental contracts for dewatering and wastewater projects around the world. Renting the pump-to-depth pumps 000 in addition to the vessels 101 & 201 enables SOScarbon operators to essentially eliminate costs whenever sargassum is not threatening beaches by returning pumps 000 and vessels 101 & 201 back to owners during these periods. It is recommended that a solids-handling pump with self-priming capability be used because the pumps will likely be mounted onboard the vessels 101 & 201 in most cases.

Note that the 12” 5000GPM pump 000 could have also been axial flow instead of centrifugal, and/or submersible instead of skid/pedestal mounted, and/or hydraulic or electric instead of integrated diesel. If the 12” 5000GPM pump 000 were replaced by a submersible pump, the self-priming capability would obviously become unnecessary. Another advantage of using a submersible pump is that the 12” pump suction hoses 107 & 210 could be eliminated (and with them the common concern of clogging in the 12” pump suction hose 107 & 210 would be eliminated). A system using a submersible pump could integrate the transverse auger pump inlet 010, submersible pump, and a hose reel similar to hose reel 060 into a single, compact module perhaps deployable on an autonomous vessel. However, there are advantages to using pumps mounted onboard larger vessels, the primary being that keeping said pumps onboard, as opposed to submersible, allows the use of much larger pumps than would be otherwise possible.

Increasing capacity of the SOScarbon system embodiments contained in FIGS. 2 & 3 for executing pumping-to-depth methods 100 & 200, respectively, would involve using more pumps similar to the 12" 5000GPM pump 000 and/or using pump(s) larger than the 12" 5000GPM pump 000 (centrifugal pumps, for example, can provide flowrates >100,000GPM given there is space and holding capacity for them onboard vessels 101 & 201). The former option of using more pumps, each with their own pump inlet device, in parallel, is the preferred method for increasing SOScarbon vessel capacity.

One can imagine systems very similar to those in FIGS. 2 & 3 but with many 12" 5000GPM pumps 000, suction inlet devices 010 & 030, and booms 105 & 203 in parallel, deployed from both sides of vessels similar to, but larger than, vessels 101 & 201.

For example, a high capacity version of the system in FIG. 2 may use 3 transverse auger suction inlets 010 in parallel, in the same apex of funneling boom 105 where the length and angle of inclination of said funneling boom 105 are increased to 60m and 45 degrees, respectively (to increase the collection width of funneling boom 105 to 45m such that 50% solids concentration is maintained at the increased pumping capacity), are used to feed 3 independent 12" 5000GPM pumps 000, which in turn pump-to-depth through 3 independent hose reels 060. The same parallelized set of 3 pumps, pump inlet devices, and hose reels could be deployed from both sides of the larger version of vessel 101, to achieve a total pump-to-depth capacity of 30,000GPM. Very large oilfield utility vessels, for example, may be able to accommodate even more pump-to-depth capacity by simply increasing funneling boom 105 collection width and/or adding more pump, pump inlet, hose reel sets in parallel.

Similarly, a high capacity version of the system in FIG. 3 may use 3 sump suction inlets 030 in parallel, feeding 3 independent 12" 5000GPM pumps 000, which pump-to-depth through 3 independent hose reels 060. The same arrangement could be deployed from both sides of the larger version of vessel 201, to achieve a total pump-to-depth capacity of 30,000GPM. In order to maintain a high solids concentration at the increased pumping capacity, booms 203 could be pulled proportionally faster than the initial recommended pulling speed of 0.5-2m/s so long as said boom reel 207 (or larger coiling pad deploying longer boom 203 lengths) is powerful enough to overcome increased drag, and, more importantly, that the booms 203 do not suffer arching, bridging, submergence, mechanical failure or concentrate encircled sargassum 206 so much that its submerged thickness exceeds the skirt depth of the booms 203. Very large oilfield utility vessels, for example, may be able to accommodate even more pump-to-depth capacity by simply increasing booms 203 pulling speed and/or adding more pump, pump inlet, hose reel sets in parallel.

The latter option of using larger pump(s) for increasing SOScarbon system capacity would require that larger hose/pipe be used (5000GPM is about the limit of what should be pumped through 12" hose/pipe) or multi-suction/multi-discharge (multiple hoses/pipes are used to carry the full flowrate into/out of the pump), making hoses/pipes more expensive, heavier, less flexible and, therefore, harder to implement. Not to mention, pumps larger than 12" 5000GPM pump 000, for example, can start to become harder to operate – for example, larger pumps may exhibit

a higher susceptibility to cavitation and/or a narrower best efficiency region and/or be more susceptible to general mechanical failure if conditions are not tightly controlled.

One of the prime advantages of the pump-to-depth method is its extremely low specific energy consumption (SEC; J/m3 sargassum consumed to pump-to-depth). This low energy consumption is owed to the fact that pumping-to-depth essentially experiences zero static head loss – the total dynamic head of the pumping process being comprised only of friction losses and geometric losses (bends and/or entry/exit losses) in the hoses/pipes. As an example, assuming the 12" 5000GPM pump 000 operating at ~5000 GPM (1100 cubic meters per pump per hour), with a pump hydraulic efficiency of 41% (the low end of the efficiency range for the Godwin DPC300 pump represented by the 12" 5000GPM pump 000), then applying viscosity, slurry, and solids correction factors, the specific energy consumption of pumping-to-depth is calculated as 1.53 MJ/m^3. Tests of a system very similar to the system embodiment contained in FIG. 2 for executing pumping-to-depth methods 100, confirmed this low energy consumption.

The only reason for using larger pumps/hoses/pipes would be to achieve better hydraulic efficiencies. However, because pumping-to-depth is already so energy efficient compared to other costs (other process costs and the presumed overhead for running an SOScarbon operation), it not considered to be worth the added capital and mechanical complication. Pump/hoses/pipes might actually better be reduced from the 12" sizes imposed by the 12" 5000GPM pump 000, perhaps to 8-10" systems, in order to reduce capital cost and ease of implementation.

In summary, the essential elements in the pump-to-depth systems are: (1) vessels, (2) pump(s), (3) hose(s), and (4) inlet device(s), the latter three connected, by necessity, by piping or hoses. Each length of piping can be either short, meaning the components at the nodes are immediately adjacent, or extended, perhaps allowing for independent mobility between the components. Additionally, pump(s) can either be onboard the vessel, or deployed in the water with the inlet device(s). Many independent series of (1) vessels, (2) pump(s), (3) hose(s), and (4) pump inlet device(s) can be deployed in parallel on the same vessels.

The pump collection mechanisms described herein can match/far exceed the capacity of currently employed conveyor systems (deployed on aforementioned barges for collecting sargassum from in front of barriers), require much less maintenance (robust construction and a single moving part, the impeller), and are much more dispatchable as they can be quickly installed/uninstalled on any ordinary vessel (no need for custom-built vessels or invasive retrofitting), shipped around the world, many times operating on a lease/rental basis (which is particularly useful to sargassum management as its arrival is a seasonal phenomena).

Moreover, by sinking carbon content present in the sargassum deep in the ocean, avoiding landfill/coastal methanogenesis, and increasing the overall biological pumping capacity of the Caribbean, SOS represents a new method of carbon reduction/offsetting with great potential (on the order of 100s of millions of tons CO2 equivalent per year).

Pumping-to-depth offers a more sustainable (physically more space), more eco-friendly (no methane emissions or heavy metal leakage to surroundings) disposal method than landfilling, the current management practice. Pumping-to-depth is the single most reliable way of sequestering sargassum in the deep ocean. By sinking the sargassum in a whole state, direct from the surface, to a depth where hydrostatic pressure completely compresses its buoyant pneumatocysts so it continues to sink in its whole state, naturally, the pollution/landfall potential is minimized. Other methods of rendering sargassum negatively buoyant at the surface, like crushing with rollers, may not completely rupture 100% of pneumatocysts (which is necessary for inducing negative buoyancy), leaving sargassum sufficiently buoyant to remain afloat, whereas not a single bladder will be able to escape hydrostatic pressure at depth, leading to much more reliable sinking.

Specialty Vessels

While system embodiments contained in FIGS. 2 & 3 for executing pumping-to-depth methods 100 & 200, respectively, show how pump-to-depth systems could be deployed on repurposed/retrofitted vessels 101 & 201, of generic design, there are many specialty vessels already in existence, or that could be custom-built, to be specifically conducive towards carrying pump-to-depth systems. Examples of said specialty vessels already in existence include purse seine fishing vessels, benthic trawling vessels, whaling ships, outrigger (shrimping) trawlers, large workboat catamarans, etc.

FIG. 4 shows an example of an alternative system 300 to the system embodiment contained in FIG. 2 for executing pumping-to-depth method 100, that uses a specialty vessel for carrying a pump-to-depth system. In FIG. 4, an outrigger (shrimping) trawler 301 is equipped with planing pump inlet devices 302 along the entire length of its outriggered trusses 303. As opposed to the system embodiment contained in FIG. 2 for executing pumping-to-depth method 100, wherein funneling boom 105 is used to provide the desired collection width, system 300 accomplishes its collection width by stringing a plurality of planing pump inlet devices 302 along the entire span of its outrigger trusses 303. The planing pump inlet devices 302 operate by using partially submerged planes 305, with a positive angle of attack, to push water and sargassum 306 underwater, similar to a 0-degree deadrise planing hull, where it encounters pump inlets (perhaps also containing co-axial or transverse augers to meter the flow of solids into the pump inlets).

Another example of a specialty vessel for deploying a pump-to-depth system may comprise a hybrid vessel with, ideally a cata-/tri-maran that uses its hulls as funneling structures for sargassum, with a pitching wall with a conveyor/rake excavator on one side and a planing wall and auger device pump inlet on the other. The interchangeable conveyor and pump inlet, combined with the low draft of the cata-/tri-maran would enable such a vessel to perform collection near shore or in offshore water not appropriate for sequestration (because of insufficient depth or another reason) and then transport the same lot to deep water for sequestration. Alternatively, such a vessel could operate as an open ocean in-situ sequestration

vessel (wherein sargassum is not collected and rather immediately pump-to-depth – or otherwise sequestered).

There are many more specialty vessels that could be particularly conducive to carrying pump-to-depth systems, each prompting slightly different system construction (making it impractical to summarize them all in the present submission), but all use the same basic pump-to-depth methods 100 and/or 200 and system elements of (1) vessels, (2) pump(s), (3) hose(s), and (4) pump inlet device(s), with similar system architectures to those illustrated in FIGS. 2 & 3, that sequester sargassum by transporting it to/below the critical depth (150-200m).

Pump Inlet Devices

It is important to note the transverse auger pump inlet 010 and sump pump inlet 030 in FIGS. 2 & 3 are two of five pump inlet devices in the current submission. While each pump inlet has a preferred implementation – the transverse auger pump inlet 010 being better suited for method 100 and sump pump inlet 030 being better suited for method 200 – any of the pump inlet devices could be used in any of the pump-to-depth system embodiment, because they all accomplish the same basic functional requirements: (1) concentrate sargassum, (2) transport sargassum underwater where it will encounter suction inlets (suction inlets must remain below waterline at all times for aforementioned reasons), and (3) maintain a consistent, high sargassum flow into suction inlets. The five pump inlet devices of the present submission are: transverse auger suction inlet 010, co-axial auger suction inlet 020, sump suction inlet 030, suction boom 040, and suction tee 050.

Again, each suction inlet device concept has an optimal system architecture associated with it. While each inlet device has a use-case in which it might perform best, it is maintained that any of the inlet devices could be used in any possible scenario: open ocean, barrier cleaning, marina cleaning, power plant water intake cleaning, emergency response, open ocean disposal, and/or beach cleaning; mounted on any vessel: utility boat, barge, etc; and either discharged into a receptacle for transport, or directly into a pump inlet to be transported deep below the surface of the ocean (150-200m) for sequestration. Note that a two-stage system wherein an onboard pump-to-depth pump is fed by a conveyor (bucket or rake) or a modified snow blower that collects sargassum from the surface of the ocean, instead of a suction inlet, is also possible.

Transverse/Co-Axial Auger Suction Inlet Devices

FIGS. 5 & 6 show transverse auger suction inlet 010 and co-axial auger suction inlet 020, two pump-to-depth suction inlet devices that use augers of different orientations (transverse and co-axial with the suction hose, respectively) to meter sargassum flow into suction openings.

In FIG. 5, showing the transverse auger suction inlet 010, a left-handed/right-handed (center-feed), 12” OD, 12” pitch, 8ft-long, transverse auger 011 is of mild steel construction with solid, helical flighting and turns inside a schedule 10, 12” pipe steel casing 0110. Steel casing 0110 has two windows cut that form the suction inlets 013. Steel casing 0110 has an exit in it back-center where there is a welded saddle joint to another schedule 10, 12” pipe neck 0112 to which the pump suction hose attaches and extracts collected sargassum from the transverse auger suction inlet 010. The steel casing 0110 and neck 0112 are reinforced with welded splines 0113 and 019.

The transverse auger suction inlet 010 has a solid, four-sided, converging funnel 014 made from marine grade, 0.75”-thick plywood that is 3m wide at its opening. The panels 014a, 014b, and 014c, are bolted together along their seams with bent sheet metal sandwiches 018 bearing mating bolt patterns that accept ¼”-20 bolts, making for an rigid joint. The top panel 014a of funnel 014 acts like an inclined plane, transporting sargassum down towards the suction inlets 013, as sargassum enters the wooden funnel 014. The side panels 014b act like funnels, concentrating sargassum towards suction inlets 013. The bottom panel 014c acts like a scoop to prevent sargassum from escaping beneath the funnel 014. The panels 014a, 014b, and 014c of funnel 014 are attached to steel casing 0110 by a bolted sandwich connection to splines 019.

The funnel 014 relies on the relative motion of the water/sargassum entering it to force sargassum downward, towards the suction inlets 013, where sargassum becomes entrained in inlet flow and is pulled towards suction inlets 013. Upon entering steel casing 0110, the transverse auger 011 feeds sargassum towards the back-center of the steel casing 0110 where it enters the pump suction hose through neck 0112 and travels through a suction hose to the pump inlet. The transverse auger prevents suction hose and pump clogs by imposing a set sargassum flowrate (limiting the solids concentration of the flow through suction hose and into the pump).

In FIG. 6, showing the co-axial auger suction inlet 020, a right-handed, 12” OD, 30” pitch, 4ft-long, co-axial auger 011 is co-axial with and extends into suction inlet 023 (extending in by at least one full flight, which is necessary for imposing a solids flow rate). The co-axial auger 021 is of mild steel construction with spoked, helical flighting and turns inside a schedule 40, 12” aluminum pipe suction inlet 023. It is recommended that the co-axial auger 021, supported by motor 025 (through a rigid, keyed coupling 0213) on one end, also be supported on the other end by another bearing/bushing mounted inside the suction inlet 023 pump. Once sargassum enters the suction inlet 023, it moves directly to the pump suction hose, which extracts collected sargassum from the co-axial auger suction inlet 020.

The co-axial auger suction inlet 020 has a four-sided, converging, pervious funnel 024 made up of a welded aluminum frame 022 that is 3m wide at its opening. The frame 022 is wound with high strength fishing line (alternatively braided wire, string, etc.) wound in a high resolution (perhaps a wind everything 0.25” along the four crossbars 0210), radial pattern 028 (only in the radial direction on not in the circumferential direction) around the suction inlet 023, covering all four sides of the frame 022. Each side of the frame 022 is wound with a single piece of fishing line wound around crossbars 0210 and pegs 0211 near suction inlet 023, with 50-100lbs of tension in

each span. The resulting funnel 024 is pervious to water, but not to sargassum. The radial winding pattern 028 conveys sargassum towards the suction inlet 023 without the clog risk of woven netting, or other water-pervious coverings for the frame 022. The top panel 024a of funnel 024 acts like an inclined plane, transporting sargassum down towards the suction inlet 023, as sargassum enters the pervious funnel 024. The side panels 024b act like funnels, concentrating sargassum towards suction inlets 023. The bottom panel 024c acts like a scoop to prevent sargassum from escaping beneath the funnel 024.

The funnel 024 relies on the relative motion of the water/sargassum entering it to force sargassum downward, towards the suction inlet 023, where sargassum becomes entrained in inlet flow and is pulled towards suction inlet 023. Upon entering suction inlet 023, the co-axial auger 021 limits the rate of solids ingress into the inlet where-after it enters the pump suction hose through fitting 0212 and travels through a suction hose to the pump inlet. The co-axial auger prevents suction hose and pump clogs by imposing a set sargassum flowrate (limiting the solids concentration of the flow through suction hose and into the pump).

Note that funnel 014 from FIG. 5 could be a pervious funnel similar to funnel 024 in FIG. 6 and funnel 024 from FIG. 6 could be a solid funnel like funnel 014 in FIG. 5. The pervious funnel 024 in FIG. 6 with the radial pattern 028 is the preferred embodiment of funnels 014 & 024 because it has demonstrated, in practice, a considerable reduction in wave forces experienced by auger inlet devices 010 & 020 and a considerable increase in inlet feed efficiency. The solid funnel suffers from two primary issues: (1) even at moderate forward speeds of 0.5m/s (in pump-to-depth moving method 100, for example) the positive pressure head created in front of the solid funnel is enough to overcome the negative pressure gradient imposed by the suction inlets 013 & 023 inside the funnels 014 & 024, preventing sargassum from entering the funnels 014 & 024 altogether, and (2) when the solid funnel heaves up and down in waves, solid panels 014a/024a act like wedges, displacing seawater and sargassum as they crash in and out of the water. Because the panels are solid, the displaced water has nowhere to go but around the edges of the funnel, creating strong eddies at the edges of the solid funnel, which pull sargassum out of the funnel, around the edges. Water-pervious funnels are not susceptible to the same failures. Overall, the waves forces experienced by the solid funnel are extremely disruptive to suction inlet 013 & 023 feed efficiency. Therefore, water-pervious funnels, with the radial pattern 028 shown in FIG. 6, are the preferred embodiments of funnels 014 & 024 in auger inlet devices 010 & 020.

The transverse auger suction inlet 010 & co-axial auger suction inlet 020 address a major issue with funneling sargassum towards suction inlets 013 & 023: stable arch formation. Just as bulk materials can form stable arches in the bottoms of hopper discharge bins (preventing mass flow of material), stable arches of sargassum floating on the surface of the ocean can form in the apexes of funnels 014 & 024. This will prevent further feeding of sargassum as long as the arch is present. The transverse auger suction inlet 010 prevents an arch of sargassum forming in the funnel 014 because the rotating transverse auger 011 does not allow the formation of stable arch “feet” (because transverse auger 011 spans the entire apex of the funnel 014 and constantly rotates). The co-axial auger suction inlet 020 prevents arch formation by disrupting the formation

of said arch “keystone” because the co-axial auger 021 physically interrupts this region of the arch.

The particular embodiments of transverse auger suction inlet 010 and co-axial auger suction inlet 020 in FIGS. 5 & 6, respectively, show a post 074 extending upward. This post 074 is meant to insert into a sleeve 073 of crane 070, shown in FIG. 11. This sleeve 073 allows post 074 to slide freely inside it (this interface may be greased with a waterproof grease to reduce friction). The linear degree of freedom afforded by sleeve 073 allows the transverse auger suction inlet 010 and co-axial auger suction inlet 020 to wave-follow, . The goal of this wave-following is to keep the top of suction inlets 013 and 023 at least 12” below the free surface. Insufficient still-water depths and/or hydrostatic preload of the auger inlet devices 010 & 020 could lead to unsatisfactory wave-following, especially likely in aggressive wave states, causing the suction inlets 013 & 023 to repeatedly come out of the water aspirating the suction hoses and causing pumps to repeatedly lose suction. Ballast for auger inlet devices 010 & 020 is provided by the weight of the devices themselves, each weight 300-500lbs. Floatation for auger inlet devices 010 & 020 is provided by 55 gallon barrels 016 & 026 and 30 gallon barrels 017 & 027. The floatation barrels 016, 026, 017 & 027 are secured using ratchet straps that pull said barrels into the vees formed by the sides of funnels 014 & 024 and purpose-built plates (see plates 029 in FIG. 6, for example). These different sizes of floatation barrels (55 gallon and 30 gallon) can be rearranged and/or filled with water (or other ballast) in order to fine tune the floatation of auger inlet devices 010 & 020. Once floatation is finalized, floatation barrels 016, 026, 017 & 027 should be sealed with silicone sealant.

The post 074 is retained inside the sleeve 073 by a set of high strength pins inserted through the holes in post 074 above the sleeve 073 (such that when the crane 070 is lifted, a pin in post 074 will interfere with the top of the sleeve 073 and the entire transverse auger suction inlet 010 can be lifted out of the water).

Note that the auger inlet devices 010 & 020 could be held rigidly, without the linear degree of freedom afforded by sleeve 073, but this would require a deeper still-water depth (>12”) to keep the suction inlets 013 & 023 underwater in waves (without the ability to wave-follow). With suction inlets 013 & 023 farther below the free surface, more sargassum will need to accumulate and/or funnels 014 & 024 will need higher relative speeds in order for sargassum to be pushed down far enough to encounter suction inlets 013 & 023. Not to mention, if the auger inlet devices 010 & 020 are rigidly coupled to vessels 101 or 201, for example, then wave forces could be prohibitively strong and suction inlet 013 & 023 submergence could still become an issue if vessel 101 & 201 roll is out of phase with incident waves (which is usually the case).

Transverse auger 011 and co-axial auger 021 are driven, through rigid, keyed couplings, by 5000in-lbs hydraulic wheel motors 015 & 025. The motors have heavy-duty bearings (at least 4000-5000lbs of radial load capacity) and are capable of turning between 0-900rpm. This range allows the augers 011 & 021 to turn slowly in the case of high concentrations of incoming sargassum and also turn fast enough to essentially be “hydraulically invisible”, meaning the auger flighting is moving at the same linear speed as the fluid flowing through suction inlets 013 & 023

with the 12” 5000GPM pump 000 (which is ~4.5m/s in 12” plumbing). However, submerged auger flighting turning at high rates tends to throw off repulsive radial/centrifugal flow because the flighting is acting like a paddle/blower. This repulsive flow prevents sargassum from entering flighting of augers 011 & 021 and suction inlets 013 & 023. In practice, it has been found that 12” auger speeds should be limited to 200-300rpm max to avoid this problem.

Despite transverse auger 011 being solid/12” pitch/12” OD and co-axial auger 021 being spoked/30” pitch/12” OD in the embodiments of FIGS. 5 & 6, the augers 011 and 021 could both be of varying sizes (ODs and pitch:OD ratios), geometries, and designs – spoked/not, serrated/not, compliant/not, finger/brushes/rigid flighting, tapered/not, paddles/not, variable pitch/not, variable shaft diameter/not, cusped/not, shafted/shaftless, etc. To prevent wedging of flotsam and jetsam, or other unwanted pelagic debris, between augers 011 & 021 and casings, a number of countermeasures may be employed: spring-preloaded walls, serrated/interrupted flighting, compliant auger flighting material, force-limiting clutch/shear pins, brushes/compliant trim on the flight edges, and/or simply chamfered flighting edges. Finally, it is maintained that clogging may not be a concern in some cases (when suction hose is short and relatively straight, for example) and provisions are made to remove the auger(s) 011 & 021 from auger suction inlets 010 & 020, such that suction inlets 013 & 023 are left unobstructed.

While the auger suction inlets 010 & 020 could be used for pump-to-depth methods 100 or 200 (in place of sump suction inlet 030 in FIG. 3), the auger suction inlets 010 & 020 are naturally more suited to moving pump-to-depth method 100. The auger suction inlets 010 & 020 could also be mounted on a powered barge or other vessel, whereupon a pump and a container for storing collected sargassum exists, to aid/replace the conveyor vessels currently used (eg. by Algae Nova) to clean along floating barriers near shore, without pumping-to-depth (sargassum collected along barriers could then be transported to deeper water for pumping-to-depth; such a two-stage system is discussed again later in this submission).

Sump Suction Inlet Device

An embodiment of the sump suction inlet, shown in FIG. 7 relies on a specific submerged depth of a weir 031 to provide the desired flowrate and solids concentration, further relying on the constrained geometry (limited cross-sectional area) of the sump 032 to create sufficient downward velocity inside the sump such that sargassum is transported towards submerged suction piping against its natural rate-of-rise in seawater (~0.2m/s). This makes the sump inlet more appropriate as a stationary device that is “fed” with sargassum by natural current or by various booming operations (preferably pump-to-depth method 200). However, a moving version of the sump inlet could be realized at low speeds, about 1-2 knots, and in relatively small waves < 0.5m.

Any shape could be used for the sump, but a slender rectangle of high aspect ratio, 3:1 to 10:1, has the highest perimeter to surface area ratio allowing it to sustain large flowrates, at low

weir depths, while still maintaining plenty of downward velocity inside the sump. Whether the sump is free-floating or constrained by a 1 or 2 degree of freedom, rotary and/or linear linkage (the embodiment in FIG. 7 has a 1 degree of freedom pivot 033, below the deck, close to the waterline, that allows it to wave-follow) attached to the deployment vessel, an instability exists in that if, even for a moment, the flow of water over the weir is less than the pump flowrate, the sump will become more and more buoyant, eventually exiting the water and forcing the pump to run dry. A countermeasure to this risk is to heavily hydrostatically preload the sump (using ballast 0311 and floatation 034 & 035) such that the force balance on the sump depends relatively little on the standing water level in the sump. This sensitivity may also be addressed by optimizing the shape of the weir 031 to maximize the discharge coefficient by using an ogee curve, labyrinth weir, or a piano key weir (commonly used to maximize the discharge capacity of spillways in large dams) such that there is more flow per unit head above the weir and the sump is kept as full as possible at all times. The exterior hydrodynamic form of the sump is designed to minimize surge and sway forces that are out of phase with the heave forces the sump (hence the drafted form of the sump) is meant to mimic while still holding enough volume to give ample time to respond in case of dry-running.

The sump suction inlet 030 in FIG. 7 is designed for use with 12” 5000GPM, requiring it to be 1.75m long and for the weir 031 to be 0.2m underwater at least (sump designed for larger pump could be as long as 15-30m taking up the entire side of the deployment vessel). Here, the sump is deployed and retracted with a hydraulic/pneumatic cylinder 037, which may also provide some spring stiffness and damping. Here, a purse seining boom 036 (pump to depth method 200) is used to pull sargassum into the sump, creating a seal against floatation 034. Deck frame, 0310 is pinned to the deck of the deployment vessel.

The sump-inlet must be capable of providing a consistent, high volumetric solids concentration to the pump inlet. The sump must prevent itself from running dry, even in rough water, as failing to do so might cause damage to the pump, but moreover makes the sequestering process extremely inefficient as the pump will be required to continuously re-prime itself. This risk may be accentuated in waves because the waterline may recede below the inlet edge of the sump across large sections, or for long periods of time. The inlet of a sump’s given shape/size is limited by the surface area/cross-sectional area ratio. Streamlining the inlet edge of the sump extends this range. While increasing the depth of the sump’s inlet edge below the free surface of the water also extends this range, it is detrimental to providing a high solids concentration and should not be used as a means of increasing allowable volumetric flowrate. Wave amplitude has a great effect on volumetric solids concentration while wavelength has negligible effect. Both the concentration imposed by the collection boom, and the depth of the leading edge of the sump below the water, can be used to control and maximize the solids concentration of the sargassum-seawater slurry flowing into the pumps.

A slender rectangular sump has a much smaller footprint than a circular sump rated for the same volumetric flowrate, meaning that it takes less space (it could perhaps even be stored in an outboard position) and can be deployed immediately next to the ship (decreasing the size and complexity of the deployment mechanism). A rectangular sump is easy to make, transport,

install, and maintain. A rectangular sump is lighter and more compact than a circular sump of equivalent rated volumetric flow, meaning it will have less effect on ship dynamics. Lastly, a rectangular sump lends itself to sealing against the collection boom(s).

FIG. 7 shows the sump suction inlet geometry specifically designed for a 5000GPM pump, comprising a rectangular prism with drafted floor. Sargassum and seawater flow over the leading edge into the sump. A filleted leading edge maximizes flowrate to decrease the chance of dry-running and allowing the leading-edge to remain close to the free surface, maximizing volumetric solids concentration. The remaining planes are all flat, zero draft tessellations. The cross-sectional area of the sump is small enough such that the volumetric flowrate out (via the pump) causes sufficient downward velocity inside the sump to pull sargassum down (against its natural rate-of-rise) towards suction inlet piping.

Typically, there will be one sump for every pump, so that each of the sump-pump-pipe-hose modules can act as independent units (as opposed to one sump per multiple pumps or one pump with multi-suction inlet). This allows variable sinking rate and allows continued operation in the case that one module is out of service. Only the distal edge of the sump acts as the "leading edge," lying below the free surface and sustaining a flow of sargassum and seawater over it (the proximal edge of the sump is above the waterline).

Suction Boom and Suction Tee

An embodiment of the "suction boom" 040, shown in FIG. 8, comprises an extended suction pipe/hose 041, with its distal end 042 capped/sealed, with distributed inlets 043 spread along the entire length. The design goal of the suction boom 040 is to maximize the length of continuous suction region where the inlet velocity is divided but still locally high enough to entrain sargassum. Distributed inlets 043 (at least 5" OD) should be spaced 3-5 diameters center-to-center (suction cones should overlap to avoid gaps in the suction field for sargassum to escape through). Because pressure losses between inlets 043 is much less than the pressure losses through the inlets 043 themselves, there is approximately equal flowrate through each inlet along the entire length of the boom. Floatation 045 and chain ballast 044, attached frequently along the length, counteract wave forces and internal forces from flow through the suction boom 040 as it adopts the curvature of ocean waves. The inlets 043 may be of varying size/shape/spacing. Funnels and/or weirs may be added near each inlet 043 to increase the capture efficiency of sargassum.

A large scale SOScarbon system for implementing pumping-to-depth may wish to use very large pumps (>100,000 GPM) to increase capacity and efficiency. A challenge exists here because very large pumps with single inlets must be fed with sargassum very quickly – otherwise the operator would pump only seawater and very little sargassum. Instead of driving the collection vessel very quickly, or pulling a boom extremely fast, the suction boom's extended length will allow collection from a wide swathe, at relatively low velocity locally. Therefore, the suction

boom might be very useful, especially if large pumps are considered. It is important to note that the extended suction device not only enables the use of a large pump, but it requires it, otherwise local inlet velocity will not be sufficient to entrain nearby sargassum amidst other ocean forces.

The suction boom may be rigid or flexible. FIG. 9 shows a rigid suction "tee" 050 that might incorporate anti-roll floatation 052 & 054 in the form of a "tee" 053 to prevent roll and emergence of inlet openings 051 on the underside of the device in large waves. Because a rigid suction boom cannot be compacted, its length is limited by the size of ship and deployment system used.

The suction boom 040 and suction tee 050 might also be semi-permanently installed along/between floating sargassum barriers or in powerplant cooling water intakes for regular removal of sargassum.

Summary of Suction Inlet Devices

One should notice that the principles of one inlet device embodiment may be used with others. It is quite easy to imagine many hybrid combinations of the various inlet devices. The true ingenuity of the inlet devices exists in their fundamental operational principles – vees concentrating, gravity-feeding, planing, weirs to pull across the free surface and control solids concentration, high downward velocities in confined cross-sectional areas to entrain sargassum, augers to transport/feed/prevent clogging, and impellers to throw and/or transport using water as a carrying fluid - not in their exact manifestation/implementation. While each inlet is presented in its purest form herein, it is maintained that hybrids of these devices, or their constituent components, have also been considered.

Hose Reel

A singular hose reel 060 is what was used on the SOS pilot vessel and is ideal for installing small SOS systems on other repurposed vessels in the future, that only require a single hose, where space may be limited, and where considerable obstacles to placement and securing may exist. Several hose reels 060 could also be implemented in parallel to enable systems with large pump-to-depth capacity. FIG. 10 shows the preferred embodiment of the hose reel 060 with a curved roller conveyor 063, or "stinger", that conveys the hose from a 45-degree start angle, through a 10-ft radius, over the side of the ship, to a 0-degree angle where the hose hangs vertically as it enters the water and extends to the critical depth (150-200m).

The 200m lay-flat discharge hose (109 & 209 in FIGS. 2 & 3, respectively) deployed and recollected on the hose reel 060, is retained inside the hose reel 060 via a custom integral fitting 068 bolted inside the hose reel 060 center. Care is taken to make sure there are no edges or

sharp corners anywhere inside the wagon wheel 064 or curved roller conveyor 063. The hose reel 060 wagon wheel 064 is hexagonal in construction such that the major tip-to-tip diameter of the wagon wheel 064 is 102” (enough to hold >200m of 12” ID, 0.25”-thick polyurethane lay-flat hose), but the minor flat-to-flat diameter is only 89” such that the wagon wheel 064 could fit inside a standard intermodal container.

The hose reel 060 wagon wheel 064 is actuated by a 5000in-lbs wheel motor 0611 that transmits torque from a 12-tooth drive sprocket, through a heavy duty ANSI 100 grade chain, to a 120-tooth driven sprocket 0612 on the wagon wheel 064. When the 200m lay-flat discharge hose is completely recollected, it wraps around a set of six 2” rungs 0610 in the center of the hose reel 060 wagon wheel 064. When the hose is completely recollected, the kickdown stand 069 is laid over the opening on the distal end of the curved roller conveyor 063, so that the hose weight at the end of the 200m lay-flat discharge hose (109 & 209 in FIGS. 2 & 3, respectively) can rest on the kickdown stand 069 and the tension removed from the 200m lay-flat discharge hose during transit.

The curved roller conveyors starting height, radius, and starting angle, can be used to avoid obstacles such as railings, bollards, padeyes, gunwales, etc. This designed also allows the entire footprint of the hose reel to remain on the deck of the vessel, which is better for securing. It is not recommended that a radius any tighter than 10ft be used to support a lay-flat hose, otherwise the hose may kink, restricting flow, or cause undo stress in the top and outer edges of the lay-flat hose. Another embodiment of the hose reel 060 could be cantilevered out over the edge of the vessel. Such a configuration offers an advantage in that the hose is straight and does not have to adopt the relatively sharp curvature imposed by the curved roller conveyor 063 in the preferred embodiment, while pumping. However, the 10ft radii imposed by the built and tested curved roller conveyor 063 showed no detrimental effect on hose dynamics or pumping performance, and overall it worked quite nicely and is recommended in the future.

The hose reel 060 wagon wheel 064 is connected to the hose reel base 065 with sealed, heavy-duty (>5000lbs of radial load capacity) rotary bearings 066 bolted to the hose reel base 065. The hose reel base 065 is ultimately secured to the deck with at least four high-strength pins inserted in pinholes 067, through pairs of padeyes that straddle the legs of hose reel base 065 and are welded/bolted to the deck. Thus far, all connections to the deck have been made using pins. This practice is recommended in the future, especially when installing SOS systems on repurposed vessels. The padeyes used on the SOS pilot vessel featured a pattern of staggered holes in both the x and y directions so that one combination of holes always lines up with the holes in the base of the hose reel (or other devices – ie. cranes and pumps), despite the unevenness of the deck, or errors in manufacturing.

Crane

FIG. 11 shows the crane 070 used to deploy the auger suction inlets 010 & 020 in system embodiments in FIGS. 2 & 3 for executing pump-to-depth methods 100 & 200, respectively. The crane 070 comprises one powered rotary degree of freedom 071 (actuated by a pair of 2.5" 3000psi double-acting hydraulic cylinders 076, one passive rotary degree of freedom at pivot 072, and one passive linear degree of freedom provided by sleeve 073. Auger suction inlets 010 & 020 were attached to post 074 via the 12-bolt flange 075 (pipe section 0713 at the bottom of post 074 connects between the auger suction inlet exits and the pump suction hose; collected sargassum and seawater flow through auger suction inlets 010 & 020 and pass through pipe section 0713, before entering the pump suction hose). The auger suction inlets 010 & 020 are able to wave-follow via the linear degree of freedom afforded by sleeve 073. Post 074 is ultimately retained inside the sleeve 073 by a high strength pin inserted into the holes in the top of post 074, above the tope of sleeve 073.

The crane 070 provides the critical function of deploying the auger suction inlets 010 & 020 and retracting the auger suction inlets 010 & 020 for transit. When retracted, the post 074 swings, via pivot 072, into catch 0710 and is locked with a pin so it is secure during transit. When the crane arm 079 is retracted, it is secured to crane base 0711 with high-strength pins inserted in safety pin holes 077 & 078. The entire crane 070 is ultimately secured to the deck with at least four high-strength pins inserted in pinholes 0712, through pairs of padeyes that straddle the legs of crane base 0711 and are welded/bolted to the deck.

Like the aforementioned hose reel 060, this crane 070 proved quite useful for installing the SOS pilot system on a repurposed vessel, avoiding inevitable unplanned obstacles, and securing it to the deck.

Sequestration Barge/Submarine

FIG. 12 demonstrates a two-stage, ex-situ pump-to-depth system 400 architecture. In areas 402 where immediate, in-situ pump-to-depth is not possible (ie. near shore where the water depth is shallower than the critical depth of 150-200m), 12" 5000GPM pump(s) 000 and any of the suction inlet devices 010, 020, 030, 040, & 050 (represented by generic suction inlet 401 in FIG. 12) could still be used to collect sargassum 406 into a sequestration barge 410 (either directly pumped into sequestration barge 410, through discharge hose 403, as shown in FIG. 12, or via collection in smaller containers that are then transported to a central loading location for sequestration barge 410) for subsequent transport, by a tug 404, to areas over the deep ocean, where sargassum 406, previously collected, can be pumped-to-depth by 12" 5000GPM pump 000.

This two-stage, ex-situ pump-to-depth system 400 is an important system architecture because such a service could be immediately useful as a means of sustainably disposing of the hundreds of thousands of metric tons of sargassum currently collected from beaches and barriers in places like Punta Cana and Cancun. In emergency situations where an abnormally large and/or unexpected sargassum mat poses an imminent threat to coastline, the sequestration barge 410

can be used to collect this sargassum near shore and then transport it out to deep water for pumping-to-depth. This type of service could be particularly useful to small islands, in the Lesser Antilles, for example, that lack the resources to sustain regular protection/cleanup systems for sargassum, but still stand to suffer a great deal when hit by a large sargassum mat.

FIG. 13 shows one embodiment of the sequestration barge 410, that uses augers 412 to discharge the sargassum 411 payload from the storage hopper 413 to the suction inlet area 414, where flow into the pump suction hose 415 is facilitated by a co-axial auger suction inlet 020 (may or may not be necessary in practice because the bin discharge augers already meter the flow from the storage hopper 413 into the suction inlet area 414). The 12" 5000GPM pump 000 then pumps-to-depth through pump discharge hose 417, hose reel 060, and 200m lay-flat discharge hose 418, which extends to/below the critical depth (150-200m). Note that the sequestration barge contains all the necessary equipment (including HPUs and diesel power for pump) for pumping-to-depth such that it can be towed by any vessel (so long as said vessel can pull the sequestration barge).

The sequestration barge 410 storage hopper 413 would have a vee-bottom that ensures all sargassum feeds down towards the pump inlet or auger (it does not have to be designed for mass flow but it is advantageous). The hopper vee bottom must be fully live with augers 412 to ensure egress of all sargassum. The hopper walls must be either vertical (perhaps extending upward to provide more carrying capacity) or inclined at or above the angle of friction of sargassum and the hopper at the expected pressure (appropriate vertical/horizontal shear strength and wall friction tests must be conducted). In FIG. 13 the storage hopper has a vertical wall section 416 (for expanded carrying capacity) and a converging wall section 419, which forms the aforementioned vee-bottom. There is a tradeoff between steepness of the walls, lost carrying capacity, and the number of augers required to achieve a fully live bottom. The hopper geometry may further comprise diverging endwalls 4110 (~10 degrees) and a lengthwise beam 4111 to create an "expanded flow" condition and reduce the risk of an arch forming (a common problem in bulk material processing). Additionally, widthwise beams 4113, bear the brunt of the weight of sargassum 411 (piled high and inclined at its angle of repose), so as to minimize the pressure at the bottom of the storage hopper 413, limiting the starting torque of augers 412 and decreasing the friction force between the sargassum 411 and the converging wall section 419 in the vee-bottom.

The embodiment of sequestration barge 410 in FIG. 13 is ~50m long and has a holding capacity of approximately 1000-5000m^3, uses 4ea, ~40m-long augers 412 that are 20" OD. Support of augers 412 is difficult because of their length. Intermediate bearings along the auger shaft would require that the flighting be interrupted and could pose a major clogging risk. The support of such long screw lengths could be addressed by (1) supporting the augers along their entire length on an HDPE or Teflon liner in the casing, (2) support the screws with intermediate, circumferential inserts with HDPE/Teflon linings, (3) inserting rollers on the edges of the screw flights, (4) using intermediate bearing width smooth transitions between screw sections and support bearings, and/or (5) endwalls 4110 may also be converging to reduce the length of augers 412. The augers 412 themselves could be of a variable, stepped pitch from ~1/3x to 1x the flight

OD along the length (7” pitch at the towed end 4112 and stepping by 1”, every 10ft, so that there is a 20” pitch leading into the suction inlet area 414; the pitch lengthening, never shortening, from the drive side to the discharge side) to even out the extraction pattern from the hopper and decrease the starting and operating torque of the drive motors (smaller motors, smaller HPU/generator). The augers 412 can be individually driven or coupled by chains or spur gears. An auger actually has the most draw-down capacity on the upward moving side of the flight, as it uncovers the void beneath. In order to help mass flow near the edges of the live bottom of augers 412 and prevent buildup-up of material (which leads to arching), both edges of the live bottom should have upward moving flight faces. To accomplish this, maintain symmetry, and have all augers 412 feed towards the same end of the hopper, an even number of both left-handed and right-handed augers is required.

FIG. 14 show an end-view of the sequestration barge 410 embodiment from FIG. 13.

Fig. 15 shows an alternative embodiment of the sequestration barge 420 (a separate embodiment from the sequestration barge 410) wherein, instead of a live bottom auger discharging to a pump inlet area, the hopper is continuously filled with seawater (from immediate surrounding in the chosen pump-to-depth location), by passive inlets 422 in the barge hull 429, below the waterline 423, or by actively pumping seawater from the surrounding into the hopper region 424 (using secondary pump(s) 425, suction hose(s) 426, and discharge hose(s) 427 to inject seawater into the hopper region 424. The resulting seawater/sargassum mixture in the hopper region 424 bottom is then pumped out through a suction hose 428 equipped with an auger suction inlet device (similar to 010 or 020; to meter the flow of solids), to 12” 5000GPM pump 000, and pumped-to-depth (or fed to another sequestration process).

A special manifestation of the sequestration barge is a submarine container, a soft shelled (perhaps netting or rubber), reinforced (to it holds it shape under suction), streamlined (to reduced towing power consumption) container. Such a container would require less power to tow and require less floatation (less structure) than a surface barge that carries all its payload above the waterline. The preferred embodiment would have the reinforced structure of the submarine covered with rubber or another lightweight, cheap, strong, low friction material impervious to water. The submarine would be roughly ellipsoidal with orifices on both ends of the major axis. Such a submarine container could be loaded at a quayside or at sea via injecting it with a pump from another water laden sargassum container (through one of said orifices). The submarine container could then be discharged via reversing the suction and discharge hoses and pumping the sargassum out, to the critical depth (or to another sequestration process). During both injecting and discharging, there is mass flow of water and sargassum (at differing rates) along the length of the submarine (through the two orifices in both ends), so there is no need for any active discharging components. Alternatively, discharge of sargassum (only discharge) could happen through an extended suction boom along the upper edge of the ellipsoid (the sargassum will float to the top of the submarine container where it will encounter the distributed suction). The submarine will require it be kept afloat with floatation of minimum cross-sectional area and towed through its center of buoyancy.

Ideally, all equipment for sequestration should be mounted on the sequestration barge/submarine itself so that it can be towed by any ordinary tug boat and so that tugs can be rented from maritime operations companies only when needed for journeys to deep water.

Roller crushing systems

While pump-to-depth is considered the preferred sargassum sequestration method, crushing and mechanically, irreversibly compromising sargassum pneumatocysts renders sargassum negatively buoyant as well. This could conceivably be done with large rolling crushers (grinding the sargassum or otherwise compromising it could make a mess of things and won't 100% compromise every pneumatocyst, which is quite necessary for negative buoyancy). While crushing systems are not the preferred embodiment of the present invention, several crushing systems are summarized below.

One embodiment of this system calls for a modified tanker/landing craft's bow ramp to be outfitted with a pair of rolling crushers. The cylinders could be rigidly attached to the bow ramps, the dipping into the water and the plane formed between their axes being parallel to the bow ramp. This ramp may or may not be controlled by an active heave compensated winch such that it remains in the water even in rough seas. Alternatively, the rolling pair could be arranged perpendicular to the direction of the ship motion, floating in the water (not rigidly attached to the ship, and with a coefficient of friction and/or submerged depth and/or diameters such that the sargassum is lifted out of the water and into the contact patch of the cylinders.

Another onboard implementation of rolling crushers involves placing one, or several, pair(s) of rolling crushers onboard the landing craft 506, shown in FIG. 16, which has a large deck space in front of the bridge. The bow ramp 505 would be outfitted with a conveyor that dips into the water, lifting sargassum 501 out of the water and depositing it into the rolling crushers 503. The conveyor system could also incorporate a separating section 507 to remove turtles from the sargassum (similar to a separator used to separate chicks from their egg shells in hatcheries). Next, a conveyor supported by load cells could provide verification of the amount of sargassum collected and crushed (and this measurement can be corroborated by inline NIR optical spectroscopy). The rolling crushers 503 used could be those already used in mineral processing facilities. After being crushed and rendered negatively buoyant by the rolling crushers 503, the sargassum 501 could be jettisoned through one or more moonpools 504 cut into the hull of the ship, thereby reentering the ocean and sinking. It is recommended that the acquired vessel be "unrestricted" class, or, at least 70m in length to ensure stability at sea. Both the pushed and the onboard implementations could benefit from the use of a concentrating funnel to increase the collection width. Instead of moonpools 504, sargassum 501 could merely exit on additional conveyors that jettison it over/through the gunwales of the ship.

The systems can be thought of in terms of where the rolling crushers are placed (on deck or in the water) and how they are oriented (vertical or transverse). One can also imagine a system with outriggered rollers on the port and starboard sides of a ship, driven by outboard actuators, that are deployed in and crush sargassum in the water, without the need to remove it from the water. The implementation could be deployed on either a landing craft or supply-type ship – any vessels with enough deck space for the hydraulic arms, HPUs, repairs, and maintenance.

Rolling crushers may not be able to 100% crush all sargassum pneumatocysts (necessary for sinking) and, even if they do, there may still be entrained air that can keep the plant afloat for an unknown period of time. It cannot be presumed that ocean mixing will remove air over time as the associative forces responsible for entrained air are quite strong. Even if crushing causes complete annihilation of vesicles and leaves such that they cannot entrain air, discharging the remnants of sargassum onto the surface of the ocean leaves the possibility that the sargassum will be carried, by ocean currents, to undesired locations, before finally coming to rest (shallow areas with photosynthesizing plants, critical habitats, or even coastal/beach areas). Hence pumping the crushed sargassum to 10m or greater depth is preferred so pump turbulence will disrupt and free air bubbles.

SOScarbon Planning Model

FIG. 17 shows a planning model 600 for identifying and predicting the movement of sargassum in the Caribbean, for the purpose of directing fleets of SOScarbon vessels. Said model 600 is critical to the success of SOScarbon for several reasons:

1. SOS will become prohibitively expensive if any and all sargassum near critical coast is sunk indiscriminately. Planning model 600 will direct an SOScarbon fleet, in real-time, so that SOScarbon vessels can precisely target pump-to-depth efforts on sargassum that is destined for critical coastline, without managing sargassum that is destined for uninhabited areas, for example.
2. Planning model 600 could help to plan for and study the potential feasibility and/or effectiveness of SOScarbon implementation in new areas.
3. Planning model 600 could be used to verify the additionality of carbon offsets generated by SOScarbon, by determining where sequestered sargassum would have otherwise landed, and what would've happened to its carbon content.

600a shows results of a particle forward-tracking model in the Mona Passage wherein the original "stain" of 1000 particles is released at 17.85 N. 292.65 E. and HYCOM ocean current data from 02/18/2019 to 02/25/2019 is used to evolve the simulation. From models like 600a, it can be determined that sargassum bound for Punta Cana 601 flows westward, in tight proximity to the south coast of Puerto Rico 602, and enters the Mona Passage in the southeastern corner of the channel. In the Mona Passage, sargassum drifts in an S-curve, first due north, then northwest

across the channel, and then transitioning northward again, before, presumably, being trapped by coastal currents and making landfall. The entire crossing takes approximately 7 days. The overlay of output from these models from historical data, shipping traffic maps, knowledge of sargassum mat shapes in particular areas (from satellite imagery), bathymetric maps, etc., can be used suggest potential SOScarbon operational strategies. Satellite imagery shows that sargassum mats appear more concentrated, dense, and concentric near its entrance to the Mona Passage and upon turning northward after crossing the channel. While crossing the Mona Passage, sargassum is strung out in long "windrows" aligned with the direction of the wind. This suggests that either area 607 or area 609 are most advantageous for pumping-to-depth, with area 609 having the added benefit that it is deep enough there to claim carbon offsets for pumping-to-depth in that location.

Similarly, a particle backtracking model in 600b shows that almost all the sargassum hitting Cancun 605 travels straight through the straight between Cozumel 606 and the mainland 604. A favorable location for pumping-to-depth, therefore, is area 610, just south of the straight, where depth is sufficient and sargassum is crowded into large mats because of the bottleneck nature of the straight.

In the future, real time planning must occur with even higher accuracy and resolution to direct real SOScarbon vessels. The historical trend (from recent, monthly, or perhaps yearly backtracking models) and the 7-10 day forward tracking model should be used in concert to develop a "landfall probability index," assigned to each ~0.08° x ~0.08° bin (resolution of HYCOM dataset) in the area of interest, indicating the relative probability of sargassum hitting critical coast. With mats identified and prioritized based on "landfall probability index", optimized paths for SOScarbon vessel(s) can be suggested to collect mats in advantageous locations (eg. where mats are large and concentrated) using as little fuel/time as possible. Weights applied to the output from backtracking (of historical data) and outputs from forward-tracking (of futuristic forecast data) should be defined through Spearman correlation (Spearman, 1918) with actual sargassum landfall observations from satellite imagery. The model can be further improved by in-situ measurement of salinity, temperature, surface velocity/direction, and current velocity/direction performed by SOScarbon vessels in the area of operation.

In the future, a current dataset different from HYCOM may be used. HYCOM gives daily data for ocean surface currents with 0.08° resolution from satellite observation and direct measurement (Putnam et al., 2018). The datasets capture fronts, filaments, and eddies (Chassignet et al., 2007, Putman and He, 2013), but not wind-induced currents ("Stommel shear"; Rio et al., 2014; Bonjean & Lagerloef, 2002), direct momentum transfer from wind to pelagic debris ("windage"; Trinanes et al., 2016), or waves ("Stokes drift", Monismith & Fong, 2004).

Additionally, in the future, Lagrangian models could be specifically improved for modeling sargassum – the effect of surface currents, windage, and waves on the path of a Lagrangian drifter depends on its buoyancy, form-factor, and surface texture (Putnam et al., 2018). These characteristics likely change with aging/damage (from waterlogging and feeding), encrustation,

etc. (Johnson and Richardson, 1977, Woodcock, 1993, Zhong et al., 2012). There is a large degree of sophistication yet to be harnessed.

In the future it may also be wise to incorporate 3D ocean, benthic currents, not only for the purpose of better predicting sargassum movement, but also for the purpose of predicting where sunken sargassum will migrate and accumulate.

Sequestration Platform

Instead of a specially designed barge/submarine, the sargassum laden barge/submarine could transfer its payload to a semi-permanent platform comprising a gantry-like crane bearing an open-bottomed weighted cage that pushes sargassum down to a depth of ~150-200m before pulling the cage back up to the surface to perform the operation again. Such an ocean platform is illustrated in Fig. 18. Various barge configurations exist that might make unloading sargassum into the open ocean platform most efficient (side-dump/bottom-dump barges, etc), however all concepts revolve around the open ocean platform with the open-bottomed weighted cage. The open ocean platform may have various containment devices, comprising fences, walls, and booms, to contain the sargassum as it is emptied into the platform. In the case of a sequestration submarine as described immediately above, the submarine container itself could be lowered to depth and then bottom of the submarine open via an ultrasonic release, for example, the sargassum released and the submarine container lifted back to the surface.

The system described herein is also applicable to other types of floating biomass or debris in different parts of the world, such as algae, seaweed, jellyfish, and plastic in the great garbage patch. Preferred embodiments of methods and machines to collect and sequester sargassum, have been described, but their utility beyond application to sargassum is apparent in applications involving other types of floating biomass or pollution in many different parts of the world.

Another auger embodiment is the “modified snowblower” is similar to a commercial snowblower, used in the northeast for clearing roads for example, except for several key differences that optimize it for collecting waterborne sargassum. The blower does not have the issue of a pump being starved of flow cavitating. First, the blower may be fitted with a funneling structure (a vee/plane/scoop), partially mesh/wire/cable/string/chain link and partially solid, to funnel sargassum toward the impeller. Further, the left-handed/right-handed auger is supported only from the sides, features no dimension smaller than the characteristic dimension of sargassum, and may comprise fingers/brushes in addition to solid flighting. The primary advantage of the modified snowblower is that, just like an impeller pump, it will “throw” water and sargassum, except that it will feed regardless of its depth in the water whereas a pump will lose suction if its inlet comes out of the water and its inlet is relatively smaller making it very difficult to self-feed without pulling water and exploiting it as a carrier fluid for sargassum. The blower could be mounted on the front of a barge and the discharge chute of the blower can be directed into to a container onboard. Such a system could aid or replace the conveyor barges

currently being used to clean barriers. An exemplary illustration of the core module in the modified snowblower is shown in Fig. 8. The blower may also feature optimized impellers, partially or completely, of elastic material, or with preloaded rigid impeller blades, to improve the transfer of momentum from the impeller blades to sargassum. Soft impeller materials will also allow the impeller blade to touch the volute (whereas a metal impeller requires healthy spacing) which will reduce materials wedging between the impellers and the volute.

The systems described herein are also applicable to other types of floating biomass or debris in different parts of the world, such as red/green algae, seaweed, jellyfish, and plastic in the great garbage patch.

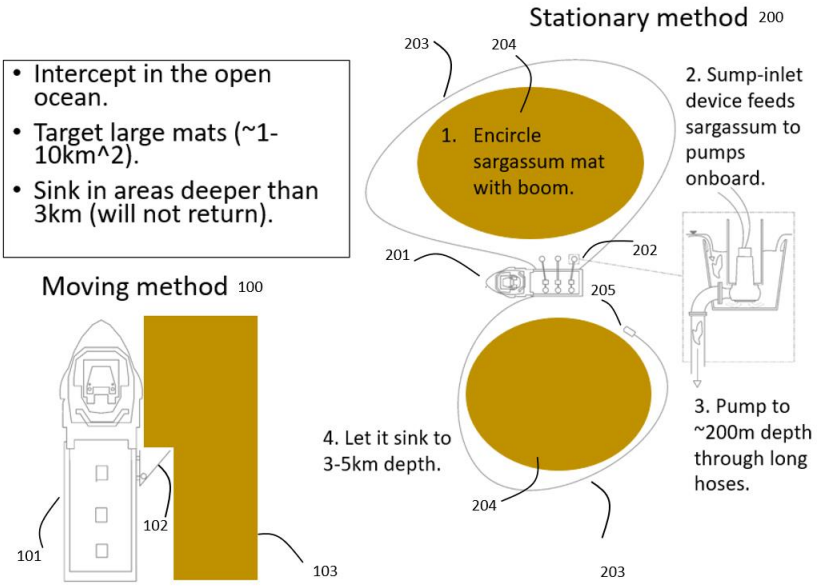

Fig. 1

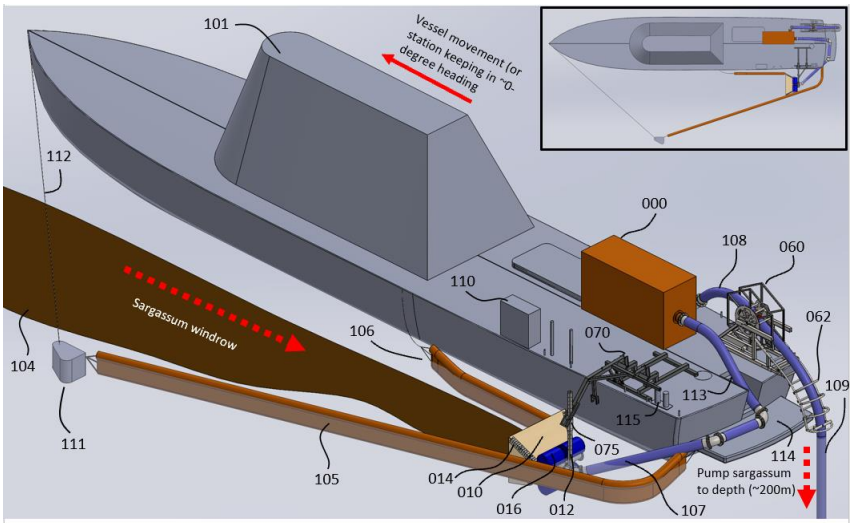
101
Vessel movement (or station keeping in ~0-degree heading
112
000
108
060
110
062
106
070
104
Sargassum windrow
113
109
115
111
075
114
105
014
010
016
012
107
Pump sargassum to depth (~200m)

Fig. 2

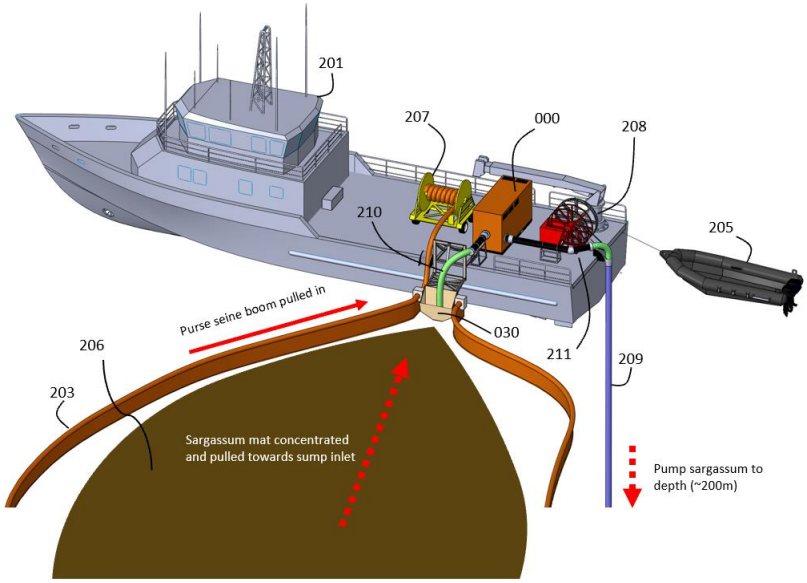
201
207
000
208
210
205
Purse seine boom pulled in
030
206
211
209
203
Sargassum mat concentrated and pulled towards sump inlet
Pump sargassum to depth (~200m)

Fig. 3

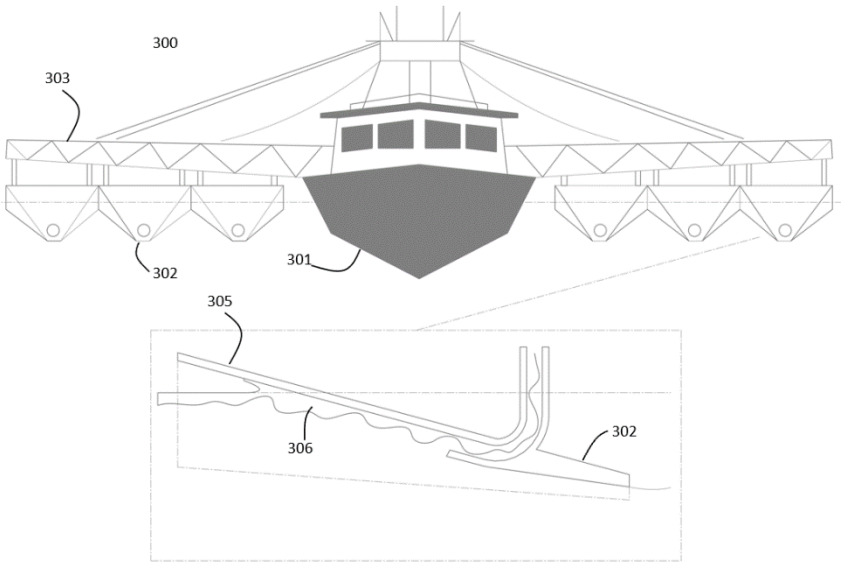
300
303
302
301
305
306
302

Fig. 4

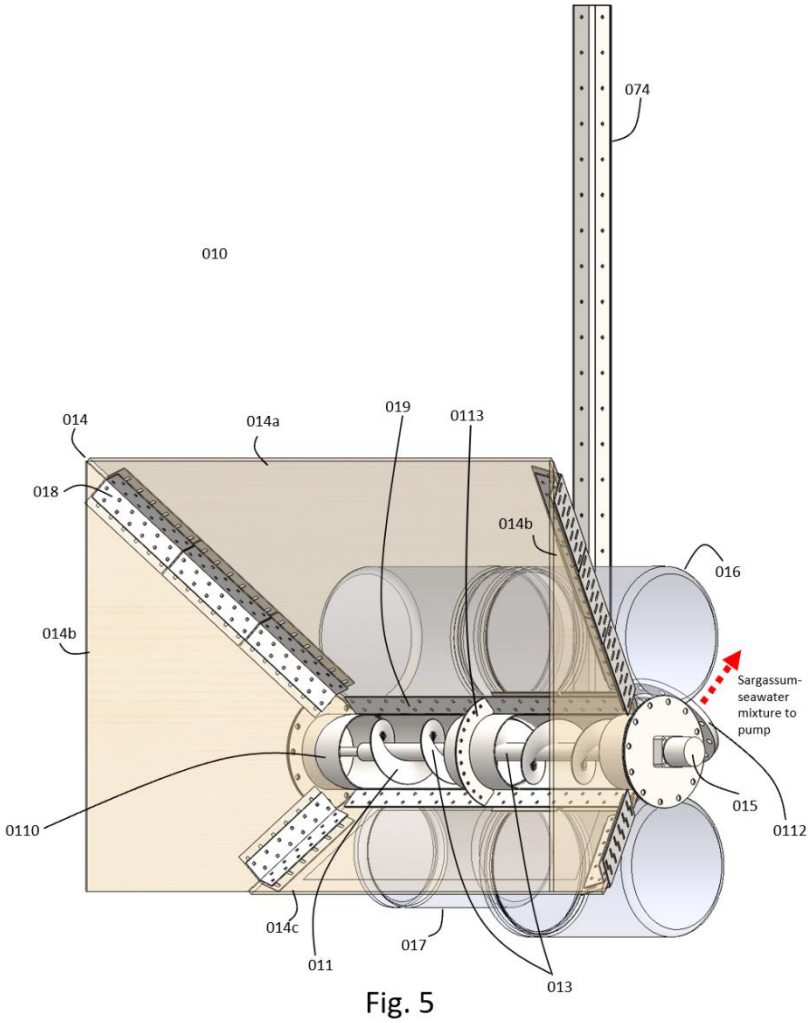
074
010
014
014a
019
0113
018
014b
016
014b
Sargassum-seawater mixture to pump
0110
015
0112
014c
011
017
013

Fig. 5

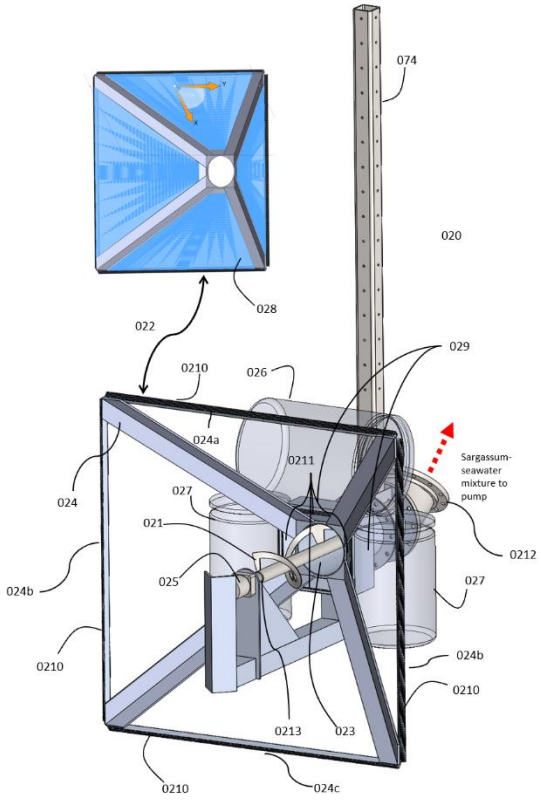
074
020
028
022
029
0210
026
024a
0211
Sargassum-seawater mixture to pump
024
027
021
0212
025
024b
027
024b
0210
0210
0213
023
0210
024c

Fig. 6

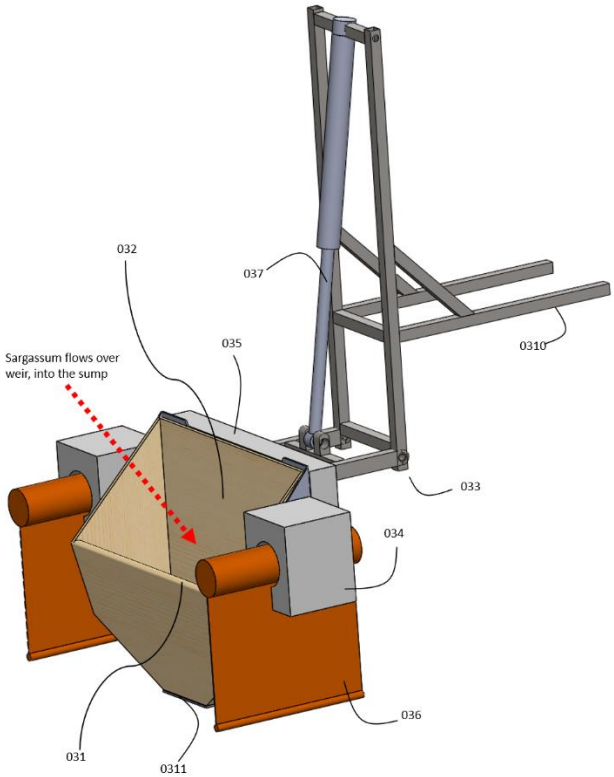
032
037
0310
035
Sargassum flows over weir, into the sump
033
034
036
031
0311

Fig. 7

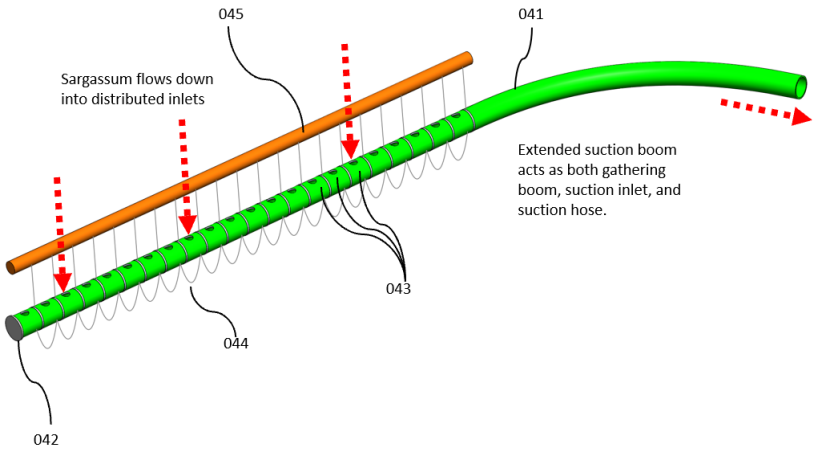
045
041
Sargassum flows down into distributed inlets
Extended suction boom acts as both gathering boom, suction inlet, and suction hose.
043
044
042

Fig. 8

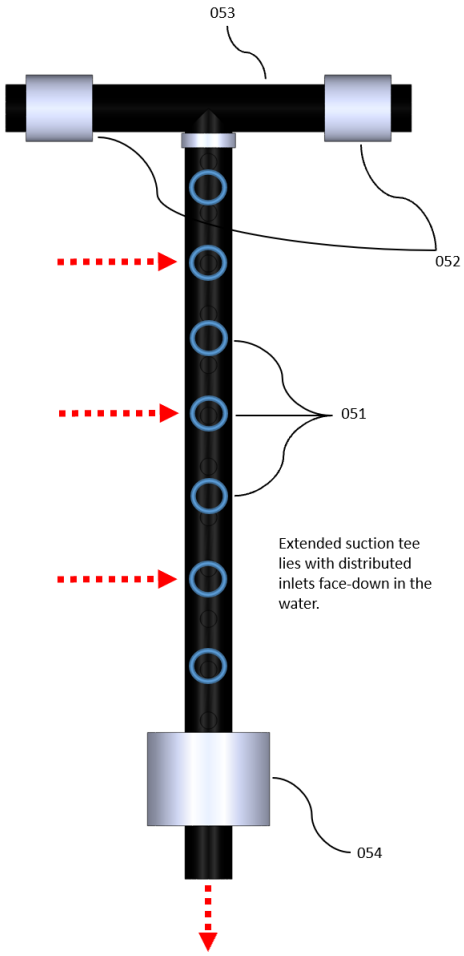
053
052
051
Extended suction tee lies with distributed inlets face-down in the water.
054

Fig. 9

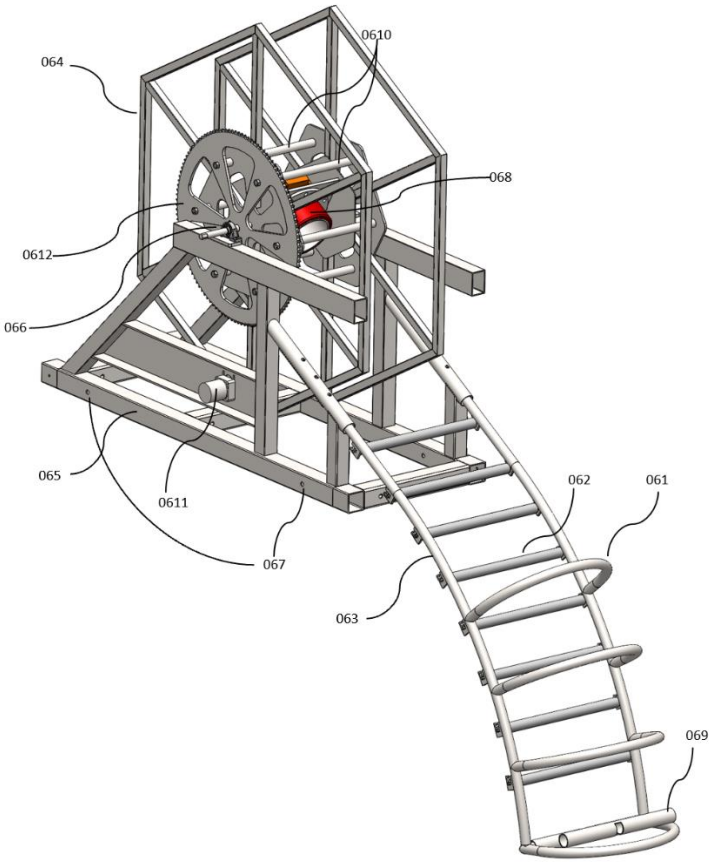
064
0610
068
0612
066
065
0611
067
062
061
063
069

Fig. 10

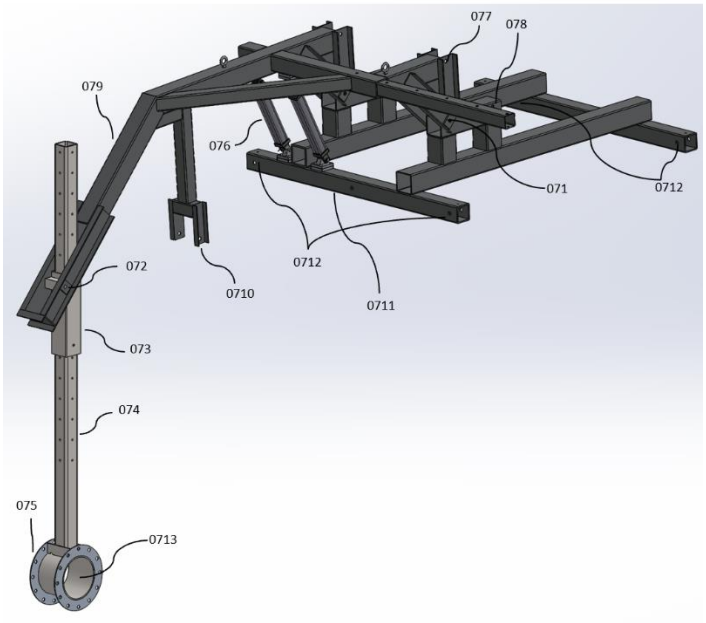
077
078
079
076
071
0712
0712
072
0710
0711
073
074
075
0713

Fig. 11

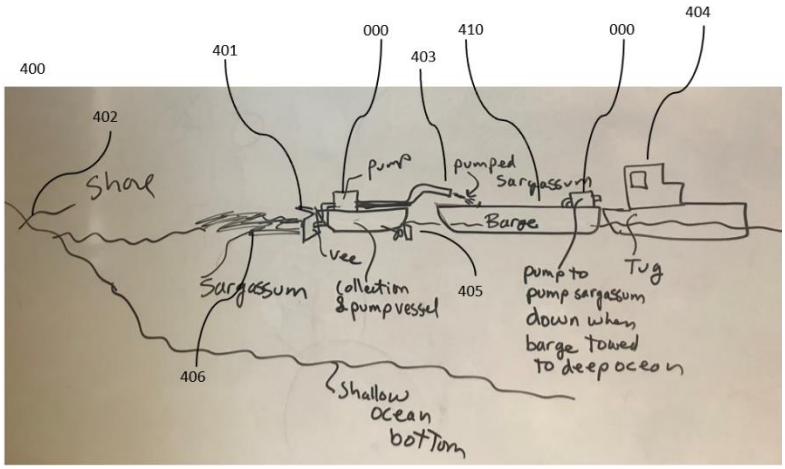
400
401
000
403
410
000
404
402
Shore
pump
pumped Sargassum
Barge
Tug
vee
collection & pump vessel
405
Sargassum
406
pump to pump sargassum down when barge towed to deep ocean
Shallow ocean bottom

Fig. 12

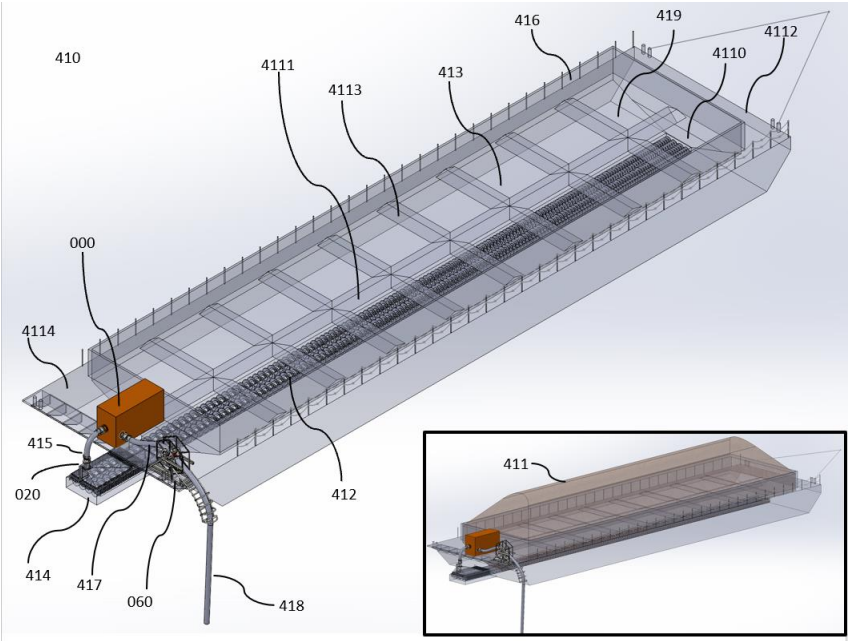
410
4111
4113
413
416
419
4112
4110
000
4114
415
020
414
417
060
418
412
411

Fig. 13

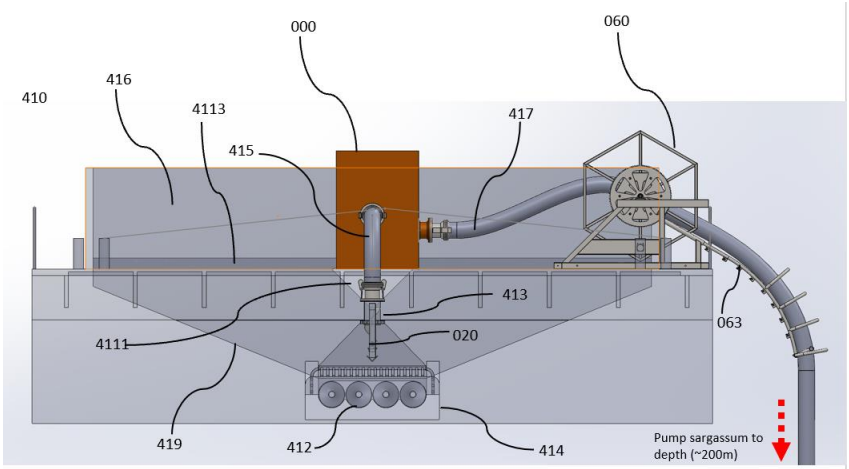
000
060
410
416
4113
417
415
413
4111
020
063
419
412
414
Pump sargassum to depth (~200m)

Fig. 14

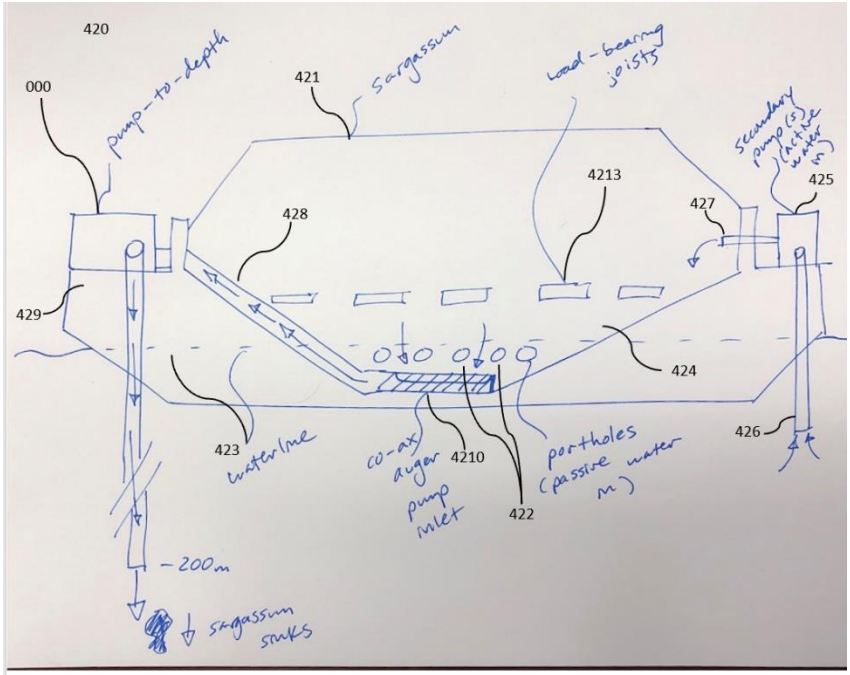
420
000
pump-to-depth
421
sargassum
load-bearing joists
secondary pump (s) (active water in)
4213
425
427
428
429
424
423
waterline
co-ax auger pump inlet
4210
422
portholes (passive water in)
426
~200m
sargassum sinks

Fig. 15

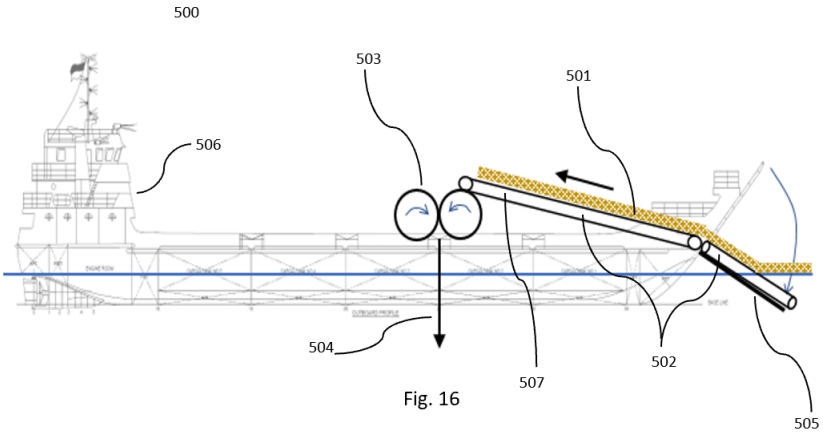
500
503
501
506
504
507
502
505

Fig. 16

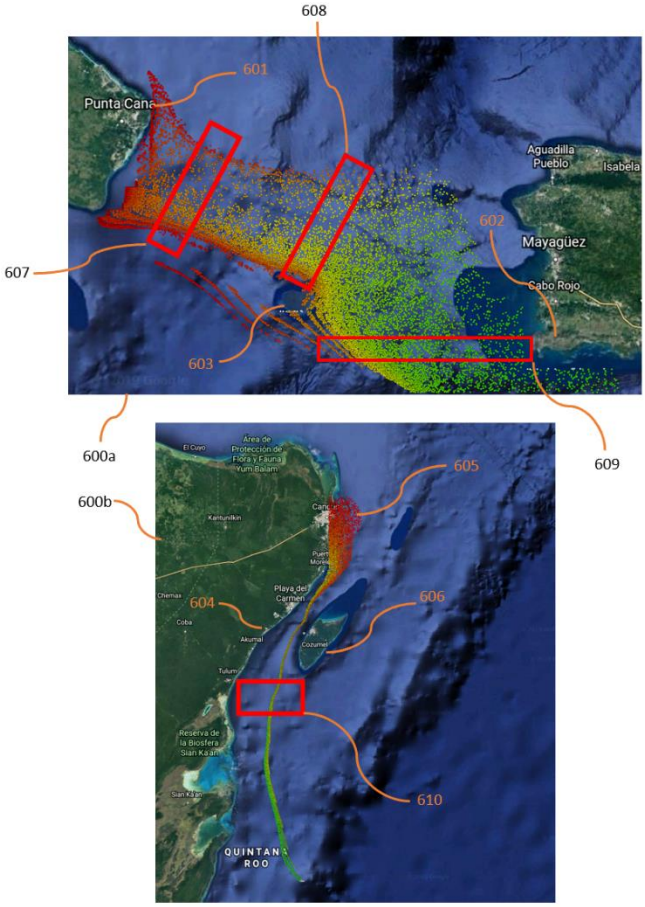
608
601
Punta Cana
Aguadilla
Pueblo
Isabela
602
Mayagüez
607
Cabo Rojo
603
600a
609
605
600b
604
606
610
QUINTANA
ROO

Fig. 17

7.2 Artisanal Collection Vessel Provisional

MODULAR SYSTEMS FOR RETROFITTING ARTISANAL WATERCRAFT AS COLLECTION BOATS FOR MARINE DEBRIS

FIELD OF THE INVENTION

The present invention relates to systems for retrofitting artisanal watercraft for collecting floating marine debris.

STATEMENT REGARDING FEDERALLY FUNDED RESEARCH

This invention was made without US government support.

BACKGROUND

BACKGROUND IS REDACTED BECAUSE ALREADY INCLUDED IN SECTION 2

The present invention describes systems for retrofitting local artisanal vessels for collecting sargassum near shore or on shore to: reduce cost & visual pollution, increase scalability of collection systems, reduce carbon footprint of cleanup efforts, reduce design and manufacturing/maintenance time, and help artisanal fishers (and other boat owners) earn a living wage while fishing is not as profitable.

OBJECTS OF THE INVENTION

The primary method described herein, for collecting sargassum using nets deployed from artisanal vessels, involves skimming long nets through the surface of the water where sargassum is floating. The nets are deployed from the vessels using modular, rapidly installed/removed arms with adjustable fixturing such that the same modular design fits many different types and sizes of artisanal vessels. When nets are filled, each net is tied closed and left floating at the barrier/or on the beach (wherever collection is happening) for subsequent pickup and towing, perhaps in chains of nets, to final disposal.

Accordingly, the following objects of the invention include:

A principal object of this invention is to provide a simple, low-cost modular system that rapidly installs/uninstalls onto many different types and sizes of artisanal vessels, to provide a structural member from which nets are efficiently and conveniently deployed, skimmed, removed, and replaced.

A further object of the invention is to provide a mass-manufactured sausage-like net that is easily secured, filled, detached, closed, towed, lifted, emptied, cleaned, and folded for repacking back inside the artisanal collection vessel for reuse.

A further object of the invention is to an anchoring module, perhaps comprising screwed/bolted plates for anchoring to artisanal vessels. An alternative anchoring mechanism is to employ a dual-screw clamp that is fixed around the gunwales of the vessels.

A further object of the invention is a widthwise, port-to-starboard, spanning member as the structural backbone of the device and mounting structure for additional objects.

A further object of the invention is long rotating arms that can be pinned in an up (translating/net reloading) and down (collection) position. The arms extend out over the side of the artisanal vessels

A further object of the invention is net holders, comprising circular rolled tubing, that fix nets and hold them open.

A further object of the invention is to use Vernier hole/slot patterns on said spanning member and anchoring module to ensure the intended pin can always be inserted, regardless the beam/width of the artisanal vessel, to lock the spanning member to the anchoring module.

A further object of the invention is to secure the net holders to the rotating arms via pins inserted through vertical posts extending from the net holders and tubes attached to the ends of the rotating arms.

A further object of the invention is to provide a number of pinholes on said vertical post extending from said net holders, such that the vertical position of said net holders can be adjusted to accommodate the freeboard of different artisanal vessels.

A further object of the invention is to provide a number of said tubes attached to the ends of the rotating arms such that the radial position of said net holders (relative to the pivot point of said rotating arms) can be adjusted to accommodate the beam/width of different artisanal vessels.

A further object of the invention is to provide safety pin holes in said spanning member such that said rotating arms can be secured in the “up” (transit and net changing mode) and “down” (skimming/collection mode) positions.

A further object of the invention is to provide rolling members on the outboard sides of the said net holders to provide rolling contact with any obstacles (ie. barriers) sargassum is accumulated against (to prevent damage to said obstacles and/or the net holders themselves).

A further object of the invention is to provide a funnel-like structure on the inboard sides of said net holders such that sargassum deflected by the hull of said artisanal vessel, as it moves through a mat of sargassum, is directed into said sausage-like nets, increasing the effective collection width of the system (to include the beam of the artisanal vessel) and improving the collection efficiency (less leakage), lowering the filling time of a single net for a given vessel speed.

A further object of the invention is to provide a sausage-like net that can be opened/closed on either end and gravity discharged by lifting through its axis and opening the bottom end.

A further object of the invention is to provided a sausage-like net with circumferential and lengthwise structural lines for towing and lifting out of the water (for emptying via a slip knot or drawstring).

A further object of the invention is to provide a sausage-like net with a sufficiently fine mesh such that sargassum can be gravity discharged without too much sargassum clinging/entangling in said mesh.

A further object of the invention is to provide a sausage-like net with solid/reinforced ends for structural purposes and to create lengthwise tension during initial towing (due to a "parachute effect") such that the nets are parallel to said artisanal vessels and said sausage-like net remains open along its length to reduce resistance to sargassum filling.

A further object of the invention is to provide a sausage-like net made from nylon/polyester or other manufactured materials (ie. Dyneema) that is buoyant, or neutrally buoyant, such that the nets float when filled with sargassum.

A further object of the invention is to tow sausage-like nets in daisy chains, through the water, by connecting said lengthwise structural lines of each net.

A further object of the invention is to provide a structure around said vessel's propellers such that barriers, other infrastructure in the collection area, and the propellers themselves, are not damaged – a particular risk when operating in the dark.

A further object of the invention is to provide lights for operation in the dark.

A further object of the invention is to equip said artisanal vessels with >60hp motors for optimal operation, even in thick sargassum mats.

A further object of the invention is to use two artisanal vessels in parallel, connected by structural members, to tow even larger nets between them.

A still further object, is to forego using said anchoring module, spanning member, rotating arms, and net holders by simply towing said sausage-like nets behind said artisanal vessel(s).

Other and further objects will be explained hereinafter and more particularly delineated in the appended claims.

SUMMARY

In summary, in the preferred embodiment of the present invention, screwed/bolted or clamping anchoring modules fix a spanning member onto an artisanal vessel, using Vernier hole/slot pattern with a pinned connection such that the module will fix to vessels of variable width. Connected to the spanning members are rotating arms with net holders on their ends, which secure sausage-like nets, hold them open, and deploy/fix them in the water on the port and starboard sides of said artisanal vessel. Sausage-like nets are towed simultaneously (or one at a time while one of the two nets is being changed) on the port and starboard sides of the artisanal vessel, sargassum floating at the surface of the water being collected into said sausage-like nets in the process. The net holders are secured to the rotating arms via pins inserted through vertical posts with a pattern of holes that allows the vertical position of the nets to be adjusted to accommodate the freeboard of different artisanal vessels. There are multiple insertion points for said vertical posts on said rotating arms such that the radial position of said net holders (relative to the pivot point of said rotating arms) can be adjusted to accommodate the beam of different artisanal vessels. Safety pins are provided on said spanning members to fix said rotating arms in both the “up” (transit and net changing mode) and “down” (skimming/collection mode) positions. Said artisanal vessels may be outfitted with a structure around said vessel’s propellers such that barriers, other infrastructure in the collection area, and the propellers themselves, are not accidentally damaged, a particular risk when operating in the dark. Said artisanal vessel may be outfitted with lights for operating in the dark (often required so that beaches are clean at the start of the day for tourist use). Said artisanal vessels are fitted with a motor of at least 60hp for operation in think mats of sargassum. Additional, reused sausage-like nets are stored in various available space around the artisanal vessel for rapid/sustained replacement of filled nets. Sausage-like nets can be open/closed on both ends, designed to be buoyant, they are reinforced with circumferential and lengthwise structural lines such that they can be towed away (perhaps daisy-chained together) through the water, then lifted and opened from the bottom such that they can be gravity discharged into a barge or truck, etc. A variation of this system involves connecting two monohulled collection vessels via structural members such that a larger net can be towed/filled between them. An alternative to port-starboard deployment is to simply tow the sausage-like nets behind the vessel in a surface-trawling fashion. These systems are also applicable to other types of floating biomass or debris in different parts of the world, such as algae, seaweed, jellyfish, and plastic in the great garbage patch.

Best mode and preferred designs and techniques will now be described.

DRAWINGS

The present invention can be best understood in conjunction with the accompanying drawing, in which:

FIG. 1 An example of a system for retrofitting an artisanal boat as a sargassum collection vessel, which collects sargassum by skimming nets through the surface of the water where sargassum is floating;

FIG. 2 One method by which filled nets of sargassum are towed away through water (instead of being transported through land) by a jet ski (could also be an artisanal vessel, the collection vessel itself, or another specially designed vessel). The nets can be daisy chained together as shown;

FIG. 3 The fishing village in Cabeza del Toro, Dominican Republic, centrally located between tourist areas of Bavaro and Punta Cana. The village is one of many in the Caribbean that is hard hit by sargassum, which corrodes and damages their equipment. Fishing harvests have also been on the decline due to changing fisheries populations and fish travel patterns, a further negative effect of sargassum. Many locally constructed (pictured are wooden/fiber glass vessels made in Miches, Dom. Rep.) artisanal vessels sit idle, or in disrepair, as a result.

FIG. 4 A sargassum collection experiment carried out using a large skimming net secured between two artisanal fishing vessels, showing how two artisanal vessels may work together to fill larger nets;

In the drawings, preferred embodiments of the invention are illustrated by way of example, it being expressly understood that the description and drawings are only for the purpose of illustration and preferred designs, and are not intended as a definition of the limits of the invention.

PREFERRED EMBODIMENT(S) OF THE INVENTION

FIG.1 shows the preferred embodiment of the invention. Artisanal vessel 1 moves relative to sargassum 2 accumulated on barrier 3 (barriers are not required – collection can also be done offshore or along the beach so long as sargassum is in water of sufficient depth to accommodate draught of said artisanal vessel 1), collecting said sargassum 2 into sausage-like net 4 (FIG. 1 shows only one net deployed but usually both nets, port and starboard of artisanal vessel 1, would be deployed). Boom module 100 is attached artisanal vessel 1 and can lower arms 7 & 10 from vertical stowed position to horizontal deployed position. Net 4 is held by net holder 5 via loops and hooks 6. Net holder 5 is attached to rotating arm 7 via a vertical post 8 pinned inside insertion tube 9. The plurality of pinholes on vertical post 8 and insertion tubes 9 on rotating arm 7 allow the vertical and radial adjustment of the net holder 5 to accommodate different artisanal

vessel freeboard and beam/width, respectively. There are rotating arms 7 & 10 and net holders 5 & 11 on both the port and starboard sides of the artisanal vessel 1.

Normally, two nets would be deployed simultaneously on both sides of the artisanal vessel, using both sets of rotating arms 7 & 10 and net holders 5 & 11, and the bow of the artisanal vessel 1 would split the sargassum mat to flow around it and into both deployed nets. But FIG. 1 shows the portside rotating arm 10 in the "up" position to facilitate loading a new net onto the portside net holder 11. Safety pins and pinholes are provided to fix the rotating arms 7 & 10 in the "up" and "down" position for sargassum collection and net-replacement/transiting, respectively. The arms 7 & 10 are better supported against large hydrodynamic drag forces by the triangular frame structures 33a & 33b, respectively.

The rotating arms' (7 & 10) pivots are in spanning member 12. Spanning member 12 is the main structural member tying both sides of the system together. Spanning member 12 is fixed to the artisanal vessel 1 via screwed/bolted plate 14. Spanning member 12 is pinned to screwed/bolted plate 14 via a series of staggered "Vernier-style" holes/slots 13 such that a pin can always be inserted through both spanning member 12 and screwed/bolted plate 14, accommodating variable beam/width of the artisanal vessel 1. Screwed/bolted plate 14 is attached directly to the gunwale and structural member of the artisanal vessel 1 (here a bulkhead which also serves as a seat – a design common in the Dominican Republic). Screwed/bolted plate 14 (and the attached pin-block with Vernier holes) always remain attached to the vessel once installed (minimal interference if the sargassum module is removed and the artisanal vessel 1 returns to its normal function – fishing, water taxi, etc.), but screwed/bolted plate 14 could also be a clamp for complete, rapid removal (depending on boat construction – wood or fiberglass).

While not shown in FIG. 1, a further evolution of the design might provide rolling members on the outboard sides of net holders 5 & 11 to provide rolling contact with any obstacles (ie. barriers) sargassum is accumulated against (to prevent damage to said obstacles and/or the net holders themselves).

A further evolution of the design might also provide a funnel-like structure on the inboard & outboard sides of said net holders 5 & 11 such that sargassum deflected by the hull of said artisanal vessel 1, as it moves through mat of sargassum 2, is directed into sausage-like net 4, increasing the effective collection width of the system (to include the beam of the artisanal vessel 1) and improving the collection efficiency (less leakage), lowering the filling time of a single net for a given vessel speed.

Headlights 15 (and other cabin lights not shown) aid operation in the dark (which is often required such that beaches are clean for tourists at the start of each day).

Artisanal boat 1 is outfitted with an outboard motor 16 with >60hp for optimal operation, even in thick sargassum mats.

Artisanal boat 1 is outfitted with stern guard 17 to protect barriers, and other structures in the collection area, from collision with the propeller of outboard motor 16.

Additional, reused sausage-like nets 19 are stored in various available space around the artisanal vessel 1 for rapid/sustained replacement of filled nets. Sausage-like nets can be open/closed on both ends, designed to be buoyant, they are reinforced with circumferential and lengthwise structural lines 18 such that they can be towed away (perhaps daisy-chained together) through the water, then lifted and opened from the bottom such that they can be gravity discharged into a barge or truck, etc. Net 4 may have solid/reinforced ends 20 for structural purposes and to create lengthwise tension during initial towing (creating a “parachute effect”) such that the nets are parallel to artisanal vessel 1 and said net 4 remains open along its length to reduce resistance to sargassum filling.

These systems are best used next to barriers (they offer the advantage that these lightweight craft can clean very close to barriers whereas other specialized conveyor boats currently used cannot, meaning sargassum always sit next to the barrier where it bio-fouls said barrier and dissolves/rots, dyeing water brown, emitting a terrible smell, and passing through the barrier in small pieces, eventually landing on beaches) and while moving against the current (to promote feeding at lower vessel speed and increasing controllability next to barriers and other obstacles). However, these vessels could be used to clean immediately next to beaches so long as accumulated sargassum is still in a depth sufficient to accommodate the draught of the artisanal vessel 1 (sargassum that has already made landfall and been pushed up onto the beach could also be pushed back into the water for collection with this system – this is better than trying to collect from the beach directly because it avoids collecting much sand with the sargassum and compacting the sand with heavy machinery).

FIG. 2 shows the preferred method for towing away filled nets 23 of sargassum through the water (by their lengthwise structural lines 18). This is more cost-effective and preferred to the present method of bringing sargassum through resort areas (through narrow/limited access points – sometimes even tourist throughways) to be loaded onto a truck (because of reduced visual pollution for tourists). Shuttling craft 21 are used to pickup and tow filled nets 23, that are left floating against barriers/beaches after being filled (this allows collection and transport to continue at the maximum rate without depending on any synchronization between the two processes). Jet skis are the ideal shuttling craft 21 because they have a high power-to-drag ratio (don’t waste power moving the shuttling craft 21 itself), a wide power band (can move at high speed with low load and low speed at high load) which means, after finishing a tow, they can return to the collection area very quickly to pick-up more filled nets 23 (which means less shuttling craft 21 are required in a given area). Note that the shuttling craft 21 could also be the collection vessel itself (not ideal as these vessel should continue collecting), or another specially designed vessel (as some resort areas have a ban on jet skis because of noise pollution). Filled nets could be daisy-chained together by connecting their lengthwise structural lines 18 together at junctions 24. The shuttling craft 21 should be separated from the nearest filled net 23 by an

adequate length of towline 22 such that momentum can be efficiently imparted to the water/shuttling craft.

Once towed away from beaches/barriers, filled nets 23 can be emptied into barges moored offshore, for further transport (or disposal at sea), or loaded onto trucks for transport to proper landfills (so long as no toxicity present) or to transformation facilities (to make products - so long as no toxicity present).

FIG. 3 shows the fishing village at Cabeza del Toro, a small resort area between Punta Cana and Bavaro. This village is hit hard by sargassum. Fishing boats are corroded and damaged by sargassum. Fishing profit is severely diminished because fisherfolk are forced to clean their own beach instead of fish and also because fishing harvests have been severely diminished due to changing fisheries (species populations and travel patterns), as a result of sargassum blooms. Many artisanal fishing vessels sit idle, or in disrepair, at fishing outposts throughout Punta Cana. These vessels and fisherfolk manpower could be utilized immediately to clean beaches and help improve the lives of communities traditionally reliant on fishing.

FIG. 4 shows a makeshift test using two monohulls attached by structural members working together to fill a large net between them. Such a dual-vessel system could be an alternative to the single vessel system shown in FIG. 1.

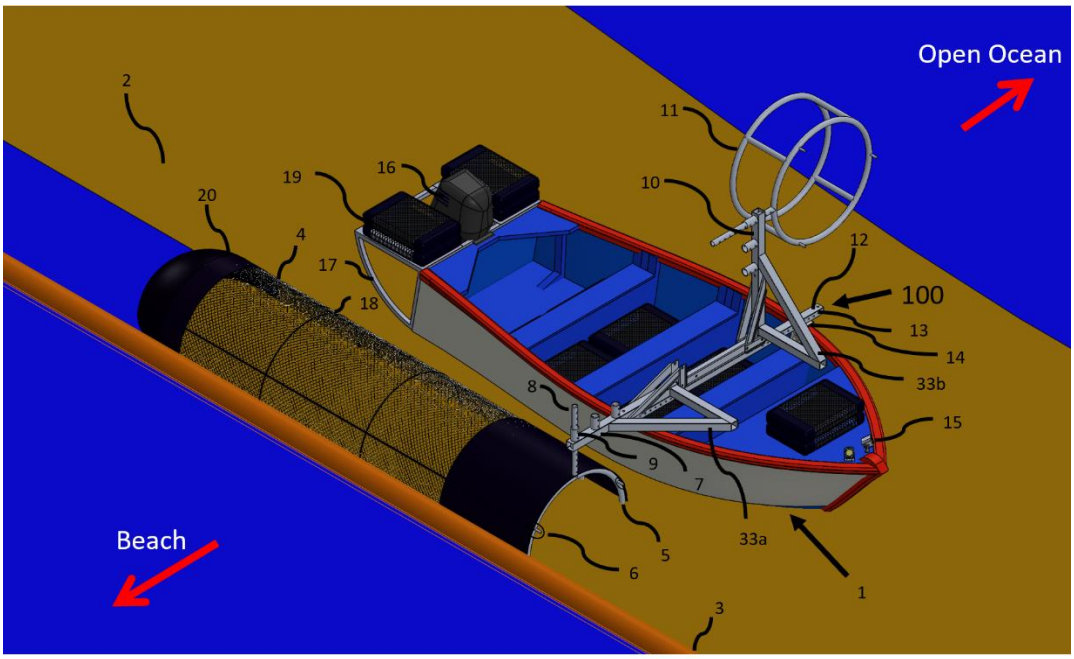

FIG 1

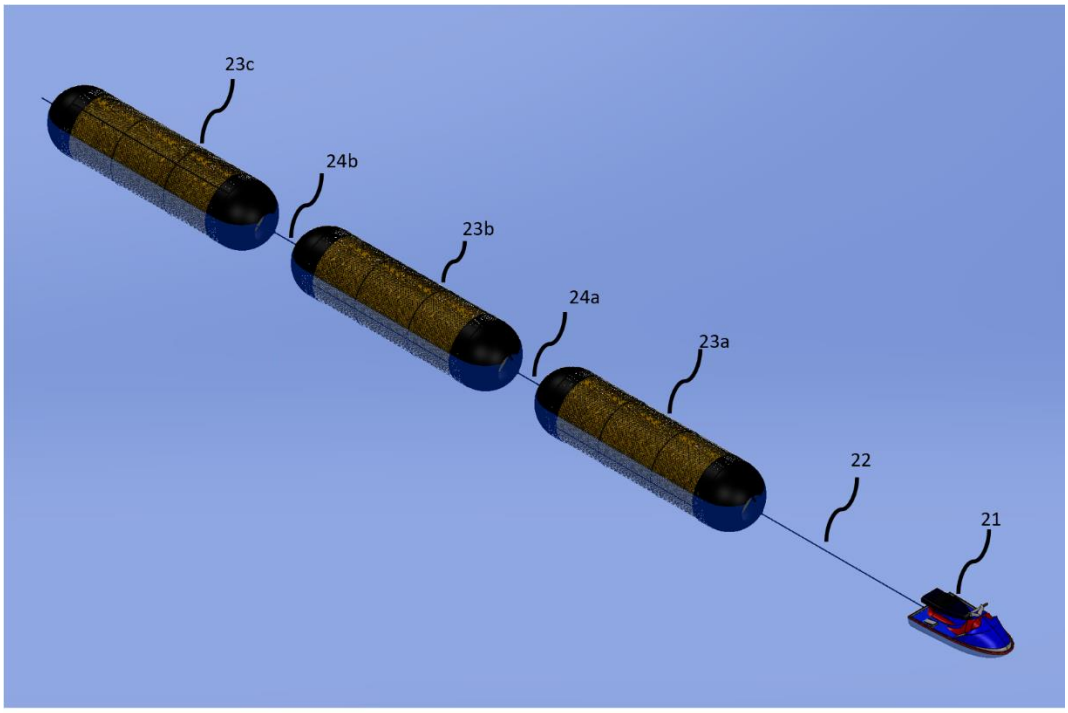

FIG 2

FIG 3

FIG 4

8. Conclusions

This thesis documents an investigation and systems analysis of the sargassum problem in the Caribbean. It documents the design/building/testing of low-cost systems for collecting sargassum and sequestering it in the deep ocean.

The inventors chose a strategy of "sargassum ocean sequestration of carbon" (SOS Carbon) which comprises a method wherein sargassum is "pumped-to-depth" in the ocean (150-200m) where ambient hydrostatic pressure compresses sargassum pneumatocysts and renders the entire plant negatively buoyant such that is continues sinking to the bottom of the ocean.

Because pumps came central to this disposal strategy, the inventors designed and built many pump inlet devices that could collect sargassum near- or off-shore. This thesis identifies two primary systems by which the SOS method, and the associated pump-inlet devices, could be implemented to begin reducing sargassum landfall in the Caribbean - (1) ex-situ system and (2) in-situ system.

The ex-situ system uses pump inlet devices or artisanal working boats to collect sargassum from beaches/barriers, into nets, that are then towed offshore and deposited in a barge. When filled, this barge is then towed out to deep water (250m → >3km) for disposal via pumping-to-depth.

The in-situ system comprises a fleet of sea-going vessels operating near an area of interest, that addresses sargassum mats in the open ocean, collecting and pumping-to-depth simultaneously.

The team did proof-of-concept tests of the pump-to-depth method in the Dom. Rep. in January, 2019.

With the support of a cohort of donors from the U.S. and the Dom. Rep., the team constructed an SOS Carbon Pilot system and tested it onboard a Dom. Rep. navy vessel. This system showed that a large-capacity pump-to-depth system could be built quickly, by a small team, and for a low cost. The test also showed that the system could be seamlessly installed and operated on a vessel of a generic design. Lastly, the test showed that the system could process sargassum at a high solids concentration and pump-to-depth with a very low energy consumption.

It was not within the scope of the pilot tests to do open ocean tests on wild sargassum mats because none were present at the time the SOS Pilot vessel construction was finished (sargassum was instead collected from elsewhere and jettisoned overboard for tests). Pilot equipment is still installed on the navy vessel at the time of this submission and the team is actively seeking to perform tests on wild mats of sargassum in the near future.

Co-benefits of the SOS method, also discussed herein, include avoiding heavy metal leaching from the practice of dumping sargassum in pits near resorts, and carbon offsets that could be generated as a result of sequestering sargassum in the deep ocean.

Appendix A – Carbon Offset Potential

Sargassum, like other macroalgae and microalgae, plays a natural role in oceanic carbon sequestration; natural senescence and sinking of sargassum biomass (Stoner, 1983), the release of recalcitrant dissolved organic carbon (rDOC) (Bauer, Williams, & Druffel, 1992), and faecal pellets from animals grazing on sargassum (Itoh et al., 2007), are all ways in which sargassum helps sequester carbon in the ocean. While the latter two sources have been quantified as contributing 4.3×10^{10}gC/yr, the amount of carbon sequestered via sargassum sinking is not known (International Union for Conservation of Nature, 2014).

Could the SOS strategy be subsidized, or even be made profitable, by selling carbon credits? Sinking carbon in the ocean could affect the carbon cycle in three ways: (1) the net carbon comprising the biomass of the sargassum being sunk, (2) the avoided methane emissions that would result, should sargassum make landfall and be put into landfills or decay in anaerobic coastal waters, and (3) the carbon sequestered as a result of sargassum area coverage being replaced by more productive phytoplankton, thereby increasing the net biological pumping capacity of the ocean.

We estimate that the pump-to-depth process, by consuming so little fuel to sink sargassum, could sequester 0.258 MTCO2 per MTSW (metric ton sargassum wet). If all the sargassum entering the Caribbean each year were sequestered at the bottom of the sea, we estimate an upper limit on carbon reduction potential of 100 million MTCO2/year. FIG 101 shows these results in the spreadsheet tool developed. FIG 102 shows how SOS Carbon could compare to alternative negative emissions technology.

Common problems with past and present offset schemes include (1) uncertain effects of the project (ie. afforested plots of land take decades to grow and are subject to wildfires and disease which means they might never reach the carbon sequestering potential that the offsets represent), (2) perverse incentives (ie. the realized market for sequestration or destruction of the GHG might cause the offset agent to create more of that pollutant), (3) the additional offset value of a project (ie. there is often controversy over whether or not an offset would happen in spite of the project), (4) permanence (ie. sequestering carbon in terrestrial plants runs the risk of the carbon being reintroduced if the plants are later harvested), and (5) leakage (ie. activity of the offset project may, itself, create emissions or cause emissions in a related industry to increase). Not only will cap-and-trade systems limit the influx of these "voluntary" credits, but entities who buy these controversial offsets risk severely damaging their brand.

Unlike some controversial offset projects, sinking sargassum has a certain, immediate, and permanent carbon offset value. Not only this, but the fact that sinking sargassum solves a significant problem for the Caribbean, means that any agent that sinks sargassum may be able to claim "co-benefits" on top of the value of the net, sequestered carbon. Because sargassum is known to absorb toxic elements/heavy metals in the ocean, there may also be grounds to claims co-benefits from sequestering these elements in the deep ocean. Doing this in growing Caribbean nations that simultaneously lack a sizable portfolio of offset projects, could make SOS a very attractive offset scheme. With the general trend towards environmental stewardship, promotion of carbon taxation, and more far-reaching cap and trade programs, the future appears promising for offset businesses.

While cap and trade systems place limits on the amount of outside credits that can be sold into their carbon markets, private companies committed to carbon-neutrality may choose to buy their credits

from anywhere, and in any amount so long as they meet their internal standard (usually these companies pay credit auditors to verify offsets). If this private customer proves to exist, it could mean that the monetization of SOS offsets could happen much sooner, through private 3rd party auditors, than if they were to be issued through the UN. For these companies, the credits they buy can have a large impact on their brand. Just like buying unaudited credits may hurt their brand, buying credits that have the co-benefit of helping the Caribbean may be particularly attractive, perhaps even warranting a premium price.

Quantity Description	Variable	Value	Formula	Reference/Explanation
Calculations related to the open ocean elimination strategy...				
Sargassum coverage in the Central Western Atlantic (CWA) (km^2)	C	2,000		(Wang and Hu, 2015)
Wet weight of sargassum in the GASB (tonnes)	WW	2.20E+10		(Wang & Hu estimate from June 2019, Gower and King, 2011, estimated 2 million tonnes in the GoM and the Atlantic combined)
Doubling time of sargassum in open ocean, phosphorous poor (days)	DRp	33.3		(Lapointe, 1986)
Rate of sargassum egress from the Central Western Atlantic @ s.s. (m^2/yr)	ER	2.19E+10	365*C*1000000/DRp	Based on doubling rate, this is the rate at which sargassum leaves the CWA to maintain s.s. coverage.
Dry weight of sargassum that could be sunk each year (tonnes/yr)	DWmax	7.01E+06	ER*area density*DW/1000000	Converting to weight/year.
Above is for is sargassum is collected in the CWA... if operation happens closer to shore, we need to account for sargassum growing en route to the Caribbean...				
Doubling time of sargassum in neritic water, phosphorous rich (days)	DRr	12.5		(Lapointe, 1986)
Radius of the Earth (m)	Re	6.37E+06		Used below to calculate the approximate distance traveled by sargassum.
Approximate circumferential distance from 0° N, 30° W to Punta Cana (18° N, 68° W) (m)	dist	4.68E+06	(((2*PI())/360)*18*Re)^2+(((2*PI())/360)*38*Re)^2)^(0.5)	Punta Cana is taken as the center of the problem area in the Caribbean.
Avg wind/wave speed at sea (m/s)	vwave	2		For a surface wave.
Approximate transit time of sargassum from the CWA to the Eastern Caribbean (days)	TT	27	dist/vwave/60/60/24	Or slower because of meandering.
Approximate annual total of sargassum that arrives on Caribbean shores (m^2/year)	AT	9.8.E+10		Assuming, on average, a mat reaches the Eastern Caribbean without sinking naturally.
1. Landfill space and emissions saved by stopping sargassum from reaching shore and/or decomposing in coastal water...(EPA WARM model)				
Density of pelagic sargassum wet (g/m^2)	area density	4000		(Parr, 1939)
Sargassum wet weight prevented from reaching shore (tonnes/yr)		392,779,770	AT*area density/1000000	
Sargassum dry weight prevented from reaching shore (tonnes/yr)		31,422,382		
Landfill gas recovery?		NO		As of 2006, no Caribbean island collected LFG (World Bank Group, 2006) but this may change in the future.
Landfill gas recovery efficiency		n/a		Note results may change depending on current state of LFG recovery in Caribbean.
Flash or reuse recovered gas?		n/a		Note results may change depending on current state of LFG recovery in Caribbean.
Average distance from source to landfill (miles)		20		Data for Hawaii available.
Dry or wet digestion?		Moderate		Wet not possible for mixed organics.
Using Hawaii as the state in which the study is being performed...				
CO2 reduced from preventing sargassum landfall in the Caribbean (tonnesCO2e/yr)	tCO2/yr1	43,797,849	from warm model	B31 --> EPA WARM model (no option to "sink" so approximated as "Tons Source Reduced" "Food Waste"
Value of carbon credit ($/MTCO2)	$/tCO2	$ 30.00		This value may also be subject to change as a universal price on carbon gains footing.
Carbon credit value from avoiding sargassum entering landfills ($/year)	$/yr1	$ 1,313,935,474	(tCO2/yr)*($/tCO2)	
2. Sequestration of carbon via the direct sinking of sargassum to the abyssal ocean...				
Carbon as a percentage of dry weight of sargassum	CP	50%		(Gower, 2006)
Dry weight as a percentage of wet weight for sargassum	DW	8%		(Gower, 2006)
Carbon sequestered each year via sinking sargassum as it exits the CWA (tonnesC/yr)	tC/yr	15,711,191	AT*area density*DW*CP/1000000	Same as the rate at which we collect in the open ocean calculated above.
Ratio of CO2 absorbed to carbon content in organic matter	mmr	3.67		Based on molar masses of carbon and oxygen.
CO2 sequestered each year via sinking sargassum as it exits the CWA (tonnesCO2/yr)	tCO2/yr2	5.76E+07	tC/yr*mmr	From sinking the carbon incorporated into the biomass of the sargassum itself.
Equivalent in carbon credit value ($/year) from sinking sargassum biomass	$/yr2	$ 1,728,230,986	tCO2/yr2*$/tCO2	While relatively small compared to the offset from avoiding landfill, this offset is still substantial.
3. Net effect on the oceanic biological pump by removal of sargassum from the CWA...				
Average coverage of sargassum in the Caribbean (km^2)	Ctot	3,769	((DRr/LN(2))*(ER/365)*2*(TT/DRr)-(DRr/LN(2))*(ER/365))/1000000	Integration over days of travel from CWA to the Caribbean.
Carbon Net Primary Production (NPP) of Sargassum in the Caribbean (mgC/g_dry/hr)	NPP	1.4		(Carpenter and Cox, 1974) from the continental shelf in October 1971.
Photosynthesizing hours per day	H	10		(IUCN, 2014)
Annual Carbon NPP of Sargassum in the Caribbean (gC/m^2/year)	NPPyr	1635	NPP*area density*DW*(H/24)*8760/(1000)	Much less than that of phytoplankton.
Dissolved Organic Carbon (DOC) as a percentage of NPP	DOC	40%		(Hanson, 1977) for macroalgae in general.
Recalcitrant Dissolved Organic Carbon (rDOC) as a percentage of DOC	rDOC	15%		(Hanson, 1977) for macroalgae in general.
Percentage of total NPP that sinks to the sea floor as faecal pellets	%pellets	10%		(Itoh, 2007) for Japanese coastal species.
Lost CO2 sequestration from rDOC and faecal matter (ignoring sinking) from sargassum in Caribbean (MTCO2/yr)	lost	3.62E+06	NPPyr*1000000*Ctot*mmr*(DOC*rDOC+%pellets)/1000000	Removing sargassum from the CWA and/or the Caribbean means this activity will no longer happen...
Phytoplankton NPP that takes sargassum's place (gC/m^2/year)	pNPP	400		Sargassum only about 0.5% and 10% of phytoplankton NPP in the Sargasso and GOM, respectively (Carpenter and Cox, 1974; Gower, 2006)
Photosynthesizing hours per day		10		(IUCN: The Significance and Management of Natural Carbon Stores in the Open Ocean, 2014)
Phytoplankton NPP gained as a result of increased surface area (gC/yr)	pNPPyr	1.51E+12	pNPP*Ctot*1000000	While sargassum is gone in some capacity, less area coverage will allow more phytoplankton to grow.
Percent of phytoplankton biomass that is sequestered to the deep ocean	%phyto	20%		(IUCN: The Significance and Management of Natural Carbon Stores in the Open Ocean, 2014)
CO2 sequestered each year via increase in phytoplankton (tonnesCO2/yr)	gained	1.11E+06	pNPPyr*mmr*%phyto/1000000	
Net change in the sequestration productivity of the biogical pump in the Caribbean (tonnesCO2/yr)	change	-2.51E+06	gained-lost	
Equivalent in Carbon Credit value ($/yr) due to changes in biological pump in the Caribbean	$/yr3	$ (75,311,278)	change*$/tCO2	
Total annual Carbon offset in the Caribbean (tonnesCO2e/yr)		98,895,171	TCO2/yr1+tCO2/yr2+change	
Potential Carbon Credit Revenue from sinking sargassum in the CWA ($/yr)	$tot	$ 2,966,855,182	$/yr1+$/yr2+$/yr3	Assuming we sink 100% of sargassum leaving the CWA.
Revenue per metric ton of wet sargassum ($/tonne)	$/tonne	$ 34	$tot/(DWmax/DW)	Still process revenue even with "crashed" $$/tCO2
Total Specific Carbon Offset Value of Sargassum (TSCOV) (tCO2/tWS)	TSCOV	0.258	DW*CP*mmr	tonnes CO2 for tonnes wet sargassum

FIG 101 Spreadsheet tool developed to predict the total potential of SOS Carbon offsets in the Caribbean.

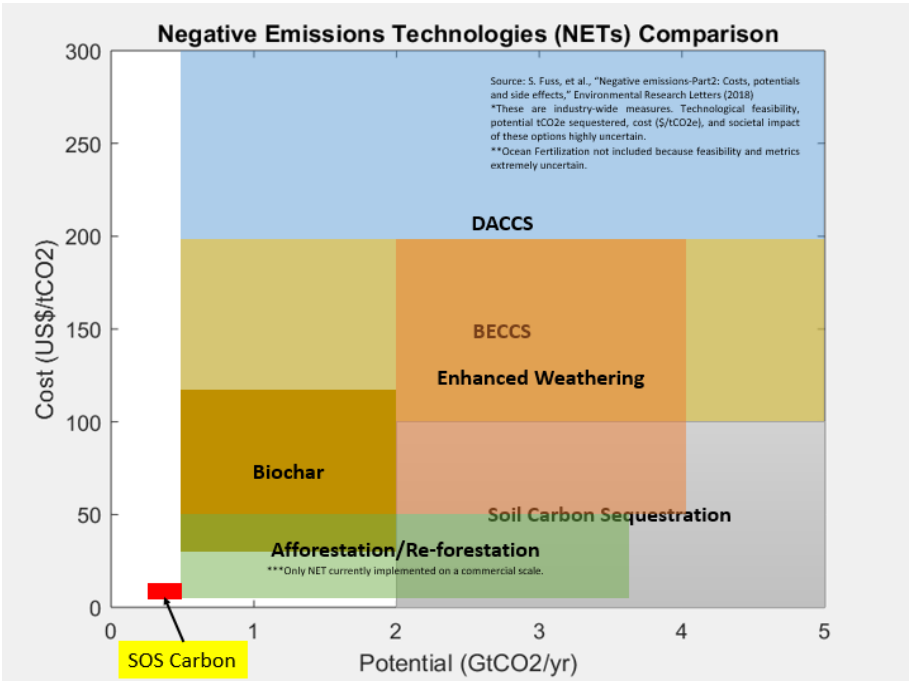

FIG 102 A comparison between SOS Carbon and other (global-scale) negative emissions technologies (NETs). SOS Carbon is considerably cheaper and boasts a large potential for a project with a relatively small geographic footprint and capital cost.

In Fall 2018, the IPCC released a report, the Intergovernmental Panel on Climate Change (IPCC) "Special Report". It's primary conclusion were:

C.1 "In model pathways with no or limited overshoot of 1.5°C, global net anthropogenic CO2 emissions decline by about 45% from 2010 levels by 2030 (40–60% interquartile range), reaching net zero around 2050 (2045–2055 interquartile range)… (high confidence)."

C.2 "Pathways limiting global warming to 1.5°C with no or limited overshoot would require rapid and far-reaching transitions in energy, land, urban and infrastructure (including transport and buildings), and industrial systems (high confidence)."

C.3 "All pathways that limit global warming to 1.5°C with limited or no overshoot project the use of carbon dioxide removal (CDR) on the order of 100–1000 GtCO2 over the 21st century... (high confidence)."

The report calls for urgent action to limit global warming to 1.5°C and asserts that accomplishing this goal will require than just efficiency improvements and decarbonization – it will require carbon dioxide removal (CDR; the same as "negative emissions technologies" or "NETs") from the atmosphere. A solution portfolio approach is recommended – technical risk should be spread over many different types of CDR/NETs technologies, rather than making a large bet on a single method.

All things considered, pumping-to-depth could be welcomed as a new model for carbon offsetting in the Caribbean and these revenues could provide a means to subsidize the campaign against sargassum invasion.

Appendix B - Toxicity Analysis of Sargassum in Punta Cana

It is well known that almost all sargassum currently collected from beaches across the Caribbean, is deposited in local landfill. It is also not surprising, that most “landfills” in the Caribbean are unsanitary, meaning there is no containment or landfill gas capture - they are open pits. It has been widely reported that heavy metals, and other toxic elements, have been found in beaching sargassum at alarming levels, unfit for human consumption or products (Mexico News Daily, June 2019). The MIT team, with the help of Harvard Chemistry Prof. Nocera and PhD Candidate Sam Verouneau, performed mass spectrometry on samples of sargassum from landfills and beaches in Punta (Bavaro, Punta Cana, and Cap Cana, respectively).

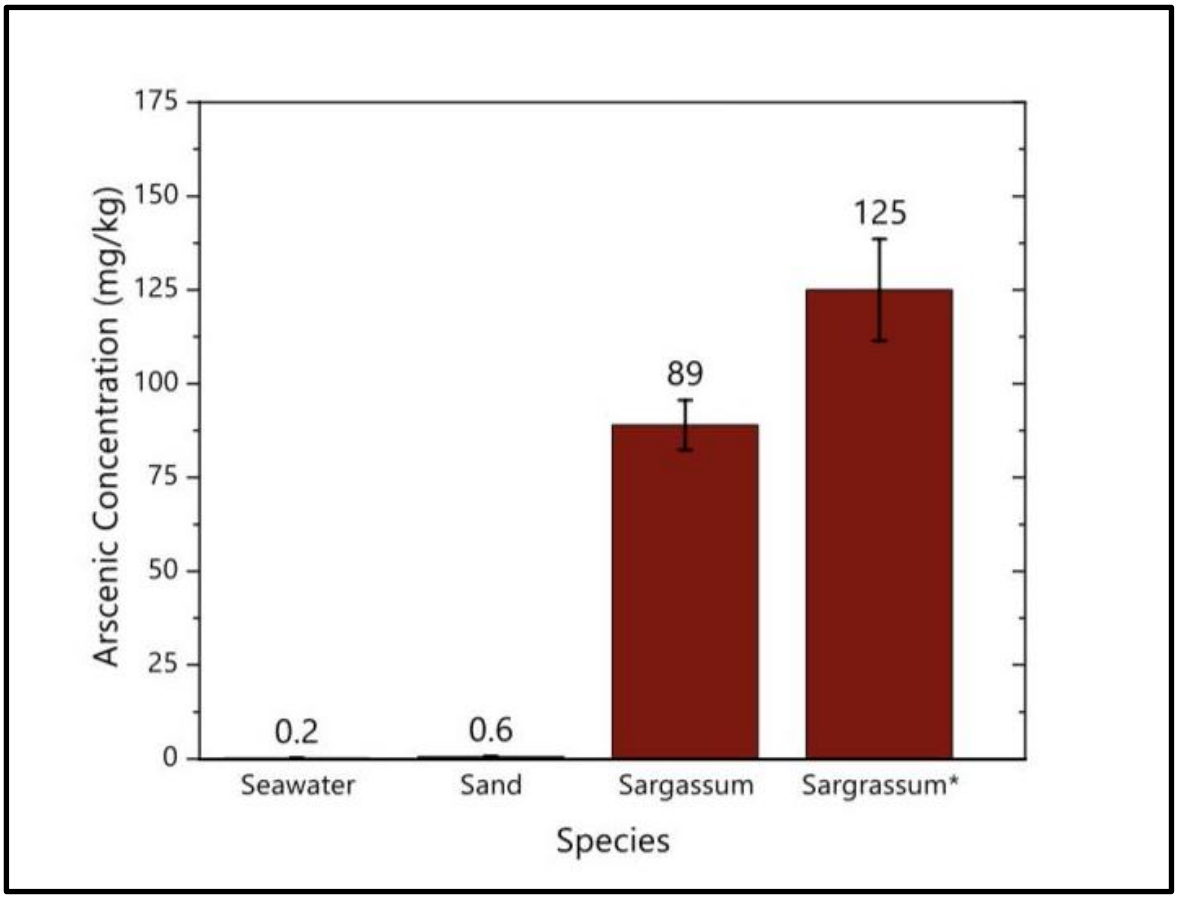

This data has been shared with potential initial customers, and it is one of the major reasons why the SOS Carbon pump-to-depth barge is a desirable service (as an alternative disposal method to landfilling). Even if resorts were to begin bringing sargassum to proper landfills with containment, these landfills would no longer be free (like unsanitary landfills within resort properties currently are) and the SOS Carbon pump-to-depth barge would then undercut the cost of these more distant, paid landfills.

Appendix C – Environmental Impact Statement

Environmental Impact

The steady-state population of sargassum in the Central Western Atlantic (CWA) stores a large amount of carbon. However, as sargassum is carried out of the open ocean, making landfall in many places, primarily in the Caribbean, the sargassum dies and begins decomposing, creating the anaerobic conditions necessary for methanogenesis. Rotting sargassum mats in shallow water are almost always littered with dead fish that have been suffocated – a testament to these anaerobic conditions. Sargassum that lands on valuable tourist coastline is collected and deposited in landfills where methane production is certain. It is well-known that methane has ~86x the global warming potential (GWP) of carbon dioxide. Therefore, it is highly likely that the recent blooms of sargassum in the CWA have a net positive global warming effect. By permanently sinking sargassum, sustainably as it exits the open ocean, SOS is eliminating these coastal methane emissions while leaving the oceanic steady state carbon sink intact.

However, the environmental impact of SOS extends beyond the global carbon cycle, to the immediate pelagic and deep sea ecologies. First of all, it is important to recognize that while sargassum in the Sargasso Sea (Northern Atlantic) is protected because of its long-standing ecological role in the region, sargassum in the CWA, which has existed there for less than a century and only grown into a sizable population in the last decade, does not necessarily deserve the same protection. In contrast, it is painfully clear that sargassum from the CWA has a negative effect on pelagic ecology in the Caribbean, where it devastates fisheries, coral reefs, and several species of sea turtle. With regard to deep sea ecology, sargassum has been found at depths as great as 3200m, where it is used as shelter and nourishment by deep sea organisms. However, since relatively little is understood about these deep sea areas, it is hard to reason about the potential impact SOS would have. What is certain is that these deep sea areas receive large amounts of organic enrichment from many sources, not just sargassum. Therefore, the uncertainty surrounding sargassum's effect on deep sea ecology is best answered by ongoing monitoring, similar to the approach currently being taken by deep sea mining.

Without any reason for concern, Caribbean nations appear ready and willing to permit the operation of SOS in their national waters, as the immediate benefits to tourism, standards of living, and coastal ecology are immense. Therefore, it is in the interest of the scientific community to understand the impact such activity will have. SOS is creating an incentive to not only understand sargassum and its role in global carbon accounting, but SOS is also creating the opportunity to finally understand some of the deepest ecosystems in the entire Atlantic. A peer-reviewed study should be undertaken to:

1. Investigate the effect of SOS on pelagic/coastal ecology (fisheries, phytoplankton populations, coral reefs, etc).
2. Forecast the range of scenarios (from best-case to worst case) that SOS could have on deep sea ecology.
3. Propose concrete measures and monitoring processes to evaluate the ongoing impact of SOS on pelagic, coastal, and deep sea areas.
4. Quantify the exact carbon content of sargassum (by percent weight), the methanogenesis from sargassum's decomposition in coastal waters and landfill, respectively, and the relative amounts of sargassum that hit critical, non-critical coastline, or sink naturally, thereby establishing a historical accounting of sargassum's carbon contribution and enabling the auditing of SOS offsets

in the future (and also understanding better the role of an important macroalgae in the global carbon cycle).

The same methods taken to pursue this study could be applied to other macroalgaes, microalgaes, and other floating biomass in general. Increasing ocean temperatures, acidity/alkalinity, and nutrient upwelling is causing a more and more cases of invasive ocean species; red tide, green tide, and nomura jellyfish are just a few. Therefore, sustainable ocean sequestration of floating biomass, especially invasive species, could become a widespread management method and produce a large carbon offset as a consequence. It is important to understand the environmental impact of these actions.

Risks and legal framework protecting pelagic sargassum

The Sargasso Sea is a linchpin in the ecology, culture, history, and economy of the Northern Atlantic. It is considered an area of ecological significance, sargassum itself being home to 10 endemic species, playing the role of a nursery and breeding grounds for several endangered or threatened species of turtle and eel, respectively, and playing host to many long distance travelers like bluefin tuna, whale sharks, and manta rays, among many others. The historical extraction of sargassum from the Sargasso Sea for use in fertilizer and cattle feed has been recognized as a direct threat to the environment (Sargasso Sea Alliance, n.d.). There is a gestalt of national and international law aimed at protecting oceanic ecosystems, specifically those protecting pelagic and deep-sea ecosystems which may be affected by SOS.

With the authority granted under the Magnuson-Stevens Fishery Conservation and Management Act (Magnuson-Stevens, 1976), the South Atlantic Fishery Management Council's Fishery Management Plan (FMP) for the Pelagic Sargassum Habitat prohibits the harvest of all sargassum in the South Atlantic EEZ south of the 34° North Latitude (South Atlantic Fishery Management Council, 2003). We are not aware of a legal framework to protect sargassum in the Dominican Republic or other areas in the Caribbean, however, the "precautionary principle" adopted by most conservationist institutions could mean that SOS Carbon will receive some pushback.

The protected populations of sargassum in the South Atlantic EEZ of the United States and in the Sargasso Sea (international waters) are very different from the sargassum population in the Caribbean (spawning from the CWA). While sargassum has been observed in the Sargasso Sea for hundreds of years, sargassum natans weren't observed in the CWA until 1931 (Széchy et al., 2012). Satellite images suggest a relatively dormant population in the region (Wang & Hu, 2016) until 2011 when the Brazilian Air Force mistook large mats for oil spills (Széchy et al., 2012). During this period, the existence of sargassum natans in the CWA was considered abnormal, or even doubtful (Széchy et al., 2012). This begs the question: is sargassum integral to the wellbeing of the marine ecosystem in the CWA and the Caribbean?

While pelagic sargassum serves as an essential nursery for some populations of sea turtle, there are many populations that breed in locations without any sargassum drift lines. This observation lead to the conclusion that young turtles will inhabit any inanimate floating debris (Carr, 1986). The regional dependency of other species on sargassum is yet to be defined.

Sargassum in the Caribbean, especially in the present amounts, is extremely abnormal and has caused numerous deleterious effects on the marine ecosystem. Ongoing research, effective monitoring,

and the swift implementation of countermeasures to observed adverse impacts (ie. artificial debris as nurseries for sea turtles) could effectively stem environmental risks. The biodiversity and wellbeing of the marine ecosystem is of critical importance, but the emergent and severe harm that sargassum is inflicting on Caribbean regions cannot be allowed to continue.

Risks and legal protection of the deep-sea

The Convention on the Prevention of Marine Pollution by Dumping of Wastes and Other Matter (1972) ("London Protocol") represents an international pact to protect deep-sea resources and ecology. Many of the Caribbean nations are signees, pledging to enact any and all regulation in the spirit of the convention (London Protocol, 2006). This likely means that permits to sink, record-keeping of amounts sunk, and monitoring of the seafloor will be required from SOS Carbon. Caribbean nations could receive significant international pressure to implement antagonizing regulation, should sargassum sinking activity commence.

Despite this precedent, it should be recognized that sargassum is significantly different from the pollutants that the London Protocol addresses. Surface productivity in the form of microalgae, macroalgae, wood, carcasses and other organic matter is the primary energy input and driver of deep-sea ecological processes. Sargassum has been found at depths as great as 3200m (International Union for Conservation of Nature, 2014), and could theoretically exist at greater depths. Camera and bait experiments have identified several invertebrates that are attracted to and readily eat sargassum (Fleury & Drazen, 2013; Lawson, Tyler, & Young, 1993; Schoener & Rowe, 1970).

What percent area coverage will sinking of sargassum cause in the area of interest? This necessarily means studying benthic currents to predict how sargassum is being scattered across the ocean floor. Does SOS contribute significantly to the organic enrichment that is already happening, due to natural sinking and accumulation of sargassum and other marine biomass, in the area of interest?

While the importance of organic enrichment, specifically in deep-sea canyons, by sinking biomass has been recognized and quantified in specific cases, little is known about the ecological effect of this phenomena (Harrold, Light, & Lisin, 1998). What is certain is that deep-sea canyons in the Caribbean must be receiving significant amounts of sargassum at present. This provides a unique opportunity to study the ecological dynamics associated with organic enrichment in a vast and little-explored area.

Should SOS be implemented, associated risks, like sunk sargassum missing or migrating far from its intended resting place, should be thoroughly monitored. While little is known about the depths of our oceans, the immediate effects of sargassum on Caribbean civilization and the simultaneous lack of a sufficient or working solution should justify SOS.

Appendix D – Sump-Inlet Hydrodynamics Model

This model has not been peer-reviewed and was never used to build a real device or otherwise tested. The sump inlet never ended up being used, but there was considerable work done on it and it holds promise for the future. The sump is such a simple device that it is probably undeserving of the level of analysis presented hereafter, however, L. Gray was interested in learning more about hydrodynamics and making the linear dynamics model.

The primary objective of the floating sump-inlet is to provide a high, consistent solids concentration to the pump inlet piping, while preventing dry-running and shocks to the system. This requires control of the depth and angle of the leading edge of the sump, relative to the free surface. It is envisioned that this be accomplished using a passive structure comprising a single DOF arm deployed from the SOS vessel. This system is illustrated as a stick figure in FIG 103, below.

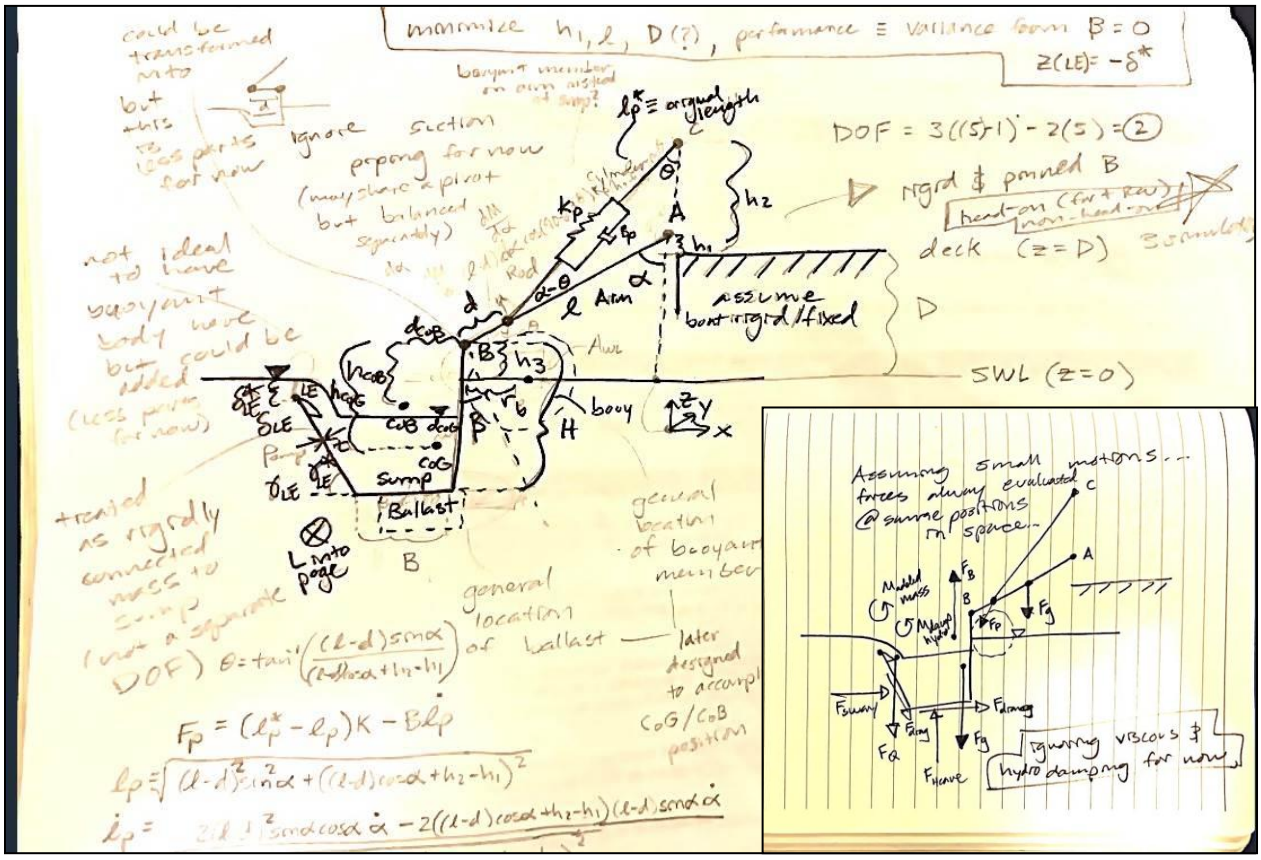

FIG 103 The sump-inlet is envisioned as an outriggered linkage system of at least one degree of freedom (pin at Point A). There is the possibility of adding a second degree of freedom at Point B, if the dynamics model indicates it is advantageous. There is also the possibility of adding stiffness and/or damping with a hydraulic/gas piston between Point C and a variable position on the arm. Above shows the set of parameters chosen to describe the system, which will be evolved through the use of the dynamics model. Also shown is an FBD of the sump-inlet. The primary forces acting on the system are gravitational, hydrostatic, incident wave forces, viscous forces, as well as thee sump's own added mass and damping forces.

Hereafter, a hydrodynamics model for the motion of the sump-inlet in ocean waves is used to reasonably optimize the design of these elements to achieve these basic objectives in as wide a range of expected sea states as possible:

1. Avoid undesirable phenomena: resonance, swamping, skipping, submergence, shocks to system.
2. Maintain the average depth and angle of the leading edge of the sump at the desired depth.
3. Reduce the size, weight, and impact on ship dynamics of the structure.
4. Reduce the length of suction piping required (horizontal distance from vessel to sump).
5. Reduce the required preload, stiffness, and damping.

By varying the inputs:

a. Degrees of freedom (Point B rigid or rotary or other configuration).
b. The ideal set of construction parameters (sizing of arm and sump, ballast, buoy, etc).
c. The vessel orientation (head-on, non-head-on waves, cross waves).

The current goal of this model is to design a sump-inlet to be deployed aboard the SOS pilot vessel in summer 2019. Upon completion of the pilot tests, the refined model will be used to design the first full-scale SOS vessel.

The hydrodynamics model will also serve as an exercise to better understand the forces in the submerged sump-inlet, which will inform the structural design of the sump, arm, frame, and connections therein, in the next section.

Using NOAA WAVEWATCH III data for the Mona Passage for the last 3 years, the average significant wave height ($H_{1/3}$; the average crest-to-trough height of the largest third of ocean waves) and average peak wave period (T_p) were calculated. This values are summarized in Table X.

Table X: The mean significant wave height and peak wave periods in the Mona Passage from XXXX to XXXX.

Significant wave height ($H_{1/3}$; m)	Peak wave period (T_p; sec)	Wave velocity (U; m/s)
1.2m	10 sec	0.5 m/s

The distribution of sea states was then modeled using the Bretschneider spectrum, which takes the significant wave height and peak wave period as inputs. The Bretschneider spectrum is used instead of the Pierson-Moskowitz spectrum as it is not limited to the long-fetch assumption, and models both developing and decaying waves (A.H. Techet, 2005).

$$Bretschneider\ Spectrum: \quad S(\omega) = \frac{5}{16}\frac{\omega_m^4}{\omega^5}H_{1/3}^2 e^{-5\omega_m^4/4\omega^4}$$

$$H_{1/3} = 4\sqrt{\int_{-\infty}^{\infty} S(\omega)d\omega} \qquad \omega_m = 0.4\sqrt{g/H_{1/3}}$$

ω is wave frequency in [rad/sec], ω_m is mean wave frequency ($T_p = 2\pi/\omega_m$). From this distribution, we select 8 sea states, each with associated probability of occurrence, ρ, to be used as inputs to the hydrodynamics model of the sump. These sea states are listed in Table Y and the spectrum is shown in FIG 104. In total, these sea states cover ~99% of the expected sea states in the Mona Passage. We assume that SOS vessels will not operate in storm conditions, and so these extreme sea states are not weighed into the hydrodynamic optimization (although the structural design in the next section considers an encounter with a rogue wave). Nevertheless, the Breitschneider spectrum indicates that most sea states in the Mona Passage are categorized between "Calm" and "Moderate" according to the World Meteorological Organization Sea State Codes (Codes 0-4 inclusive).

Table Y: Representative sea states, and associated probabilities, in the Mona Passage.

Sea State	Significant wave height ($H_{1/3}$; m)	Wave period ($T = 2\pi/\omega$; sec)	Wave velocity ($U = A\omega$; m/s)	Probability (ρ)
1	1.2	8.38	0.90	3.94%
2	1.2	5.98	1.26	32.66%
3	1.2	4.65	1.62	30.69%
4	1.2	3.81	1.98	16.45%
5	1.2	3.22	2.34	8.23%
6	1.2	2.79	2.7	4.28%
7	1.2	2.46	3.06	2.36%
8	1.2	2.20	3.42	1.37%

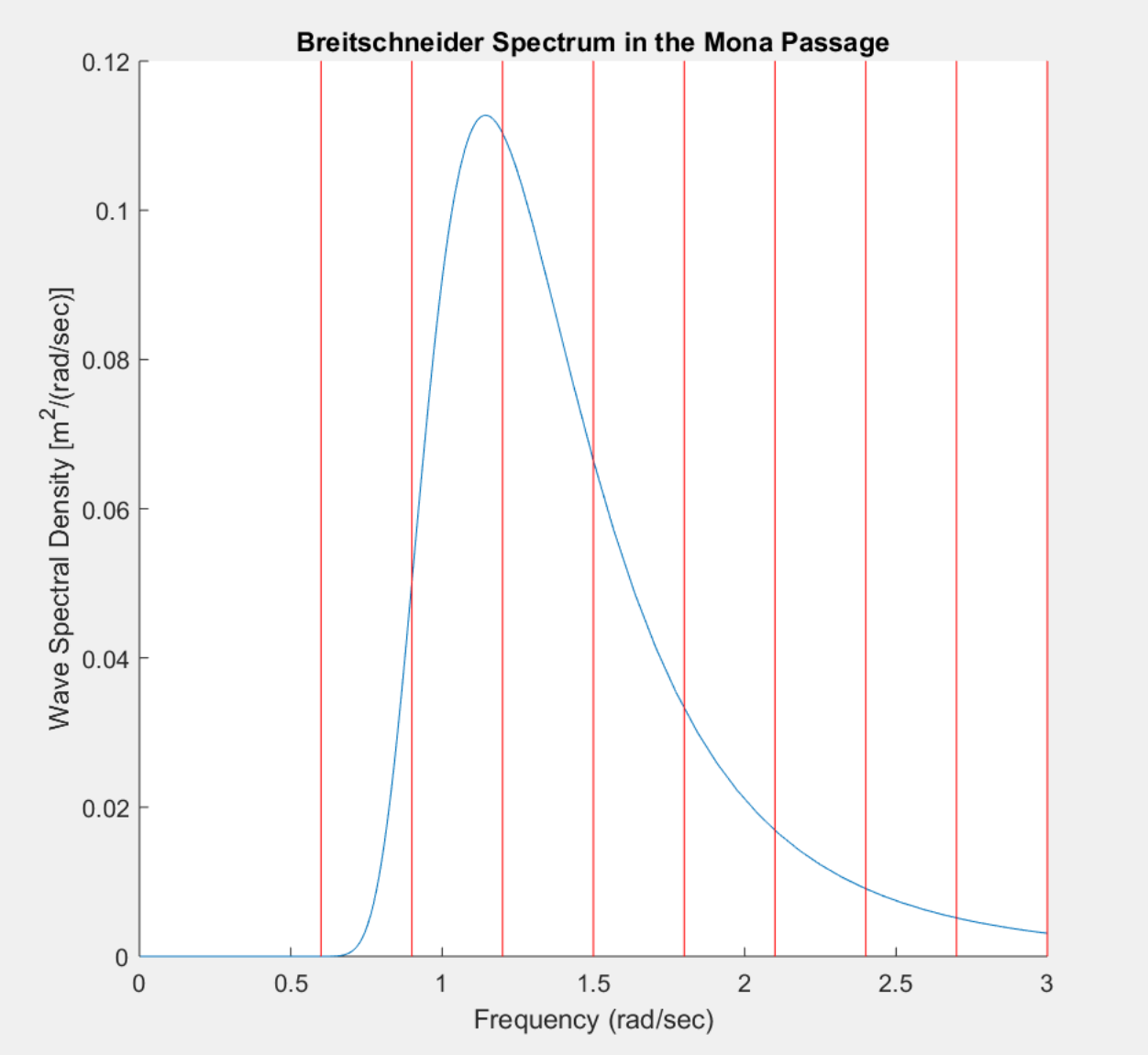

FIG 104 A Breitschneider spectrum showing the wave spectral density of waves in the Mona Passage.

$$Nordenstrom\ (1969): \begin{cases} H^{1/3} = 1.68(H_v)^{0.75}\ [m] \\ \overline{T} = 2.83(T_v)^{0.44}\ [seconds] \end{cases}$$

The performance of each parameter set can be assigned a score in each of these states. Performance is quantified by the time averaged deviation of the depth and angle of the leading edge from those desired. An overall composite score for each configuration, orientation, and set of parameters (the weighted average of each with the probability of that state) can be used to deterministically converge on a reasonably optimized design for the sump-inlet.

The behavior of the sump-inlet is governed by complex phenomena. It is necessary to make several simplifying assumptions, in order to build an operational model for the sump-inlet dynamics. The analytical model of the sump-inlet comprises the aforementioned system of a rigid arm link and submerged sump, connected to each other, and the SOS vessel, by single DOF pivot joints. The SOS vessel is assumed to be fixed in space. The origin is defined as the intersection of the still water line (SWL) and the vertical line through the pin connecting the arm and the SOS vessel. The entire set of system parameters describing the structure are summarized in Table Z.

Table Z: Parameters describing the sump-inlet system. Some variables are only defined in the reference (still water) position.

Parameter	Description
D	The freeboard between the ship deck and the still water line. [m]
h_1	The height of the arm-vessel pivot joint, Point, A above the deck of the vessel. [m]
h_2	The height of the piston-frame pivot joint, Point C, above Point A. [m]
l	The length of the arm linkage. [m]
n	Number of arms.
d	The distance of the rod-arm pin joint from the arm-sump pivot joint, Point B. [m]
h_3	The height of the arm-sump pivot joint, Point B, above the still water line. [m]
H	The height of the sump in the z-direction. [m]
B	The width of the sump in the x-direction. [m]
L	The length of the sump in the y-direction, along the length of the vessel. [m]
w	The flat length along the bottom of the sump. [m]
s	Height of the zero-draft sides of the sump. [m]
γ_{LE}^*	The constant construction draft angle of the leading edge and sump bottom. [rad]
γ_{LE}	The angle between the leading edge (LE) of the sump and horizontal. [rad]
δ_{LE}^*	The set still water depth of the leading edge (LE) below the still water line. [m]
δ_{LE}^{min}	The threshold depth of the leading edge to prevent dry running in operation. [m]
δ_{LE}	The variable depth of the leading edge (LE) below the still water line. [m]
d_{CoG}	The x-direction distance from the arm-sump pin joint (B) to the sump CoG. [m]
d_{CoB}	The x-direction distance from the arm-sump pin joint (B) to the sump CoB. [m]
h_{CoG}	The z-direction distance from the arm-sump pin joint (B) to the sump CoG. [m]
h_{CoB}	The z-direction distance from the arm-sump pin joint (B) to the sump CoB. [m]
h_{weir}	The height between leading edge and free surface of water in the sump. [m]
n_p	Number of pistons.
$F_{preload}$	The pre-load force generated by the rod-cylinder assembly in still water. [N]
l_p^{SW}	The still water length of the rod-cylinder assembly (pre-loaded). [m]
l_p	The in-situ length of rod-cylinder assembly during operation. [m]
k_p	The axial stiffness of the rod-cylinder assembly. [N/m]
B_p	The damping coefficient of the rod-cylinder assembly. [Ns/m]
θ	The in-situ angle between the rod-cylinder assembly and vertical. [rad]
θ_{SW}	The in-situ angle between rod-cylinder assembly and vertical in still water. [rad]
Q	The volumetric flowrate out of the sump, to the pump. $[m^3/s]$
t_b	Thickness of the rectangular buoy. [m]
H_b	Height of the rectangular buoy. [m]
l_b	Radial length from Point A to the central axis of the rectangular buoy. [m]

α	The in-situ angle between the arm link and vertical. [rad]
α_{SW}	The still water angle between the arm link and vertical. [rad]
β	The in-situ angle between the sump and the arm link. [rad]
β_{SW}	The still water angle between the sump and arm link. [rad]
$\Delta\alpha$	Angular offset between arm and the centroidal axis of the rectangular buoy. [rad]
t	Thickness of sump walls. [m]
t_f	Thickness of the I-beam flanges. [m]
t_w	Thickness of the I-beam web. [m]
b_f	Thickness of the I-beams. [m]
h_{I-beam}	Height of the I-beams. [m]

Below is a list of assumptions underlying the present model, accompanied by justification:

A. While the actual mass, displaced volume, and relevant centers of the sump-inlet will be affected by the eventual addition of brackets, weldments, nuts, bolts, etc. it is sufficient for now to assume the system only comprises the sump, arm linkage, ballast, and buoy.
B. Waves are assumed plane progressive regular waves. Ambient flow is assumed to be irrotational, inviscid potential flow. Waves excitation forces arise from incident, diffracted, and radiated velocity potentials. Waves are deterministic, generated by the model as pure sinusoids (rather than stochastic).
C. Diffraction and radiation forces are assumed to be negligible because the characteristic length of the sump ranges from L=[0,15] m (min and max dimensions), therefore L/λ < 0.2 with $\lambda = T^2 + \frac{T^2}{2}$ = [90, 200] m (P. Sclavounos, 2015).
D. Because diffraction effects are negligible, long-wavelength approximations are adopted for calculating wave excitation forces, added mass, and damping coefficients. This implies that body motions are small compared to waves such that wave-body forces are linear. This is, in general, a good assumption for gravity waves, unless they are breaking (not the case in deep water).
E. Viscous fluid forces are ignored because the Keulegan-Carpenter number, $K_C = UT/B = 2\pi A/B \approx 3$. For $K_C \gg 2$, flow separation occurs, viscous effects are comparable to buoyancy and pressure forces (inertial forces), and therefore are non-negligible. If nonlinear viscous effects need to be accounted for later, this can be done with Morison elements, which are based on incident potential flow (A.H. Techet, 2004).

FIG 105 shows a helpful diagram with the relevant regimes in both assumptions D and E.

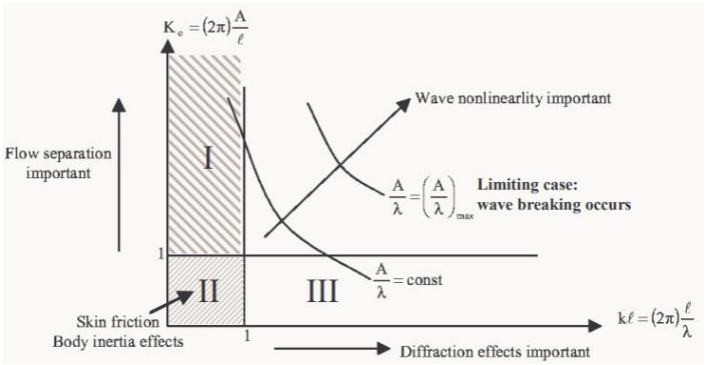

FIG 105 Showing the appropriate regimes for evaluating wave forces on submerged bodies. When wave height is small compared to the size of the body ($2\pi A/l \leq 1 \rightarrow 2$) then there is no flow separation and viscous effects are limited to the boundary layer. Furthermore, if the wavelength of the incident waves is much greater than the characteristic length of the submerged body $l/\lambda \ll 1$ then diffraction effects are negligible (D. Yue, 2005). For the sump-inlet, $2\pi A/l \approx 3$ therefore flow separation occurs and Morrison's formula must be used to calculate viscous forces. However, because $B/\lambda \ll 1$, diffraction effects can be ignored.

F. There is no elastic deformation of the sump, arm, or any connections in between that would require additional degrees of freedom in the dynamics model. Furthermore, assumed to be no clearance in the pivot joint(s). Only the angular degree of freedom about Point A is considered. While such a model would usually be carried forward in 2D, and later translated to 3D, we elect to solve for the equation(s) of motion in 3D directly.
G. The water in the sump is taken to be a solid mass rigidly connected to the sump, eliminating the need for this additional degree of freedom. This assumption ignores the possible presence of a rate-dependent coupling between the water and the sump, and any sloshing dynamics that arise.
H. There are no memory effects. In other words, the motion of the sump is dominated by the incident velocity potential and not dependent on radiated waves caused by its historical motion.
I. We assume that the system is at steady state. In other words, waves have been impinging for an infinite amount of time.
J. There is no reaction moment caused in the pivot joint(s) (no friction in the joints or very small compared to wave forces). Any friction generated here would be vanishingly small compared to the moments generated from gravity and hydrodynamic forces.
K. The SOS vessel is assumed to be fixed, creates boundary layer interactions, and no diffraction or radiation waves that affect the motion of the sump-inlet. Essentially, the model completely neglects the presence of the vessel except that the Point A is kept fixed in space.

Depending on the size of the ship and the sea state, the assumption that the ship is fixed in space can be somewhat problematic. While sway, surge, and yaw, of the SOS vessel may be small, the composite vertical displacement of the mounting Point A – due to heave, pitch, and roll of the vessel – may have a significant effect on the dynamics of the sump-inlet. While the future SOS vessel may be very large, the pilot vessel will still be a relatively small platform. Currently, one option for the pilot vessel is [Length, Beam, Draft] = 25m X 7m X 2m. A simulation in MAXSURF was used to calculate the composite maximum vertical displacement of such a vessel in sea state 8, according to speed and heading. These results are shown in Figure 106, below.

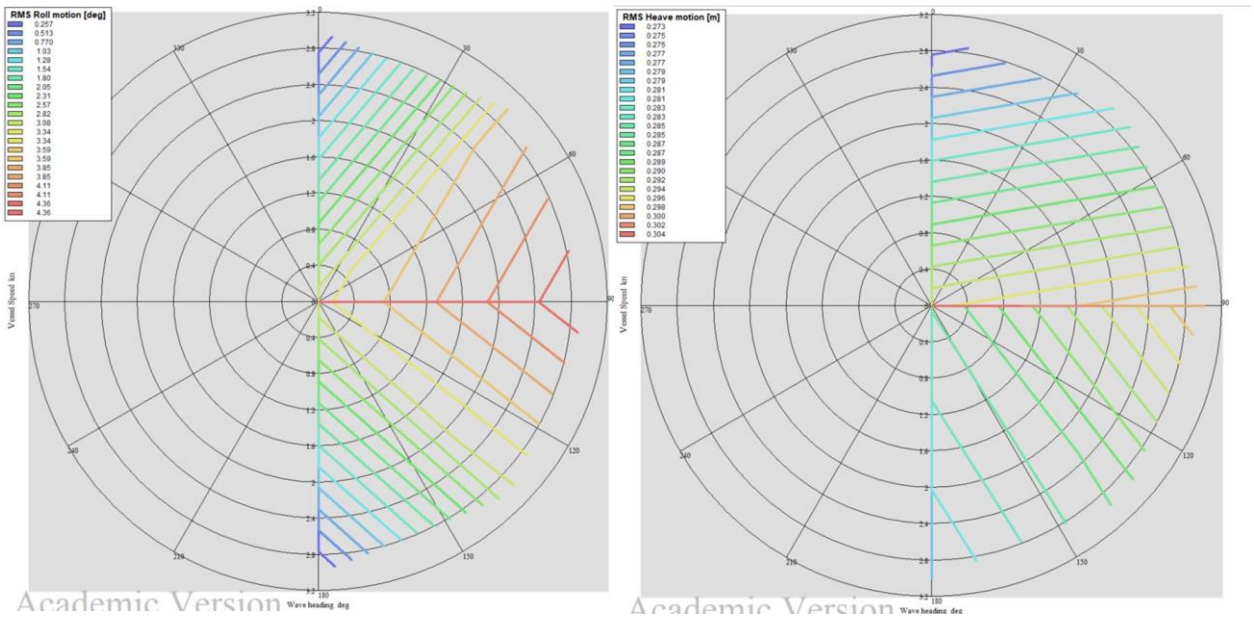

FIG 106 A simulation calculation of the heave and roll motions of the intended pilot vessel with [Length, Beam, Draft] = 25m X 7m X 2m according to vessel speed and heading. With zero velocity and 90° heading, the max displacement of the sump-inlet attachment at Point A is $\sim$0.5m

In the worst case condition, with zero vessel velocity and 90° heading, the maximum vertical displacement of the sump-inlet mounting at Point A is $\sim$0.5m. While this displacement would certainly affect the dynamics of the sump-inlet, it is a worst case. Furthermore, the contribution to sump-inlet motion will depend on the geometry of the linkage system. For example, if the mounting at Point A is very close to the still water line, disturbance to the sump-inlet is relatively small. For now, the motion of the SOS vessel is neglected. The merit of the fixed vessel assumption will be reevaluated considering the design of the sump-inlet at the end of this section.

Hereafter the physical model of the system will be described. The degrees of freedom considered in this analysis are:

$$\vec{x}_{sump-inlet} = [\alpha] \quad \text{(1 DOF) measured in radians.}$$

Where α is the angle formed at Point A, between the arm and vertical. While the current system is rigid at Point B, a provision is made for including the angle β as a DOF by making Point B a pivot joint (β is the angle formed between the proximal side of the sump, connected to Point B, and the arm linkage). Therefore, the still water values of α and β are $\alpha_{SW} = \cos^{-1}\left(\frac{D-h_3}{l}\right)$ and $\beta_{SW} = 180 - \alpha_{SW}$. The depth of the leading edge of the sump at any point in time can be calculated from α and β as:

$$\delta_{LE} = D + h_1 - lcos(\alpha) - Hcos(\beta + \alpha - 180) + Bsin(\beta + \alpha - 180) + \left(\frac{H - h_3 - \delta^*_{LE}}{\sin(\gamma^*_{LE})}\right)\sin(\beta + \alpha - 180 + \gamma^*_{LE})$$

And the angle of the leading edge relative to horizontal at any point in time is evaluated as:

$$\gamma_{LE} = \gamma_{LE}^{*} + \beta + \alpha - 180$$

Because Point B is rigid is the present system, $\beta = \beta_{SW}$ always. The value of θ, the angle formed between the cylinder and vertical at any point in time, can be calculated as:

$$\theta = \tan^{-1}\left(\frac{(l-d)\sin(\alpha)}{(l-d)\cos(\alpha) + h_2}\right)$$

And the length and time derivative of the rod-piston assembly at any point in time can be calculated as:

$$l_p = \sqrt{(l-d)^2 \sin^2(\alpha) + \big((l-d)\cos(\alpha) + h_2\big)^2}$$

$$\dot{l_p} = \frac{(l-d)^2 \sin(\alpha)\cos(\alpha)\,\dot{\alpha} - \big((l-d)\cos(\alpha) + h_2\big)(l-d)\sin(\alpha)\dot{\alpha}}{\sqrt{(l-d)^2 \sin^2(\alpha) + \big((l-d)\cos(\alpha) + h_2\big)^2}}$$

In order for the equations of motion describing α to be derived, it is necessary to understand the forces acting on the sump and arm linkage. Figure Y shows free body diagrams of the system.

Figure Y: A free body diagram of the floating sump-inlet. Positive moments are defined in the CCW direction.

The piston-cylinder assembly is modeled as a spring-dashpot and assumed massless (force contribution small compared to its stiffness and damping). The internal forces (bending, etc.) will be considered in the next section. Sway and heave hydrodynamic forces act on the side and bottom of the sump, respectively. The gravitational force and hydrostatic buoyant forces act vertically. Lastly, there is an impulse generated on the leading edge from the flow of fluid over it, which impinges on the free surface of the fluid inside the sump. Therefore, the equation of motion describing α in the current system is simply the moment balance about Point A:

$$L_A\ddot{\alpha}(t) + B_A\big(\dot{\alpha}(t)\big) + C_A\big(\alpha(t)\big) = \mathcal{M}_{piston} + \mathcal{M}_g + \mathcal{M}_{LE} + \mathcal{M}_{hydro}(A, \omega, t) \qquad (1)$$

Where L_A is the rotational inertia of the sump and linkage about Point A.

$$L_A = \int r_A^2 dm + A_A$$

Wherein A_A is the rotational added mass of the sump. The hydrodynamic damping moment contribution of the sump is denoted $B_A\big(\dot{\alpha}(t)\big)$ and the hydrostatic stiffness moment contribution is

$C_A\left(\dot{\alpha}(t)\right)$. $\mathcal{M}_{hydro}(A,\omega,t)$ is the net moment created by the sway and heave forces on the sump at a given time. The remaining moment contributions are:

$$\mathcal{M}_{piston} = -\left(F_{preload} + k_p\left(l_p^{SW} - l_p\right)\right)h_2\sin(\theta) + B_p\dot{l_p}h_2\sin(\theta)$$

$$\mathcal{M}_g = -\left(m_{sump} + m_{arm} + m_{ballast}\right)x_{CoG}$$

$$x_{CoG} = \frac{\left(m_{sump}x_{CoG,sump}(\alpha) + m_{arm}x_{CoG,arm}(\alpha) + m_{ballast}x_{CoG,ballast}(\alpha)\right)}{\left(m_{sump} + m_{arm} + m_{ballast}\right)}$$

$$\mathcal{M}_{LE} = -\rho_w Q\sqrt{2gh_{weir}}\left(lsin(\alpha) + (H + h_3)sin(\beta + \alpha - 180) + Bcos(\beta + \alpha - 180) + \frac{H - h_3 - \delta_{LE}^*}{\sin(\gamma_{LE}^*)}\cos(\gamma_{LE}^* + \beta + \alpha - 180)\right)$$

The hydrodynamic moment, hydrostatic stiffness, hydrodynamic damping, and added mass about Point A require more analysis. This will require a brief introduction to potential flow theory. For more detail, the reader is referred to (J. Newman, 2017).

Wave forces on a body can comprise both inertial – Froude-Krylov forces, diffraction forces, radiation forces resulting from potential flow wave theory – and viscous forces – form drag and friction drag resulting from fluid flow over the body (which we are neglecting for the time-being).

Inertial forces

With incident waves of the form $a(x,t) = Acos(\omega t - kx) = A \times Re\left(e^{i\omega t - ikx}\right)$, with zero phase defined relative to x=0 ($\omega = \frac{2\pi}{T}$ and $k = \frac{2\pi}{\lambda}$), it can be shown (by applying the appropriate boundary and free surface conditions and deriving the nonlinear dispersion relation between wave frequency and wavelength) that the velocity potential of a plane progressive wave is (P. Sclavounos, 2002):

$$\Phi_I(x,z,t) = Re\left(A\varphi_I(x,z)e^{i\omega t}\right) = Re\left(\frac{igA}{\omega}\frac{\cosh(k(z+H))}{\cosh(kH)}e^{-ikx+i\omega t}\right) = Re\left(\frac{igA}{\omega}e^{kz-ikx+i\omega t}\right)$$

Where $k = \omega^2/g$ and H is the bottom depth, and where

$$\varphi_I(x,z) = \frac{ig}{\omega}\frac{\cosh(k(z+H))}{\cosh(kh)}e^{-ikx}$$

is the complex potential. Where of course $\nabla^2\Phi_I = 0$ everywhere and $\frac{\partial^2\Phi_I}{\partial t^2} + g\frac{\partial\Phi_I}{\partial z} = 0$ at z=0. The velocity at any point (x, z) is simply $\vec{v}_I(x,z,t) = \nabla\Phi_I(x,z,t)$ and hydrodynamic pressure is $P_I = -\rho\frac{\partial\Phi_I}{\partial t} = Re\left(\rho gA\frac{\cosh(k(z+H))}{\cosh(kH)}e^{-ikx+i\omega t}\right)$. The diffraction velocity potential caused by the presence of a body in the fluid is: $\psi(z) = Re\left(\varphi_7(x,z)e^{i\omega t}\right)$ where $\varphi_7(x,z)$ represents the scattered, outgoing waves created by the body. Together they must satisfy BC $\frac{\partial}{\partial n}(\Phi_I + \psi)$=0 on the surface area, and $\left(-\omega^2 + g\frac{\partial}{\partial z}\right)\varphi_7 = 0$ at z=0. It follows that (P. Sclavounos, 2002):

$$P = -\rho \frac{\partial}{\partial t}(\Phi_I + \psi) = -\rho Re\left(i\omega(\varphi_I + \varphi_7)e^{i\omega t}\right) = \rho g A\, Re\left(\left(e^{kz-ikx} + \frac{\varphi_7 \omega}{igA}\right)e^{i\omega t}\right)$$

This boundary value problem is solved for $\varphi_7(x,z)$, usually with panel method. However, because diffraction effects are negligible, we do not consider these relations. From these relations the inertial hydrodynamic forces can be evaluated.

By definition, $\overrightarrow{F_i} = \iint P\vec{n}ds$ where i=1,3 (heave, sway) over the surface area (P. Sclavounos, 2002):

$$F_{heave} = \iint P\vec{n}_{heave}dS = Re\left(\vec{f}_{heave}(\omega)e^{i\omega t}\right) \rightarrow \vec{f}_{heave}(\omega) = \rho g A \iint \left(e^{kz-ikx} + \frac{\varphi_7 \omega}{igA}\right)\vec{n}_{heave}dS$$

$$F_{sway} = \iint P\vec{n}_{sway}dS = Re\left(\vec{f}_{sway}(\omega)e^{i\omega t}\right) \rightarrow \vec{f}_{sway}(\omega) = \rho g A \iint \left(e^{kz-ikx} + \frac{\varphi_7 \omega}{igA}\right)\vec{n}_{sway}dS$$

$$\vec{M}_{roll} = \iint P(\vec{X}_G \times \vec{n}_{all})dS = Re\left(\vec{f}_{roll}(\omega)e^{i\omega t}\right) \rightarrow \vec{f}_{roll}(\omega) = \rho g A \iint \left(e^{kz-ikx} + \frac{\varphi_7 \omega}{igA}\right)(\vec{X}_G \times \vec{n}_{all})dS$$

Each of these forces can be decomposed into their Froude-Krylov and Diffraction components, respectively (P. Sclavounos, 2002):

$$\vec{f}_j(\omega) = \vec{f}_j^{FK}(\omega) + \vec{f}_j^{Diff}(\omega) \text{ where j = heave, sway, roll}$$

And because we ignore the diffraction component, the Froude-Krylov components are simply (P. Sclavounos, 2002):

$$\vec{f}_{heave}(\omega) = \rho g A \iint \left(e^{kz-ikx}\right)\vec{n}_{heave}dS$$
$$\vec{f}_{sway}(\omega) = \rho g A \iint \left(e^{kz-ikx}\right)\vec{n}_{sway}dS$$
$$\vec{f}_{roll}(\omega) = \rho g A \iint \left(e^{kz-ikx}\right)(\vec{X}_G \times \vec{n}_{all})dS$$

An alternative method for calculating the wave excitation forces goes as follows (D. Yue, 2005). Because $B \ll \lambda$ for the sump in all expected sea states, the incident wave field is not affected by the presence of the sump, therefore diffraction and radiation forces can be neglected and the Froude-Krylov approximation can be used to calculate the Froude-Krylov wave forces (D. Yue, 2005):

$$\Phi \approx \Phi_I$$

$$P \approx P_I = -\rho\left(\frac{\partial \Phi_I}{\partial t} + gz\right)$$

$$\vec{F}_{FK} = \iint -\rho\left(\frac{\partial \Phi_I}{\partial t} + gz\right)\hat{n}dS$$

Applying divergence theorem, we can rewrite $\vec{F}_{FK}$ as (D. Yue, 2005):

$$\vec{F}_{FK} = -\iint P_I\hat{n}dS = -\iiint \nabla P_I dV$$

And since the body is small compared to the wavelength of incident waves, we can take ∇P_I to be approximately constant throughout the body volume, and approximately equal to the value at the body center (D. Yue, 2005):

$$\vec{F}_{FK} \cong (-\nabla P_I)|_{\substack{body \\ center}} \iiint dV = V(-\nabla P_I)|_{\substack{body \\ center}}$$

While incident waves are not affected by radiation and diffraction fields, the motion of the sump in the water still creates radiation fields, which in terms creates inertial forces on the body (D. Yue, 2005).

$$\vec{F}_R = \iint -\rho\left(\frac{\partial \Phi_R}{\partial t}\right)\hat{n}dS = -m_{ij}\dot{U}_{b\,j} - b_{ij}U_{b\,j}$$

And these are accounted for by the added mass and hydrodynamic damping coefficient discussed in a moment, where U_b is the velocity of the body.

Yet another alternative to calculating the wave excitation forces, under the long wavelength assumption, is to use the GI Taylor approximation to calculate the incident wave forces (P. Sclavounos, 2002):

$$F_{sway} = -\left(V_{disp} + \frac{A_{sway}}{\rho}\right)\frac{\partial P}{\partial x}_{x=0}$$

$$F_{heave} = -\left(V_{disp} + \frac{A_{heave}}{\rho}\right)\frac{\partial P}{\partial z}_{z=-H+h_3}$$

Where the force is divided into Froude-Krylov and diffraction components (left and right term in the parenthetical, respectively). From Euler's equations this set of equations can be rewritten (P. Sclavounos, 2002):

$$\frac{\partial U}{\partial t} + U\frac{\partial U}{\partial x} \cong -\frac{1}{\rho}\frac{\partial P}{\partial x} \quad \text{where} \quad U = \frac{\partial \Phi_I}{\partial x} = Re\left(\frac{igA}{\omega}(-ik)e^{kz-ikx+i\omega t}\right)$$

$$F_{sway} = \left(\rho V_{disp} + A_{sway}\right)\left(\frac{\partial U}{\partial t} + U\frac{\partial U}{\partial x}\right)_{x=0} - A_{sway}\frac{\partial^2 x_{sway}(t)}{\partial t^2}$$

Where U does not take body disturbance into account and the last term is only included if the body is moving in the sway-direction. And when the ambient velocity is arising from plane progressive waves (P. Sclavounos, 2002):

$$\left| U \frac{\partial U}{\partial x} \right| = O(A^2)$$

Where A is the amplitude of the incident waves and so it can be omitted (P. Sclavounos, 2002):

$$F_{sway} = \left(\rho V_{disp} + A_{sway}\right)\left(\frac{\partial U}{\partial t}\right)_{x=0} + O(A^2)$$

For a deeply submerged object (such as an oil rig leg), the surge/sway force must be added up be integrating dF_z along the entire length. In long waves, the surge/sway force receives even contributions from the Froude-Krylov and the Diffraction components. In heave, the Froude-Krylov component is the leading contributor to the force. In long waves, the heave exciting force is approximately equal to the hydrostatic force (P. Sclavounos, 2002):

$$F_{heave} \cong F_{heave}^{FK} = \rho g A \iint e^{kz - ikx} n_{heave} dS$$

$$Taylor\ Series: e^{kz-ikx} = 1 + (kz - ikx) + O(kB)^2$$

$$F_{heave} = \rho g A_{SWL} A$$

Where A_{SWL} is the cross-sectional area of the object and A is the long wave amplitude.

The GI Taylor approximation is the most commonly used method for wave force calculations under the long wavelength approximation, so it will also be used here. The heave and sway forces acting on the sump can be calculated as:

Approximated as a rectangular prism with $[Length, Width, Height] = [L,\ \ B + \frac{H-h_3}{2\tan(\gamma_{LE}^*)},\ \ H - h_3]$ very small compared to wavelength and small motions compared to wavelength

$$F_{sway}(t) = \int_{z'=-H+h_3}^{z'=0} df_{sway} = \int_{z'=-H+h_3}^{z'=0} \left(2\rho L\left(B + \frac{H-h_3}{2\tan(\gamma_{LE}^*)}\right)\right) \frac{\partial U}{\partial t}\Big|_{\substack{x=lsin(\alpha_{SW})+B+\frac{H-h_3}{2\tan(\gamma_{LE}^*)} \\ z=z'}} dz'$$

Or if we assume the pressure gradient and time derivative is approximately constant along the side of the sump, then the sway force simply becomes:

$$F_{sway}(t) = (H-h_3)\left(2\rho L\left(B+\frac{H-h_3}{2\tan(\gamma_{LE}^*)}\right)\right)\frac{\partial U}{\partial t}\Big|_{\substack{x=lsin(\alpha_{SW})+B+\frac{H-h_3}{2\tan(\gamma_{LE}^*)} \\ z=\frac{-H+h_3}{2}}}$$

$$= (H-h_3)\left(2\rho L\left(B+\frac{H-h_3}{2\tan(\gamma_{LE}^*)}\right)\right)Re\left(\frac{igA}{\omega}\left(-\frac{i\omega^2}{g}\right)(i\omega)e^{k\left(\frac{-H+h_3}{2}\right)-ik\left(lsin(\alpha_{SW})+B+\frac{H-h_3}{2\tan(\gamma_{LE}^*)}\right)+i\omega t}\right)$$

$$= (H-h_3)\left(2\rho L\left(B+\frac{H-h_3}{2\tan(\gamma_{LE}^*)}\right)\right)\left(iA\omega^2 e^{k\left(\frac{-H+h_3}{2}\right)}e^{i\left(\omega t-k\left(lsin(\alpha_{SW})+B+\frac{H-h_3}{2\tan(\gamma_{LE}^*)}\right)\right)}\right)$$

$$= -(H-h_3)\left(2\rho L\left(B+\frac{H-h_3}{2\tan(\gamma_{LE}^*)}\right)\right)A\omega^2 e^{k\left(\frac{-H+h_3}{2}\right)}\sin\left(\omega t-k\left(lsin(\alpha_{SW})+B+\frac{H-h_3}{2\tan(\gamma_{LE}^*)}\right)\right)$$

Similarly, the heave force can be calculated as:

$$F_{heave}(t) = \int_{x\prime=lsin(\alpha_{SW})+B+\frac{H-h_3}{2\tan(\gamma_{LE}^*)}}^{x\prime=lsin(\alpha_{SW})} df_{heave}$$

$$= -\int_{x\prime=lsin(\alpha_{SW})+B+\frac{H-h_3}{2\tan(\gamma_{LE}^*)}}^{x\prime=lsin(\alpha_{SW})}\left(\frac{3}{2}\rho L(H-h_3)\right)\frac{\partial V}{\partial t}\Big|_{\substack{x=x\prime \\ z=-H+h_3}} dx'$$

Or if we assume the pressure gradient and time derivative is approximately constant along the bottom of the sump, then the heave force simply becomes:

$$F_{heave}(t) = -\left(B+\frac{H-h_3}{2\tan(\gamma_{LE}^*)}\right)\left(\frac{3}{2}\rho L(H-h_3)\right)\frac{\partial V}{\partial t}\Big|_{\substack{x=lsin(\alpha_{SW})+\frac{B}{2}+\frac{H-h_3}{4\tan(\gamma_{LE}^*)} \\ z=-H+h_3}}$$

$$= -\left(B+\frac{H-h_3}{2\tan(\gamma_{LE}^*)}\right)\left(\frac{3}{2}\rho L(H-h_3)\right)Re\left(\frac{igA}{\omega}\left(\frac{\omega^2}{g}\right)(i\omega)e^{k(-H+h_3)-ik\left(lsin(\alpha_{SW})+\frac{B}{2}+\frac{H-h_3}{4\tan(\gamma_{LE}^*)}\right)+i\omega t}\right)$$

$$= -\left(B+\frac{H-h_3}{2\tan(\gamma_{LE}^*)}\right)\left(\frac{3}{2}\rho L(H-h_3)\right)Re\left(-A\omega^2 e^{k(-H+h_3)}e^{i\left(\omega t-k\left(lsin(\alpha_{SW})+\frac{B}{2}+\frac{H-h_3}{4\tan(\gamma_{LE}^*)}\right)\right)}\right)$$

$$= \left(B+\frac{H-h_3}{2\tan(\gamma_{LE}^*)}\right)\left(\frac{3}{2}\rho L(H-h_3)\right)A\omega^2 e^{k(-H+h_3)}\cos\left(\omega t-k\left(lsin(\alpha_{SW})+\frac{B}{2}+\frac{H-h_3}{4\tan(\gamma_{LE}^*)}\right)\right)$$

These equations can be directly used to calculate the reaction forces, in time, at the pivot joint at Point A. Moreover, they indicate the forces which will be experienced by the sump, arm, and joints in operation. The next section uses these forces to inform the structural design of the sump and arm.

However, the forcing of interest in the linear dynamics model is the roll moment caused by wave excitation about Point A, which can be readily calculated as:

$$M_{A,roll} = \int_{z'=-H+h_3}^{z'=0} (D + h_1 - z') df_{sway} + \int_{x\prime=lsin(\alpha_{SW})+B+\frac{H-h_3}{2\tan(\gamma_{LE}^*)}}^{x\prime=lsin(\alpha_{SW})} x' df_{heave}$$

$$= \int_{z'=-H+h_3}^{z'=0} (D + h_1 - z') \left(2\rho L \left(B + \frac{H-h_3}{2\tan(\gamma_{LE}^*)}\right)\right) \frac{\partial U}{\partial t}\Big|_{\substack{x=lsin(\alpha_{SW})+B+\frac{H-h_3}{2\tan(\gamma_{LE}^*)} \\ z=z'}} dz'$$

$$- \int_{x\prime=lsin(\alpha_{SW})+B+\frac{H-h_3}{2\tan(\gamma_{LE}^*)}}^{x\prime=lsin(\alpha_{SW})} x' \left(\frac{3}{2}\rho L(H-h_3)\right) \frac{\partial V}{\partial t}\Big|_{\substack{x=x\prime \\ z=-H+h_3}} dx'$$

Or if we, again, assume the pressure gradient and time derivative is approximately constant throughout the volume of the sump, then the roll moment about Point A simply becomes:

$$M_{A,roll} = (H-h_3)(D + h_1 + \frac{H-h_3}{2}) \left(2\rho L \left(B + \frac{H-h_3}{2\tan(\gamma_{LE}^*)}\right)\right) \frac{\partial U}{\partial t}\Big|_{\substack{x=lsin(\alpha_{SW})+B+\frac{H-h_3}{2\tan(\gamma_{LE}^*)} \\ z=\frac{-H+h_3}{2}}}$$

$$- \left(B + \frac{H-h_3}{2\tan(\gamma_{LE}^*)}\right) \left(lsin(\alpha_{SW}) + \frac{B}{2} + \frac{H-h_3}{4\tan(\gamma_{LE}^*)}\right) \left(\frac{3}{2}\rho L(H-h_3)\right) \frac{\partial V}{\partial t}\Big|_{\substack{x=lsin(\alpha_{SW})+\frac{B}{2}+\frac{H-h_3}{4\tan(\gamma_{LE}^*)} \\ z=-H+h_3}}$$

$$M_{A,roll} = -(H-h_3)\left(D + h_1 + \frac{H-h_3}{2}\right)\left(2\rho L\left(B + \frac{H-h_3}{2\tan(\gamma_{LE}^*)}\right)\right) A\omega^2 e^{k\left(\frac{-H+h_3}{2}\right)} \sin\left(\omega t - k\left(lsin(\alpha_{SW}) + B + \frac{H-h_3}{2\tan(\gamma_{LE}^*)}\right)\right)$$
$$+ \left(B + \frac{H-h_3}{2\tan(\gamma_{LE}^*)}\right)\left(lsin(\alpha_{SW}) + \frac{B}{2} + \frac{H-h_3}{4\tan(\gamma_{LE}^*)}\right)\left(\frac{3}{2}\rho L(H-h_3)\right) A\omega^2 e^{k(-H+h_3)} \cos\left(\omega t - k\left(lsin(\alpha_{SW}) + \frac{B}{2} + \frac{H-h_3}{4\tan(\gamma_{LE}^*)}\right)\right)$$

This is the expression used in the hydrodynamic model of the sump to calculate the moment contribution of the wave forces.

2.9.2 Viscous forces

If viscous forces need to be accounted for in the future, the following method can be implemented. Viscous forces comprise form drag (pressure drag resulting from separated boundary layer over a significant portion of the body) and friction drag (due to shear stress inside of a boundary layer). The body size is comparable to wave amplitudes so viscous effects important except in very calm waters. As $2\pi A/l \approx 3$, the viscous force on a body in unsteady viscous flow can be evaluated by Morrison's Equation.

$$F_i(t) = \rho C_m(Re, K_C) V_{sub} \dot{U} + \frac{1}{2} \rho C_d(Re) A U|U|$$

Assuming linear ("Airy") wave theory, the drag and mass coefficients can be obtained from Blasius: These coefficients could vary significantly in different flows, in time, even within the span of a single wave period. However, here they are assumed constant for the purpose of attaining a rough estimate of viscous forces.

2.9.3 Added mass and hydrodynamic damping contributions

In general, the added mass and hydrodynamic damping coefficients for a floating object are attained by solving for the diffraction potential caused by the fluid disturbance around the object. This requires solving the free-surface boundary value problem, typically using the panel method.

$$\omega^2 A_{ij}(\omega) - i\omega B_{ij}(\omega) = -\rho \iint \psi_i \frac{\partial \psi_j}{\partial n} dS$$

$$A_{ij}(\omega) = Re\left(-\frac{\rho}{\omega^2} \iint \psi_i \frac{\partial \psi_j}{\partial n} dS \right)$$

$$B_{ij}(\omega) = Im\left(-\frac{\rho}{\omega} \iint \psi_i \frac{\partial \psi_j}{\partial n} dS \right)$$

Without ψ_i available on the surface area (because we neglect diffraction effects), we instead use derivations for simple cross sections to evaluate the sway, heave, roll

Added mass represents the additional resistance to the acceleration of a submerged (or partially submerged) object that it caused by the presence of the ambient fluid. In other words, added mass represents the mass of fluid that is accelerated with the body. Therefore, it is direction-dependent. Hydrodynamic damping represents the dissipation of energy as surface waves. These two parameters are collectively referred to as "impedance hydrodynamic coefficients." These are usually also attained by using the panel method to solve the boundary value problems for the velocity potentials (radiative) of the fluid disturbances caused by the motions of the body in the fluid. We will instead use the long wavelength approximations to evaluate the impedance hydrodynamic coefficients.

For a slender body, the 3D added mass coefficient can be estimated as the sum of the added mass coefficients of the 2D slices perpendicular to the longitudinal axis. Approximating the sump as a rectangular prism of square cross-section with length L and width/height $H - h_3$, a 2D slice of the sump perpendicular to the longitudinal axis (in the fore-aft direction, parallel to the still water plane) has added masses:

$$in\ 2D \rightarrow \quad m_{sway} \cong 4.754\rho(H - h_3)^2 \quad m_{heave} = \frac{1}{2}\rho\,(H - h_3)^2 \quad m_{roll} \cong 0.725\rho(H - h_3)^4$$

By integration of these 2D slices along the longitudinal axis of the sump, the 3D sway, heave, and roll added masses of the sump can be evaluated. Because System 1 considers a 1 DOF system in roll, the only added mass component of interest is the roll added mass. Because the center of rotation is not at the center of the submerged shape, roll causes linear displacement, both sway and heave. Therefore, the coupled added mass for rotation about the remote center of rotation at Point A can be found by first writing the moment generated by the sump experiencing an angular acceleration in the water about Point A, $\ddot{\alpha}$:

$$M_{A|_{mass}^{added}} = m_{roll}\ddot{\alpha} + m_{sway}\cos(\alpha)\left(\frac{H}{\sqrt{2}} + l\right)^2 \ddot{\alpha} + m_{heave}\sin(\alpha)\left(\frac{H}{\sqrt{2}} + l\right)^2 \ddot{\alpha} = m_{\alpha,A}\ddot{\alpha}$$

Factoring out $\ddot{\alpha}$ and integrating along the longitudinal axis of the sump (strip theory):

$$m_{\alpha,A} = L\left(0.725\rho(H-h_3)^4 + 4.754\rho(H-h_3)^2\cos(\alpha_{SW})\left(\frac{H}{\sqrt{2}} + l\right)^2 + \frac{1}{2}\rho\,(H-h_3)^2\sin(\alpha_{SW})\left(\frac{H}{\sqrt{2}} + l\right)^2\right)$$

This is similar to the result one would get by, again, approximating the sump as an elongated square with side length $H - h_3$, length L, with diagonal collinear with the central axis of the arm, and integrating:

$$m_{\alpha,A} = \rho\int_{r=\sqrt{2}(H-h_3)+l}^{r=l+\frac{H-h_3}{\sqrt{2}}}\left(2\left(\sqrt{2}(H-h_3)+l-r\right)\right)Lr^2dr + \rho\int_{r=l+\frac{H-h_3}{\sqrt{2}}}^{r=l}\left(2(r-l)\right)Lr^2dr$$

$$= 2L\rho\left(\frac{\left(\sqrt{2}(H-h_3)+2l\right)\left(l+\frac{H-h_3}{\sqrt{2}}\right)^3}{3} - \frac{\left(l+\frac{H-h_3}{\sqrt{2}}\right)^4}{2} - \frac{\left(\sqrt{2}(H-h_3)+l\right)^4}{12} - \frac{l^4}{12}\right)$$

By using the Haskind relations to express the wave excitation forces, one can circumvent solving the diffraction problem in finding the hydrodynamic damping contribution. The diagonal damping coefficients can be evaluated given that the hydrodynamic forces are already known [Newman 174]:

$$in\ 2D \quad \rightarrow \quad B_{roll} = \frac{|dM_{roll}|^2}{2\rho g V_g}\ where\ V_g = \frac{g}{2\omega}\ in\ deep\ water$$

$$dM_{roll} = \left(-(H-h_3)\left(D+h_1+\frac{H-h_3}{2}\right)\left(2\rho\left(B+\frac{H-h_3}{2\tan(\gamma_{LE}^*)}\right)\right)A\omega^2 e^{k\left(\frac{-H+h_3}{2}\right)}\sin\left(\omega t - k\left(lsin(\alpha_{SW})+B+\frac{H-h_3}{2\tan(\gamma_{LE}^*)}\right)\right)\right.$$
$$+\left(B+\frac{H-h_3}{2\tan(\gamma_{LE}^*)}\right)\left(lsin(\alpha_{SW})+\frac{B}{2}+\frac{H-h_3}{4\tan(\gamma_{LE}^*)}\right)\left(\frac{3}{2}\rho(H-h_3)\right)A\omega^2 e^{k(-H+h_3)}\cos\left(\omega t\right.$$
$$\left.\left.-k\left(lsin(\alpha_{SW})+\frac{B}{2}+\frac{H-h_3}{4\tan(\gamma_{LE}^*)}\right)\right)\right)dy$$

This can be trivially extended to the 3D case using strip theory. For now, damping contributions are neglected because, for small oscillatory sump motions, accelerations are high and velocities low, therefore the added mass contribution is much larger than the hydrodynamic damping contribution.

$$B_A\big(\dot{\alpha}(t)\big) = 0$$

2.9 Hydrostatic stiffness contribution

The buoyancy of the sump can be modeled as a spring that supplies a hydrostatic restoring force/moment. Hydrostatic stiffness primarily depends on the SWL area. For an unconstrained floating rectangular prism (6 DOF) the heave hydrostatic stiffness is $C_{heave} = \rho g A_{SWL}$,the pitch and roll hydrostatic stiffness are $C_{ptich/roll} = \rho g V_{sub} z_{centroid,sub} - mgz_{centroid,sub}$, and the sway, surge, and yaw stiffness are all 0 (there is no restoring force for motions in these directions). For the 1 DOF (System 1) sump-inlet, we consider only the roll hydrostatic restoring moment. The restoring moment is not linear with α, therefore we cannot define a linear "stiffness." We must consider the total nonlinear resultant buoyant restoring force.

The buoyant body will be of a rectangular construction with length L, thickness t_b height H_b where $H_b - h_3$ is the draft of the buoyancy in still water. Because the prism is rigidly attached to the arm linkage, the centroidal axis travels on a circular arc of radius l_b. The prism should be tangent to the proximal side of the sump in still water (to maximize its action arm and reduce its required displacement). In still water, the coordinates of the centroidal axis of the prism are:

$$Centroid_{buoy}^{SW} = \left(x_{Cent}^{SW}, z_{Cent}^{SW}\right) = \left(lsin(\alpha_{SW}) - \frac{t_b}{2} \quad , \quad D + h_1 - \ lcos(\alpha_{SW}) - \frac{H_b}{2}\right)$$

The constant radial distance from Point A to the centroidal axis of the rectangular buoy, l_b, is:

$$l_b = \sqrt{\left(lsin(\alpha_{SW}) - \frac{t_b}{2}\right)^2 + \left(lcos(\alpha_{SW}) + \frac{H_b}{2}\right)^2}$$

As α changes, there remains a constant angular offset between the arm linkage and the radius from Point A to the centroidal axis of the rectangular buoy:

$$\Delta\alpha = \alpha_{SW} - \sin^{-1}\left(\frac{lsin(\alpha_{SW}) - t_b/2}{l_b}\right)$$

The coordinates of the centroidal axis of the buoy can then be simply calculated for any α:

$$Centroid_{buoy} = (x_{Cent}, z_{Cent}) = \left(l_b sin(\alpha - \Delta\alpha) \quad , \quad D + h_1 - l_b \cos(\alpha - \Delta\alpha) - A\sin(\omega t - l_b \sin(\alpha - \Delta\alpha))\right)$$

And the displaced volume of water can be readily calculated for any α:

$$V_{disp,buoy} = \begin{cases} 0 \ if \ z_{Cent} \geq h_{far} \\ L\left(\frac{\left(h_{far} - z_{Cent}\right)^2}{2}\left(\tan(\beta_{SW} + \alpha - \pi) + \tan\left(\frac{3\pi}{2} - \beta_{SW} - \alpha\right)\right)\right) \ if \ h_{near} \leq z_{Cent} < h_{far} \\ L\left(\frac{t_b^2}{2}\tan(\beta_{SW} + \alpha - \pi) + t_b\left(\frac{H_b}{2} - \frac{Z_{Cent}}{\cos(\beta_{SW} + \alpha - \pi)} - \frac{t_b}{2}\tan(\beta_{SW} + \alpha - \pi)\right)\right) if \ 0 \leq z_{Cent} < h_{near}) \\ L\left(\frac{t_b^2}{2}\tan(\beta_{SW} + \alpha - \pi) + t_b\left(-\frac{Z_{Cent}}{\cos(\beta_{SW} + \alpha - \pi)} - \frac{t_b}{2}\tan(\beta_{SW} + \alpha - \pi) + \frac{H_b}{2}\right)\right) if - h_{near} < z_{Cent} < 0 \ and \ \alpha \geq \alpha_{SW} \\ L\left(\frac{t_b^2}{2}\tan(\pi - \beta_{SW} - \alpha) + t_b\left(-\frac{Z_{Cent}}{\cos(\pi - \beta_{SW} - \alpha)} - \frac{t_b}{2}\tan(\pi - \beta_{SW} - \alpha) + \frac{H_b}{2}\right)\right) if - h_{near} < z_{Cent} < 0 \ and \ \alpha < \alpha_{SW} \\ L\left(H_b t_b - \frac{\left(h_{far} + z_{Cent}\right)^2}{2}\left(\tan(\pi - \beta_{SW} - \alpha) + \tan\left(\beta_{SW} + \alpha - \frac{\pi}{2}\right)\right)\right) \ if \ - h_{far} < z_{Cent} \leq -h_{near} \\ LH_b t_b \quad z_{Cent} \leq -h_{far} \end{cases}$$

Where,

$$h_{near} = \begin{cases} \sqrt{\left(\frac{H_b}{2}\right)^2 + \left(\frac{t_b}{2}\right)^2}\cos\left(\beta_{SW} + \alpha - \pi + \tan^{-1}\left(\frac{t_b}{H_b}\right)\right) & \text{for } \alpha > \alpha_{SW} \\ \sqrt{\left(\frac{H_b}{2}\right)^2 + \left(\frac{t_b}{2}\right)^2}\cos\left(\tan^{-1}\left(\frac{t_b}{H_b}\right)\right) & \text{for } \alpha = \alpha_{SW} \\ \sqrt{\left(\frac{H_b}{2}\right)^2 + \left(\frac{t_b}{2}\right)^2}\cos\left(\pi - \beta_{SW} - \alpha + \tan^{-1}\left(\frac{t_b}{H_b}\right)\right) & \text{for } \alpha < \alpha_{SW} \end{cases}$$

is the vertical height between the centroid and the near corners and,

$$h_{far} = \begin{cases} \sqrt{\left(\frac{H_b}{2}\right)^2 + \left(\frac{t_b}{2}\right)^2}\cos\left(\beta_{SW} + \alpha - \pi - \tan^{-1}\left(\frac{t_b}{H_b}\right)\right) & \text{for } \alpha > \alpha_{SW} \\ \sqrt{\left(\frac{H_b}{2}\right)^2 + \left(\frac{t_b}{2}\right)^2}\cos\left(\tan^{-1}\left(\frac{t_b}{H_b}\right)\right) & \text{for } \alpha = \alpha_{SW} \\ \sqrt{\left(\frac{H_b}{2}\right)^2 + \left(\frac{t_b}{2}\right)^2}\cos\left(\pi - \beta_{SW} - \alpha - \tan^{-1}\left(\frac{t_b}{H_b}\right)\right) & \text{for } \alpha < \alpha_{SW} \end{cases}$$

is the vertical height between the centroid and the far corners.

The center of buoyancy of the rectangular buoy for any given α is approximated as $x_{CoB}^{buoy} = l_b \sin(\alpha - \Delta\alpha)$. Then the moment around Point A generated by the buoy at any given time can be expressed as:

$$M_{A,buoy} = \begin{cases} 0 \;\; if \;\; z_{Cent} \geq h_{far} \\ \rho_w g x_{CoB}^{buoy} L \left(\frac{\left(h_{far} - z_{Cent}\right)^2}{2} \left(\tan(\beta_{SW} + \alpha - \pi) + \tan\left(\frac{3\pi}{2} - \beta_{SW} - \alpha\right) \right) \right) \;\; if \;\; h_{near} \leq z_{Cent} < h_{far} \\ \rho_w g x_{CoB}^{buoy} L \left(\frac{t_b^2}{2} \tan(\beta_{SW} + \alpha - \pi) + t_b \left(\frac{H_b}{2} - \frac{Z_{Cent}}{\cos(\beta_{SW} + \alpha - \pi)} - \frac{t_b}{2} \tan(\beta_{SW} + \alpha - \pi) \right) \right) \; if \; 0 \leq z_{Cent} < h_{near}) \\ \rho_w g x_{CoB}^{buoy} L \left(\frac{t_b^2}{2} \tan(\beta_{SW} + \alpha - \pi) + t_b \left(-\frac{Z_{Cent}}{\cos(\beta_{SW} + \alpha - \pi)} - \frac{t_b}{2} \tan(\beta_{SW} + \alpha - \pi) + \frac{H_b}{2} \right) \right) \; if - h_{near} < z_{Cent} < 0 \; and \; \alpha \geq \alpha_{SW} \\ \rho_w g x_{CoB}^{buoy} L \left(\frac{t_b^2}{2} \tan(\pi - \beta_{SW} - \alpha) + t_b \left(-\frac{Z_{Cent}}{\cos(\pi - \beta_{SW} - \alpha)} - \frac{t_b}{2} \tan(\pi - \beta_{SW} - \alpha) + \frac{H_b}{2} \right) \right) \; if - h_{near} < z_{Cent} < 0 \; and \; \alpha < \alpha_{SW} \\ \rho_w g x_{CoB}^{buoy} L \left(H_b t_b - \frac{\left(h_{far} + z_{Cent}\right)^2}{2} \left(\tan(\pi - \beta_{SW} - \alpha) + \tan\left(\beta_{SW} + \alpha - \frac{\pi}{2}\right) \right) \right) \;\; if \;\; - h_{far} < z_{Cent} \leq -h_{near} \\ \rho_w g x_{CoB}^{buoy} L H_b t_b \;\; z_{Cent} \leq -h_{far} \end{cases}$$

The total hydrostatic restoring force must incorporate the displaced fluid from the sump itself, assuming small motions such that it stays submerged:

$$C_A = -M_{A,buoy} - p_w g x_{CoG,sump} V_{sump,shell}$$

Where the displaced volume of the sump shell is:

$$V_{sump,shell} = t \Bigg(w \left(\frac{(H - h_3)}{\sin(\gamma_{LE}^*)} + B + (H - h_3) \right) + 2 \Bigg(sB + s \frac{H - h_3 - s}{\tan(\gamma_{LE}^*)} + \frac{s^2}{2\tan(\gamma_{LE}^*)} + \frac{s(L - w)}{2} + \frac{(L - w)(H - h_3 - s)}{4} + \left(B + \frac{(H - h_3 - s)}{2\tan(\gamma_{LE}^*)} \right) \sqrt{(H - h_3 - s)^2 + \left(\frac{L - w}{2} \right)^2} + \frac{s(L - w)}{2\sin(\gamma_{LE}^*)} + \frac{(H - h_3 - s)(L - w)}{4\sin(\gamma_{LE}^*)} \Bigg) \Bigg)$$

Model Results and System Optimization

The model is solved using Matlab's ode45() function (which uses an adaptive time-step Runge-Kutta scheme), given the initial conditions $\alpha(t = 0) = \alpha_{SW}$ and $\dot{\alpha}(t = 0) = 0$.

First, the sump geometry is specified according to the pump flowrate (everything is driven by the hydraulic efficiency of pumping sargassum). Given the pump flowrate $Q_{pump} = 4500 \text{ GPM} = 0.284 \text{ m}^3/s$ the geometry of the sump inlet is specified. Given inputs for the geometry of the sump $C_d, L, \delta_{LE}^*, w, H, B, s, \gamma_{LE}^*$ the sump must satisfy the constraints:

$$\frac{Q_{pump}}{A_{sump}|_{z=0}} = \frac{Q_{pump}}{L\left(B + \frac{H - h_3}{\tan(\gamma_{LE}^*)}\right)} \geq 0.2 \; [m/s] \equiv \text{natural rate-of-rise of sargassum.}$$

Which ensures sargassum will flow downwards despite its natural rate-of-rise.

$$\frac{V_{sump}}{Q_{pump}} = \frac{L\left(\left(B+\frac{H-h_3-s}{\tan(\gamma_{LE}^*)}\right)s+\frac{s^2}{2\tan(\gamma_{LE}^*)}\right)+\frac{B(H-h_3-s)(w+L)}{2}+\frac{(H-h_3-s)^2}{\tan(\gamma_{LE}^*)}\left(\frac{w}{6}+\frac{L}{3}\right)}{Q_{pump}} > 3.75\ [sec] \equiv \text{dry-run response time}$$

Which ensures the hydraulics will have time to force the sump underwater again.

$$\delta_{LE}^* > \delta_{LE}^{min} = \left(\frac{Q_{pump}}{\frac{2}{3}C_d\sqrt{2g}L}\right)^{\frac{2}{3}}$$

If the still water depth of the LE is less than the threshold then it certainly won't in waves.

The values $B = s = 0.5\ [m]$ are given based on approximate proportionality with the suction piping diameter and the expected freeboard of the sargassum containment boom expected to be used.

The length of the sump, L, is set by construction and cannot be changed. In contrast, the still water depth of the leading edge can be changed by moving the tubular buoy vertically relative to rest of the sump-inlet. Therefore, the length of the sump is set by the length required to prevent dry-running in still water when the leading edge is at its minimum depth of $\delta_{LE}^* = 0.2\ [m]$

$$L = \frac{Q_{pump}}{\frac{2}{3}C_d\sqrt{2g}{\delta_{LE}^*}^{3/2}} = 1.79\ [m]$$

This happens to be about the same width of the pump, which means the number of pumps onboard is not limited by outboard space. Of course, with hydraulic efficiency as the primary design consideration, it is recommended that additional capacity is added with bigger pumps, not more, smaller pumps. Since this length is an exact number, the threshold depth of the leading edge to prevent dry-running $\delta_{LE}^{min} = \delta_{LE}^* = 0.2\ [m]$. This is the depth that δ_{LE} must remain below during operation.

Note that L and δ_{LE}^{min} can be decreased by increasing the discharge coefficient, $C_d = 0.602$ of the leading edge. C_d can be improved beyond the capacity of an ogee curve by using a labyrinth or piano key weir profile. This is discussed in section XXX and could significantly improve the stability of the sump-inlet.

Next, the rest of the sump dimension must be defined to minimize cross sectional area at the waterline and ensure sufficient volume so that there is time to respond to dry-running (constraints 1 and 2). Using the first geometrical constraint on $Q_{pump}/A_{sump}\big|_{z=0}$ and setting the desired vertical velocity to 0.2 [m/s], the width of the sump at z=0 can be calculated as:

$$\left(B+\frac{H-h_3}{\tan(\gamma_{LE}^*)}\right) = \frac{Q_{pump}}{0.2L} \rightarrow \frac{H-h_3}{\tan(\gamma_{LE}^*)} = 0.29\ [m]$$

Where B is already known. The equality will give the most flexibility with the remaining geometric terms $w, H-h_3, \gamma_{LE}^*$. Because the cross-sectional area of the sump decreases with depth, the downward

velocity will increase. Even if prior calculations and experiments prove untrustworthy and sargassum is not carried down immediately by a surface velocity of 0.2 m/s, it is weakly buoyant, meaning upstream sargassum will readily push downstream sargassum downwards, towards suction piping, where it will encounter even higher downward velocities.

Even with the second geometrical constraint, the quantities $w, H - h_3, \gamma_{LE}^*$ are still under-constrained. We introduce the additional constraint that $w, H - h_3, \gamma_{LE}^*$ should be chosen to reduce the sway force on the sump-inlet that cause unnecessary stresses in the sump, linkage, frame, and connections at points A and B. There is also reason to believe that reducing the moment around Point A caused by horizontal wave forces has a beneficial impact on sump-inlet dynamics, because these forces are out of sync with the heave motions that the sump-inlet is intended to mimic.

There is no quickly derivable objective function for the sway force that takes account for the complex geometry of the sump-inlet. Such a function could only be attained by finite element methods and CFD, confirmed by physical experiments. For now, the projected frontal area of the sump-inlet can be used as a pseudo-objective function for reducing the sway force on the sump-inlet. Choosing $\gamma_{LE}^* = 75° \approx 1.31\ [rad]$ to given sufficient bias for non-sargassum-laden seawater to flow under, not over, the leading edge of the sump, $H - h_3 = 0.29\tan(\gamma_{LE}^*) = 1.1\ [m]$ and w can be readily calculated according to constraint 2:

$$w = \frac{3.75Q_{pump} - L\left(\left(B + \frac{H - h_3 - s}{\tan(\gamma_{LE}^*)}\right)s + \frac{s^2}{2\tan(\gamma_{LE}^*)}\right) - \frac{B(H - h_3 - s)L}{2} - \frac{(H - h_3 - s)^2 L}{3\tan(\gamma_{LE}^*)}}{\frac{B(H - h_3 - s)}{2} + \frac{(H - h_3 - s)^2}{6\tan(\gamma_{LE}^*)}} = 0.53\ [m]$$

Next the model sizes the I-beam arm linkages between points A and B, using the analysis in Appendix A.

With the geometry of the sump and arm linkage completely defined, the model then solves for the thickness of the rectangular buoy, t_b, given its height $H_b = s = 0.5\ [m]$. The model checks to make sure that this buoyancy is enough to render the entire sump-linkage system positively buoyant, should it detach from the SOS vessel at Point A. This should also provide enough reserve buoyancy to prevent the sump from being dragged underwater.

Preliminary model results show the obvious result that designs which perform well in sea state 8, in head-waves (90° heading) perform even better in sea states 1-7 with other vessel orientations. Therefore, the goal of the parameter sweep became to converge on a set of parameters, $[\delta_{LE}^*, h_1, l, h_2, h_3, d, k_p, B_p, F_{pre}, m_{ballast}]$ that best meet objectives 1-5 in this worst case scenario.

While the hydraulic cylinders can provide damping (via and open/float centered directional control valves), external preload, F_{pre}, and stiffness, k_p, can only be imposed by the addition of a pneumatic spring in parallel with the hydraulic cylinder (or another more complicated means). Because $m_{ballast}$ and the rectangular buoy, together, can provide a tremendous amount of hydrostatic preload

with no added complexity, it was decided that external preload and stiffness would not be included ($F_{pre} = kp = 0$).

Not only is the hydrostatic preload created by $m_{ballast}$ and the rectangular buoy critical to the dynamics of the sump-inlet, it also ensures the stability of the sump-inlet. For a sump without any ballast, for example, disturbances will cause Q_{pump} to be instantaneously larger than Q_{weir}. This would cause the sump's standing level of water to decrease, making the sump more buoyant and bringing the leading edge of the sump closer to the free surface. This would in turn increase the discrepancy between Q_{pump} and Q_{weir} leading to a runaway effect that lifts the sump out of the water as it runs dry. Not only will this interrupt operation, but dry-running could severely damage the pump. The preload provided by $m_{ballast}$ solves this issue by reducing the effect the standing level of water in the sump has on the depth of the leading edge. In others words, for a heavily ballast sump, a decrease in the standing water level inside has a negligible effect on the buoyancy of the sump, making the rise of the leading edge small. The ballast, $m_{ballast}$, is the primary means by which the still water depth of the leading edge, δ_{LE}^{*}, is set. Across the entire range of sea states, this sump may require between 100-500kg of ballast.

Simulations immediately showed that locating the pivot, Point A, closer to the water line leads to increased performance. However, to avoid increase drag on the ship and increase rate of corrosion in the pivot, $h_1 = -0.75\ [m]$ was chosen as the maximum distance below the ship deck such that the pivot would not collide with traverse waves during transit.

Because the sargassum collection boom can only sustain a concentrated sargassum mat thickness as deep as its skirt (~0.75), it is preferable not to let δ_{LE}^{*} exceed this depth, or else the ability to achieve a maximal solids concentration in these sea states would be diminished. It is found that, in sea state 8, the depth of the leading edge must be set to 0.75 [m] in order for the leading edge to remain below the threshold depth.

We wish to minimize the length, l, of the arm linkage to, in turn, minimize the length of suction piping required. This length is chosen to be , $l = 1\ [m]$ as the minimum safe distance while also avoiding possible detrimental dynamics effects from diffraction waves made by the vessel.

It is shown that, for a ballast of 100kg, the required damping ranges from 0 [Ns/m], in SS1, to 15,000 [Ns/m], in SS8. The most common sea state 2 requires damping of about 8000 [Ns/m]. This damping will be provided by means of the directional control valve in the hydraulic cylinder (either a float-centered or open-centered valve).

FIG 107 shows the model output for this reasonably optimized set of parameters and Table R shows the parameters, or range of parameters, used to achieve the simulated output.

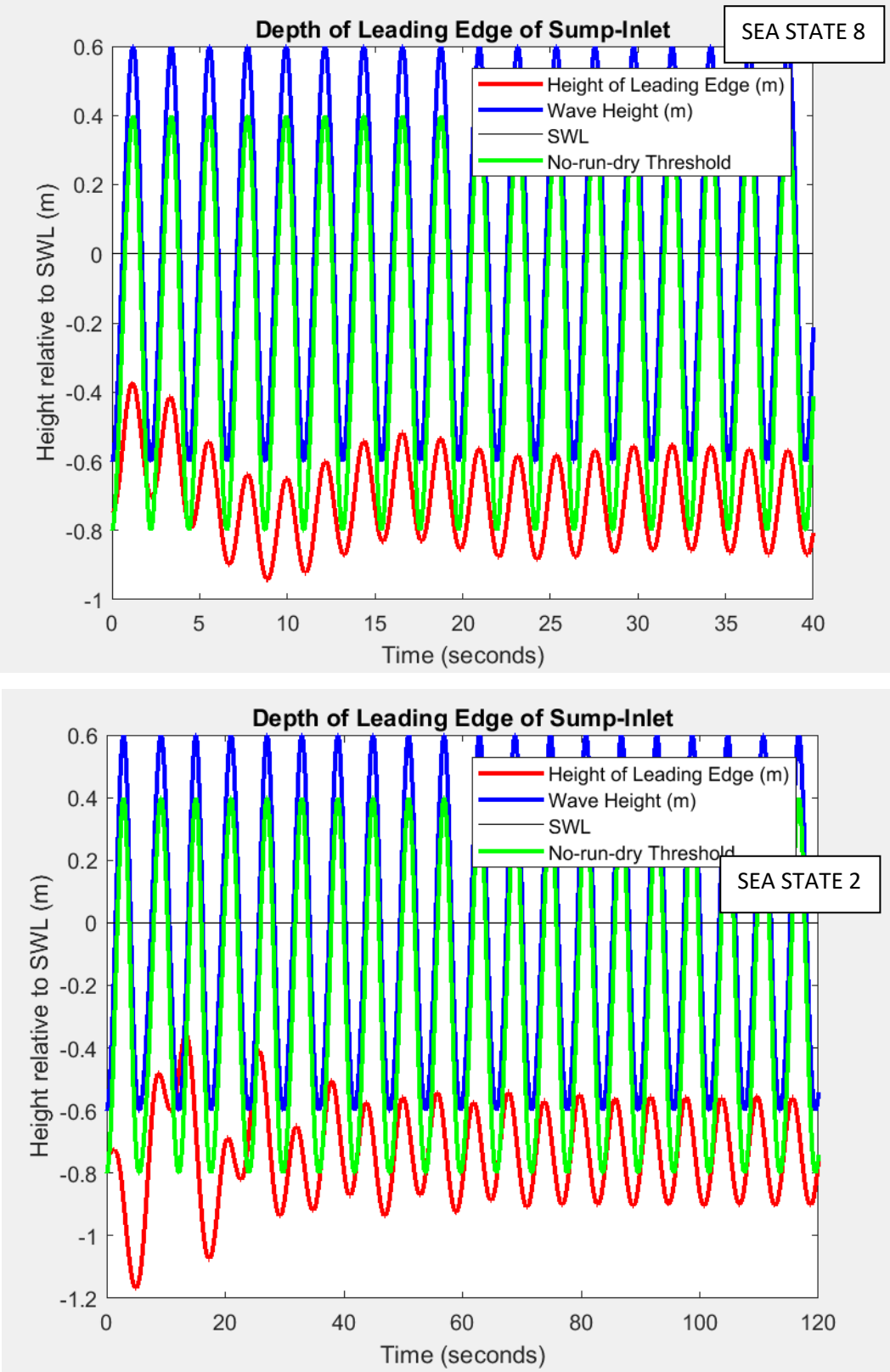

FIG 107: Example outputs of the linear dynamics model of the sump-inlet used to design an example device for a pump with a volumetric flowrate of 4500 [GPM], the first in SS8 and the second in SS2.

Table R: A table showing example numbers for a sump designed to meet a volumetric flowrate of $Q = 4500$ [GPM]. The same linear dynamics model and structural analysis models can be used to design a sump for an arbitrary volumetric flowrate in the future.

Parameter	Value	Explanation
Q	4500 [GPM]	This is the approximate expected size of the pilot pump.
D	1.5 [m]	This is the freeboard of the pilot vessel.
h_1	-0.75 [m]	Max. depth below deck to avoid traverse waves in transit.
h_2	2 [m]	Could change while increasing the damping commensurately.
h_3	0.5 [m]	Lowers α_{SW} further (closer to free floating).
l	1 [m]	Minimizes suction piping and still safe from diffraction waves.
d	0.5 [m]	Reduces cylinder length and allows reasonable stroke to lift.
H	1.6 [m]	Necessary to provide desired volume in sump.
B	0.5[m]	Necessary to allow full submergence of suction pipe in sump.
L	1.79 [m]	Necessary to prevent dry-running with minimum $\delta_{LE}^* = 0.2$.
w	0.53 [m]	Reduces projected frontal area.
s	0.5 [m]	Necessary mounting surface for ballast, boom guides, funnel.
γ_{LE}^*	1.31 [rad]	Creates minimum downward bias for flow, minimizes lift.
δ_{LE}^*	0.2-0.75 [m]	Necessary to prevent dry running in SS8.
n_{arm}	2	This small sump only requires 2 arms with cross bracing.
n_p	1 or 2	Could be easily changed to one centrally mounted cylinder.
$F_{preload}$	0 [N]	This is accomplished with ballast to avoid gas springs for now.
l_p^{SW}	2.18 [m]	Could be shortened by reducing h_2 and increasing damping.
k_p	0 [N/m]	Hydrostatic stiffness is accomplished with ballast and buoy.
B_p	8000-15,000 [Ns/m]	A small amount of damping is required to eliminate
α_{SW}	1.32 [rad]	Very close to 90° means operation is close to free-float.
t_b	0.11 [m]	Could be bigger to increase hydrostatic stiffness (add ballast).
H_b	1 [m]	Enough freeboard to allow for the addition of ballast.
t_{sump}	0.03 [m]	To prevent failure of the plywood with minimal ribbing.
t_{box}	0.00635 [m]	Standard box extrusion thickness.
w_{box}	0.07 [m]	Sized to provide infinite life in operation.
h_{box}	0.14 [m]	Sized to provide infinite life in operation.
$m_{ballast}$	100-500 [kg]	Used to control the still water height of the leading edge.

Again, this system has served as merely an example of how the linear dynamics model might be used to design a sump for a given flowrate and set of sea states with 90° heading, as close to deterministically as possible. While it is not informed deterministically by the dynamics model or the required geometry of the sump, the heading of the boat and the possibility of additional degrees of freedom at Point B, may improve the dynamics of the sump further. A -90° heading will cast a wave shadow on the sump, decreasing the wave forces it experiences. Furthermore,

Scaled wave tank tests could be done to verify this model.

Appendix E - Fleet Planning Tool

A “fleet planning tool” would take present and/or historical satellite imagery & environmental data (current and wind data) in an area of interest, identify sargassum mats with high resolution (particularly those with concentration and shape factor that makes SOS interception feasible), quantify the probability that each mat is likely to hit critical coastline, and the optimize a path for SOS vessels to sink these mats. A fleet planning tool is critical for realizing phase 2 of SOS Carbon - a fleet of open-ocean, in-situ SOS Carbon vessels - for the following reasons:

1. Feasibility Studies and Operation of SOS Carbon – Before a fleet of SOS vessels is deployed to a given area, there must be some reasonable expectation for how much reduction in sargassum landfall SOS could have there and, conversely, what size fleet is needed to create the desired impact. The fleet planning tool can be used to analyze historical data in the area of interest to study how an SOS fleet would operate there, what impact it could have, and if profitable. If these initial studies show that the venture is worthy then an automated version of the fleet planning tool would be used, in practice, to direct SOS vessels. If the initial studies show that drift patterns in the area of interest are very consistent, then SOS vessels can simply sink all mats within an identified area (these assumptions should be checked periodically with real time data).
2. Carbon accounting - Because the dominant scenario under which phase 2 would be pursued would be in the case that carbon offsets are granted, knowing where pumped-to-depth sargassum would have made landfall (if not sunk) is critical to determination of additionality.

The SOS Carbon team has used ICHTHYOP v.2 particle tracking software to generate the initial proof-of-concept model. The model uses Global HYbrid Coordinate Ocean Model (HYCOM) surface velocity data for the Mona Passage. FIGS 108 & 109 shows the output of the particle backtracking/forward-tracking model in the Mona Passage. The original “stain” of 1000 particles is released at 18.5 N 291.5 E. and 17.85 N 292.65 E in the backtracking and forward-tracking models, respectively.

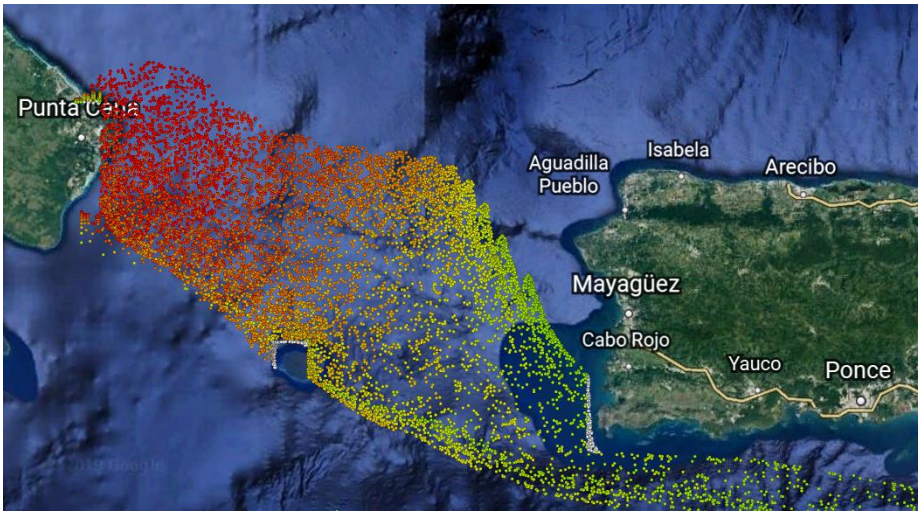

FIG 108 The output of a proof-of-concept backtracking model, which uses HYCOM surface velocity data (this example between 02/18/2019 to 02/25/2019) to trace virtual particles from Punta Cana to its entrance to the Mona Passage, near the southeast corner of the channel. Such models will be useful for analyzing real-time current data and directing fleets of SOS ships.

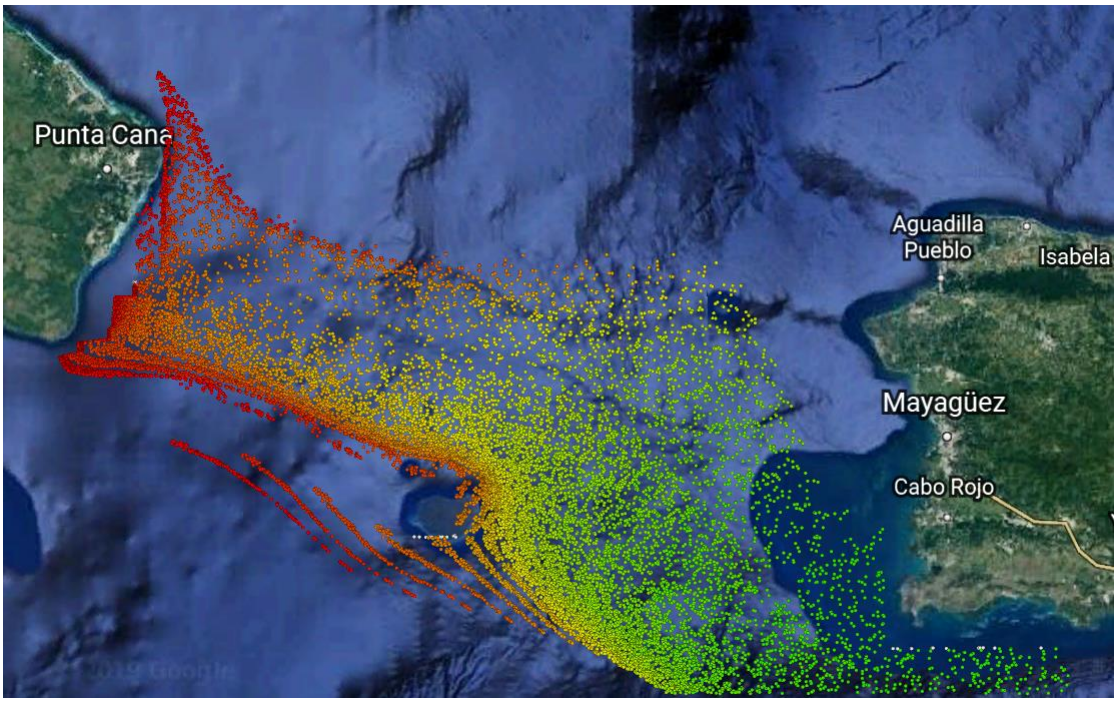

FIG 109 The output of a proof-of-concept forward-tracking model, which uses HYCOM surface velocity data (this example between 02/18/2019 and 02/25/2019) to trace virtual particles from Punta Cana to its entrance to the Mona Passage, near the southeast corner of the channel. Such models will be useful for analyzing real-time current data and directing fleets of SOS ships.

These preliminary models show that sargassum hitting Punta Cana flows westward, in tight proximity to the south coast of Puerto Rico, and enters the Mona Passage in the southeastern corner of the channel. In the Mona Passage, sargassum drifts in an S-curve, first due north, then northwest across the channel, and then transitioning northward again, before, presumably, being trapped by coastal currents and making landfall. The entire crossing takes approximately 7 days. This is thought to be the predominant path by which sargassum reaches Punta Cana. On some days, currents are completely different. It should also be noted that some current models differ considerably from HYCOM.

The current practice to verify and improve these types of models (resolving the influence of advection phenomena, surface currents, windage, waves, buoyancy, form-factor, surface texture, aging/damage, encrustation, Stommel shear, windage) is to use actual satellite observation of sargassum movement (Landsat, MODIS, MERIS; Gower et al., 2013, Hu et al., 2016, Wang & Hu, 2016, Wang & Hu, 2017). So far, models like this have identified the NERR as the source location for sargassum entering the Caribbean (Putnam, et. al., 2018) and has enabled analysts to provide periodic, albeit low resolution, forecasts of sargassum landfall.

SOS Carbon is working with French satellite surveillance company CLS (the makers of the sargassum forecasting service SAMtool) to perform an initial feasibility study of how an SOS fleet would operate, and what impact it could have, in Punta Cana. FIG 110 shows how this study is performed.

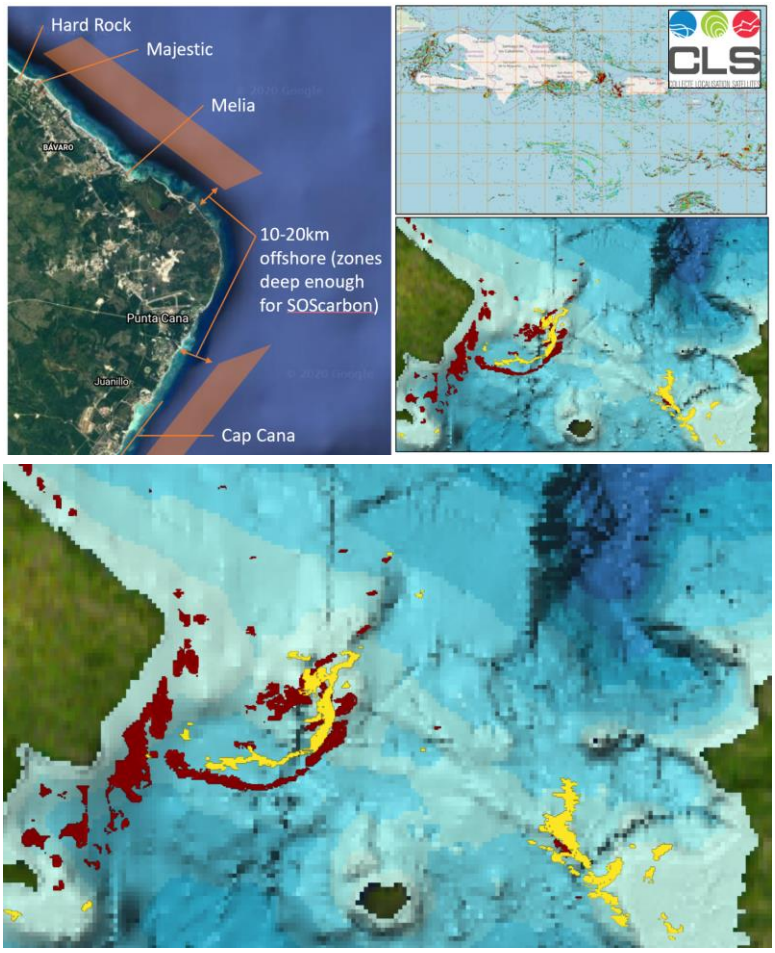

FIG 110 An example of data from CLS's SAMtool. This data is being used to study how an open ocean SOS fleet would operate in Punta Cana, DR, and how effective it could be in reducing sargassum landfall. Historical data from June-August 2018 & 2019 is being used to identify every mat of a critical size, determine its mass quantity, and if it would have been able to be addressed by SOS.

Appendix F - Alternative to Artisanal Collection Vessel

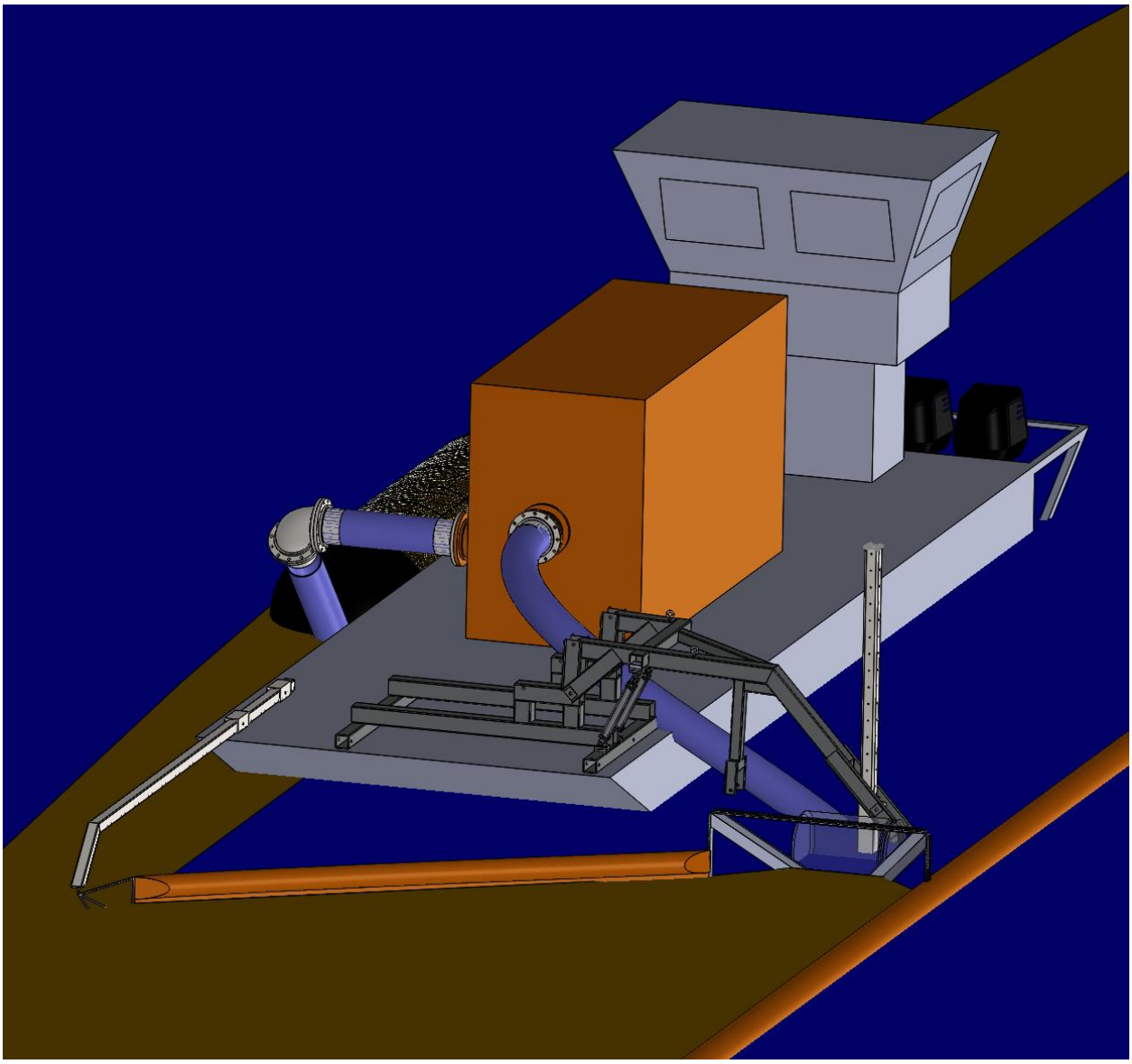

FIG 111 A higher capacity alternative to artisanal collection boats is a pump-based system, comprising a skid-mounted pump installed onboard an off-the-shelf “deck utility boat”. These are easily acquired vessels with sufficiently shallow draft for operating next to barriers. While more capital intensive than artisanal boats, these systems are still built for lower cost and less time than special conveyor vessels currently employed, and retain very high resale value (the crane arm and inlet device being the only custom hardware). The pump-based collection boat shown in FIG XXX below is a “next best” option for near shore collection. It fits into phase exactly in the place of the artisanal collection vessels - it fills the same sausage-like nets that are then towed to the SOS pump-to-depth barge offshore.

Appendix G – International Conferences

During the build phase in Bow, NH, the SOS Carbon team was invited to speak at several international conferences about the pump-to-depth strategy (FIG 112).

FIG 112: (A) GTRCM roundtable on sargassum (Jamaica), (B) 1st International Conference on Sargassum (Guadeloupe) (https://m.facebook.com/RegionGuadeloupe/videos/vl.543795413020606/560074328072032/?type=1).

This contributed some non-zero amount to the validity of the project and the ability to secure funds. The conferences also afforded the opportunity to meet face-to-face with scientists concerned with sargassum and the ecological impact of sargassum management.